THE NUMERICAL MODELLING OF COMPOSITE FLOORS EXPOSED TO FIRE

by

Mrs. Samia Nama

Submitted in fulfilment of the
requirement of the award of
degree of Doctor of Philosophy
in Civil Engineering

Engineering Structures Research Centre
School of Engineering and Mathematical Sciences
City University
London

July 2008

DECLARATION

No portion of the work referred to in the thesis has been submitted in support of an application for other degree or qualification of this or any other university or other institute of learning.

I grant powers of discretion to the City University Library to allow this thesis to be copied in whole or in part without any reference to me. This permission covers only single copies made for study purpose subject to normal condition of acknowledgement.

ACKNOWLEDGEMENTS

I would like to particularly acknowledge Professor Kuldeep S. Virdi, under whose supervision this investigation was carried out, for his continuous guidance, expert advice, constant encouragement and valuable suggestions without which this study would have never been completed.

I gratefully acknowledge and specially thank Dr. P. Stephens the senior tutor for research students in the School of Engineering and Mathematical Sciences for his support during the course of the research.

I would also offer my thanks to my colleagues in our research group for their suggestions and discussion on my work.

Finally, I sincerely thank my family, friends and most of all Max for their faith and support throughout the duration of this work.

ABSTRACT

This thesis deals with the influence of fire on the behaviour of steel concrete composite floors. A theory has been developed to calculate deflections during the fire and the ultimate strength of the composite floor under such conditions. The solution is based on the finite difference method. It takes temperature-dependent material properties into account.

The method of analysis comprises two parts; the first is thermal analysis, enabling temperatures to be calculated as a function of fire exposure time. The second is strength analysis for calculating the strength of composite floor with material properties affected by temperature.

For the heat flow analysis, the cross-section is divided into mainly rectangular elements. Sloping boundaries are approximated by triangular elements. The heat transfer from the fire to the surface is considered as well as heat conduction to the neighbouring points. At internal points, heat conduction to all the neighbouring points is considered.

To calculate the deflections, the floor is divided into a two-dimensional mesh. The deflections are calculated for each mesh point based on orthotropic plate theory. The differential operators are replaced by the finite difference formulae. This reduces the governing differential equation into a system of linear algebraic equations. To calculate the plate rigidities, it is necessary to find curvatures for all mesh points in the two planes using finite difference operators. The thermal strains are superimposed on the mechanical strains associated with curvatures to find the net strains, and then stresses are calculated using the non-linear temperature dependent stress-strain curves. Integrating the stresses, the internal stress resultants are calculated. The above method has been programmed in Visual Basic.

To validate this method, a comparison with a number of fire tests has been carried out for both thermal and mechanical behaviour. The temperatures at comparable points are generally close to each other. Comparisons have also been carried out for calculated mid-span deflections by this method and the published test results. The results show excellent correlation between the tests and the new method.

A parametric study has carried out on floors with different boundary conditions when subjected to in-plane forces for two fixed and simple ends. Comparison of mid-span deflections between the fixed and simple end conditions has shown that fixed edges have better fire resistance than simply supported when not subjected to in-plane forces. It has found that in-plane forces had little effect on deflection rates at initial stages of the fire. These only appeared at later stages. When subjected to in-plane forces in one direction only the floor showed better response.

The conclusion from the parametric study is that in-plane forces at different edges play a significant role in the behaviour, as the surrounding structure provides restraint increasing the fire resistance of the structure within the fire compartment.

To check the applicability of this method, a comparison between Bailey's design method and the present numerical analysis method was carried out. The maximum deflections were calculated by the new method using the Span/20 criterion for deflection. Good agreement was obtained with the Bailey's design method for slabs with both simply supported edge conditions and clamped edge conditions.

The developed method has been shown to accurately predict the nonlinear response of composite floors in fire and gives satisfactory prediction of thermal and mechanical behaviour of composite floors in fire. It has been shown that the new method is an appropriate tool for the analysis of composite floors exposed to fire.

CONTENTS

LIST OF FIGURES

NOTATION

C	heat capacity
dA	mesh element area in mm^2
$dt_{proposed}$	Proposed time increment
dt	appropriate time increment
D_x	the flexural rigidity of the plate in the x-direction
D_y	the flexural rigidity of the plate in the y-direction
D_{xy}	the effective torsional rigidity
E_{ao}	Young's Modulus of steel at 20 °C
f_{ayo}	Yield stress of steel at 20 °C
f'_c	compressive strength of concrete at temperature T in (N/mm^2)
f_{co}	Strength of concrete at 20 °C
$f_{a\,max}$	Tensile strength of steel at temperature T in (N/mm^2)
H_{max}	maximum value of the coefficient of heat transfer during exposure to the standard fire, $W/m^2\,°C$
K	thermal conductivity
K_c	the thermal conductivity of the concrete
K_{ct}	Reduction value for concrete

K_{max}	maximum thermal conductivity of the concrete
K_{pt}	Reduction factor for steel corresponding to f_{ayo}
K_{st}	Reduction factor for steel (in elastic range)
M_x, M_y	Moments in x and y direction respectively
n_x, n_y,	In-plane forces per unit length
p	Internal forces in the cross-section
Q	heat flow out of the bottom face in y direction at point i,j at time m
ρ	density
$\rho_c C_{cmin}$	minimum thermal capacity of the concrete
t	time in minutes
t_h	the time after the start of the fire in hours
T	Temperature
T_f	the fire temperature in (^oC)
T_o	initial temperature in (^oC)
$T_{i,j}^{m+1}$	temperature at the time *(m+1)dt*
ε_{ce}	Ultimate concrete strain in descending branch
ε_{ae}	max. Strain in descending branch
$\varepsilon_{a\max}$	Strain corresponding to $f_{a\max}$ (end of strain-hardening branch) start of Plateau
ε_{au}	Strain corresponding to $f_{a\max}$ (end of Plateau)
$\varepsilon_{bending}$	bending strain

ε_c	emissivity of the concrete
ε_f	emissivity of the fire
ε_{stress}	Strain due to stress
$\varepsilon_{thermal}$	thermal strain
ε_u	Concrete strain at the peak compressive stress, (corresponding to f_c')
σ	Stress
σ	$5.67 * 10^{-8} W / m^2 K^4$ (Stefan Boltzmann Constant)
α	coefficient of linear thermal expansion.
ν	Poisson's ratio
w	Deflection of the plate in the space coordinates
$\Delta L/L$	The rate of change of thermal expansion with temperature
$w_{m,k}$	the deflection at a general interior node of the floor
Z	the distance from the centre of the mesh element area to the neutral axis

GLOSSARY OF TERMS

Ambient temperature:	Being at room temperature (20 ^{0}C).
Coefficient of thermal expansion:	The change in linear dimension per unit length divided by the temperature change.
Conduction:	The flow of heat from one part of a substance to another part.
Conductivity:	The rate at which heat is transmitted through a material.
Convection:	A method of transferring heat by the actual movement of heated molecules.
Creep of concrete:	A time-dependent deformation that occurs while concrete is under sustained stress.
Deflection:	The displacement of the composite floor under elevated temperature.
Deformation:	The act of changing the shape or dimensions of the floor resulting from stresses.
Emissivity of fire:	The amount of radiative heat the fire emits relative to the radiative heat emitted by a perfect black body at the same temperature.
Equations of Equilibrium:	The equations relating a state of static equilibrium of the composite floor when the resultant of all forces and moments are equal to zero. Three equations must be fulfilled

	simultaneously: Sum of the forces in the X-direction must equal zero, sum of the forces in the Y-direction must equal zero, and the sum of the moments about any point must equal zero for a two dimensional structure.
Equivalent Fire Exposure:	The time during which a specified compartment or structure is submitted to ISO standard fire in order to obtain the same severity (effect) as the real fire curve.
Fire resistance:	Fire resistance is a measure of the ability of the structure to resist collapse, fire spread or other failure during exposure to a fire of specified severity.
Fire severity:	It is a measure of the destructive impact of a fire, or a measure of the forces or temperatures which could cause collapse or other failure as a result of the fire.
Fixed-End Support:	A condition where no rotation or horizontal or vertical movement can occur at that end. This type of support has no degrees of freedom. Three reactive forces exist at the rigidly fixed end.
Insulation:	Resistance to the transfer of heat, or limitation of the increase on the unexposed face. Or The rise of temperature on the unexposed face.
Integrity:	Resistance to fire protection or ability of the resist penetration by flames or hot gases through opining (e.g. cracks). For composite floors it is assumed that the integrity criterion is fulfilled because of the steel sheet. Or ability of the floor to resist penetration of flames through the

	formation of cracks and openings.
Isotropic:	A material having equal physical properties along all axes.
Moment:	The tendency of a force to cause a rotation about a point or axis which in turn produces bending stresses.
Neutral Axis:	The surfaces in the floor where the stresses change from compression to tension, i.e., represents zero strain and therefore zero stress.
Non-linear behaviour:	The strain or deflection of the floor is no longer proportional to the stress applied.
Orthotropic plate:	A plate which has different elastic properties in two mutually perpendicular directions in the plane of the plate.
Pin Connection or Support:	A connection where no moments are transferred from one member to another, only axial and shear forces. This type of support has one degree of freedom, it can freely rotate about its axis but it cannot displace in any direction. Two mutually perpendicular reactive forces exist at the pin and their lines of action pass through the centre of the pin.
Poisson's Ratio:	Defined as the ratio of the unit lateral strain to the unit longitudinal strain. It is constant for a material within the elastic range.
Proportional Limit:	The point on a stress-strain curve where the linear relationship between stress and strain ends and usually coincides with the material yield point.
Rigidity coefficients D_x, D_y:	The resistance to flexure of a plate strip having a unit width and a thickness, in the x- or y-direction, respectively.

Roller Support:	This type of support has two degrees of freedom, it can freely rotate about its axis or displace in one direction in the plane. Only one reactive force exists at a roller which acts perpendicular to the path of the displacement and its line of action passes through the centre of the roller.
Specific heat:	The rate of temperature rise of a given material to a given amount of heat energy.
Stability:	Resistance to collapse and/or excessive deflection.
Stiffness:	The resistance of a structural member to deflection due to loading.
Strain:	The shortening or elongation caused by an applied stress.
Stress:	A compression or tensile force acting on an element divided by the area which it acts.
Surface Emissivity:	The ratio between the radiative heat absorbed by a given surface and that of a black body surface, equal to heat absorptive ability of a surface.
Tensile Strength:	The longitudinal pulling stress a material can withstand without tearing apart or the maximum tensile stress the material can sustain.
Tension:	A condition caused by the action of stretching or pulling of a component.
Thermal conductivity:	The rate that heat energy is able to transfer (conduct) through a given material and is defined as the ratio of the heat flux to the temperature gradient.
Thermal diffusivity:	It is described as an index of the ease or difficulty with

	which concrete undergoes temperature change and, numerically, is the thermal conductivity divided by the product of specific heat and density.
Thrust:	The horizontal component of a reaction or an outward horizontal force.
Torsional rigidity:	The resistance of a plate element to twisting.
Yield Point (f_y):	Is that unit stress at which the stress-strain curve exhibits a definite increase in strain without an increase in stress which is less than the maximum attainable stress.
Young's modulus:	The slope of the linear portion of the stress-strain plot for a given material found by dividing the unit stress by the unit strain. This is also called Modulus of Elasticity (E).

EQUATIONS

Equation	New No.
$T_f = 750\left[1 - e^{-3.79553\sqrt{t_h}}\right] + 170.41\sqrt{t_h} + T_o$	(2-1)
$T_f = 345\log_{10}(8t+1) + T_o$	(2-2)
$f_c = f_c'(3\varepsilon_{stress}/\varepsilon_u)/(2+(\varepsilon_{stress}/\varepsilon_u)^3) \quad for: \varepsilon_{stress} \le \varepsilon_u$	(2-3)
$f_c = f_c'(1-((\varepsilon_{stress}/\varepsilon_u)/(\varepsilon_{ce}-\varepsilon_u))) \quad for: \varepsilon_u < \varepsilon_{stress} < \varepsilon_{ce}$	(2-4)
$f_c = 0 \quad for: \varepsilon_{stress} \ge \varepsilon_{ce}$	(2-5)
$f_y = (\varepsilon_{stress} * f_{ap}) / \varepsilon_{ap}$	(2-6)
$\varepsilon_{ap} = (K_{pt} * f_{ayo})/(K_{st} * E_{ao})$	(2-7)
$f_y = \frac{b}{a}(\sqrt{a^2 - (\varepsilon_{a\max} - \varepsilon_{stress})^2} + f_{ap} + c$	(2-8)
$a^2 = (\varepsilon_{a\max} - \varepsilon_{ap})(\varepsilon_{a\max} - \varepsilon_{ap} + c/E_a)$	(2-9)
$b^2 = E_a(\varepsilon_{a\max} - \varepsilon_{ap})c + c^2$	(2-10)
$c = \frac{(f_{a\max} - f_{ap})^2}{E_a(\varepsilon_{a\max} - \varepsilon_{ap}) - 2(f_{a\max} - f_{ap})}$	(2-11)
$f_y = f_{a\max}$	(2-12)
$f_y = f_{au}\frac{\varepsilon_{ae} - \varepsilon_{stress}}{\varepsilon_{ae} - \varepsilon_{au}}$	(2-13)
$dt_{proposed} = \frac{dxdy\rho_c C_{c\min}}{4K_{\max} + dxH_{\max}}$	(3.1)

$K(\frac{\Delta^2 T}{\Delta x^2}+\frac{\Delta^2 T}{\Delta y^2})=\rho C\frac{\Delta T}{\Delta t}$	(3.2)
$\frac{\Delta}{\Delta x}(K\frac{\Delta T}{\Delta x})+\frac{\Delta}{\Delta y}(K\frac{\Delta T}{\Delta y})=\rho C\frac{\Delta T}{\Delta t}$	(3.3)
$C_c=900+80(\frac{T}{100})-4(\frac{T}{100})^2$ J/kg.K	(3.4)
$K_c=2-0.24(\frac{T}{100})+0.012(\frac{T}{100})^2$ W/m.K	(3.5)
$C_s=470+20(\frac{T}{100})-3.8(\frac{T}{100})^2$ J/kg.K	(3.6)
$K_s=54-3.33(\frac{T}{100})$ W/m.K	(3.7)
$\rho_c C_c = (0.005T + 1.7) * 10^6\ Jm^{-3}\,^oC^{-1}$ For $0 \le T \le 200\ ^oC$	(3.8)
$\rho_c C_c = 2.7 * 10^6\ Jm^{-3}\,^oC^{-1}$ For $200 < T \le 400\ ^oC$	(3.9)
$\rho_c C_c = (0.013\ T - 2.5) * 10^6\ Jm^{-3}\,^oC^{-1}$ For $400 < T \le 500\ ^oC$	(3.10)
$\rho_c C_c = (-0.013\ T + 10.5) * 10^6\ Jm^{-3}\,^oC^{-1}$ For $500 < T \le 600\ ^oC$	(3.11)
$\rho_c C_c = 2.7 * 10^6\ Jm^{-3}\,^oC^{-1}$ For $T > 600\ ^oC$	(3.12)
$K_c = -0.00085T + 1.9\ \ W/mC$ For $0 \le T \le 800\ ^o$	(3.13)
$K_c = 1.22\ \ W/mC$ For $T > 800\ ^oC$	(3.14)
$\rho_s C_s = (0.004T + 3.3) * 10^6\ Jm^{-3}\,^oC^{-1}$ For $0 \le T \le 650\ ^oC$	(3.15)
$\rho_s C_s = (0.068T + 38.3) * 10^6\ Jm^{-3}\,^oC^{-1}$ For $650 < T \le 725\ ^oC$	(3.16)
$\rho_s C_s = (-0.086T + 73.35) * 10^6\ Jm^{-3}\,^oC^{-1}$ For $725 < T \le 800\ ^oC$	(3.17)
$\rho_s C_s = 4.55 * 10^6\ Jm^{-3}\,^oC^{-1}$ For $T > 800\ ^oC$	(3.18)
$K_s = -0.022T + 48\ \ W/mC$ For $0 \le T \le 900\ ^oC$	(3.19)

$K_s = 28.2 \quad W/m \qquad For \quad T > \ 900\ ^oC$	(3.20)
$-K(\frac{T^m_{i,j} - T^m_{i-1,j}}{\Delta x}\Delta y + \frac{T^m_{i,j} - T^m_{i,j-1}}{\Delta y}\Delta x)$ $= -K(\frac{T^m_{i+1,j} - T^m_{i,j}}{\Delta x}\Delta y + \frac{T^m_{i,j+1} - T^m_{i,j}}{\Delta y}\Delta x) + \rho c \Delta x \Delta y \frac{T^{m+1}_{i,j} - T^m_{i,j}}{\Delta t}$	(3.21)
$T^{m+1}_{i,j} = T^m_{i,j} + \frac{\Delta t}{\rho c \Delta x \Delta y}(\frac{K(T^m_{i,j+1} - T^m_{i,j})}{\Delta y^2} + \frac{K(T^m_{i+1,j} - T^m_{i,j})}{\Delta x^2} + \frac{K(T^m_{i-1,j} - T^m_{i,j})}{\Delta x^2}$ $+ \frac{K(T^m_{i,j-1} - T^m_{i,j})}{\Delta y^2})$	(3.22)
$K_{left} = \frac{2k_{i,j}k_{i-1,j}}{k_{i,j} + k_{i-1,j}}$	(3.23)
$K_{right} = \frac{2k_{i,j}k_{i+1,j}}{k_{i,j} + k_{i+1,j}}$	(3.24)
$K_{bottom} = \frac{2k_{i,j}k_{i,j-1}}{k_{i,j} + k_{i,j-1}}$	(3.25)
$K_{top} = \frac{2k_{i,j}k_{i,j+1}}{k_{i,j} + k_{i,j+1}}$	(3.26)
$Q = \sigma \varepsilon_f \varepsilon_c [(T^m_f + 273)^4 - (T^m_{i,j} + 273)^4]$	(3.27)
$\frac{K^m_{i+1,j} + K^m_{i,j}}{2}\frac{(T^m_{i+1,j} - T^m_{i,j})}{dx}\frac{dy}{2} + \frac{K^m_{i,j+1} + K^m_{i,j}}{2}\frac{(T^m_{i,j} - T^m_{i,j+1})}{dy}dx$ $= \frac{K^m_{i-1,j} + K^m_{i,j}}{2}\frac{(T^m_{i,j} - T^m_{i-1,j})}{dx}\frac{dy}{2} + \frac{\rho c(dxdy)}{2}\frac{(T^{m+1}_{i,j} - T^m_{i,j})}{dt} + Q.dx$	(3.28)

$$T_{i,j}^{m+1}=T_{i,j}^{m}+\frac{2dt}{(\rho c dxdy)_{i,j}}\{\frac{K(T_{i,j+1}^{m}-T_{i,j}^{m})}{dy}dx+\frac{K(T_{i+1,j}^{m}-T_{i,j}^{m})}{dx}\frac{dy}{2}$$ $$+\frac{K(T_{i,j}^{m}-T_{i-1,j}^{m})}{dx}\frac{dy}{2}+Q_{i,j}^{m}dx\}$$	(3.29)
$$T_{i,j}^{m+1}=T_{i,j}^{m}+\frac{4dt}{(\rho c dxdy)_{i,j}}\{\frac{K(T_{i,j+1}^{m}-T_{i,j}^{m})}{dy}\frac{dx}{2}+\frac{K(T_{i+1,j}^{m}-T_{i,j}^{m})}{dx}\frac{dy}{2}+(\frac{dx}{2}+\frac{dy}{2})+Q_{i,j}^{m}dx\}$$	(3.30)
$$T_{i,j}^{m+1}=T_{i,j}^{m}+\frac{dt}{(\rho_c c_c dxdy)_{i,j}+\rho_w c_w \Phi}\{\frac{K(T_{i,j+1}^{m}-T_{i,j}^{m})}{dy^2}$$ $$+\frac{K(T_{i+1,j}^{m}-T_{i,j}^{m})}{dx^2}+\frac{K(T_{i-1,j}^{m}-T_{i,j}^{m})}{dx^2}+\frac{K(T_{i,j-1}^{m}-T_{i,j}^{m})}{dy^2}\}$$	(3.31)
$$T_{i,j}^{m+1}=T_{i,j}^{m}+\frac{2dt}{(\rho_c c_c dxdy)_{i,j}+\rho_w c_w \Phi_w}\{\frac{K(T_{i,j+1}^{m}-T_{i,j}^{m})}{dy^2}dx$$ $$+\frac{K(T_{i+1,j}^{m}-T_{i,j}^{m})}{dx}\frac{dy}{2}+\frac{K(T_{i,j}^{m}-T_{i-1,j}^{m})}{dx}\frac{dy}{2}+Q_{i,j}^{m}dx\}$$	(3.32)
$$D_x=\frac{E_x t^3}{12(1-\upsilon_x \upsilon_y)};\qquad D_y=\frac{E_y t^3}{12(1-\upsilon_x \upsilon_y)}$$	(3.33)
$$D_{xy}=\sqrt{D_x D_y}$$	(3.34)
$$D_{xy}=D_y$$	(3.35)
$$Dx\frac{\partial^4 w}{\partial x^4}+2Dxy\frac{\partial^4 w}{\partial x^2 dy^2}+Dy\frac{\partial^4 w}{\partial y^4}=q$$	(3.36)
$$M_x=D_x(\frac{\partial^2 w}{\partial x^2}+\upsilon_y\frac{\partial^2 w}{\partial y^2})$$	(3.37)
$$M_y=D_y(\frac{\partial^2 w}{\partial y^2}+\upsilon_x\frac{\partial^2 w}{\partial x^2})$$	(3.38)
$$\phi_x=\frac{w_{o(i+1)}+w_{o(i-1)}-2w_{o(i)}}{\Delta_x^2}$$	(3.39)

$\phi_y = \frac{w_{o(i+n)} + w_{o(i-n)} - 2w_{o(i)}}{\Delta_y^2}$	(3.40)
$w_o = ASin\frac{\pi.x_m}{a}Sin\frac{\pi.y_k}{b}$	(3.41)
$\frac{d^2(w_o)_{m,k}}{dx^2} = \frac{(w_o)_{m,k+1} + (w_o)_{m-1,k} - 2(w_o)_{m,k}}{\Delta x^2}$	(3.42)
$\frac{d^2(w_o)_{m,k}}{dy^2} = \frac{(w_o)_{m,k+1} + (w_o)_{m,k-1} - 2(w_o)_{m,k}}{\Delta y^2}$	(3.43)
$\varepsilon_{thermal} = -1.8\times10^{-4} + 9\times10^{-6}\times T + 2.3\times10^{-11}T^3$ For 20 °C ≤ T ≤ 700 °C	(3.44)
$\varepsilon_{thermal} = 14\times10^{-3}$ For 700 °C < T≤ 1200 °C	(3.45)
$\varepsilon_{thermal} = -2.4\times10^{-4} + 1.2\times10^{-5}T + 0.4\times10^{-8}T^{-2}$ For 20 °C ≤ T ≤ 750 °C	(3-46)
$\varepsilon_{thermal} = -11\times10^{-3}$ For 750 °C < T ≤ 860 °C	(3-47)
$\varepsilon_{thermal} = -6.2\times10^{-3} + 2\times10^{-5}T$ For 860 °C < T ≤ 1200 °C	(3-48)
$\varepsilon_{bending} = Z.\ d^2y/dx^2$	(3-49)
$\varepsilon_{X\,bending} = Z_{x\,i,j}\times Øx_{m,k}$	(3-50)
$\varepsilon_{Y\,bending} = Z_{y\,i,j}\times Øy_{m,k}$	(3-51)
$\varepsilon_{stress} = \varepsilon_{bending} - \varepsilon_{thermal}$	(3-52)
$p = \int\sigma dA$	(3-53)
$M_x = \int\sigma_x dAZ_x$	(3-54)
$M_y = \int\sigma_y dAZ_y$	(3-55)
$D_x = \frac{M}{d^2w/dx^2}$	(3-56)

$D_y = \dfrac{M}{d^2 w / dy^2}$	(3-57)
$D_x \dfrac{w_{m-2,k} - 4w_{m-1,k} + 6w_{m,k} - 4w_{m+1,k} + w_{m+2,k}}{\Delta x^4} +$ $2D_{xy} \dfrac{4w_{m,k} - 2(w_{m+1,k} + w_{m-1,k} + w_{m,k+1} + w_{m,k-1}) + w_{m+1,k+1} + w_{m+1,k-1} + w_{m-1,k-1} + w_{m-1,k+1}}{\Delta x^2 \Delta y^2} +$ $D_y \dfrac{w_{m,k+2} - 4w_{m,k+1} + 6w_{m,k} - 4w_{m,k-1} + w_{m,k-2}}{\Delta y^4} = q$	(3-58)
$w = 0, \qquad \dfrac{\partial^2 w}{\partial x^2} + \nu \dfrac{\partial^2 w}{\partial y^2} = 0$	(3-59)
$\dfrac{\partial^2 w}{\partial y^2} = 0, \qquad \dfrac{\partial^2 w}{\partial x^2} = 0$	(3-59a)
$w_{II} = w_p$	(3-60)
$\dfrac{\partial^2 w}{\partial x^2} + \nu \dfrac{\partial^2 w}{\partial y^2} = 0, \qquad [\dfrac{\partial^3 w}{\partial x^3} + (2 - \nu) \dfrac{\partial^3 w}{\partial x \partial y^2}] = 0$	(3-61)
$\dfrac{\partial^2 w}{\partial y^2} + \nu \dfrac{\partial^2 w}{\partial x^2} = 0, \qquad [\dfrac{\partial^3 w}{\partial y^3} + (2 - \nu) \dfrac{\partial^3 w}{\partial x^2 \partial y}] = 0$	(3-62)
$(m_x)_{m,k} = -(2 + 2\nu) w_{m,k} + w_{m+1,k} + w_{m-1,k} + \nu(w_{m,k+1} + w_{m,k-1}) = 0$ $w_{m-1,k} = (2 + 2\nu) w_{m,k} - w_{m+1,k} - \nu(w_{m,k+1} + w_{m,k-1})$	(3.63)
$(\vartheta_x)_{m,k} = (6 - 2\nu)(w_{m+1,k} - w_{m-1,k}) + 2(1 - \nu)(w_{m-1,k-1} + w_{m-1,k+1}$ $- w_{m+1,k+1} - w_{m+1,k+1}) - w_{m+2,k} + w_{m-2,k} = 0$	(3.64)
$w_{m-2,k} = -(6 - 2\nu)(w_{m+1,k} - w_{m-1,k}) - 2(1 - \nu)(w_{m-1,k-1}$ $+ w_{m-1,k+1} - w_{m+1,k+1} - w_{m+1,k+1}) + w_{m+2,k}$	(3.65)
$(m_x)_{m,k+1} = -(2 + 2\nu) w_{m,k+1} + w_{m+1,k+1} + w_{m-1,k+1} + \nu(w_{m,k+2} + w_{m,k}) = 0$ $w_{m-1,k+1} = (2 + 2\nu) w_{m,k+1} - w_{m+1,k+1} - \nu(w_{m,k+2} + w_{m,k})$	(3.66)
$(m_x)_{m,k-1} = -(2 + 2\nu) w_{m,k-1} + w_{m+1,k-1} + w_{m-1,k-1} + \nu(w_{m,k-2} + w_{m,k}) = 0$ $w_{m-1,k-1} = (2 + 2\nu) w_{m,k-1} - w_{m+1,k-1} - \nu(w_{m,k-2} + w_{m,k})$	(3.67)

$\alpha^4 D_x(10.48w_{m,k}\,10.8w_{m+1,k}\,2w_{m+2,k} - 4.06w_{m,k+1} + 0.42w_{m,k+2} - 4.06w_{m,k-1}$ $+ 0.42w_{m,k-2}\,2.8w_{m+1,k-1}\,2.8w_{m+1,k+1}) +$ $\alpha^2\,2D_{xy}(-1.8w_{m,k}\,1.2w_{m,k+1}\,1.2_{m,k-1} - 0.3w_{m,k-2} - 0.3w_{m,k+2}) +$ $D_y(w_{m,k+2} - 4w_{m,k+1} + 6w_{m,k} - 4w_{m,k-1} + w_{m,k-2}) = q\Delta x^4\alpha^4$	(3.68)
$D_x \frac{d^4w}{dx^4} + 2D_{xy} \frac{d^4w}{dx^2dy^2} + D_y \frac{d^4w}{dy^4} = q + n_x \frac{d^2w}{dx^2} + n_{xy} \frac{d^2w}{dxdy} + n_y \frac{d^2w}{dy^2}$	(3.69)
$D_x(w_{i-2,j} - 4w_{i-1,j} + 6w_{i,j} - 4w_{i+1,j} + w_{i+2,j})\alpha^4 +$ $2D_{xy}(4w_{i,j} - 2(w_{i+1,j} + w_{i-1,j} + w_{i,j+1} + w_{i,j-1}) + w_{i+1,j+1} + w_{i+1,j-1} + w_{i-1,j-1} + w_{i-1,j+1})\alpha^2 +$ $D_y(w_{i,j+2} - 4w_{i,j+1} + 6w_{i,j} - 4w_{i,j-1} + w_{i,j-2}) -$ $n_x(w_{i+1,j} - 2w_{i,j} + w_{i-1,j})\Delta x^2\alpha^4 - n_y(w_{i,j+1} - 2w_{i,j} + w_{i,j-1})\Delta x^2\alpha^2 = q\Delta x^4\alpha^4$	(3.70)
$\Delta x(i) = \text{Span} - \sum \text{Lx(i)}$	(3.71)
$w_{o(1to45)} = A.\sin\frac{\pi(m-1).\Delta_x}{L_x}\sin\frac{\pi(n-1).\Delta_y}{L_y}$	(3.72)
$p_1 = \sum \sigma \times \Delta A$	(3.73)
$Z = \frac{p_1 \times NA1 - p_2 \times NA2}{p_1 - p_2}$	(3.74)

CHAPTER 1

INTRODUCTION

1.1 General

Fire safety can have a major impact on the overall conception of buildings, i.e. on architectural conception, on the design, on the cost, etc. The objectives of fire safety are a historical concept, and a properly designed building system greatly reduces the hazards to life and limits property loss. The Great Fire of London in 1666 [Malhotra, 1956] was the single most significant event which has shaped legislation of today. The rapid growth of the fire through adjacent buildings also highlighted the need to consider the possible spread of fire between properties when the rebuilding work was done. So the first building construction legislation was therefore requiring buildings to have some form of fire resistance.

The research on fire safety design started as far back as 1928 of [Inberg, 1928]. Building Control took on the greater role of Health and Safety through the first Public Health Act in 1875. This Act had two major revisions in 1936 and 1961, leading to the first set of national building standards, The Building Regulations 1965.

The Building Regulations apply to building work (i.e. in the UK) and set standards for the design and construction of buildings to ensure the safety and health for people in or about those buildings. UK Building Regulations 2000 [BR2000] specifies the specific requirements for each category of structural element in a building in terms of resistance to collapse. The minimum period of fire resistance for the elements of most structures is 30 minutes. Part B of UK Building Regulation 2006 [BR2006] covers all

fire precautionary measures that are necessary to provide safety from fire that will safeguard building occupants, persons in the vicinity of buildings, and fire fighters. Requirements and guidance cover means of escape in case of fire, fire detection and warning systems, fire resistance of structural elements, fire separation, protection, compartmentation and isolation to prevent fire spread and conflagration, control of flammable materials, and access and facilities for fire fighting.

Today the concept of fire safety design has been improved significantly and become more rational. The fire safety objectives in the present European Fire Codes are explicitly based on the life safety objective [CEC, 1990a], then to confine the fire within the compartment in which it started. From a life safety point of view, the designer must ensure that collapse of primary structural members will not occur before the occupants of the building have had a reasonable chance to reach an area of safety.

A more general objective of structural fire protection in a building is given by Malhotra, 1982, in that it is to maintain the integrity of safe areas, to restrict the size of fire and to prevent the building structure from becoming unstable.

The ability of a structure to resist collapse (in fire) depends primarily on the behaviour of its elements at elevated temperatures. The behaviour of structures exposed to fire is usually described in terms of the concept of fire resistance, which is the period of time under exposure to a standard fire time-temperature curve.The level of fire resistance required for different elements of a structure has traditionally been governed by codes based on the occupancy, height and area of a building. The codes normally require that load bearing elements and assemblies (walls and columns) have a fire resistance rating

at least equivalent to that required for the supported assembly (floor or roof), to represent the minimum levels of fire safety deemed acceptable to society. Such requirements, which are specified in terms of fire resistance ratings for different elements and assemblies, can be traced at least as far back as the publication in the USA of the first edition of the Uniform Building Code in 1927.

Structural design for fire safety is one aspect of performance based fire safety analysis and design of buildings. Over the past decade, there has been considerable interest in performance-based structural design for fire, particularly internationally.

Fire resistance requirements are fixed by National Codes in terms of the time an isolated element should resist the action of a Standard Fire as defined by the heat exposure given by ISO834. Fire resistance times of 15, 30, 60, 90, 180, and 240 minutes are specified depending upon the number of storeys; these times can also be a function of the occupancy of the building and of the fire load. For a member to fulfil a given fire resistance requirement, it is necessary to ensure that the temperature developed in the member at the required fire resistance time (taking into account its Section Factor and any insulation which may be applied) is less than the critical temperature necessary to cause failure which is also known as the "critical temperature".

The temperature-time curve was conceived as a basis for legislation and regulation in 1906. National standards for fire tests were adopted first in the USA in 1917 and subsequently in the UK and Europe. The fire resistance time is the time, in the standard ISO834 fire test, taken by the member to reach the critical temperature. This time

varies according to the section size. The thicker the floor the slower is the heating rate and therefore the greater is the fire resistance time. In a building in which a natural fire occurs the heating rate is also influenced by the member location.

The solution then requires predicting the behaviour of structural elements exposed to fire. The importance of predicting behaviour of structural elements exposed to fire, as part of the general safety of buildings, is normally based on standard fire tests [Newman G M, 1989]. However, it is now possible to predict the behaviour of a structure during a fire by numerical analysis method. The most common forms of analysis are finite element method and finite difference method. The structure under consideration is divided into many small elements, the response of each of which can easily be determined. By determining the response of the individual elements and knowing the interaction between these elements, the overall behaviour of the structure can be predicted.

1.2 Fire development

To understand the behaviour of a structure in case of fire requires determining fire development in the compartment, the temperatures in the structural elements and finally, the mechanical behaviour.

In a real fire, the speed of the increase of temperatures depends principally upon the combustible material and the level of ventilation. The temperature-time curves in a fire compartment designate the characteristics and intensity of fire developing process. A typical temperature development in the compartment is shown in Fig. 1.1, which includes three phases: fire growth, full development and decay.

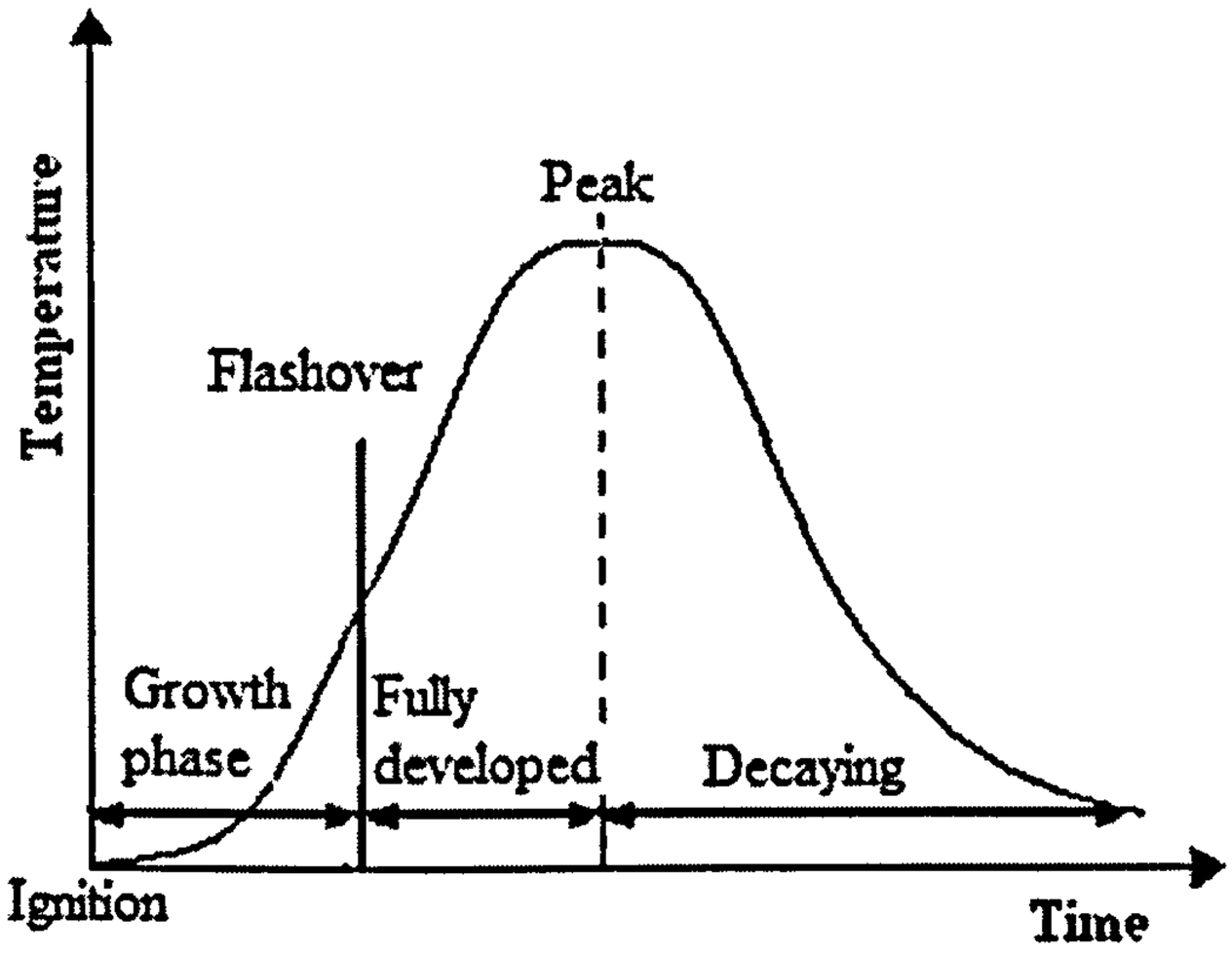

Fig. 1-1 Temperature-time curve for a typical fire

In the fire growth phase, ignition is the first event in the fire process followed by slow growth of fire. The period is important for evacuation and fire fighting. Usually, it is not of significant influence on the structure. After flashover, the second event in the fire process, the fire enters into the fully developed phase, in which the temperature of the compartment increases rapidly and the overall compartment is engulfed in fire. The highest temperature, peak event, highest rate of heating and largest flame occur during this phase, which gives rise to the most structural damage and much of the fire spread in buildings. In the decaying period, the temperature decreases gradually.

1.3 Equivalent Fire Severity

Due to the large variety of possible temperature-time curves in buildings, the assessment would be very expensive if the building elements were tested for each particular fire curve. Therefore, a standard curve is necessary to enable comparisons to be made.

According to this principle, Inberge [Inberge, 1928] obtained the first quantified relationship of equivalent fire exposure and fire load to have equivalent severity if the areas under each curve are equal, by burning office furniture and papers in a room and measuring the temperature attained. Nevertheless a lot of fire tests are submitted to standard fire curves. The most notable difference between these curves and the curve for a real fire is that the first has no phase representing the decay of temperatures after the fire load has been burnt out. They are represented in Fig. 1-2. The concept is that the effect of a real fire on a structure is equivalent to the effect of a standard fire for the duration of the equivalent time on the same structure [Franssen, 2003].

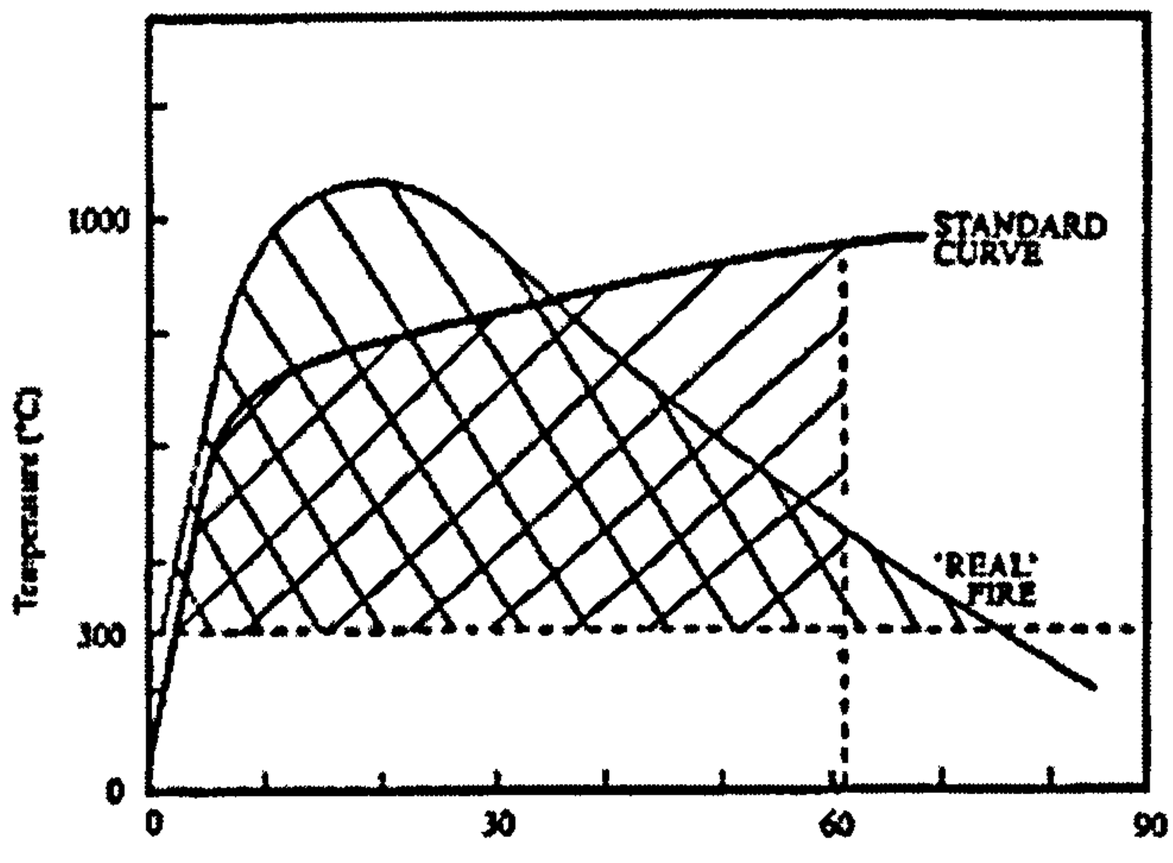

Fig. 1-2 Equivalent fire severity on equal area basis [Franssen, 2003]

The basic idea of the equivalent area hypothesis is that the area of the temperature time curve under standard fire above a certain baseline corresponding to equivalent fire exposure should be equal to that under the real fire.

1.4 Development of Numerical Methods

It thus becomes a necessity for engineers in performance based fire engineering design and also to have tools to perform this design. The behaviour of a structure in fire may be established experimentally. The experiments are performed in specially designed furnaces in which the temperature of the surrounding air changes with time according to a prescribed law. Due to reasons of economy the furnaces are often small, so that the majority of experiments have to be limited to testing of single structural elements of small size. Such a method is time consuming and the scatter of results can be wide, so that only if the number of specimens is sufficiently large, the results are statistically reliable, which makes the experiment expensive.

To overcome these drawbacks, a considerable amount of research has been directed towards the development of numerical methods which enable the behaviour of a structure to be predicted by much less expensive computer programs. Several researchers have devised models and methods in order to simulate the behaviour of structures under a fire environment. An example of the simulations is the problem of the decision whether it is more advisable to demolish and rebuild than to repair the building which has sustained a fire [Cioni et al., 2001]. A number of numerical methods of the fire resistance of reinforced concrete structures have been reviewed in Chapter 2.

The numerical analysis of the behaviour of a structure in fire requires the determination of the interaction between fire and structure. This interaction can be divided into three steps. In the first step, calculate the change of the fire temperature with time (the fire scenario) is calculated. In the second step, the change of

temperatures with time in the structure is calculated as the result of the time and space dependent heat transfer from fire into the structure. This requires a thermal analysis of the structure in which the heat conduction problem is solved. The effects of the heat radiation and the heat convection from fire to the structure surface are accounted for via the boundary conditions. The final step consists of the determination of the temperature dependent mechanical response of the structure.

1.5 Fire Resistance Analysis

Fire resistance analysis of reinforced concrete structures is important part in the design for understanding the thermo-mechanical behaviour of a structure during fire. In fire design, the ability of a structure for the exposure to heating is calculated according to the standard temperature-time curve for a specified combination and for a stated period of time [Eurocode 1 –EN1991-1-2]. The two important points of a fire design are that required period of time is based on the expertise of fire safety regulators and that the fire heating is represented by a standard temperature-time curve or natural fire curve. The Eurocodes allow the structures to be calculated either under the ISO standard fire curve or under a natural fire curve.

The ISO curve and ASTM curve are the most widely used standard fire curves for the purpose of experimental testing of elements. These curves are a very poor representation of reality. They are completely independent of conditions that will govern a real fire. For example, the same curve is used in a large industrial hall or in a small room. But for a number of years the concept of time equivalence has been used to assess natural fire severity in terms of an equivalent period of exposure to a standard heating curve. The concept relates the maximum temperature achieved by a structural

member in a natural fire to the time taken for the same member to reach the same temperature in a standard fire test. This concept has been extensively validated and provides an indication of performance relative to a fire resistance period widely understood by designers and checking authorities. The concept of equivalent fire exposure is a bridge between the realistic fire curve and the standard fire curve.

The fundamental step in designing structures for fire safety is to verify that the fire resistance of the structure (or each part of the structure) is greater than the severity of the fire to which the structure is exposed. This verification requires that the following design equation be satisfied:

$$\text{Fire resistance} \geq \text{Fire severity}$$

where fire resistance is a measure of the ability of the structure to resist collapse, fire spread or other failure during exposure to a fire of specified severity, and fire severity is a measure of the destructive impact of a fire, or a measure of the forces or temperatures which could cause collapse or other failure as a result of the fire [Buchanan, 2001].

1.6 Composite Construction

To satisfy the demand from industry for long-span solutions, which could accommodate a high degree of mechanical services and provide minimum depth solutions, research led to the innovation of composite construction; incorporating composite slab using steel decking, composite beams, composite columns and slim floor construction. Composite construction has been much more common in buildings in North America than in the UK [SCI, 2006]. However, as designers became aware of the benefits of composite construction, this form of construction has extended to UK

multi-storey commercial buildings. To develop and validate this new system, a comprehensive series of ultimate load and fire tests were undertaken in the UK and Europe.

These materials can be used in mixed structural systems where members consisting of steel and concrete act together compositely. These essentially different materials are completely compatible and complementary to each other; they have an ideal combination of strengths with the concrete efficient in compression and the steel in tension; concrete also gives thermal insulation to the steel at elevated temperatures.

It should be added that the combination of concrete cores, steel frame and composite floor construction has become the standard construction method for multi-storey commercial buildings in several countries. Much progress has been made, for example in Japan, where the structural steel/reinforced concrete frame is the standard system for tall buildings. The main reason for this preference is that the sections and members are best suited to resist repeated earthquake loadings, which require a high amount of resistance and ductility.

Building with composite elements experienced a renaissance during the 1980's, resulting in a profusion of new construction concepts and structural details [Johnson, 1985]. Single composite elements, such as isolated beams, columns and slabs are shown in Fig. 1-3.

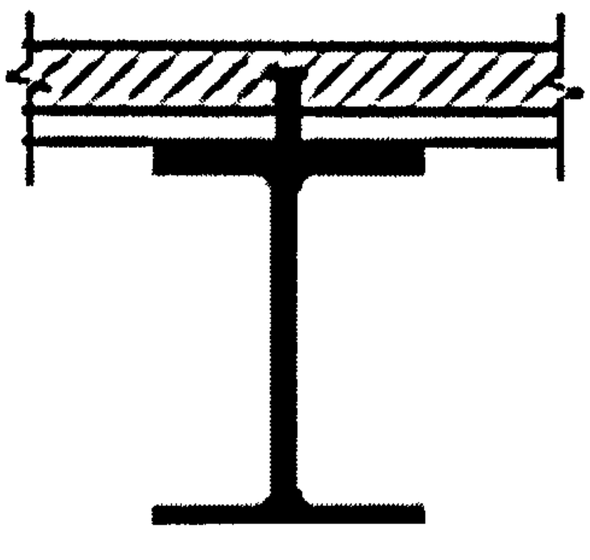

Composite Girder

Composite Floor

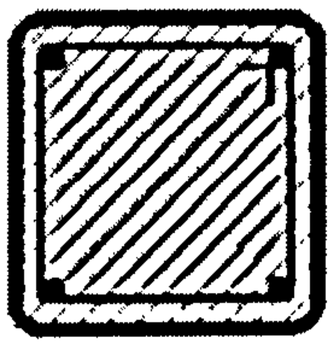

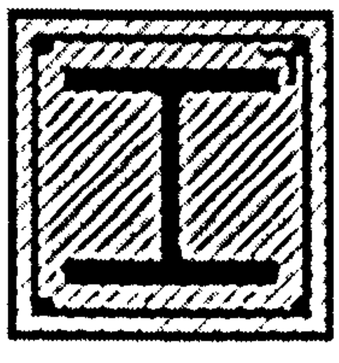

Composite Column

Fig. 1-3 Composite Elements

Attention is drawn to the effect of this form of construction on other more general problems such as fire resistance rating, speed of construction, flexibility and final fitting out.

The use of composite elements has certain advantages. In particular, a composite beam has greater stiffness and usually a higher load resistance than its non-composite counterpart [Lawson, 1989]. Consequently, a smaller steel section is usually required. The result is a saving of material and depth of construction.

Composite construction, particularly that using profiled steel sheeting, allows rapid construction. Also the weight of steelwork required in composite construction is significantly less than if the materials were used independently. There is no need for expensive false work and formwork because the steel beam is able to sustain the self weight of steel and concrete, by itself or with the assistance of a few temporary props. Formwork can be replaced by profiled steel sheeting.

The use of composite steel/concrete components in buildings is becoming increasingly important in fire resistant design because they offer several choices for influencing the rise in temperature of the steel [Eurocode 4, Part 1.1]. The two complementary materials, structural steel and reinforced concrete are shown how composite action is achieved in the case of composite, beams, columns and slabs.

1.6.1 Composite beams

Composite beam is one of the most common structural systems which have been widely used for long span floors. Composite beams are described in terms of the steel section, concrete slab and connectors used in a typical building floor. The structural behaviour of a typical composite beam is described by reference to the strain and stress in each component part. The slab usually spans between parallel steel sections and its design is normally dictated by this transverse action. Consequently the span, depth and concrete grade are determined separately and are known prior to the beam design.

Composite beams, subject mainly to bending, consist of a steel section acting compositely with reinforced concrete. The two materials are interconnected by means of mechanical shear connectors. Fig. 1-4 shows typical composite beam cross-sections.

Composite beams, even with small steel sections, have high stiffness and can carry heavy loads on long spans [Lawson, 1989]. Unpropped composite beams need the steel section to be strong and stiff enough to carry the weight of wet concrete. Simply supported composite beams, subject to sagging moments, fail by yielding of the steel section, crushing of the concrete slab or shear of the connectors.

Continuous composite beams need to be designed to resist both sagging and hogging bending. The slab reinforcement carries the tensile strain in the hogging region. The steel section must also be checked for possible buckling.

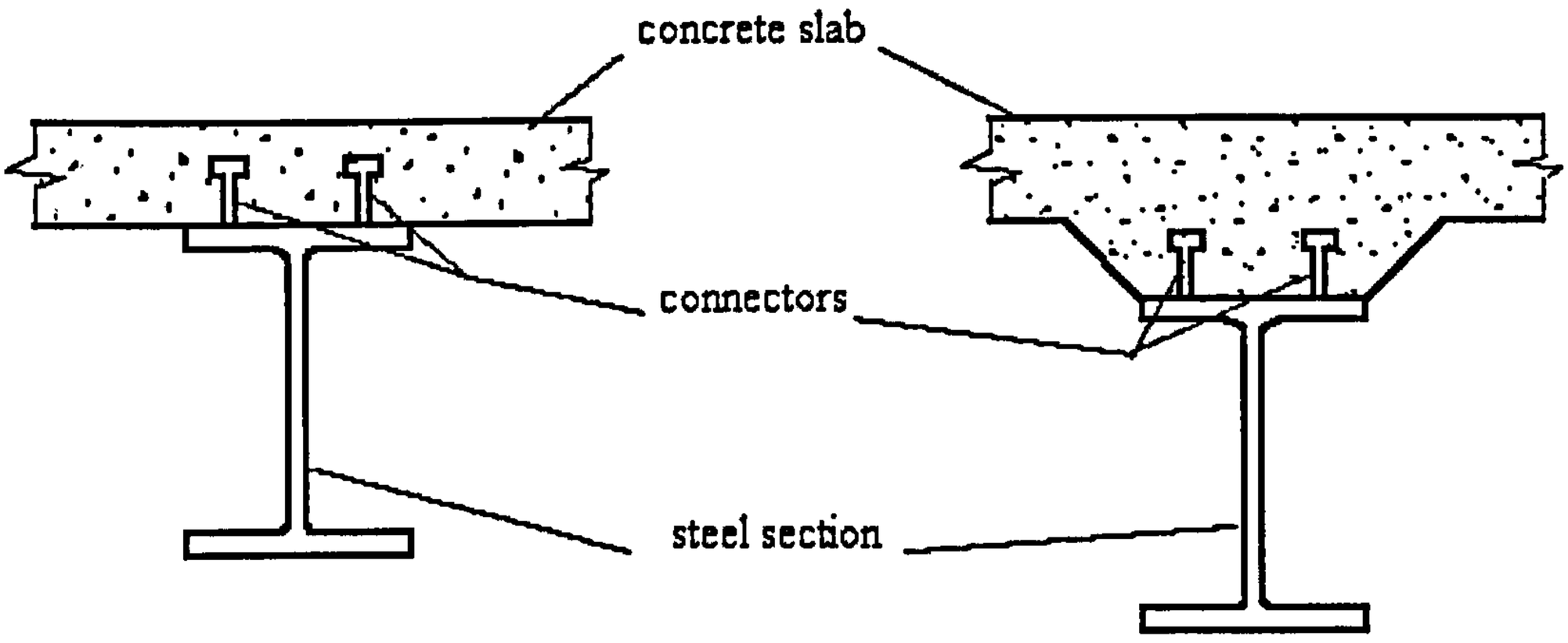

Fig.1-4 Typical composite beam cross-sections

For non-composite construction, the steel sections alone are designed to carry the load acting on the floor plus the self weight of the slab. The steel section is symmetric about its mid depth and has a neutral axis at this point. The section strains around this neutral axis and both the outer faces tensile and compressive stresses are identical. The

concrete slab is not connected to the steel section and therefore behaves independently and has its own neutral axis. The bottom surface of the concrete slab is free to slide over the top flange of the steel section and considerable slip occurs between the two.

For composite construction, the concrete slab is connected to the steel section; both act together in carrying the load as the connections resist the slip between the slab and steel section. The composite section has a single neutral axis often close to the top flange of the steel section and is non-symmetric. The tensile and compressive stresses at the outer faces are therefore dependent upon the overall moment of inertia (I) of the composite section and their distance from the single neutral axis. Fig. 1-5 shows the difference between composite and non-composite construction, for a similar load, the extreme stresses generated in the first are much smaller than generated in the second because of (I) value of the composite section is normally several times that of the steel section. This difference also has an effect on the stiffness of the beams [Eurocode 4, Part 1-1]. However the span of the beam often dictates how much of the slab may be assumed to help in the longitudinal bending action.

The connection between the slab and steel section may be made in many ways. In general it is using discrete mechanical keys. The most common form of connector is the headed stud.

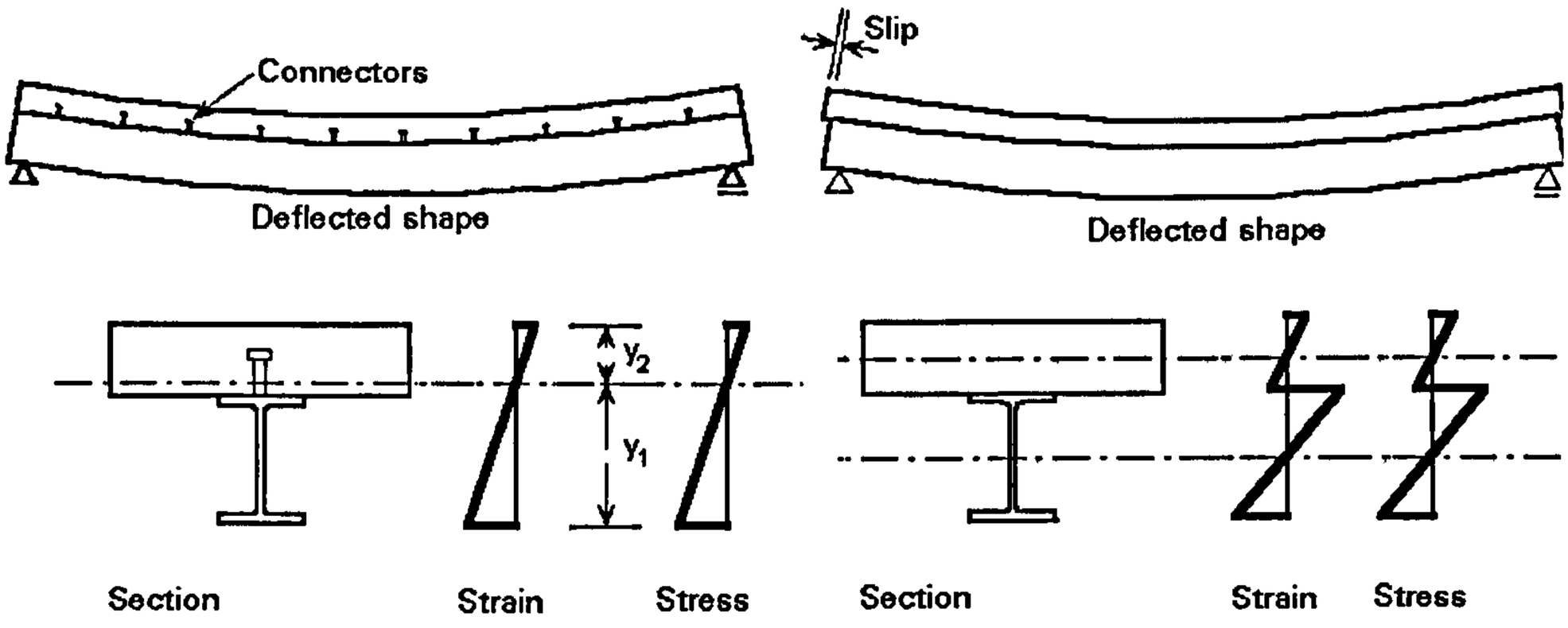

Composite Beam Non- Composite Beam

Fig. 1-5 The difference between composite and non-composite beam for a similar load

The fire resistance of composite beams may be calculated using the method described in Eurocode 4 Part1-2 [Eurocode 4 1994 Part1-2] or may be presented as a specified deflection against time using numerical analysis. The behaviour under fire conditions depends on both the thermal and structural responses. Variation in temperatures within the cross-section of composite beams supporting a concrete slab can occur when the difference in exposure to heat its parts, as the temperature of the bottom flange and the web is often much greater than that of the top flange.

In the UK, the fire performance of composite members and protection materials are typically specified up to a 2.0% maximum strain level according to BS5950 Part 8 [BSI5950] and a deflection limit of span/20 is commonly used in structural fire design practice.

1.6.2 Composite columns

In the 1960s, intensive research commenced on the assessment of resistance of columns, in which the steel cross-section acts together with the surrounding concrete. These columns could not be designed at that time by the rules for steelwork or by those for concrete structures. The result of this research work was described in various publications. Further research works have been used in [Eurocode 4, Part 1.1], which deals with composite construction in buildings. Composite columns can be either partly or totally encased open sections, or alternatively, they may be concrete filled tubes as shown in Fig. 1-6 which illustrated in [Eurocode 4, Part 1.1]. All cross-sections are symmetrical about both axes and in addition can be reinforced.

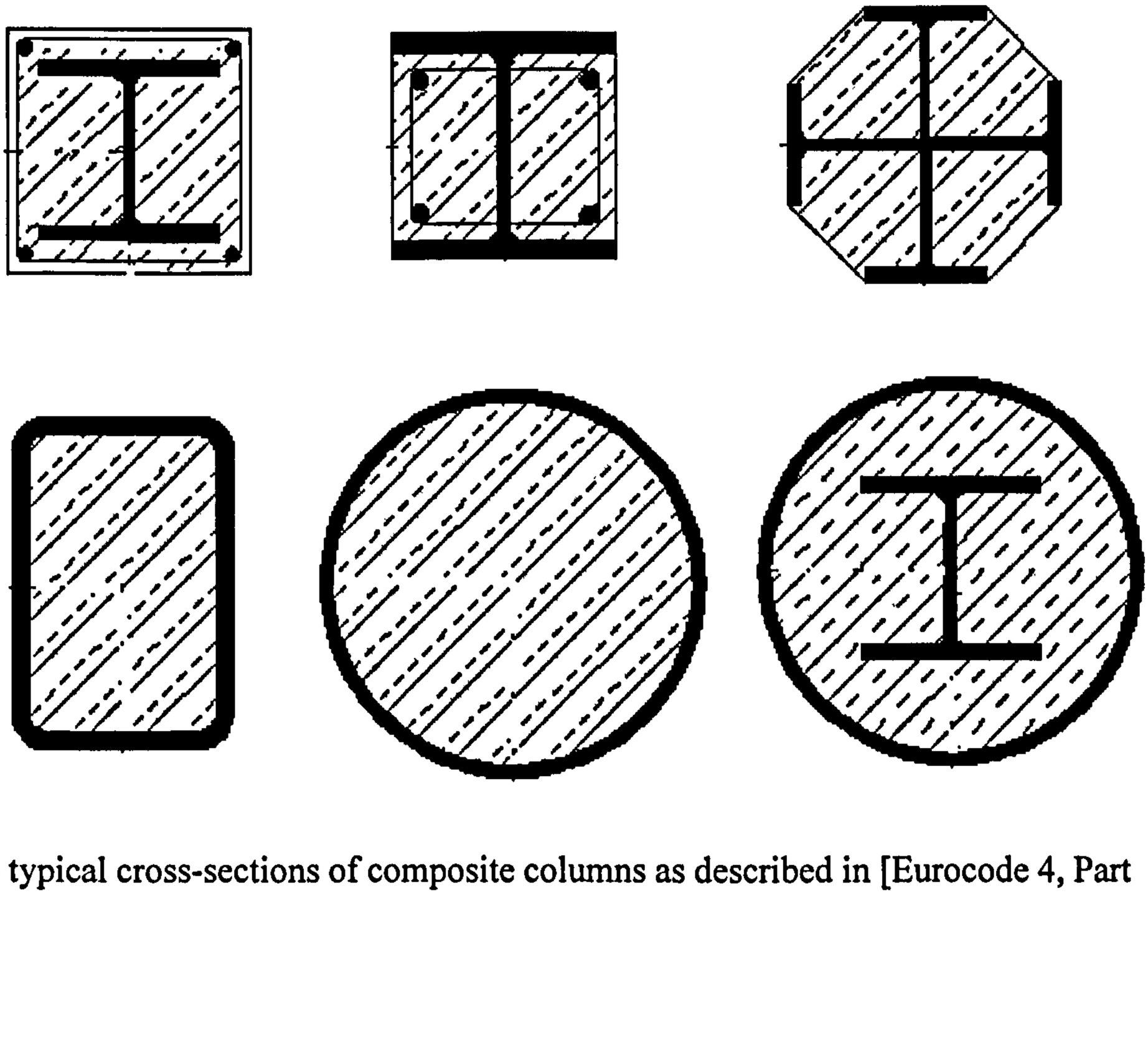

Fig. 1-6 typical cross-sections of composite columns as described in [Eurocode 4, Part 1.1]

Eurocode 4 gives limiting ratios for exposed steel parts of composite columns to ensure that local buckling does not occur [Eurocode 4, Part 1.1]. Additional to that, this code gives simplified rules for calculating the resistance of a composite column to axial load.

There are many advantages associated with the use of composite columns: small cross-sections, for example, can be designed to withstand high loads; similarly, sections with different resistances, but identical external dimensions, can be produced by varying steel thickness, concrete strength and additional reinforcement. Thus the outer dimension of a column can be held constant over a number of floors in a building, simplifying architectural detailing. Economic efficiency also results from the use of concrete - a low cost material - and from the time saved by using the highly developed connection techniques of steelwork construction.

Virdi and Dowling presented a new design method for composite columns [Virdi and Dowling, 1976]. This method unifies the design of concrete filled circular tubular section, under concentric loading with that of other types of concentrically loaded composite columns, such as encased sections and rectangular filled tubes.

For fire protection, higher percentages of reinforcement can be provided, but may not be taken into account in the design, according to Eurocode 4 [Eurocode 4, Part 1.1]. Lie [Lie, 1994] outlines the mathematical model used to calculate the fire resistance of circular concrete filled steel columns without testing. Also Franssen outlined a review of simplified calculation methods applicable to steel columns and underline some

characteristics of their behaviour in frames under fire conditions. In addition, they illustrate the analysis of the fire resistance of a real structure [Franssen et al, 1992].

Sebastjan, Bojan, Miran and Igor presented a finite element formulation for the thermo-mechanical, transient, and non-linear analysis of reinforced concrete columns in fire [Sebastjan et al., 2004]. They determined the temperature distributions over the cross-sections of the column in fire as a function of time. They compared their numerical results for the resistance time with the calculations based on Eurocode 2, 2002.

1.6.3 Composite Floors

The use of the solid reinforced concrete slab is being replaced more and more by metal decking. Orthotropic metal-decked composite slabs have been widely used in recent decades. Due to this large increase in the use of composite floor systems in buildings, it is necessary to give a light on some important issues of using composite floor and to understand their behaviour in case of fire. Profiled steel sheeting acts as permanent formwork during concreting. The principal components of a composite floor system are shown in Fig. 1-7. It consists of:

-Steel I Beam

-Profiled steel decking

-Concrete topping

-Shear studs

-Reinforcement

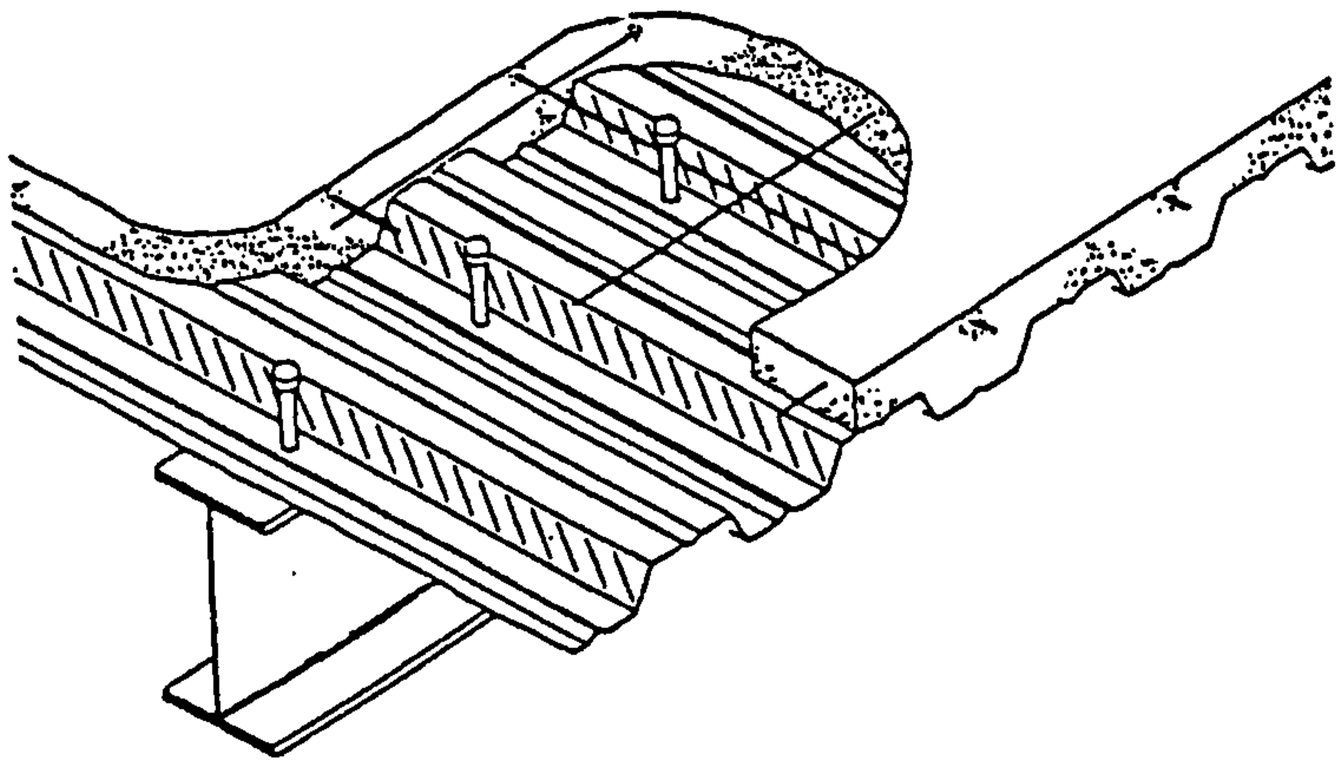

Fig.1-7 Basic components of the composite floor system [Newman G M, 1989]

The profiled steel sheet and concrete topping are interconnected in such a manner that horizontal shear forces can be resisted at the steel-concrete interface. Slip at the interface must be prevented completely or partly, as should vertical separation of the steel decking from the concrete topping.

The overall depth is usually 100 to 150 mm. The height of the steel sheet varies between 45 and 80 mm with a thickness between 0.7 and 1.5 mm. It acts as permanent formwork and as reinforcement to the concrete as well as preventing evaporation of water content on the fire exposed surface and prevents spalling. The steel sheet, also, plays an important part in improving integrity (the ability of the floor to resist penetration of flames through the formation of cracks and openings) and insulation aspects fire resistance; it acts as a diaphragm preventing the passage of flame and hot gases, as a shield reducing the flow of heat into the concrete [Newman G M, 1991]. Normally, the concrete is reinforced with a light anti-crack mesh, and may also contain additional bars, usually placed within the ribs. The reinforcement, in many instances a

standard reinforcing mesh, is either A142 (142mm^2/m reinforcement) or A193 (193mm^2/m reinforcement).

Rapid construction minimises costs. The use of the decking as a safe working platform during construction speeds up the work of other trades. The minimal steel reinforcement required can be fixed quickly and large areas of floor poured using pumped concrete. By shortening the construction programme, the impacts on the public within the construction site zone, such as noise, dust and traffic congestion are minimised. Due to the intrinsic efficiency of composite construction and the displacement of concrete by the profile shape, considerably less concrete is used than in conventional reinforced concrete construction [Corus, 2006].

Composite flooring systems are structurally efficient, thereby minimising the resources used in constructing and reducing the waste generated when it is necessary to deconstruct it. Less resources means fewer site deliveries and less localised traffic congestion. Composite floor systems are stiffer, stronger and lighter than many other floor systems. This means that the weight and size of the primary structure and the foundations can often be reduced; again minimising resource consumption and end-of-life waste generation. Steel can be recycled without degradation in terms of its properties or performance. The recovery rate of steel construction products from UK demolition sites is more than 90% [Ley et al., 2002]. Using resources carefully through design, has positive environmental benefits and low cost.

Composite flooring has several health and safety benefits, both in the factory during production and on site during construction. Decking is manufactured under factory

conditions that provide a much safer and less hostile working environment than the construction site. Steel decking provides a safe working platform for workers on that floor and protects workers below from falling objects. Steel decking can be efficiently stacked in bundles, minimising site storage and easing access and movement around the construction site.

Composite floor systems offer good fire resistance because the deck plays an important part in maintaining integrity and insulation. Several fire tests performed in the UK have shown that the composite floor can achieve 30 minutes fire resistance without any additional fire protective measures. Actual fires in steel buildings in England, Broadgate and Churchill Plaza, and full scale fire tests have shown that the unprotected composite slabs do not collapse during a severe fire [Bailey et al., 1999].

1.7 Summary

Given the importance of performance of composite floors in the behaviour of the entire structural frame, as highlighted in Section 1.6.3 above, it will be shown in the next Chapter that research on composite floors has focused on either fire tests or on numerical analysis based on finite element method. Recognizing the complications involved in modelling the behaviour of composite floors using the finite element method, a need was perceived to develop an alternative method, based on the finite difference approach, which would be simpler to use but would provide sufficiently accurate results.

1.8 Objectives of the Present Study

The objectives of the present research are:

- To develop a numerical method based on the finite difference approach to analyse the thermal and mechanical behaviour of composite floor exposed to fire.
- To investigate fire resistance of the composite floor by developing a user friendly computer program for simple and rapid determination based on the above mentioned numerical method.
- To verify the developed numerical method and the associated computer program by using experimental and calculation data published in literature.
- To investigate the effects of in-plane force and boundary conditions for the composite floors subjected to fire.
- To demonstrate the applications of the numerical method in developing design aid.

1.9 Scope of work

A review of literature is given in Chapter 2. It includes technical methods for analyzing, computer programs available, material properties, and fire tests on composite floors.

Chapter 3 describes a new technique for analyzing composite floors subjected to non-uniform temperature distribution across the depth of the cross-section. The floor is

divided into a two-dimensional mesh, the plate rigidities are calculated taking into account the effect of temperature on the internal stress. There are substituted in the governing differential equations alongside the finite difference formulae for each point of the mesh. The resulting simultaneous algebraic equations are then solved to determine deflections.

Chapter 4 deals with comparison between the numerical method developed in this investigation and the experimental results carried out by other researchers on composite floor exposed to fire to verify the capability of the method for predicting fire temperature, strength, deflection and deformation.

In Chapter 5 the analytical method proposed in this thesis is illustrated through examples, the effect of in-plane forces on the composite floor subjected to elevated temperature using the computer program developed. In order to show the capability of the developed method, parametric studies on various edge and in-plane forces under fire conditions are presented.

The discussion of results, conclusions and recommendations for future studies are included in Chapter 6.

CHAPTER 2

LITERATURE REVIEW

2.1 Introduction

The literature review has been organised in the sections covering development of fire, experimental investigations, and analytical and numerical modelling.

2.2 Development of Fire

The establishment of the British Fire Protection Committee (BFPC) at the end of 19th century marks the beginning of a scientific approach to research into structural fire resistance [Malhotra, 1956]. In 1932 the publication of a standard (BS476) defined tests for fire resistance.

In Japan, Kawagoe [Kawagoe, 1958] first proposed that one might be able to estimate the outcome of a fire scenario. He found that the rate of mass loss and the rate of heat released by the fire were proportional to the ventilation factor of the compartment vertical opening.

Kawagoe and Sekine [Kawagoe et al., 1963], have computed temperature-time curve by integrating the energy balance of compartment fires with the time. Due to the lengthy computation needed at that time, Lie [Lie, 1974] has proposed a parametric expression fitted to Kawagoe's computed temperature-time curves. The parametric

method is easier to apply (as it has no iterative process) and is expected to lead an equivalent quality of the results.

There are different ways of determining the fire resistance rating of structural members and assemblies (columns, beams and floors). Since the early 1920's, the most common method is the furnace test using gas as the fuel. The temperature history in the furnace is controlled by a designated fire curve, typically those of "standard fires". Usually, furnaces are equipped with devices to measure temperatures, and deformations, and to load specimens. Fire tests in furnaces are carried out by exposing certain surfaces of a test specimen to heating in a manner that simulates its exposure to heating in a fire [Abrams and Gustaferro 1968]; [Wade 1992]. A specimen is considered fire resistant during a test up until the point it does not satisfy certain testing criteria with respect to stability, integrity, and thermal insulation. The greatest disadvantage of this conventional design approach is that designers must conform to every essential detail of the tested assemblies for the fire resistance ratings to be applicable in actual construction. A modification in the design requires testing of a new specimen or a detailed engineering evaluation to show that the proposed modification will not be detrimental to the fire resistance rating of the assembly. This situation has severely restricted structural design innovation by enticing the design professional to specify already-tested designs instead of engineering new systems [Gosselin, 1987].

In the late 1960's, empirical equations presenting correlations of fire resistance test results with important design parameters of steel and concrete became available [SNBCC, 1985]. Some of these equations were developed on the basis of theoretical predictions, which were themselves validated by test results. A narrow database limits

the usefulness of the empirical equation, as only a limited range of design parameter values become available to the designer. The numbers of test results used in the establishment of the empirical relationship are also considered, to evaluate the confidence level one can place on the predicted results. Also, care is taken to ensure that the proposed construction materials are similar to the ones tested in all important aspects, such as resistance to cracking or spalling and thermal conductivity.

Full-scale fire tests are performed on structural systems. These tests give a more realistic representation of fire performance because they simulate the performance of a system as opposed to the study of discrete elements or small-scale assemblies. The major drawback of full-scale testing is that it is extremely expensive in comparison with furnace testing. The full-scale testing took place in 1995 in Cardington, UK. A series of fire tests were carried out on an eight-storey, steel-concrete composite structure. As an outcome of the Cardington tests, numerous numerical and theoretical models have been developed to simulate the performance of the structure.

Lie [Lie 1992] defined Standard fire test time-temperature curves for various countries which are idealized simulations of room fires. The heat load imposed on a test specimen is calculable at any point during testing. The most widely used standard test conditions are the ASTM E119 (United States and Canada) and ISO 834 (Australia, New Zealand, and England) [Buchanan 2001]. A simplified equation that approximates the ASTM E119 curve is given by [Lie 1992]:

$$T_f = T_o + 750\left[1 - e^{-3.79553\sqrt{t_h}}\right] + 170.41\sqrt{t_h} \qquad (2\text{-}1)$$

Temperature values for the ISO 834 fire follow this equation:

$$T_f = T_o + 345\log_{10}(8t + 1) \qquad (2\text{-}2)$$

Where:

T_o: Initial temperature in °C

t : time in minutes

t_h : is the time after the start of the fire in hours

Other national standards include British Standard BS 476 Parts 20-23 [BS 1987], Canadian Standard CAN/ULC-S101-M89 [ULC, 1989] and Australian Standard AS 1530 Part 4 [SAA, 1990]. All other international fire resistance test standards specify similar time-temperature curves [Lie, 1995].

In recent years, considerable research has been undertaken with a view to developing analytical methods for calculating the fire resistance of structural elements and assemblies which rely on structural mechanics and heat transfer principles to assess structural response under fire conditions. Procedures are being validated against fire resistance test results for columns, beams and floor slabs. These represent the newest design approach and open the way to an entire field of design possibilities. Thus, the complete problem of designing for fire resistance can be broken down into three components:

- prediction of fire severity,
- determination of the heat transmission from fire to the structural elements,
- calculation of the strength and deformation of structural elements.

The events following the attack on the World Trade Center showed that it is essential to have the best possible understanding of how structures will behave in the event of a fire. This requires:

- A detailed understanding of the fire conditions
- The interactions between the fire and the structural elements
- The sequence of the time for evacuation processes.

Different methods and tools have been developed to study each of these aspects. Structural and fire behaviour depend on each other. It is important to understand the relationship between fire and structural elements. Material properties will change and it is accepted that all parameters describing the material strength will deteriorate. The geometrical features of structures are also affected by fire since materials expand with temperature and the constraints inherent to the geometry of the structure result in significant generation and redistribution of stresses.

The coupling of structure and fire could be examined by testing each individual element against a standard fire curve and obtaining the failure time of the structural element. The test could be substituted by calculations that use as input the standard fire ISO-834 [ISO834], "parametric curves" [Petterson et al., 1976], or the output of the calculations performed from the design fires. Time equivalences between the standard tests, the "parametric curves" and "computed fires" can be established [Law M]. A parametric temperature–time curve for structural fire design purposes is developed for small and medium compartment fires [Zhongcheng et al., 2000] based on fire load and compartment properties. The parametric curves are proposed in the Eurocode 1

[Eurocode 1-ENV 1991-1-2] published in 1993 dealing with the action on structures exposed to fire. [Ma and Makelainen 2000], [Barnett 2002] proposed two other methods for obtaining parametric temperature-time curves. In these methods the shape of the curves is closer to the temperature-time curve measured during full-scale fire tests.

Fire safety engineers have in their hands a large number of reliable and sophisticated design tools. These tools can still be improved but currently are in many cases appropriate for design purposes. Modern structural design for fire is making more and more use of these tools. The advantage of this approach is that it introduces more physical analysis to the design process and allows a more adequate quantification of performance and uncertainty. The evolution of design, and of the tools used in the process, is geared towards an increase in integration and efficiency and a constant reduction in uncertainty and error.

2.3 Experimental Investigations

However, to accurately predict the fire resistance of a composite structure, it is important to understand the behaviour of each element in case of fire. The understanding in this field of research and development has increased significantly in the last two decades in particular. The measurement or assessment of fire resistance has traditionally been done by subjecting a representative specimen to a standard fire test. Although this technique has provided regulatory authorities with a useful classification scheme and has improved our understanding of the fire performance of various structural systems, its cost has been a major deterrent to design innovation. In recent years, theoretical calculation procedures and numerical analysis have been

developed and used in research and consultancy to engineer fire resistance which offer an economical alternative to testing.

There have been a number of natural fire tests and real building fires in a number of countries. Complementary analytical and experimental research projects have investigated the behaviour of natural fires and helped to improve knowledge of material, component and behaviour of structure at elevated temperatures. This was shown throughout the 1980s and 1990s, when the investigation of the fire event developed in a large scale building fire test in (1981, American Iron and Steel Institute), a partly completed 14-story office block on the Broadgate development in (1990, London), fire tests in William Street (1992, Australia), full-scale fire tests on an 8-storey composite steel-framed building in Cardington (1995, 1996, UK), and a fire test at TNO in the Netherlands in September 1996 as part of an ECSC research project.

2.3.1 Large Scale Building Fire Test: 1981, (AISI)

The American Iron and Steel Institute (AISI) undertook a fire research project as part of a Research Associate program at the National Bureau of Standards (NBS, now the National Institute of Standards and Technology—NIST) [Gewain, 1982a; Gewain, 1982b]. In 1981, a two-story, four-bay steel frame structure was erected on the NIST campus in Gaithersburg, MD.

The structure dimensions were 9.75m× 12.20m and 6.1m high. The frame was sized to represent a floor at mid-height of a 20-story office building and was fabricated of hot rolled structural steel sections fastened to columns with high-strength bolts. The floor slab at the second floor level was subjected to a design live load of 3.8kN/m^2 and

consisted of normal weight concrete on a steel deck. During each of the tests, one 4.88m× 6.1m × 3.05m high bay of the test frame was exposed to fire and the structural steel and metal deck protected with spray-applied fire protection material.

Temperature measurements were recorded during and after the tests through the slab thickness, along the beam profile, on the columns in the test bay, and within the fire compartment. Vertical deflections were measured across the exposed portion of the floor slab and horizontal deflections were measured along the columns and spandrel beams of the test bay and in the fire compartment. During the test, the compartment peak mean temperature reached 1059°C, and the maximum temperature on the steel beam, protected by the 1.24cm of spray-applied material, reached 640°C. At the conclusion of this test, the floor assembly had a deflection of 16.51 cm. and continued to carry the load.

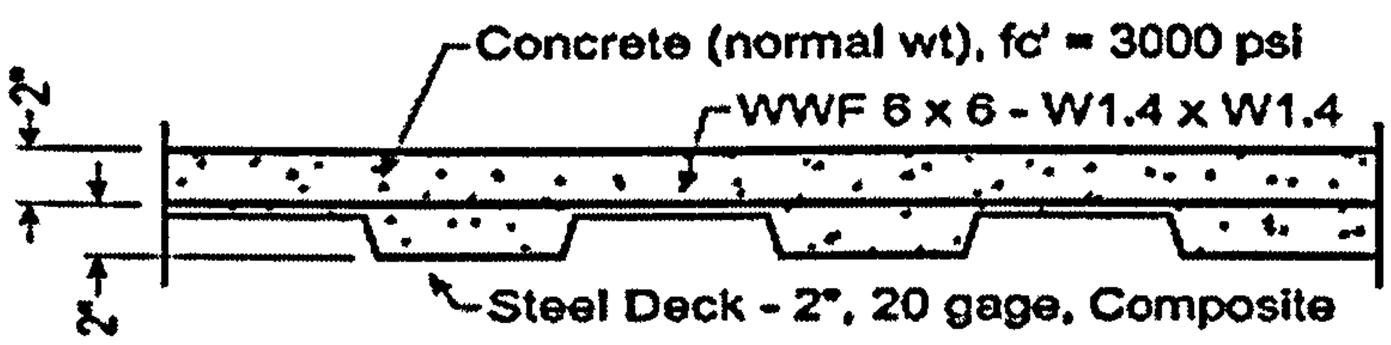

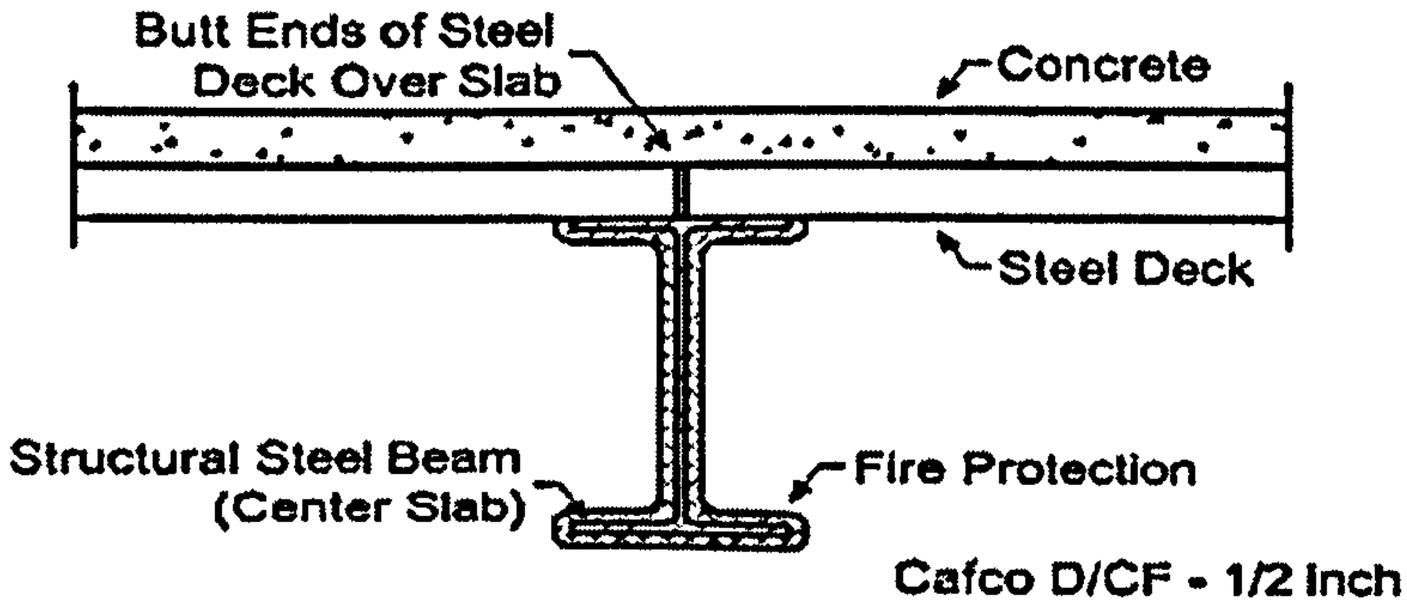

2-8 Details of beam and floor assembly for large scale NBS tests [Richard, et al., 2001]

2.3.2 Cardington fire Test

In June 1990 a fire developed on the first floor of the 14-storey Broadgate building in London, UK during construction. The total duration of the fire was in excess of four-and-a-half hours, atmosphere temperatures in the fire were estimated to have reached over 1000°C.

The floor was constructed using composite long-span lattice trusses and composite beams supporting a composite floor slab. The floor slab was designed to have 90 minutes fire resistance. The steel structure was partially unprotected at this stage of the construction. Despite some large deflections there was no collapse of any of the columns, beams, or floors.

At the time of the fire, not all the steel columns were fire protected. In cases where they were unprotected, the column had deformed and shortened by approximately 100 mm. These columns were adjacent to much heavier columns that showed no signs of permanent deformation. It was thought that this shortening was a result of restrained thermal expansion. The restraint to thermal expansion was provided by a rigid transfer beam at an upper level of the building, together with the columns outside the fire affected area.

The composite floor suffered gross deformations with a maximum permanent vertical displacement of 600 mm some failure of the reinforcement was observed. In some

areas, the steel profiled decking had debonded from the concrete. This was considered to be caused mainly by steam release from the concrete, together with the effects of thermal restraint and differential expansion. No structural failure had occurred and the integrity of the floor slab was maintained during the fire

The Broadgate fire prompted BRE to conduct a large scale test program on an 8 storey composite steel frame at their test facility in Cardington, UK. The Cardington frame fire tests [Kirby 2000] in the 1990s provided a wealth of experimental evidence about how whole frame composite steel-concrete structures behave in fire.

The Cardington frame survived a number of full scale fire tests despite having no fire protection on the steel beams (the unprotected steel often reached temperatures in excess of 900°C). The columns were generally protected to their full height. In all tests there was considerable deflection of the composite floor slab in the region of the fire. Furthermore, for most of the duration before runaway failure (not observed at Cardington), thermal expansion and thermal bowing of the structural elements rather than material degradation or gravity loading govern the response to fire [Usmani et al 2001]. Large deflections were not a sign of instability and local buckling of beams helped thermal strains to move directly into deflections rather than cause high stress states in the structure.

During 1995 and 1996, six fire tests were carried out on the 8-storey composite steel and concrete building at Cardington Laboratory of the Building Research Establishment (BRE) in the United Kingdom [Newman, 1999]. The purpose of these tests was to investigate the behaviour of a real structure under real fire conditions and

to collect data that would allow computer programs, which are capable of analyzing structures in fire, to be verified. The building was constructed as a modern steel framed office with composite metal deck floors. The structure was five bays wide almost 1000 m^2 in area by 33 m high, and beams in the tests were designed as simply- supported acting compositely with a concrete slab cast on metal deck. Columns were fully protected up to the steel sheet of the floors and the steel beams and steel sheet of the trapezoidal composite deck were unprotected. The fire generated temperatures of over 1200°C.The building survived without collapse of any structural element [European joint research programme, 1999]. The composite floors suffered large deflections more than span/20 but there was no structural collapse, (see Fig. 2-9). During fire, the floors provide support to the beams when they are designed to act compositely with the floor slab. The floor was effectively restrained on the boundaries. The steel beams were heated at a much greater rate than the concrete floor giving rise to a differential temperature gradient through the floor system. Eventually, the beam will reach its thermal buckling capacity and the rate of vertical deflection increases in the floor.

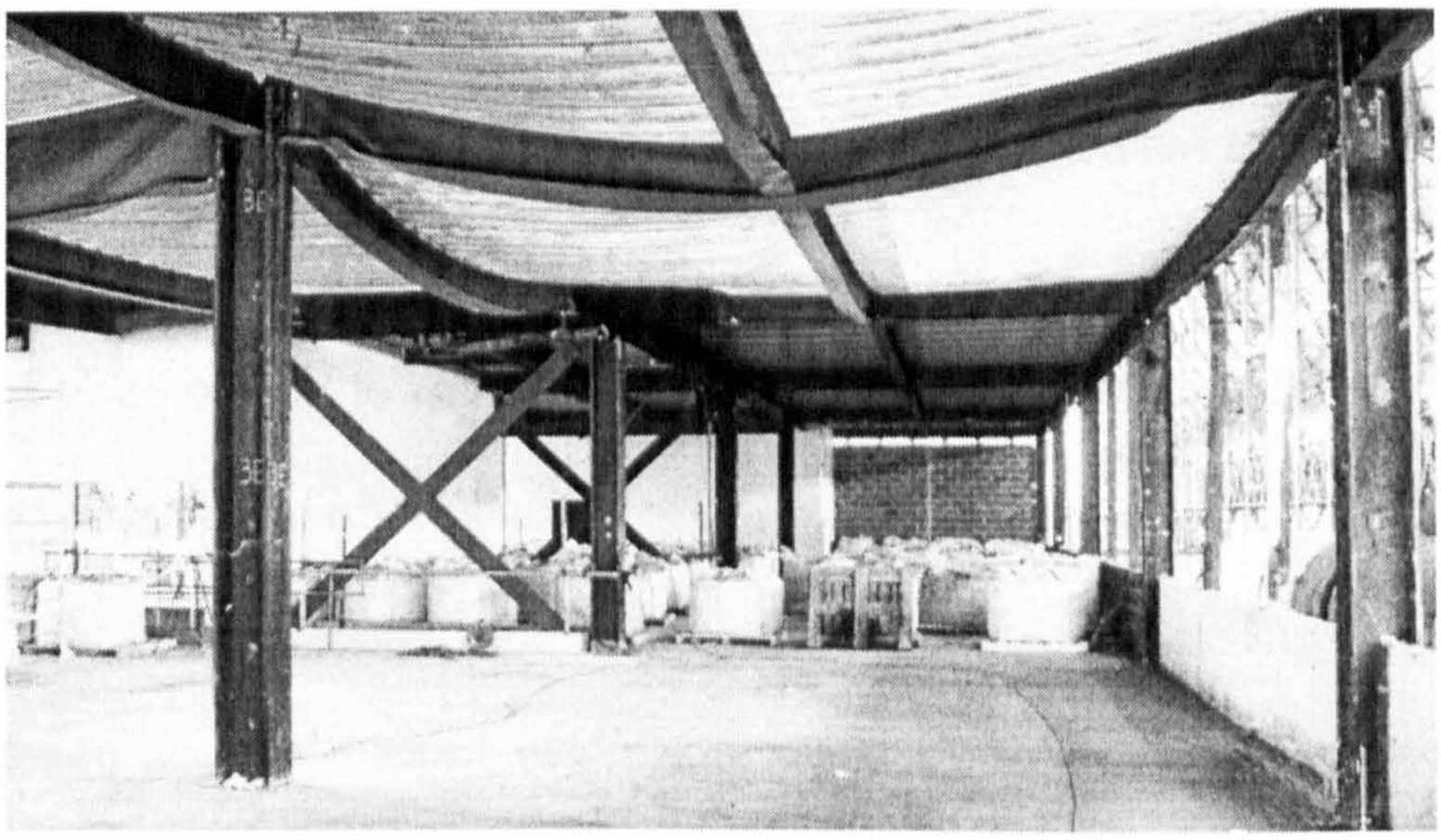

Fig. 2-9 Slab deflection after a fire in the Cardington building. No collapse occurred even though reached temperatures up to 1100°C [Bailey and Moore, 1999; Allam, Burgess and Plank, 1999]

Also the test program included one test on a restrained beam assembly on the seventh floor. During this restrained assembly test, the maximum beam temperature reached was about 900°C and the maximum deflection was about 25.4 centimetres.

At the conclusion of the test, the floor assembly continued to support its applied load. The rise in deflections in beams and restrained beams subjected to a large temperature gradient result in an increase in tensile force corresponding increase in vertical deflection. These tests provided a wealth of information about temperatures in the fire atmosphere and the protected and unprotected steel.

Unfortunately, there is considerably less information on the temperatures attained in the concrete slab. The temperatures through the depth of the slab were recorded only at a few points and in terms of the structural modelling, this has been just about adequate. There were no temperatures recorded in the slab in Test 4 (Office demonstration test).

The extensive testing of composite construction at Cardington has shown that: -

- Floors provide support to beams in fire conditions and structure stability can be maintained at very high temperatures.

- Deformation does not happen suddenly or unexpectedly but proceeds by slow, visible ductile movement.

Following the full scale tests at the Cardington steel building, an independent test was conducted at the Building Research Establishment (BRE) to simulate the behaviour of simply supported composite floor under fire conditions [Bailey and Moore, 2000].

The slab measured 9.5m x 6.5m and was built with a trapezoidal-shaped composite steel deck beneath it, which retains most of their strength at elevated temperatures, has been tested to failure at ambient temperature. The troughs of the steel deck were 60mm deep and the slab had an overall thickness of 150mm.

After the slab was cast, the steel decking was later removed from beneath the slab, leaving the concrete slab reinforced only with the reinforcement mesh. The absence of the steel decking represented the depleted strength and stiffness of the slab. However, a steel mesh was provided to resist shrinkage and temperature stresses.

The slab was vertically supported at the perimeter on beams and columns but it was horizontally unrestrained. Major differences between the tested slab and the behaviour of a heated slab in an actual building have been highlighted. The slab failed at a uniformly distributed load of 4.81 kN/m^2 with a full depth crack forming in the first instance across the shorter span of the slab followed by a full depth crack on one of the diagonals.

2.3.3 Australia, William St. fire tests

The 41-storey steel framed building at William Street in the centre of Melbourne was the tallest building in Australia when completed in 1971. The steelwork around the

inner core and the perimeter steel columns was protected by concrete encasement but the steel beams and the underside of the metal deck of the composite floors were fire protected with an asbestos-containing product. The building's sprinkler system was of a light hazard category with no sprinklers in the ceiling spaces.

After 20 years the building became due for its first refit. During a refurbishment program, a decision was made to remove the hazardous asbestos. At the time of the refurbishment, the required fire resistance was 120 minutes. Normally this would have entailed the application of fire protection to the steel beams and to the soffit of the very lightly reinforced slab (Australian regulations have been revised and now allow the soffit of the slab to be left unprotected for 120 minutes fire resistance). In addition, the existing light hazard sprinkler system required upgrading to meet the prevailing regulations.

A series of four fire tests was carried out to obtain data when the beams and slab were unprotected. The tests were to study matters such as the probable nature of the fire, the performance of the existing sprinkler system, the behaviour of the unprotected composite slab and castellated beams subjected to real fires, and the probable generation of smoke and toxic products.

A test building was constructed at the BHP Laboratories in Melbourne which simulated a section ($144m^2$) of a typical storey of the building. Natural fire tests were carried out with real office furniture.

Four fire tests were conducted. The first two were concerned with testing the performance of the light hazard sprinkler system. These two tests showed that the existing light hazard sprinkler system was adequate. The structural and thermal performance of the composite slab was assessed in Test 3. The supporting beams were partially protected. Atmosphere temperature peaked at 1254°C. The slab supported the imposed load. The maximum temperature recorded on the top surface of the floor slab was 72°C. The underside of the slab had been partially protected by the ceiling system, which remained substantially in place during the fire.

In Test 4, columns were protected, but the beams, above a non-fire rated suspended ceiling, were unprotected as well as the slab. The atmosphere temperature peaked at 1228°C. The maximum temperature reached at any point on a beam above the non-fire rated suspended ceiling was 632°C at 112 minutes with a deflection of only 120mm in a 12m span (span/100).

It was concluded from the four fire tests that the existing light hazard sprinkler system was adequate and that no fire protection was required to the steel beams or soffit of the composite slab. Any fire in the William Street building should not deform the slab or steel beams excessively, provided that the steel temperatures do not exceed those recorded in the tests. As a result of the tests and a risk assessment programme, this 41 storey building was approved by the city authorities with unprotected beams and slabs.

2.3.4 Fire Research-TNO Building and Construction Research (Netherlands, 1996)

A major fire test was carried out at TNO in the Netherlands in September 1996 as part of an ECSC research project [Corus]. The specimen tested consisted of a single span of deep-deck normal-weight concrete slab, simply supported at four corners. The overall dimensions of the test specimen were 5.6m x 4.6m, with the edge beams spanning in the shorter direction. The overall depth of the slab was 290mm. The test load including self-weight was 6.65KN/m^2, a typical office building load intensity. The slab was unrestrained against thermal expansion and was reinforced to achieve 120 minutes' fire resistance. In a numerical study, the tested material properties of structural steel, concrete and reinforcement were used. Further details are available from Reference [Corus]

2.3.5 Building Research Association of New Zealand (BRANZ) Limited

At University of Canterbury, New Zealand 2002, the fire tests of six concrete slabs were conducted to investigate the behaviour of unrestrained simply supported slabs in a controlled furnace environment. The floor slabs consisted of three reinforced concrete plain flat slabs and three different proprietary composite steel-concrete slabs.

The composite floor measured 3.3m by 4.3m and had total thickness 130mm. The floor was simply supported on all four sides over the furnace with no horizontal restraint. The slabs were subjected to a live load of 3.0kPa and were heated on the underside with the time temperature curve following the ISO 834 standard fire for three hours. The floor was supporting the loads for the full duration of three hours without collapse. By three hours, the temperatures had reached 1100 °C and high temperatures were

measured across the depth of the floor. The temperatures of the reinforcing steel exceeded 700 °C. The floor suffered extensive surface cracking and large mid-span deflections (up to 270mm). The slabs with higher steel contents and closer bar spacing suffered only surface cracking, while the slabs with the lower steel content suffered full-depth cracks.

The structural fire resistance of the slabs in the tests exceeded the predictions of code recommendations.

Before the test started, the composite floor had already cracked on the top surface due to mishandling when it was shipped [Lim, 2002]. Approximately 5 minutes after the start of the test, the steel sheet at the bottom surface started to buckle and debond from the concrete. Fig.2-10 shows the steel sheet debonding from the slab, creating a gap between the decking and the concrete. After 20 minutes, diagonal cracks started to form at the east and west sides of the slab, where the corners were held down. Small pieces of concrete also spalled off the sides of the slab. As 3 hours approached, the initial crack (due to mishandling) had widened significantly, flames started to penetrate this crack.

Fig. 2-10 Debonding of the Steel Sheet [Lim, 2002]

Fig. 2-11 shows the large deflections in the composite floor after the fire test. A large crack (up to 9mm wide) had formed across the middle of the slab in the longitudinal direction and horizontal cracks running across the short span at regular parallel spaces, which corresponded to the position of the bars of the reinforcing mesh.

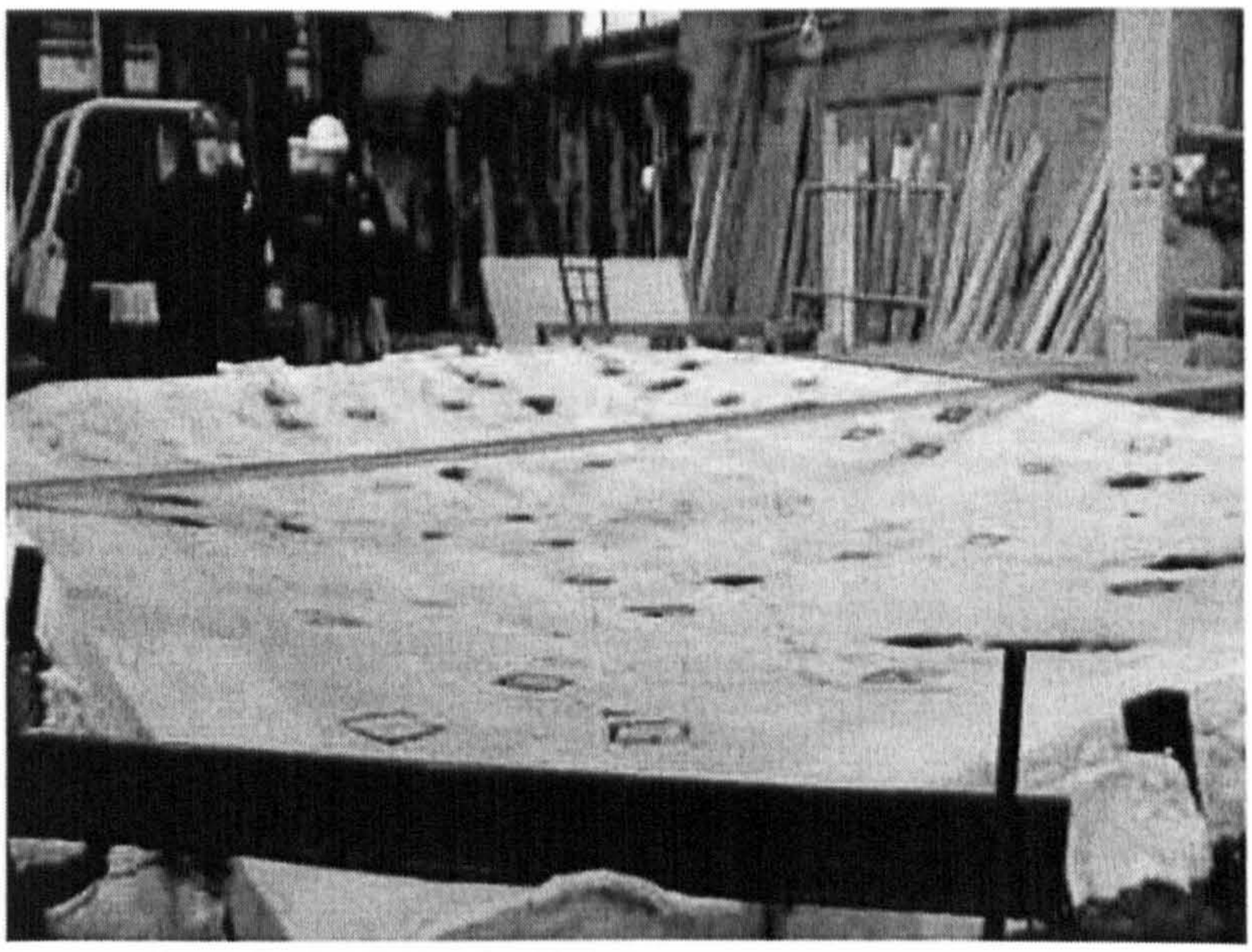

Fig. 2-11 Deflected slab after the fire test [Lim, 2002]

2.3.6 Experimental of restrained floor during a fire

[Lin et al. 1983] have conducted a large number of fire tests on restrained concrete floor slabs exposed to ASTM E119 fire. Their test results showed that the performance of the floor slabs was not greatly affected by the degree of restraint, except near the 0% and 100% restraint conditions. Under zero restraint, the floor will behave as simply supported and will result in a lower fire resistance. At full restraint, the high resisting forces could result in a compressive failure.

The Portland Cement Association has also carried out tests showed that almost any amount of restraint greatly enhanced the fire resistance of the floors as they were able to support their loads considerably longer than for the simply supported condition [Issen et al, 1970].

2.4 Analytical and Numerical Modelling

The traditional way of establishing the fire resistance of composite structural member is by test according to the British Standard [BS476] Part 20 or a similar standard such as [ISO834].

Recently, considerable research has been undertaken with a view to developing calculating methods to determine the fire resistance of structural elements. British Standard [BS5950] Part 8, describing calculation methods for the fire engineering design of steel structural members. European codes, describe simple methods of assessing fire resistance by calculation for concrete members [CEC 1990a] and composite members [CEC 1990b].

Anderberg have questioned whether the support condition occurs in real construction and have recommended simulating different degrees of restraint by different axial stiffnesses [Anderberg et al, 1982]. They have used a non-linear finite element program, CONFIRE, to investigate the structural behaviour and fire resistance of concrete members exposed to fire. Their analysis was on simply supported concrete slabs with different amount of allowable horizontal expansion of the slabs. Their analyses showed that the fire resistance of the floor slabs did not increase with increasing axial restraint.

2.4.1 Thermal Analysis

Thermal analysis is used to calculate the temperature history in each structural element. The temperature rise always lags behind the fire temperature because of the thermal inertia inherent in the material and the tendency for heat to flow to cooler material adjacent to the heated area. Insulation can greatly slow the temperature rise in protected elements.

Basic heat conduction theory can predict the temperature history in fire-exposed structures when thermal material properties of concrete, steel, and insulation are known.

There are a number of finite element computer codes that solve the heat conduction equation with fire-boundary condition like FIRES-T3 [Iding, et al., October 1977] and TASEF [Sterner et al., 1990]. All of these codes discretize the equations into a set of linear equations expressed by the matrix relationship. All thermal analyses start with discretizing the structural members into finite elements and defining boundary

conditions, both fire-exposure boundaries and other boundaries where heat may escape from the member into adjoining parts of the structure or into the environment. The thermal material properties should be defined for all components, and the time-dependent fire curve to be specified. The equations are then solved to obtain the temperature history in all parts of the structural member during the fire. Such temperatures form the basis for a structural analysis of each structural element and the structure as a whole.

Fire is usually represented by a temperature-time curve which gives the average temperature reached during the fire. International standards are based on the standard fire defined by the heat exposure given by the ISO 834 curve or similar standard curve. In some cases reference can be made to natural fires which have different temperature-time relationships depending on fire load density and ventilation conditions. However the thermal properties of the proposed material are needed. In the UK, the thermal response of various construction materials and assemblies to standard fire conditions in accordance with BS476 has been recorded in various publications since 1950s.

The response of a structural element exposed to fire is governed by the heating rate of the element which is directly related to the section factor of the element. Jose has reviewed the different approaches used to establish the thermal boundary conditions required to properly analyse a structure in the event of a fire [Jose, 2004].

The main objective of the thermal analysis is to certify that a structure fulfils the thermal requirements and to supply the full two or three dimensional temperature distribution as input for the structural analysis. In the case of composite floor systems,

the layers have different thermal conductivities in different directions. The thermal analysis for structural fire problems can be divided into two parts:

1- The heat transfer across the boundary from the fire into structural members by convection and radiation.

2- The heat transfer within structural members by conduction. The general solution of the heat transfer equation is possible by means of computer programs.

However, in fire, heat is transferred from fire to the floor system by convection and radiation which depend on the exposed area and the difference between fire and floor system temperature. The heat transferred by convection is less than 10% of the radiant heat [Trinks et al., 1961]. The temperature of the surface of the exposed object will be very close to the temperature of the environment. In this region, changes of the order of 10% will have little effect on the surface temperature and thus on the temperature in the exposed object. Therefore, to simplify the heat transfer, the convection heat transfer may be neglected and any other fire conditions can be assumed, using an input time-temperature history for the fire. Internal heat generation can be neglected; and three-dimensional problems can be considered as two-dimensional or one-dimensional idealizations.

The thermal analysis for composite floor system can define the temperature profile through the cross-section by using test data presented in tables or charts which are published in codes or design guides. These test data are generally based on standard fire conditions. [Huang 1995]'s model is used to predict temperature distribution within the cross section of the composite slab. The thermal properties of concrete and

steel (thermal conductivity, specific heat, and specific mass) are considered as temperature-dependent. The thermal conductivity decreases as a function of temperature; the specific heat increases as a function of temperature.

In Eurocode 4 composite slabs are treated as equivalent solid slabs with an effective depth (H_{eff}) and the steel decking is ignored in fire conditions. This method is not applicable to deep-deck slabs with rebar in the ribs. Eurocode 4 defines fire resistance in term of standard classes, ranging from 30 to 120 minutes (and beyond) in 30-minute intervals. Only exposure from below is considered, which in practical cases will always be decisive. As stated above, the presence of the rib makes composite slabs different from flat ones in both thermal and structural behaviour.

A number of models have been developed for modelling of composite slabs in fire.

[Gillie et al., 2001] described a method of modelling composite floor slabs using a stress-resultant approach. A drawback of this method is that the model does not allow stresses to be output from the analysis.

[Elghazouli et al., 2001] developed a model in which the composite slab was treated as an orthogonal elasto-plastic grillage of beam-column elements, and temperature variations were introduced across the two orthogonal cross-section directions as well as along the element length. The deflections were obtained from the integration of the orthogonal beam-column elements. The effects of in-plane shear and Poisson's Ratio are ignored.

2.4.2 Material Properties at Elevated Temperature

Most of the rational design methods consist of applying the usual structural mechanics design principles with due consideration given to the impact of elevated temperatures on the thermal and mechanical properties of the primary construction materials.

The mechanical properties of all common building materials decrease with elevation of temperature. Mechanical properties of concrete and steel change with increasing temperature as illustrated by means of stress-strain diagram as shown in Figs. 2-1 and Figs. 2-2. Further data available in tabular form in [Euocode 4] relates the yield stress, elastic limit, and the initial elastic modulus at a given temperature with those at 20°C. Creep is implicitly taken into account in the stress-strain relations.

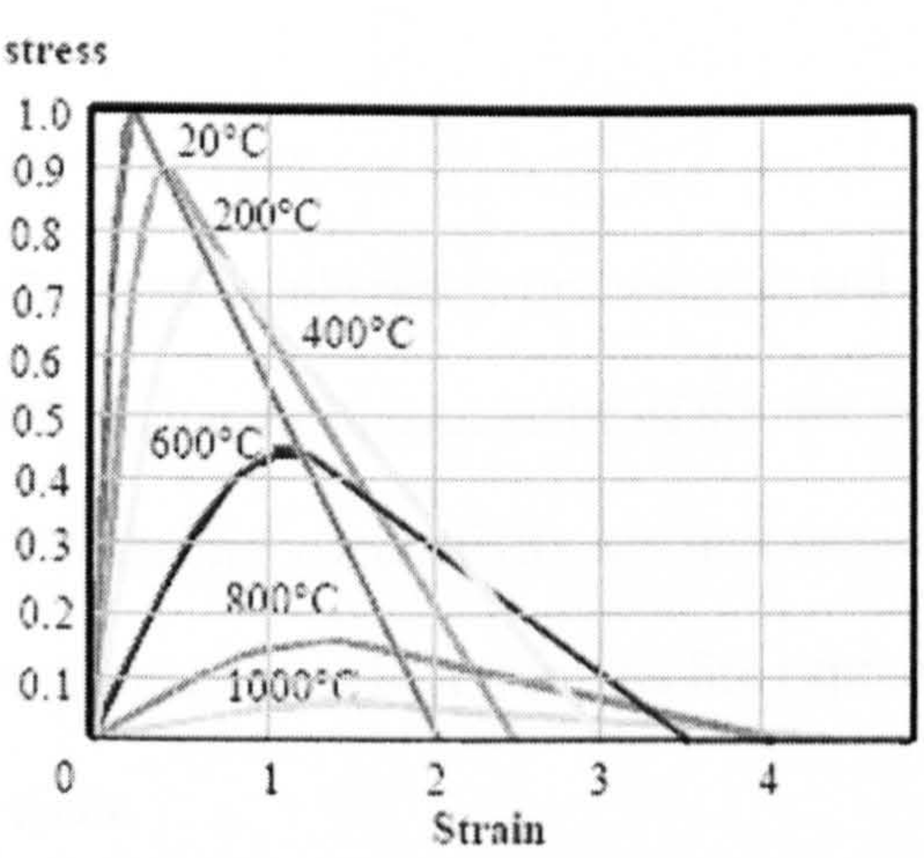

Fig. 2-1 stress-strain curve for concrete at fire temperature [Euocode4]

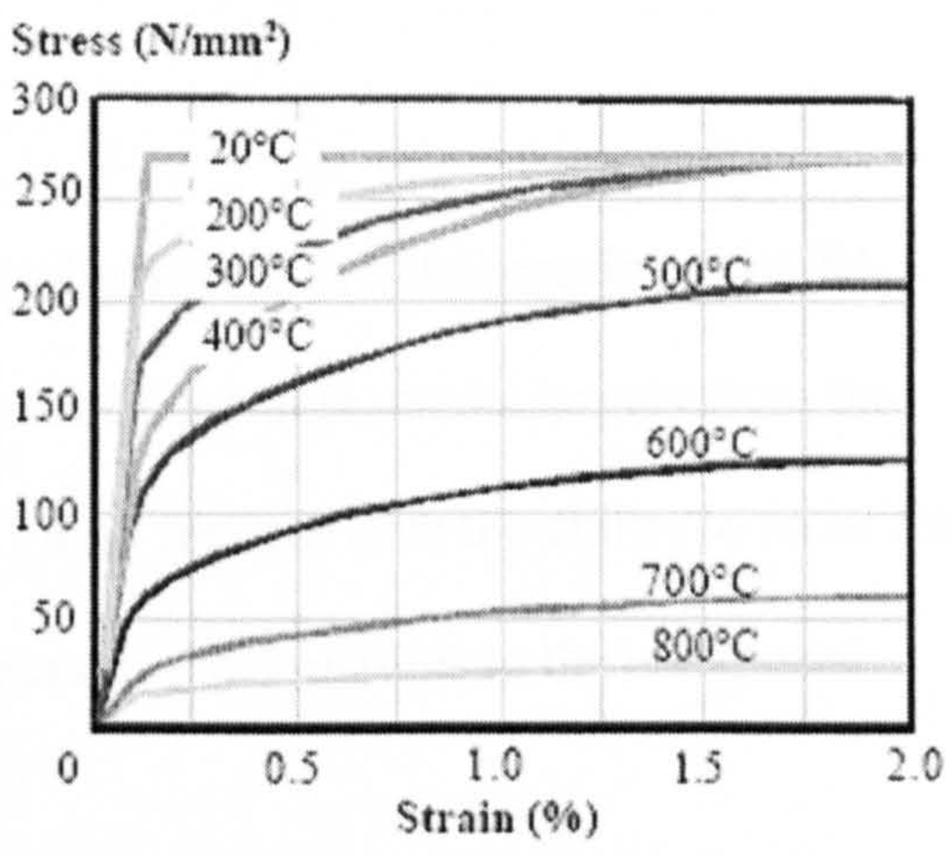

Fig. 2-2 stress-strain curve for steel at fire temperature [Euocode4]

The mechanical properties for concrete and steel have been analysed by Hertz and approved that the compressive strength, the tensile strength and the modulus of

elasticity decrease and the ultimate strain increases. For steel the modulus of elasticity, the yield stress and the tensile strength decrease [Hertz, 1999].

The properties of these materials at room temperature are well understood. During the mid-forties the Building Research Station provided some data on the high temperature properties of concrete and steel. These were based on work carried out by [Stradling, 1922] on concrete and steel. Abrams deals with concrete and steel and makes reference to their use in fire-resisting construction [Abrams, 1979].

It is essential to have a clear understanding of the material properties at elevated temperatures. Therefore needs review of previous studies on the properties of the material used.

(a) Concrete

Concrete is inherently fire resistant and is usually treated as a fireproofing material. This inherent characteristic of the fire resistance of concrete results largely from the low thermal conductivity and heat capacity. These features give the ability to resist the transmission of heat from the fire exposed faces of the structures to the unexposed faces.

Malhotra described in Fig. 2-3, the loss of compressive strength of concrete gradually under increasing temperatures [Malhotra, 1956]. So, one must make sure that structural elements have been designed with sufficient reserve strength to support the applied loads for the projected duration of fire exposure.

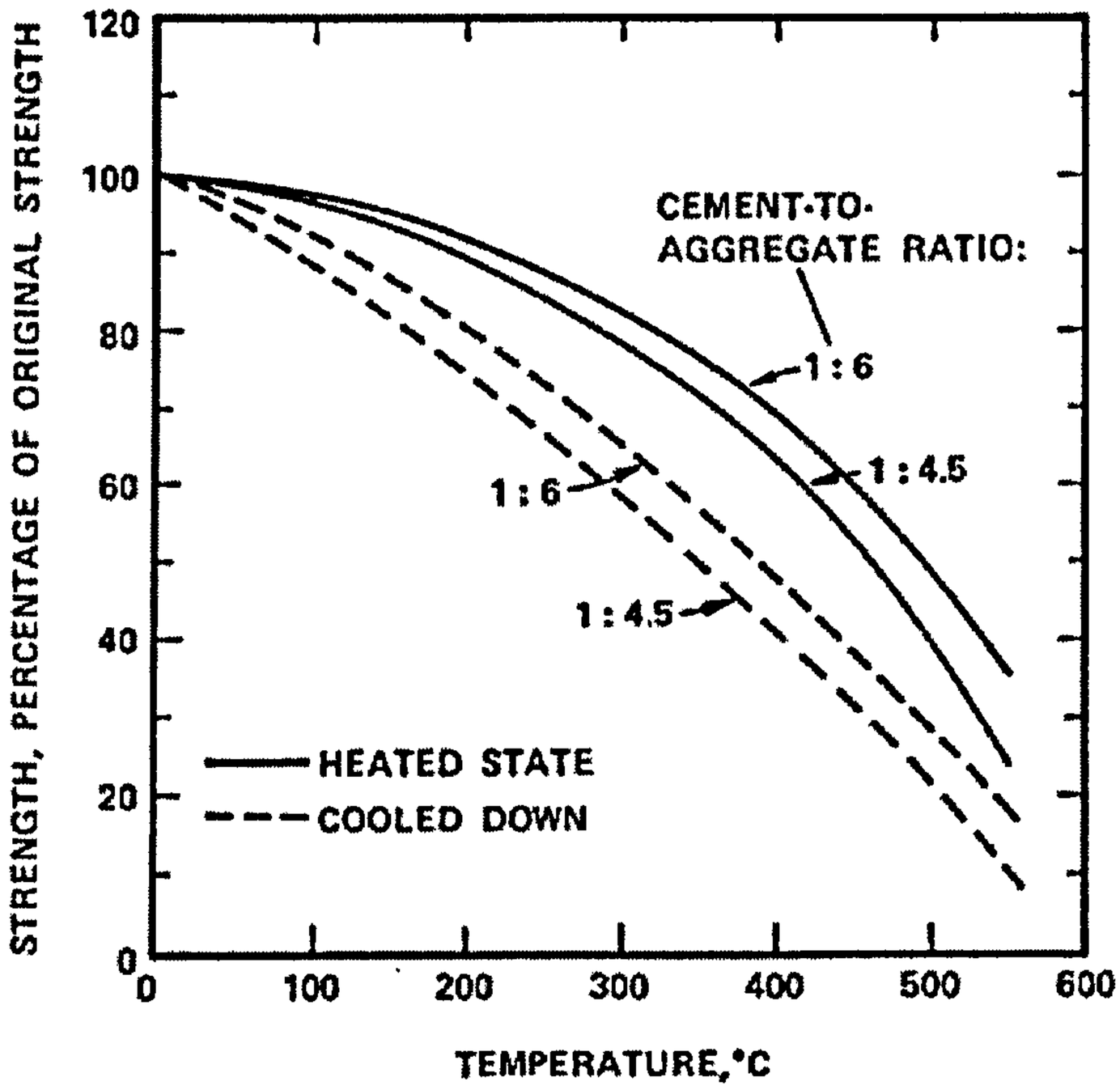

Fig. 2-3 Effect of temperature on compressive strength of concrete [Malhotra, 1956]

Some of the early experiments on the thermal deformation of concrete have been reported by [Abrams, 1979], [Bocca, et al., 2000], [Harmathy, 1970], and [Schneider, 1983], and show that deformation of concrete is dependent upon a number of factors such as type of aggregate, heating rate and the level of externally applied forces.

By referring to Fig.2-4 we can calculate the concrete stress for a given strain by the following expression [EUROCODE 4, 1994]:

$$f_c = f_c'(3\varepsilon_{stress}/\varepsilon_u)/(2+(\varepsilon_{stress}/\varepsilon_u)^3) \qquad for: \varepsilon_{stress} \le \varepsilon_u \qquad (2\text{-}3)$$

$$f_c = f_c'(1-((\varepsilon_{stress}/\varepsilon_u)/(\varepsilon_{ce}-\varepsilon_u))) \qquad for: \varepsilon_u < \varepsilon_{stress} < \varepsilon_{ce} \qquad (2\text{-}4)$$

$$f_c = 0 \qquad for: \varepsilon_{stress} \ge \varepsilon_{ce} \qquad (2\text{-}5)$$

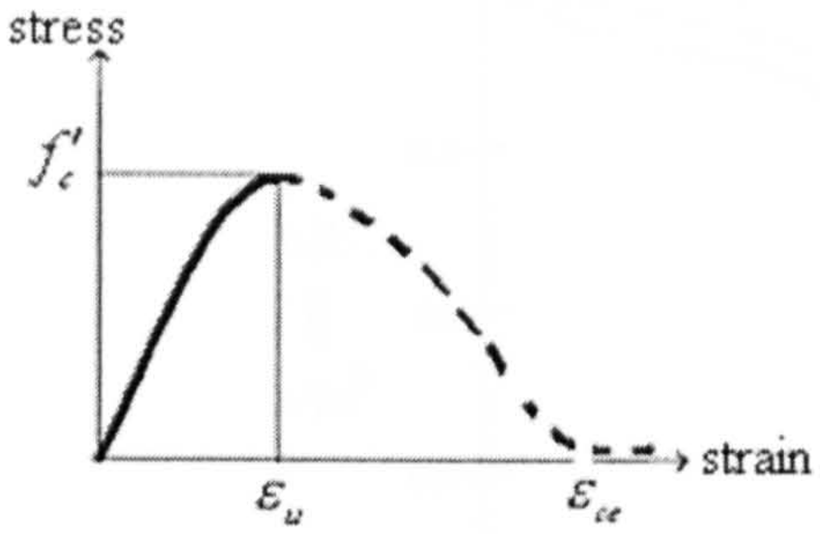

Fig. 2-4 Stress-strain relationship of concrete under compression at elevated temperature

When:

f_c' = compressive strength of concrete at temperature T, [N/mm^2] = K_{ct} * f_{co}

ε_u = concrete strain at the peak compressive stress, (corresponding to f_c')

ε_{ce} = ultimate concrete strain in descending

K_{ct} : Reduction value

f_{co} : Strength of concrete at 20 ^{o}C

(b) Steel

Steel, as concrete, has the advantage of being noncombustible but this characteristic alone means little in trying to resist collapse. Its high thermal conductivity makes steel absorb heat much more quickly than other materials; thus if the structural member has a relatively small mass, its temperature will increase very rapidly. Steel theoretically responds the same in either tension or compression. Both the yield stress and modulus of elasticity of steel are important in determining load-carrying capacity, and decrease considerably with increasing temperatures are shown in Fig. 2-5 [Cote, et al., 1986].

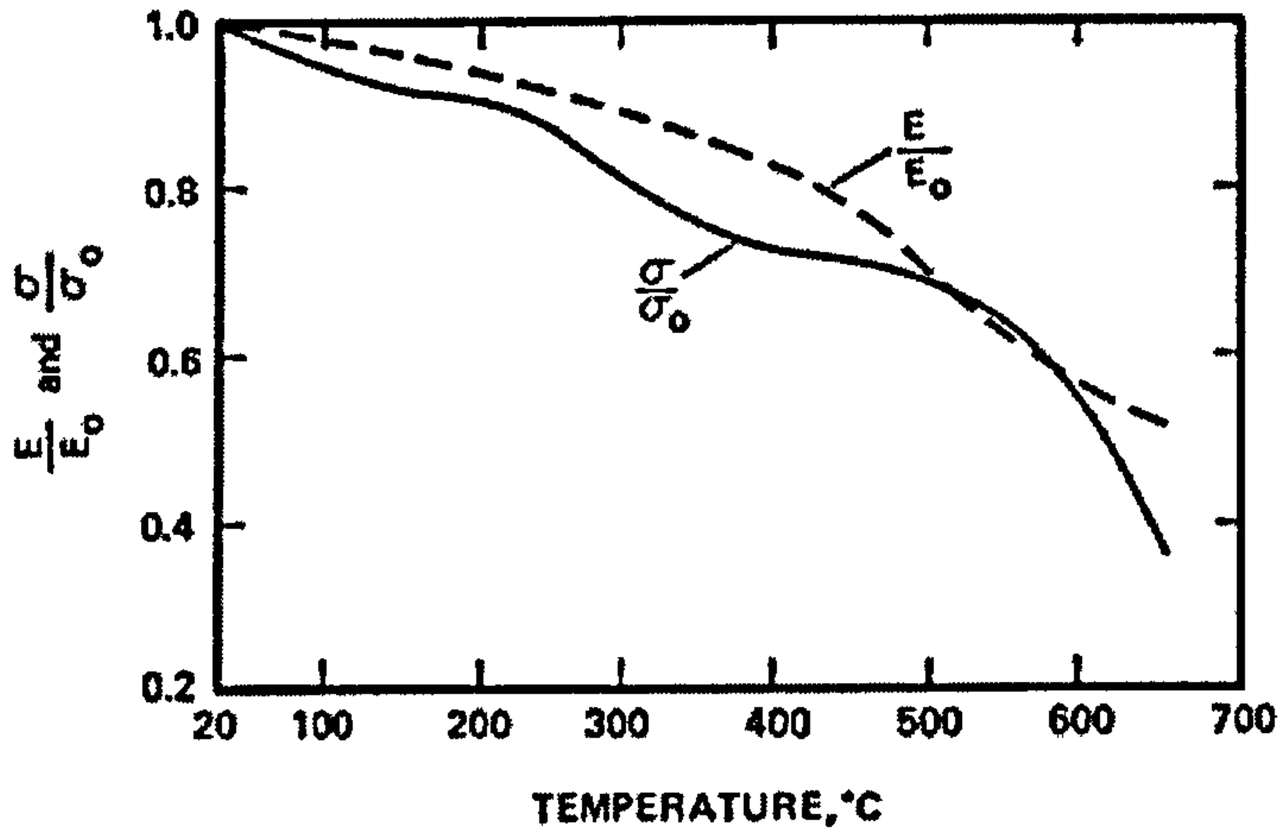

Fig.2-5 Effect of temperature on modulus of elasticity (E) and yield stress (σ) for A36 steel. E_0 and σ_0 represent ambient conditions [Cote, et al., 1986]

[NIST, 2005] has carried out tests for steel properties at high temperature. [Anderberg, 1988] and [Kirby, 2005], proposed a method to determine the stress-strain relationship of steel at elevated temperature based on the results from tensile testing. Steel loses considerable tensile strength at elevated temperatures. [Harmathy, T.Z. and W.W. Stanzak, 1970], defined the critical temperature of steel as the temperature at which only 60% of the original strength remains. The time it will take for these temperatures to be reached in a reinforced concrete member (slab, beam or column) depends on the thickness of concrete cover protecting the steel.

[Hamerlink and Twilt, 1990] investigated the influence specific heat of steel on the thermal behaviour of composite slabs; as the steel sheet is very thin, the influence of its heat capacity on the heat transfer was found to be negligible. Therefore they assumed that the steel sheet at high temperatures loses its strength completely, and the floor is then structurally equivalent to a reinforced concrete slab. The necessary steel reinforcement for this purpose is provided in the form of a mesh, typically of 6mm or 7mm diameter bars arranged in spacing of 200 or 300mm.

Also by referring to Fig. 2-6 and EUROCODE 4 we can calculate the steel stress for a given strain by the following expression.

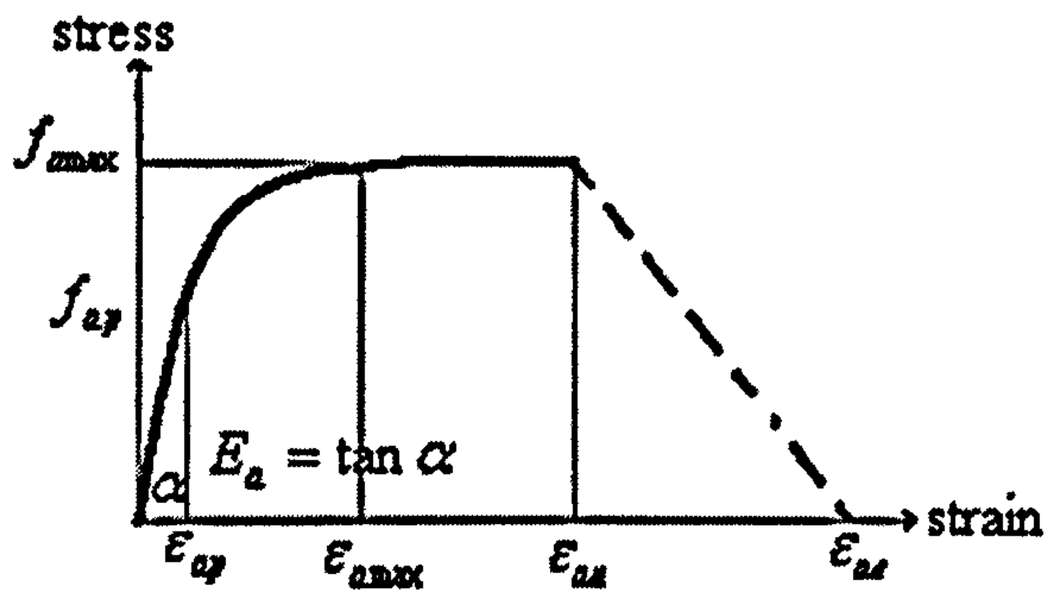

Fig. 2-6 Stress-strain relationship of steel at elevated temperature

$$for: \quad 0 < \varepsilon_{stress} \leq \varepsilon_{ap}$$

$$f_y = (\varepsilon_{stress} * f_{ap}) / \varepsilon_{ap} \qquad (2\text{-}6)$$

$$\varepsilon_{ap} = (K_{pt} * f_{ayo}) / (K_{st} * E_{ao}) \qquad (2\text{-}7)$$

K_{st} : Reduction factor for steel (in elastic range)

K_{pt} : Reduction factor for steel corresponding to f_{ayo}

E_{ao} : Young' Modulus of steel at 20 °C

f_{ayo} : Yield stress of steel at 20 °C

$$for: \quad \varepsilon_{ap} < \varepsilon_{stress} \leq \varepsilon_{a\max}$$

$$f_y = \frac{b}{a}(\sqrt{a^2 - (\varepsilon_{a\max} - \varepsilon_{stress})^2} + f_{ap} + c \qquad (2\text{-}8)$$

When:

$$a^2 = (\varepsilon_{a\max} - \varepsilon_{ap})(\varepsilon_{a\max} - \varepsilon_{ap} + c / E_a) \qquad (2\text{-}9)$$

$$b^2 = E_a(\varepsilon_{a\max} - \varepsilon_{ap})c + c^2 \qquad (2\text{-}10)$$

$$c = \frac{(f_{a\max} - f_{ap})^2}{E_a(\varepsilon_{a\max} - \varepsilon_{ap}) - 2(f_{a\max} - f_{ap})} \qquad (2\text{-}11)$$

$$for: \quad \varepsilon_{a\max} < \varepsilon_{stress} \le \varepsilon_{au}$$

$$f_y = f_{a\max} \qquad (2\text{-}12)$$

$$for: \quad \varepsilon_{au} < \varepsilon_{stress} \le \varepsilon_{ae}$$

$$f_y = f_{au}\frac{\varepsilon_{ae} - \varepsilon_{stress}}{\varepsilon_{ae} - \varepsilon_{au}} \qquad (2\text{-}13)$$

$\varepsilon_{a\max}$ = Strain corresponding to $f_{a\max}$ (end of strain-hardening branch) start of plateau

ε_{au} = Strain corresponding to $f_{a\max}$ (end of plateau)

ε_{ae} = maximum strain in descending branch

$E_a = \tan\alpha$

2.4.3 Strength Analysis

Strength analysis is to determine forces and stresses in each structural element and whether local or progressive structural collapse would occur during the fire. The increase of the temperature of structural elements subjected to fire leads to a decrease in their mechanical properties such as yield stress, Young's modulus, and ultimate

compressive strength of concrete. The response of a structural member exposed to fire is governed by the rate that it is heated because the mechanical properties of materials decrease as temperature rises and, likewise, the structural resistance of a member reduces with temperature rise.

James described an effort by the American Society of Civil Engineers (ASCE) and the Society of Fire Protection Engineers (SFPE) to develop a standard for performance-based structural fire protection analyses [James, 1999]. These methods apply to a wide variety of structural members comprised of concrete, masonry, steel, and timber. A description of the fire exposure focused on the heating conditions associated with the exposure. Material effects include material properties as a function of temperature along with physical or chemical effects of the elevated temperature exposure. Collapse occurs at the time when the structural resistance reduces to the applied action effects.

This fire resistance time can happen in a very short time when the increase of temperature is rapid. Steel elements have an unfavourable behaviour in this respect due to the very high thermal conductivity of the steel. A rapid heating of the whole profile takes place as a result. In comparison, composite elements have a favourable behaviour due to the great thermal inertia of the elements and the low thermal conductivity of the concrete.

Non-linear analysis is an effective tool to obtain an understanding of how structures behave in extreme fire conditions. Several researches are available which address the fire resistance design of composite structures, like [Lamont 2002] which represent Non-linear finite element analysis of composite structures used to assess the performance of structures in fire. The results of analyses conclude that the unprotected

steel and composite floors can survive for considerable periods without failure; also the composite slabs are effective in acting as tension and compression membranes when large deformations occur, thermal expansion and thermal bowing effects dominate the structural behaviour. Non-linear analysis gives the most accurate understanding of actual behaviour [Usmani, 2001].

An analytical study on restrained/unrestrained fire ratings used the measured temperatures at various locations along the depth of the beam and slab to determine nominal flexural strength and capacity of a beam during the ASTM fire test [Ioannides and Mehta, 1997].

Gewain and Troup [Gewain et al., 2001] offered an analytical procedure, using an assumed time-temperature history for the particular assembly and beam rating coupled with the known properties of the steel at various elevated temperatures, to calculate the nominal flexural strength of the beam. They also provided methods to increase the nominal flexural strength by accounting for the effects of rotational restraint due to connections and slab. Their study showed that, considering the combination of factors that occur in real buildings during real fires can have sufficient load-carrying capacity without even counting on any restraint.

Compared to the methods available for the design of structural members at room temperature, shows the need for further development in the elevated temperatures.

(a) Orthotropic Plates

An orthogonal-anisotropic plate is defined as a plate which has different elastic properties in two mutually perpendicular directions in the plane of the plate, designated x and y. The problem of an anisotropic plate was first studied by Gehring (1860) and Boussinesq (1879). According to Timoshenko a comprehensive treatment of an orthotropic plate, including a systematic solution of its differential equation, was first presented by Huber (1914) [Timoshenko, 1959].

Rajagopal developed a layered rectangular plate element with axial and bending stiffness in which concrete was treated as an orthotropic material [Rajagopal, 1976].

Reinforced concrete beam and slab problems have also been treated as orthotropic plates by many other investigators e.g. (Lin and Scordelis 1975; Bashur and Darwin 1978; Rots et al. 1985; Barzegar and Schnobrich 1986; Adeghe and Collins 1986; Bergmann and Pantazopoulou 1988; Cervenka et al. 1990; Kwak 1990). Many of these solutions are based on the finite difference approach

(b) Numerical Methods

Numerical methods are necessary to solve the heat flow equation. Many computer programs are available and it is now possible to carry out thermal analysis for very complex structural elements.

Numerical methods can be used to predict structural behaviour and the interactions between the fires and the structures [Torero, et al., 2004].The numerical modelling of fire scenarios has been developed and commercial software is available. Also a number

of researchers have developed numerical modelling approaches to study the behaviour of reinforced concrete structures in fire conditions. Ellingwood [Ellingwood and Lin, 1991], and Huang [Huang and Platten, 1997] developed modelling software for reinforced concrete members in fire. A simpler model has been developed by Lie for the high-temperature analysis of circular reinforced concrete columns [Lie and Celikkod, 1991].

The use of numerical methods for the calculation of the fire resistance of various structural members has been gaining acceptance [Sullivan, et al., 1997], [Kodur, et al., 1996]. These calculation methods are far less time consuming. For these calculation methods to be used with assurance, however, the material properties at elevated temperatures are required. The data on thermal and mechanical properties is being used to develop thermal and mechanical relationships, as a function of temperature. These relationships can be used as input to numerical models which in turn can be used to determine the behaviour of structural members at high temperatures. Zhuman and Hadjisophocleous [Zhuman et al., 2000] have presented numerical methods and verification examples for this development of fire in buildings and to predict fire endurance.

There are two main types of numerical method available, the Finite Element Method and the Finite Difference Method. The majority of numerical analysis used today is based on the finite element method. During recent years the fast development of the finite element method has produced several efficient computer codes for analysing thermal problems. Characteristic advantages of finite element method are suitability for generally applicable and flexibility for complex geometrical forms.

The finite-difference method was the first numerical method to be used extensively for heat conduction [Anthony, 1995]. It remains a popular method, not because it is superior to other methods for heat conduction, but because it is easier to implement and is also the most useful numerical method for heat analytical problems. Utilizing the information produced by the heat transmission analysis, it may assemble a picture of the strength and deformation characteristics of a structural member at any given stage of the heat exposure. The stress, stability and deformation analyses normally require, as a first step, the use of a numerical method to define the interdependent elements and account for the non-uniform temperature distribution within the member. As in Fig.2-7 [Lie et al. 1984], under fire conditions a non-uniform temperature distribution in the concrete over the cross-section for a reinforced concrete column for each element, the incremental strain or deformation caused by the increase in temperature is calculated and a new stress level obtained with the help of the stress-strain relationship applicable for the temperature.

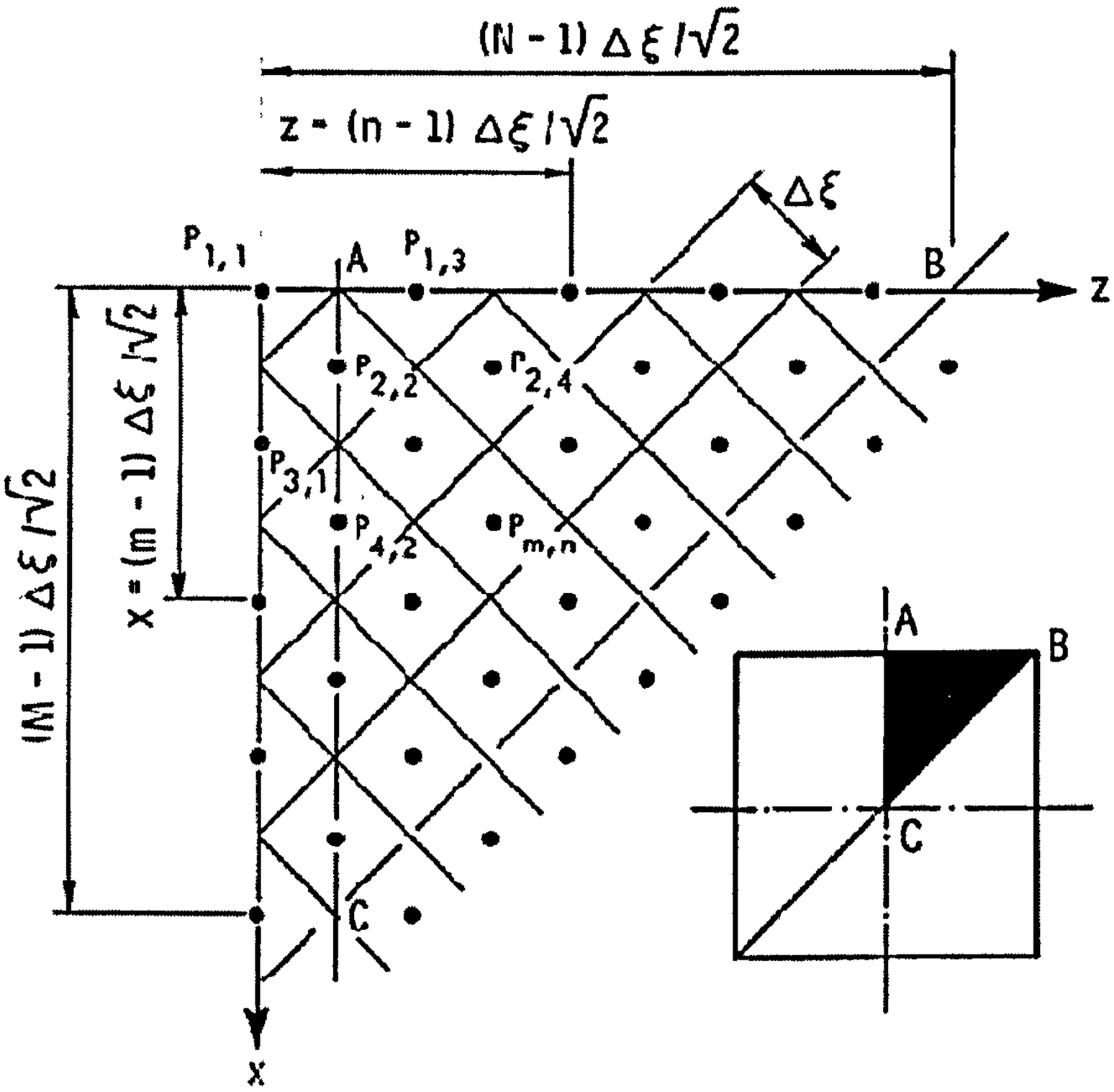

Fig. 2-7 Discretization of one-eighth section of a reinforced concrete column into an element network [Lie et al. 1984]

The ECCS Technical Note on the calculation of the fire resistance of composite columns provides design information in the form of buckling curves for various cross-section dimensions, profiles and reinforcement and for periods of standard fire exposure of 30, 60 ,90 and 120 minutes [ECCS, 1988].

Several approaches are available which address the fire resistance design of composite beams. Kruppa and Zhao represent a simple method to calculate the fire resistance of composite beams, covering both thermal and mechanical response [Kruppa and Zhao, 1995].

For this study the finite difference method has been chosen. The principal reason is that the finite difference method enables a wide variation of geometry, and material properties to be handled easily on small size computers. This method is also applied due to its simplicity in solving mathematically complex problems.

2.4.4 Development of computer programs for composite floor exposed to Fire

Several finite element packages are available for general nonlinear analysis of structure. For instance, programs available at City University include ANSYS and ABAQUS. These programs cannot be altered and therefore their capabilities are fixed. The programs cannot be conveniently used for fire analysis of composite floor.

Several computer programs were specifically designed to model these high-temperature phenomena, including FIRES-RC II [Iding et al., July 1977], FASBUS II [Iding, et al., July 1987].

DIANA and CEFICOSS are programs based on finite element method which could be used to analyse composite floors during fire exposure. Calculations with these programs take a lot of computer time on a large computer owing to the size of the problem. Furthermore, much effort is required from the user in learning the complicated structure of the code and the software producers are obliged to give much support in adapting these sophisticated programs.

In 1968, the American Iron and Steel Institute sponsored research at Illinois Institute of Technology Research Institute (IITRI) to develop a nonlinear finite element structural analysis computer program. The aim was to enable engineers to assess the structural

performance of steel deck and structural concrete floors supported by steel framing under uncontrolled fire exposure.

The program, FASBUS I (Fire Analysis of Steel Building Systems) was completed in 1972 [Chiapetta, et al., 1972]. Refinements to the program to make it more user friendly were continued in 1978 at the University of California and later at the consulting firm of Wiss, Janney, Elstner and Associates (WJE).

FASBUS II is a computer program for structural analysis only [Jeanes, 1985]. The program was completed in 1981 and is described in the WJE Final Report [Bresler and Iding, 1982].

FIRES-T3 is a computer program for calculating heat transfer from fire to structure [Iding, et al., 1977]. TASEF-2 and STABA are computer programs for thermal analysis only. HADAPT program [S. Lamont, et al., 2001] has been used to model the heat transfer to the composite steel and concrete slab. These programs are based on finite element method and have many limitations leading to very general input instruction which tend to be cumbersome.

Computer programs have also been developed based on the finite difference method such as TRAPSI [Lie, T.T. 1984] and (TACS-FIR) program [Ma, Z. and Makelainen, P., 1999] which coded in Fortran 77. The material thermal properties at elevated temperature can be selected by the user. The conductivity of concrete can be specified

to remain approximately as that at maximum temperature instead of the current temperature in the cooling phase. these programs for thermal analysis only.

VULCAN is a computer program which has been developed at the University of Sheffield to model the behaviour of composite buildings in fire. The program is based on a 3D non-linear finite element procedure in which a composite building is modelled as an assembly of beam-column, spring, shear connector and slab elements. The beam-column line element is three-noded, and its cross-section is divided into a matrix of segments to allow for variation of temperature, stress and strain through the cross-section [Huang, et al., 2004]. Slabs are modelled using nine-noded layered plate elements based on Mindlin-Reissner theory, in which each layer can have different temperature and material properties [Huang, et al., 2003]. Both material and geometric non-linearity are considered in beam-column and slab elements.

2.5 Summary

It has been shown that extensive research has taken place on fire resistance of structures. The analytical assessment of fire resistance includes four principal aspects: fire exposure, material effects, thermal response, and structural response considering the boundary conditions.

There are several ways to determining the fire resistance. The most common method is the experimental fire test. Theoretical predictions, such as empirical equations, were developed and validated by curve fitting of test results.

Full-scale fire tests are expensive. As an alternative to full-scale fire tests, numerous numerical and theoretical models have been developed to simulate the performance of a structure exposed to fire.

Considerable research has been undertaken on composite structural systems due to their characteristics of high strength and stiffness, ductility, and fire resistance.

Conclusions drawn from the extensive testing of steel deck composite construction show that:

- The ability of the beams and floors in a composite building to withstand temperatures up to 1200°C without fire protection shows that there are large reserves of fire resistance in modern steel deck composite buildings.
- Floors provide support to beams in fire conditions and structural stability can be maintained at very high temperatures.
- Floors retain their integrity and the steel deck soffit prevents spalled concrete from falling.
- Deformation, if it occurs, does not happen suddenly or unexpectedly but proceeds by slow, visible and ductile movement
- At Cardington and Broadgate, the beams were not fire protected. This had the effect of greatly increasing the distance the floor slab was spanning, but no collapse occurred. The reason is that in some of the Cardington tests the slab acted as a membrane and was supported by the colder perimeter beams and protected columns.

In view of the importance of composite floor in modern steel and composite structural systems, it becomes imperative to develop a tool for the detailed strength analysis of the floor, right up to collapse, using accurate structural mechanics. In the next chapter a new method of analysis of such floors is presented, using the versatile finite difference method.

CHAPTER 3

THEORY

3.1 Introduction

A new method of analysis for composite floor system exposed to non-uniform heating under fire forms the key part of this research. This is a three-step process involving estimate of fire exposure, heat flow analysis for calculating temperatures, followed by a strength analysis to calculate deflections and eventual failure as the fire temperature grows. The strength analysis is influenced by the thermal analysis, but it assumed that the thermal analysis is not influenced by the strength analysis.

The overall procedure is shown in Fig 3-1.

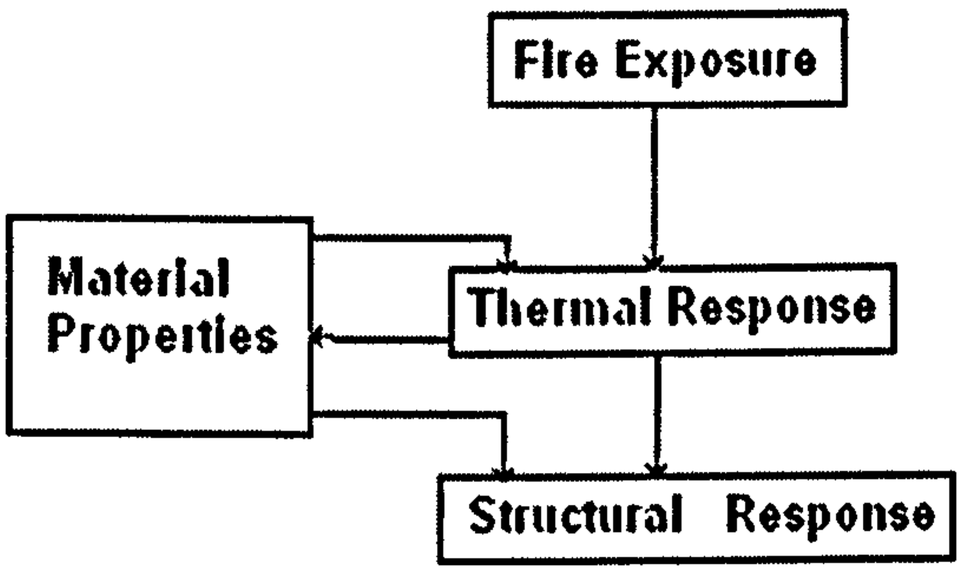

Fig. 3-1 Analytical method's framework

The finite difference method is used to solve the heat flow problem and calculate the temperature distribution within the composite floor. The temperature values influence the strains and stresses. The finite difference method is also used to solve the orthotropic plate differential equation to determine equilibrium deflections at a given

stage of fire growth. The proposed method uses a novel approved for the calculation of plate rigidities, which are needed in the solution of the orthotropic plate equation. The new method takes into account fully nonlinear stress-strain relationships for steel and concrete.

The following assumptions are made:

1- The strain distribution due to bending is linear

2- There is no slip between steel and concrete

3- Shear deformations are ignored

4- Creep is implicitly taken into account in the stress-strain relations according to Euro-code 4 (1994)

5- The influence of the air gap between the steel sheet and the concrete mass is ignored. As the air gap has an effect similar to insulation, the assumption is on the safe side.

6- The stiffness in the weak direction comes from the smaller thickness in the composite floor, ignoring the trapezoidal part of the deck. In the strong direction, a full profile of the deck is used

3.2 Fire Curves

The first step in this method is to predict the temperature of fire development. Fire exposure is usually described by a temperature–time curve of the surrounding air as experienced in typical fires. The analysis method is equally applicable for any fire curve, including user-specified natural fire curve.

3.2.1 Standard fire curves

As has been discussed in chapter 2, much of the testing and analysis is based on the standard fire curves. The most widely used test specifications are ISO 834 [ISO, 1975]. In the ISO 834 the temperature T (°C) is defined by equation (2-2).

The current analysis is equally valid for any fire curve such as the two shown in Fig.3-2.

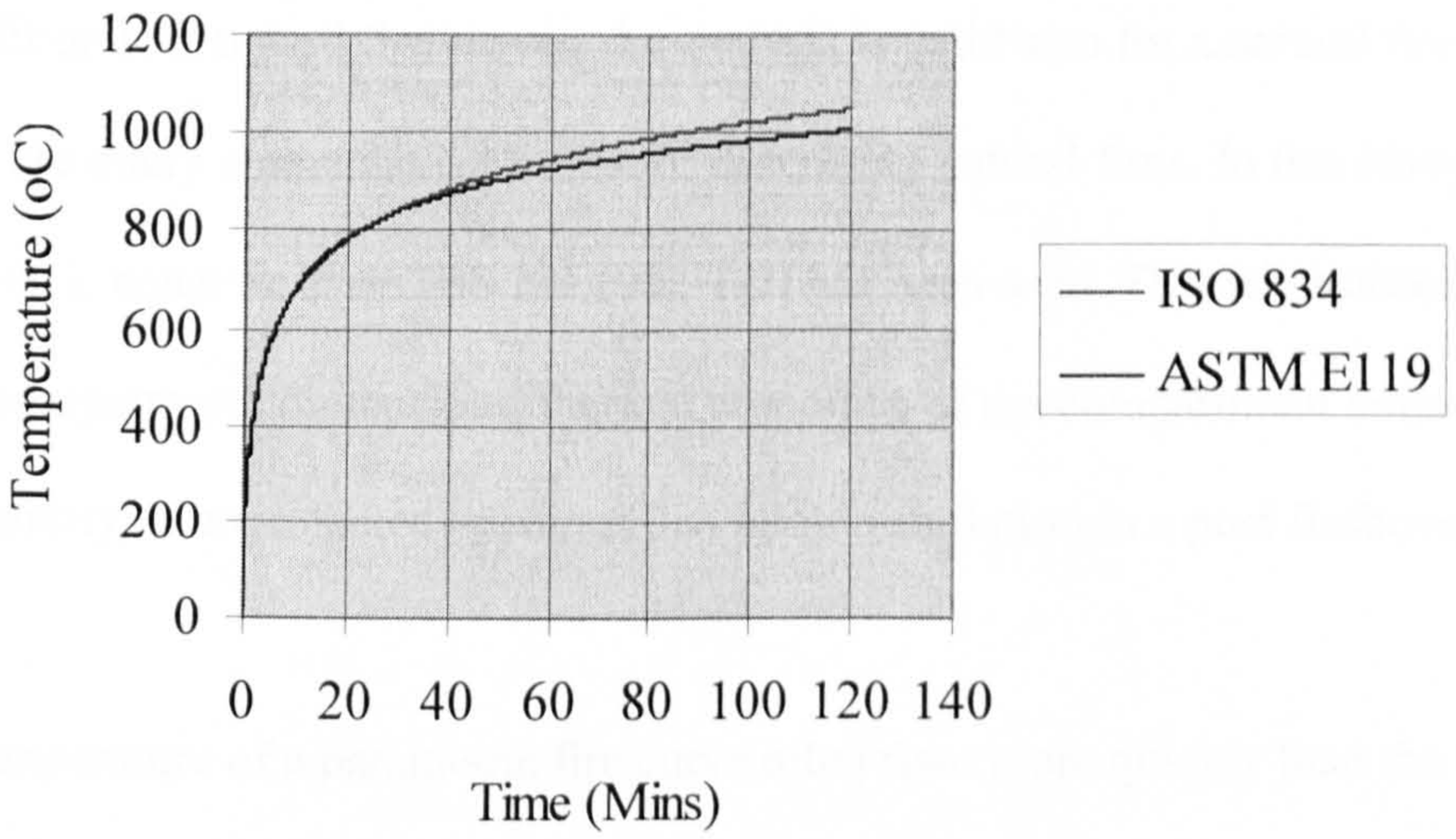

Fig.3-2 Standard fire curves

For stability and precision, a criterion relating the time step to the element width must be satisfied. An appropriate time increment should be equal or less than the proposed time increment [Lie, T.T.1992] which is given by the condition:

$$dt_{proposed} = \frac{dxdy\rho_c C_{cmin}}{4K_{\max} + dxH_{\max}} \qquad (3.1)$$

Where:

$dt_{proposed}$: Proposed time increment

$\rho_C C_{cmin}$ = minimum thermal capacity of the concrete

K_{max} = maximum thermal conductivity of the concrete

H_{max} = 675 w/m^2 ^{o}C (maximum value of the coefficient of heat transfer during exposure to the standard fire)

3.2.2 Natural Fire Curve

In addition to standard fire curves, the analysis is valid also for a natural fire curve. There are many mathematical forms for describing natural fires. In this study, the parametric equation from [BS EN 1991-1-2] has been used. This takes account of fuel load, compartment dimensions, thermal properties of the compartment boundaries, and the quantity of unprotected openings that allow ventilation in a post flashover fire.

The temperature of a parametric fire curve often rises more quickly than the standard fire curve in the early stages but, as the combustibles are consumed, it will begin to fall in temperature as illustrated in Fig. 1-2, Chapter 1.

3.3 Theory of Thermal Analysis

The thermal response is a solution of the heat transfer problem with fire at the exposed under side of the floor and the heat transfer to the floor. The types of heat transfer are conduction, convection, and radiation. Due to the profiled shape of the sheeting, heat transfer is essentially two-dimensional. Data needed for heat transfer calculation are material properties such as conductivity, specific heat and the convection and radiation

boundary conditions. Guidance on these data may be obtained from [Eurocode 4–1994, Part 1-2].

The main parameters with regard to the thermal behaviour depend on the geometry of the steel sheet, concrete depth, type of concrete and insulation. For the present, the trapezoidal profile as in Fig. 3-3 has been adopted for explanation of the method.

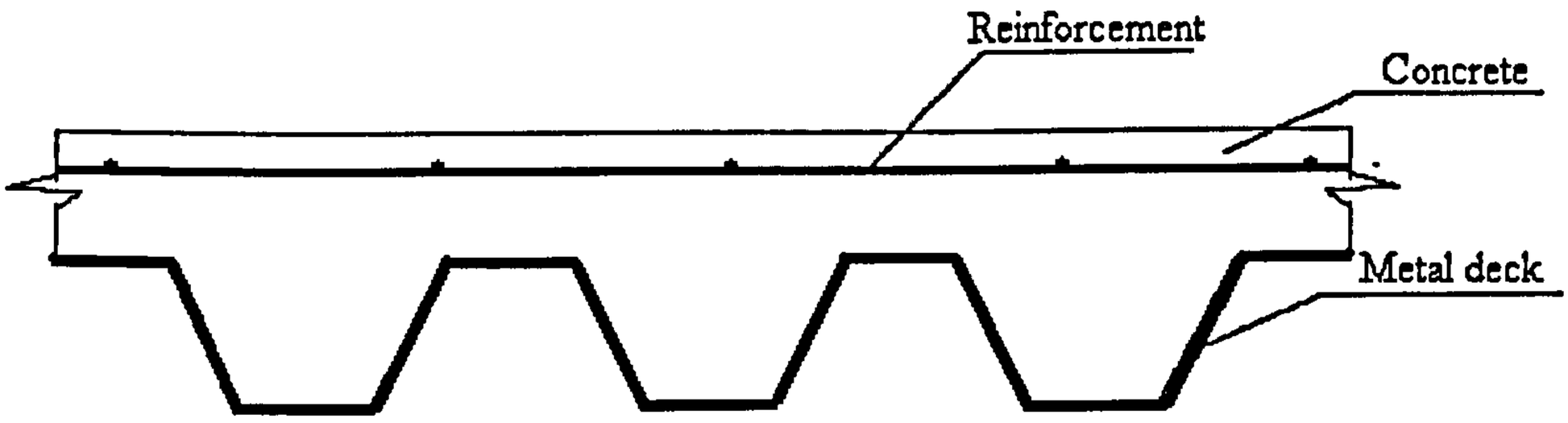

Fig. 3-3 Trapezoidal metal deck composite floor

It is assumed that the temperature of the surrounding air is a prescribed function of time. It is assumed that heat flow within the plane of the floor is negligible. To simplify the calculations it is assumed that the cross-section is symmetrical with respect to a vertical line, so that the temperature is also distributed over the section in a symmetrical way. In order to obtain the temperature and its gradients with sufficient accuracy, the cross-section has to be discretized with a relatively dense mesh, whether the calculations are done by the finite difference or the finite element method.

The steel bars occupy only a small volume as regards the whole cross-section. Hence, it is assumed that the heat transfer is not influenced by the reinforcement. The temperature of the reinforcing bar does not significantly differ from the corresponding

concrete temperature [Zhao, 2000]. Lie and Irwin [Lie, et al., 1993] show that the differences in temperature in the concrete and in the embedded steel bar at the contact are small. The temperature in the steel bar is, therefore, assumed as being that of concrete at its location.

The heat conduction problem is governed by the differential equation of heat conduction. The effects of heat radiation and heat convection from air to the floor surface are accounted for via the boundary conditions.

Fourier's dimensional equation for heat conduction can be used if the thermal properties are constant (i.e. not temperature-dependent) and the heat transfer in the composite floor without moisture, is as given below:

$$K\left(\frac{\partial^2 T}{\partial x^2}+\frac{\partial^2 T}{\partial y^2}\right)=\rho C\frac{\partial T}{\partial t} \qquad (3.2)$$

Where:

K: thermal conductivity

x and y: are the point coordinate in a two-dimensional space.

T: temperature

t: time

ρ : density

C: heat capacity

As already indicated in [Eurocode 4], the thermal properties are dependent on temperature. Equation (3.3) has to be used instead of Equation (3.2), that is:

$$\frac{\Delta}{\Delta x}(K\frac{\Delta T}{\Delta x})+\frac{\Delta}{\Delta y}(K\frac{\Delta T}{\Delta y})=\rho C\frac{\Delta T}{\Delta t} \qquad (3.3)$$

3.3.1 Thermal Properties

Material properties for concrete and steel are given in [Eurocode 4 – 1989]. There are:

- **Concrete**

$\rho_c = 2350 \ \ kg/m^3$

$$C_c = 900+80(\frac{T}{100})-4(\frac{T}{100})^2 \quad J/kg.K \qquad (3.4)$$

$$K_c = 2-0.24(\frac{T}{100})+0.012(\frac{T}{100})^2 \ W/m.K \qquad (3.5)$$

- **Steel**

$\rho_s = 7800 \ kg/m^3$

$$C_s = 470+20(\frac{T}{100})-3.8(\frac{T}{100})^2 \quad J/kg.K \qquad (3.6)$$

$$K_s = 54-3.33(\frac{T}{100}) \ W/m.K \qquad (3.7)$$

Material properties for concrete and steel are given in [Lie T.T., 1992] as the following:

- **Concrete**

-Thermal Capacity $\rho_c C_c$

$\rho_c C_c = (0.005T + 1.7) * 10^6 \ Jm^{-3} \ ^oC^{-1}$ *For* $0 \le T \le 200\ ^o$ (3.8)

$\rho_c C_c = 2.7 * 10^6 \ Jm^{-3} \ ^oC^{-1}$ *For* $200 < T \le 400\ ^oC$ (3.9)

$\rho_c C_c = (0.013\ T - 2.5) * 10^6 \ Jm^{-3} \ ^oC^{-1}$ *For* $400 < T \le 500\ ^oC$ (3.10)

$$\rho_c C_c = (-0.013\,T + 10.5) * 10^6\ Jm^{-3}\,^oC^{-1} \quad For\ 500 < T \leq 600\ ^oC \quad (3.11)$$

$$\rho_c C_c = 2.7 * 10^6\ Jm^{-3}\,^oC^{-1} \quad For\ T > 600\ ^oC \quad (3.12)$$

-Thermal Conductivity K_c

$$K_c = -0.00085T + 1.9\ \ W/m^oC \quad For\ 0 \leq T \leq 800\ ^oC \quad (3.13)$$

$$K_c = 1.22\ \ W/mC \quad For\ T > 800\ ^oC \quad (3.14)$$

- **Steel**

-Thermal Capacity $\rho_s C_s$

$$\rho_s C_s = (0.004T + 3.3) * 10^6\ Jm^{-3}\,^oC^{-1} \quad For\ 0 \leq T \leq 650\ ^oC \quad (3.15)$$

$$\rho_s C_s = (0.068T + 38.3) * 10^6\ Jm^{-3}\,^oC^{-1} \quad For\ 650 < T \leq 725\ ^oC \quad (3.16)$$

$$\rho_s C_s = (-0.086T + 73.35) * 10^6\ Jm^{-3}\,^oC^{-1} \quad For\ 725 < T \leq 800\ ^oC \quad (3.17)$$

$$\rho_s C_s = 4.55 * 10^6\ Jm^{-3}\,^oC^{-1} \quad For\ T > 800\ ^oC \quad (3.18)$$

-Thermal Conductivity (K_s)

$$K_s = -0.022T + 48\ \ W/m^oC \quad For\ 0 \leq T \leq 900\ ^oC \quad (3.19)$$

$$K_s = 28.2\ \ W/m \quad For\ T > 900\ ^oC \quad (3.20)$$

3.3.2 Solution by the Finite Difference Method

Heat flow equations can be solved either by the finite element method or the finite difference method. The finite element method is appropriate for analysis of thermal problems with complex geometry. Many general-purpose computer programs are based on this method. Although computer processing times are no longer a significant disadvantage these methods still in role, greater complexity in formulation and

programming. For two-dimensional problems with relatively simple geometries it is therefore more convenient to use the finite difference method [Jaluria and Torrance, 1986]. Hence, in this study, the thermal analysis based on the finite difference method is used to describe the heat flow in the composite floor exposed to fire.

The cross-section is divided into five parts, mainly rectangular elements. Sloping boundaries are approximated by triangular elements as shown in Fig. 3-4. The concrete depth is important as regards the temperature on the unexposed side.

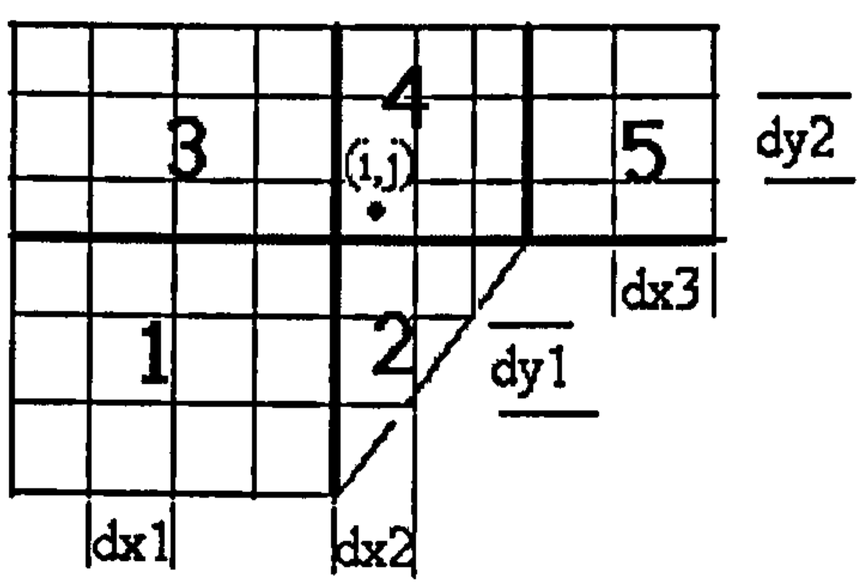

Fig.3-4 the cross-section is divided into rectangular and triangular elements

The temperature at any point is designated as $T_{i,j}$. For a problem in transient conduction the temperature at any time will be denoted by $T_{i,j}^{m}$. The next time step is labelled as m+1 and the temperature at that instant as $T_{i,j}^{m+1}$.

3.3.3 Heat Flow at an Internal Node

Whenever a temperature gradient exists, heat will flow from the higher temperature to the lower temperature region. The heat transfer is considered for the control-volume finite-difference method, as this method is widely used in the numerical simulation of heat transfer [Eymard, et al., 1998, 2000]. The method first defines the control volume,

which is a fixed region in space bounded by a control surface through which heat can pass. Next are defined all the energy flows into and out of the control volume boundaries and the volumetric terms, including the heat generation and energy storage terms. This method has been described by Frank and Mark [Frank, et al., 1993]. The current analysis is based on this method.

Fig 3-5 shows the control volume, in two-dimensional conduction for internal node. The control volume size is Δx by Δy and it is centred about the node i,j. the x nodes are identified by:

$$x_i = (i-1)\Delta x \qquad i = 1, 2, \ldots, \text{m}$$

$$y_j = (j-1)\Delta y \qquad j = 1, 2, \ldots, \text{n}$$

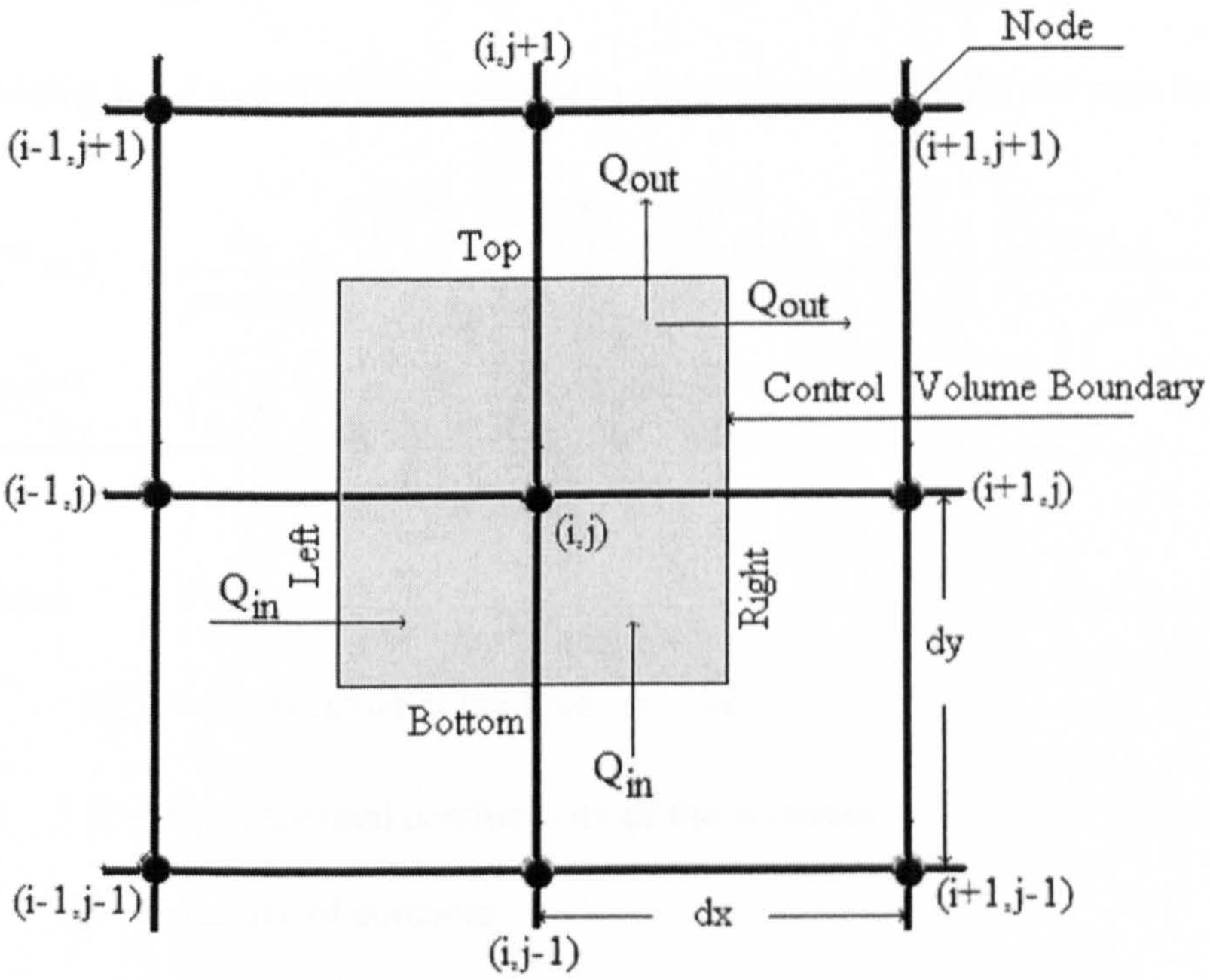

Fig. 3-5 Control Volume for Two Dimensional Conduction (Internal node)

The principle of conservation of energy for the control volume can be stated as follows:

Rate of heat conduction into control volume		Rate of heat conduction out of control volume
+	=	+
Rate of heat generation into control volume		Rate of energy storage inside volume

The overall heat balance on the control volume, ignoring heat generation into control volume is therefore:

$$-K\left(\frac{T^m_{i,j}-T^m_{i-1,j}}{\Delta x}\Delta y+\frac{T^m_{i,j}-T^m_{i,j-1}}{\Delta y}\Delta x\right)$$
$$=-K\left(\frac{T^m_{i+1,j}-T^m_{i,j}}{\Delta x}\Delta y+\frac{T^m_{i,j+1}-T^m_{i,j}}{\Delta y}\Delta x\right)+\rho c\Delta x\Delta y\frac{T^{m+1}_{i,j}-T^m_{i,j}}{\Delta t} \quad (3.21)$$

Dividing by $K\Delta x\Delta y$ therefore the inside node's temperature for the next time step is:

$$T^{m+1}_{i,j}=T^m_{i,j}+\frac{\Delta t}{\rho c\Delta x\Delta y}\left(\frac{K(T^m_{i,j+1}-T^m_{i,j})}{\Delta y^2}+\frac{K(T^m_{i+1,j}-T^m_{i,j})}{\Delta x^2}+\frac{K(T^m_{i-1,j}-T^m_{i,j})}{\Delta x^2}\right.$$
$$\left.+\frac{K(T^m_{i,j-1}-T^m_{i,j})}{\Delta y^2}\right) \quad (3.22)$$

where:

$T^{m+1}_{i,j}$ = temperature at the time $(m+1)dt$

K = the thermal conductivity of the concrete.

ρ = density of concrete

c = pacific heat of concrete

Variable thermal conductivity appropriate for determining the flux at the left and right faces of the control volume in Fig. 3-5 can be calculated as suggested by [Patankar, 1980]:

$$K_{left} = \frac{2k_{i,j}k_{i-1,j}}{k_{i,j} + k_{i-1,j}} \qquad (3.23) \qquad K_{right} = \frac{2k_{i,j}k_{i+1,j}}{k_{i,j} + k_{i+1,j}} \qquad (3.24)$$

$$K_{bottom} = \frac{2k_{i,j}k_{i,j-1}}{k_{i,j} + k_{i,j-1}} \qquad (3.25) \qquad K_{top} = \frac{2k_{i,j}k_{i,j+1}}{k_{i,j} + k_{i,j+1}} \qquad (3.26)$$

3.3.4 Heat Flow at a Boundary Node

At the boundaries of the floor (exposed and unexposed surface), relations exist between the heat transfer in the floor and the heat transfer between surface and the compartment. Since the steel sheet is very thin, the influence of its heat capacity on the heat transfer can be neglected.

At the exposed surface of the floor, it is required that the heat flow to the floor is in balance with that into the floor.

Consider the control volume $dx.\frac{dy}{2}$ as shown by the shaded area in Fig.3-6.

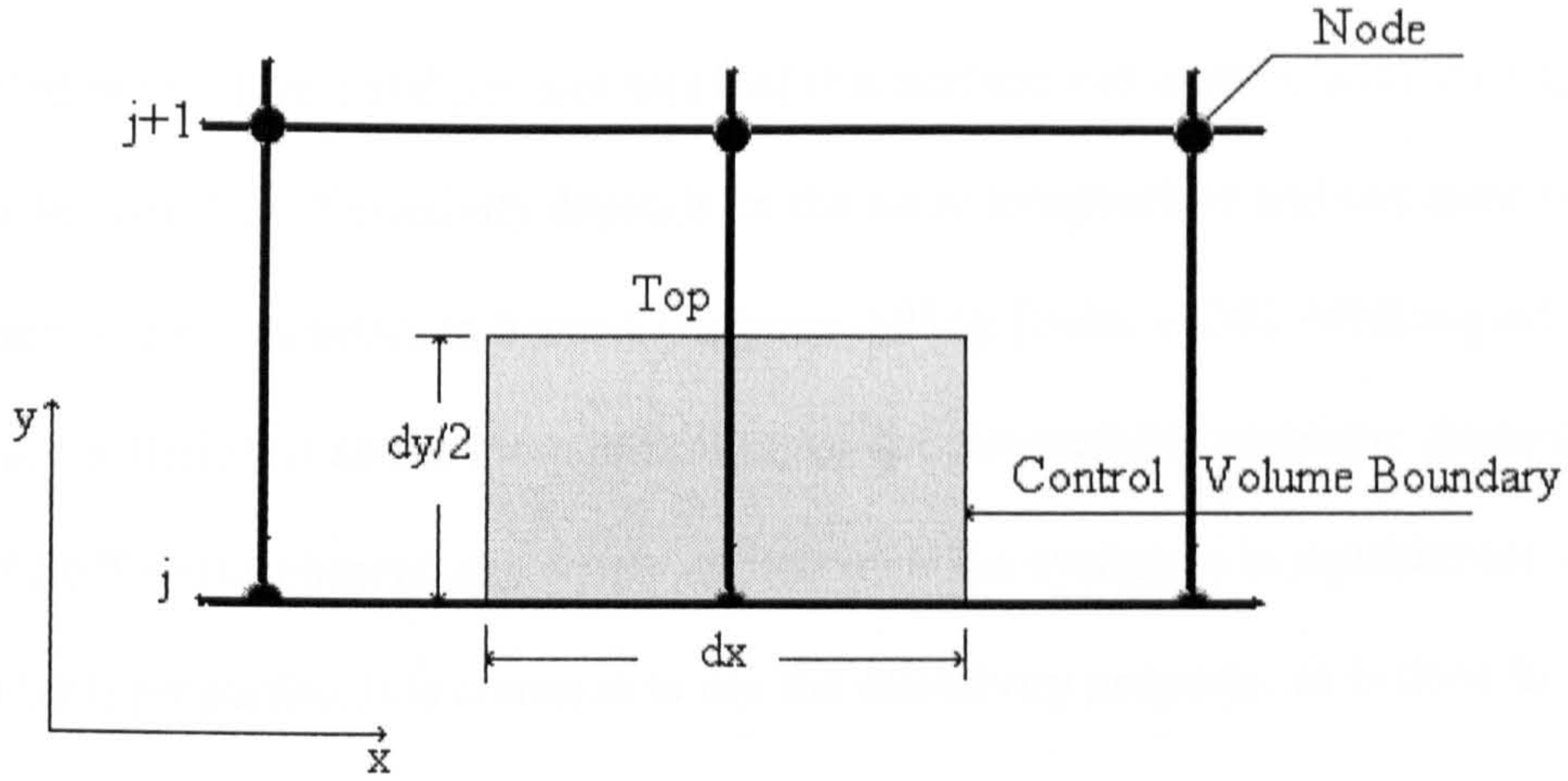

Fig. 3-6 Control Volume for Two-Dimensional Conduction (Boundary)

From point i,j, it is assumed that following same procedure of heat flow in the internal node but here the heat is transferred by conduction to the three neighbouring points. Then adding the heat transfer from fire to an elementary surface region along the boundary elements during a period which = $Q.dx$

When:

$$Q = \sigma \varepsilon_f \varepsilon_c [(T_f^m + 273)^4 - (T_{i,j}^m + 273)^4] \qquad (3.27)$$

Where:

Q = heat flow out of the bottom face in y direction at point i,j at time m

σ = $5.67 * 10^{-8} W / m^2 K^4$ (Stefan Boltzmann Constant)

ε_f = emissivity of the fire

ε_c = emissivity of the concrete

The emissivity of a surface is defined as the ratio between the emissive power, (energy emitted per unit time and per unit area), of that surface and a black body having the same temperature. Emissivity depends on the same temperature and the material of the surface and varies between 0 and 1 [Holman, 1986]; [Sala, 1986]. With regard to surface materials it seems more logical to use the absorptivity property. According to Kirchhoff's law, absorptivity equals emissivity if the system is in equilibrium. Rather than both properties, it is common to use the emissivity property, as is done in this thesis.

Then the control volume energy balance is as following:

$$\frac{K^m_{i+1,j}+K^m_{i,j}}{2}\frac{(T^m_{i+1,j}-T^m_{i,j})}{dx}\frac{dy}{2}+\frac{K^m_{i,j+1}+K^m_{i,j}}{2}\frac{(T^m_{i,j}-T^m_{i,j+1})}{dy}dx$$

$$=\frac{K^m_{i-1,j}+K^m_{i,j}}{2}\frac{(T^m_{i,j}-T^m_{i-1,j})}{dx}\frac{dy}{2}+\frac{\rho c(dxdy)}{2}\frac{(T^{m+1}_{i,j}-T^m_{i,j})}{dt}+Q.dx \qquad (3.28)$$

Equation (3.28) can be rearranged to give an equation for the boundary temperature at the next time step:

$$T^{m+1}_{i,j}=T^m_{i,j}+\frac{2dt}{(\rho c dxdy)_{i,j}}\{\frac{K(T^m_{i,j+1}-T^m_{i,j})}{dy}dx+\frac{K(T^m_{i+1,j}-T^m_{i,j})}{dx}\frac{dy}{2} \qquad (3.29)$$

$$+\frac{K(T^m_{i,j}-T^m_{i-1,j})}{dx}\frac{dy}{2}+Q^m_{i,j}dx\}$$

Following same procedure for inclined boundaries as illustrated at Fig.3-7.

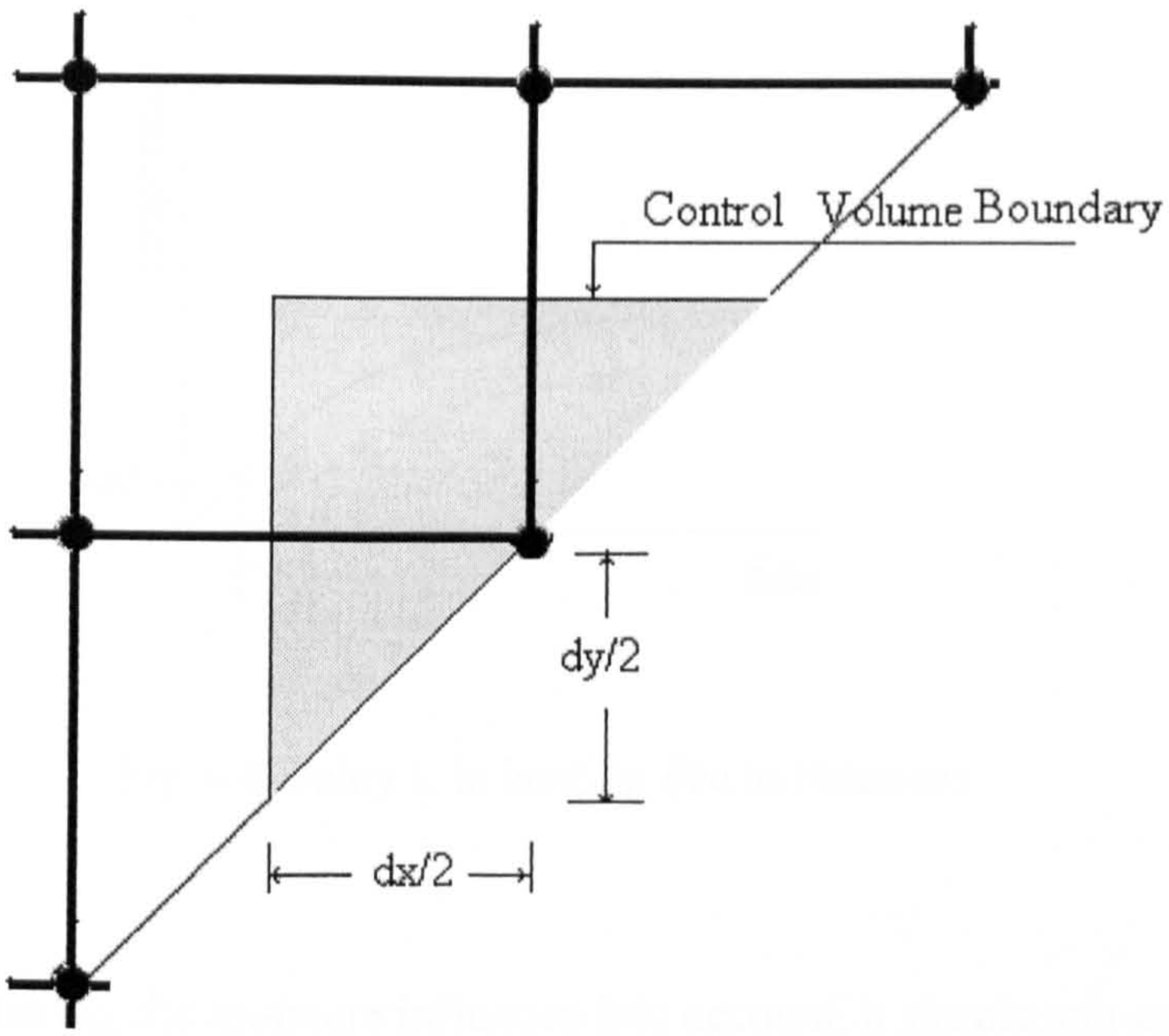

Fig. 3-7 Boundary control volume for inclined node

The inclined boundary temperature at the next time step is:

$$T_{i,j}^{m+1} = T_{i,j}^{m} + \frac{4dt}{(\rho c dx dy)_{i,j}} \{ \frac{K(T_{i,j+1}^{m} - T_{i,j}^{m})}{dy} \frac{dx}{2} + \frac{K(T_{i+1,j}^{m} - T_{i,j}^{m})}{dx} \frac{dy}{2} + (\frac{dx}{2} + \frac{dy}{2}) + Q_{i,j}^{m} dx \} \quad (3.30)$$

3.3.5 Formula which take moisture influence into account

It is assumed that the moisture evaporates as soon as a certain temperature is reached:

100°C. For evaporation of the moisture a certain amount of energy is needed. This retardation is schematically illustrated in Fig. 3-8.

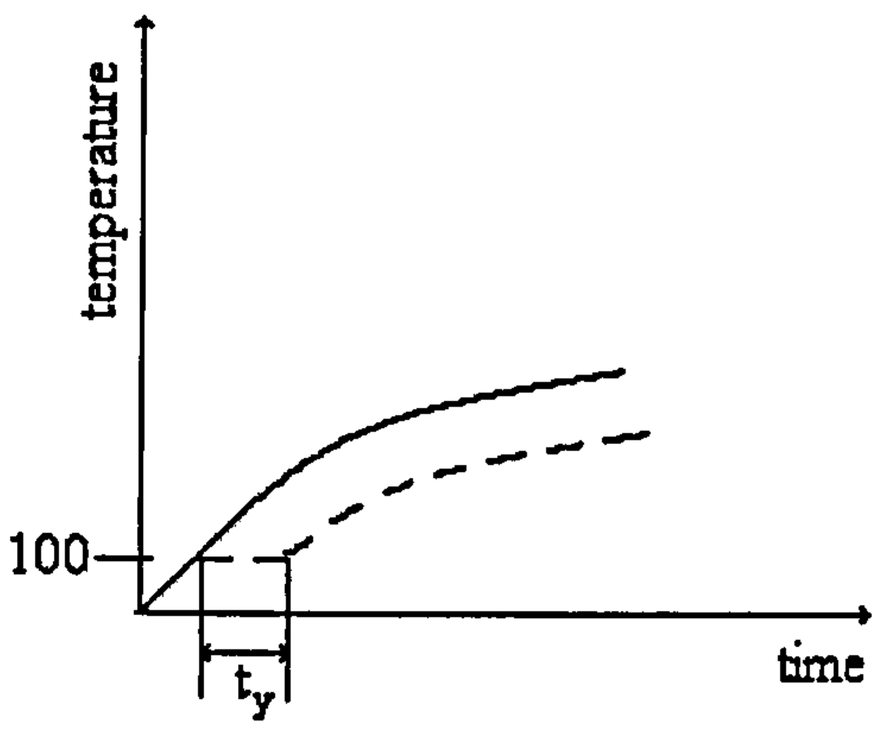

Fig 3-8 Delay t_y in heating due to moisture

For taking the moisture influence into account, a simple sub-program is used in the present research. The energy needed for this evaporation is calculated with Equation (3.31) for internal node and (3.32) for boundaries.

$$T_{i,j}^{m+1} = T_{i,j}^{m} + \frac{dt}{(\rho_c c_c dxdy)_{i,j} + \rho_w c_w \Phi} \{ \frac{K(T_{i,j+1}^{m} - T_{i,j}^{m})}{dy^2} + \frac{K(T_{i+1,j}^{m} - T_{i,j}^{m})}{dx^2} + \frac{K(T_{i-1,j}^{m} - T_{i,j}^{m})}{dx^2} + \frac{K(T_{i,j-1}^{m} - T_{i,j}^{m})}{dy^2} \} \quad (3.31)$$

Also introducing the moisture effect

$$T_{i,j}^{m+1} = T_{i,j}^{m} + \frac{2dt}{(\rho_c c_c dxdy)_{i,j} + \rho_w c_w \Phi_w} \{ \frac{K(T_{i,j+1}^{m} - T_{i,j}^{m})}{dy^2} dx + \frac{K(T_{i+1,j}^{m} - T_{i,j}^{m})}{dx} \frac{dy}{2} + \frac{K(T_{i,j}^{m} - T_{i-1,j}^{m})}{dx} \frac{dy}{2} + Q_{i,j}^{m} dx \} \quad (3.32)$$

Where:

$\rho_w C_w = 4.2 * 10^6$ $Jm^{-3}\,{}^{o}C^{-1}$ (Thermal capacity of water)

The temperature at the central point represents the temperature of the elements. The temperature of each element is stored for use in calculating the material properties in the strength analysis. The element temperature is output at the specified times.

3.4 Theory of Strength Analysis

The analysis of the strength response of a composite floor exposed to fire is essentially a solution of the deformation problem. Study of the strength response to fire leads to the understanding of the mechanisms behind the deformation response.

Orthotropic plate theory forms the basis of this analysis. The present method uses an innovative method for calculating the plate rigidities required in the analysis.

In the classical orthotropic plate theory, since the plate thickness is constant and the plate material is continuous, as required by the general conditions, the different elastic properties in the two principal directions must be due to different modulus of elasticity, $E_x \neq E_y$ and different Poisson's ratios $v_x \neq v_y$.

The elastic properties of an orthotropic plate are defined by three rigidity coefficients:

$D_x =$ the flexural rigidity of the plate in the x-direction

$D_y =$ the flexural rigidity of the plate in the y-direction

$D_{xy} =$ the effective torsional rigidity

The rigidities D_x and D_y, characterize the resistance to flexure of a plate strip having a unit width and a thickness t, in the x- or y-direction, respectively and are defined by the formulas:

$$D_x = \frac{E_x t^3}{12(1-\upsilon_x \upsilon_y)}; \qquad D_y = \frac{E_y t^3}{12(1-\upsilon_x \upsilon_y)} \tag{3.33}$$

The effective torsional rigidity, D_{xy}, characterizing the resistance of a plate element to twisting, is based on certain analytic consideration. An approximation for the effective torsional rigidity of orthotropic plate is obtained by Huber [Timoshenko, 1959] and defined by the formula:

$$D_{xy} = \sqrt{D_x D_y} \tag{3.34}$$

A reasonable approximation can be introduced. In this study the following approximation has been used:

$$D_{xy} = D_y \tag{3.35}$$

The following differential equation for orthotropic plate often referred to as Huber's equation, can be used to determine composite floor deflection [Szilard, 1974].

$$D_x \frac{d^4 w}{dx^4} + 2D_{xy} \frac{d^4 w}{dx^2 dy^2} + D_y \frac{d^4 w}{dy^4} = q \tag{3.36}$$

Where:

w = Deflection of the plate at any point in the space coordinates

q = the loading intensity at any point, expressed as a function of the co-ordinates x and y, force per unit area

D_x, D_y, D_{xy} = Rigidities of the orthotropic plate

The rigidity in the above equation, is a measure of the member's stiffness and incorporates both material and cross-section properties. As evident in these equations, for a given moment, curvature, and hence deflection, will increase with a decrease in the rigidity. The following differential equations relate the section rigidity to deflection for a given moment:

$$M_x = D_x\left(\frac{d^2w}{dx^2} + \upsilon_y \frac{d^2w}{dy^2}\right) \qquad (3.37)$$

$$M_y = D_y\left(\frac{d^2w}{dy^2} + \upsilon_x \frac{d^2w}{dx^2}\right) \qquad (3.38)$$

3.4.1 Proposed method

Strains are related to deflections through curvature, and stresses are related to strains through constitutive relations. The temperature level and its distribution across the section affect these properties. The difference in the rigidities in the two perpendicular directions results from different geometric properties rather than different modulus of elasticity of the material as in the classical orthotropic plate theory.

As a consequence of the non-uniform temperature distribution in the cross-section and changing material properties, thermal strains and stresses develop during fire exposure.

From these, it becomes necessary to consider the effect of elevated temperature on the plate rigidities as these will no longer be constant in the cross section as the fire develops.

In order to determine the plate rigidities, a new calculation method has been adopted. The innovation in the present method is that the plate rigidities are calculated taking into account the effect of temperature on the internal stresses, which in turn contribute to the internal moment. By relating curvatures to the bending moments, the plate rigidities can be calculated.

The calculation procedure can be summarized in these steps:

- The floor is divided into a two-dimensional mesh.
- The deflections are initially assumed for each mesh point. In subsequent step, previously calculated deflections will be used to predict the deflections.
- The curvatures are calculated for all mesh points in the two planes using finite difference operators.
- The curvature (ϕ_x and ϕ_y) for all the points are calculated using the finite deference formulae.

$$\phi_x = \frac{w_{o(i+1)} + w_{o(i-1)} - 2w_{o(i)}}{\Delta_x^2} \qquad (3\text{-}39)$$

$$\phi_y = \frac{w_{o(i+n)} + w_{o(i-n)} - 2w_{o(i)}}{\Delta_y^2} \qquad (3\text{-}40)$$

- The cross-section of the floor is divided into elements to determine the thermal response, using the procedure outlined in section 3.3.2 above.

- Using the mesh for the cross section as for thermal analysis, the net strains from thermal strains and mechanical strains are determined.
- Stresses are calculated using the non-linear temperature dependent stress-strain curves.
- Internal forces are calculated through summations of these forces over the rectangular and triangular elements of the cross-sectional grid.
- Iteration is needed to perform for ensuring that the value of total force matches the applied in-plane force. For unrestrained edges, the in-plane force has to be zero.
- Moments calculated in the two-directions.
- The plate rigidities may then be calculated using equations (3.36)

The framework of the strength analysis is shown in Fig. 3-9

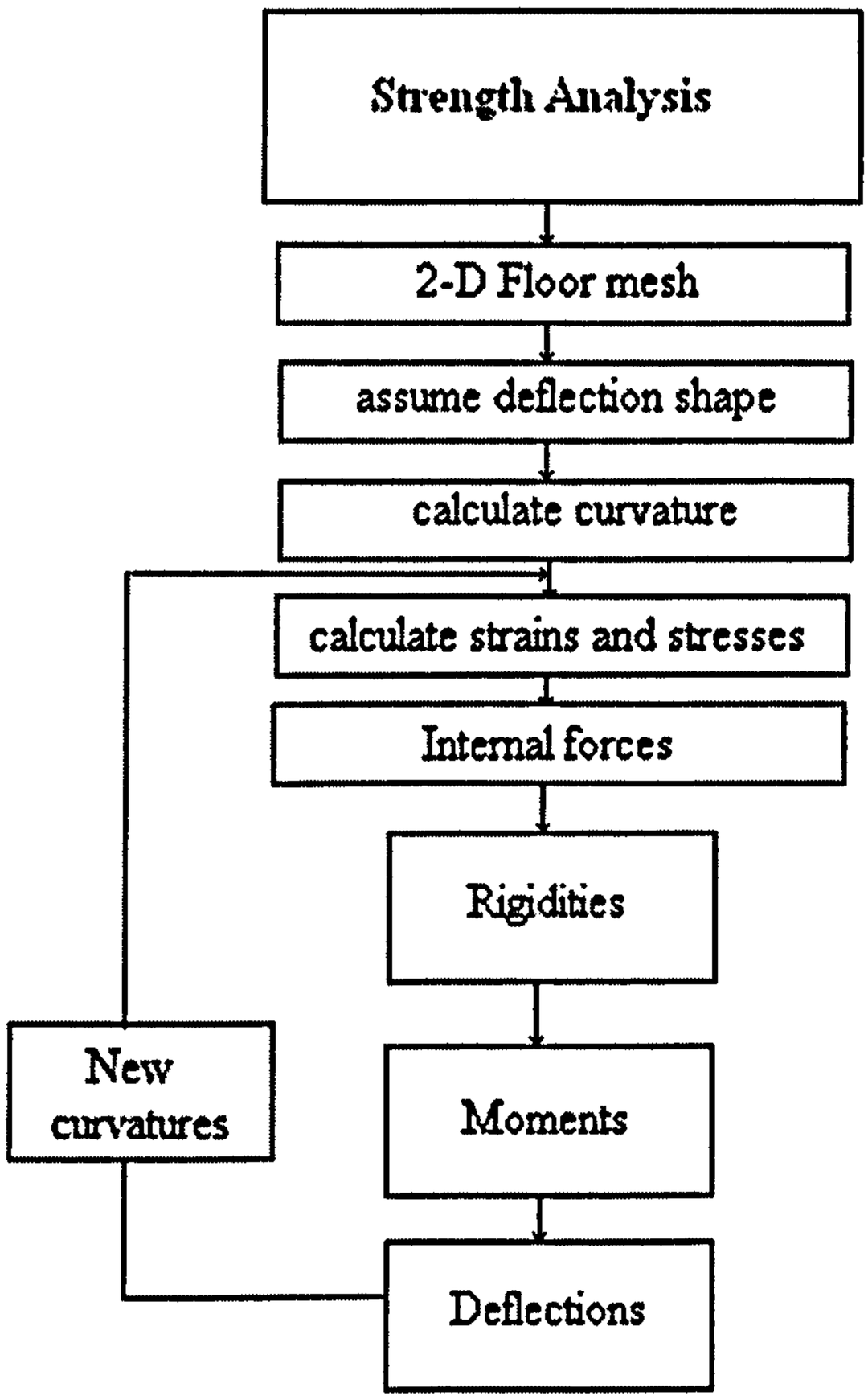

Fig. 3-9 Framework of the Mechanical Analysis

3.4.2 Solution of orthotropic plate equation

Once the time dependant distribution of the temperature over the cross-section has been determined in the thermal analysis, the novel non-linear finite difference formulation is used to determine the mechanical response of the reinforced concrete composite floor subjected to fire.

An arbitrary plan area of the floor can be divided into $n_x \times n_y$ division as shown in Fig.3-11.

For the initial deflection shape of the floor, the following formula may be used to find the initial deflection at the meshing points (m,k).

$$w_o = ASin\frac{\pi.x_m}{a}Sin\frac{\pi.y_k}{b} \qquad (3\text{-}41)$$

When:

m = 1, 2, 3,..... and k = 1, 2, 3, ...

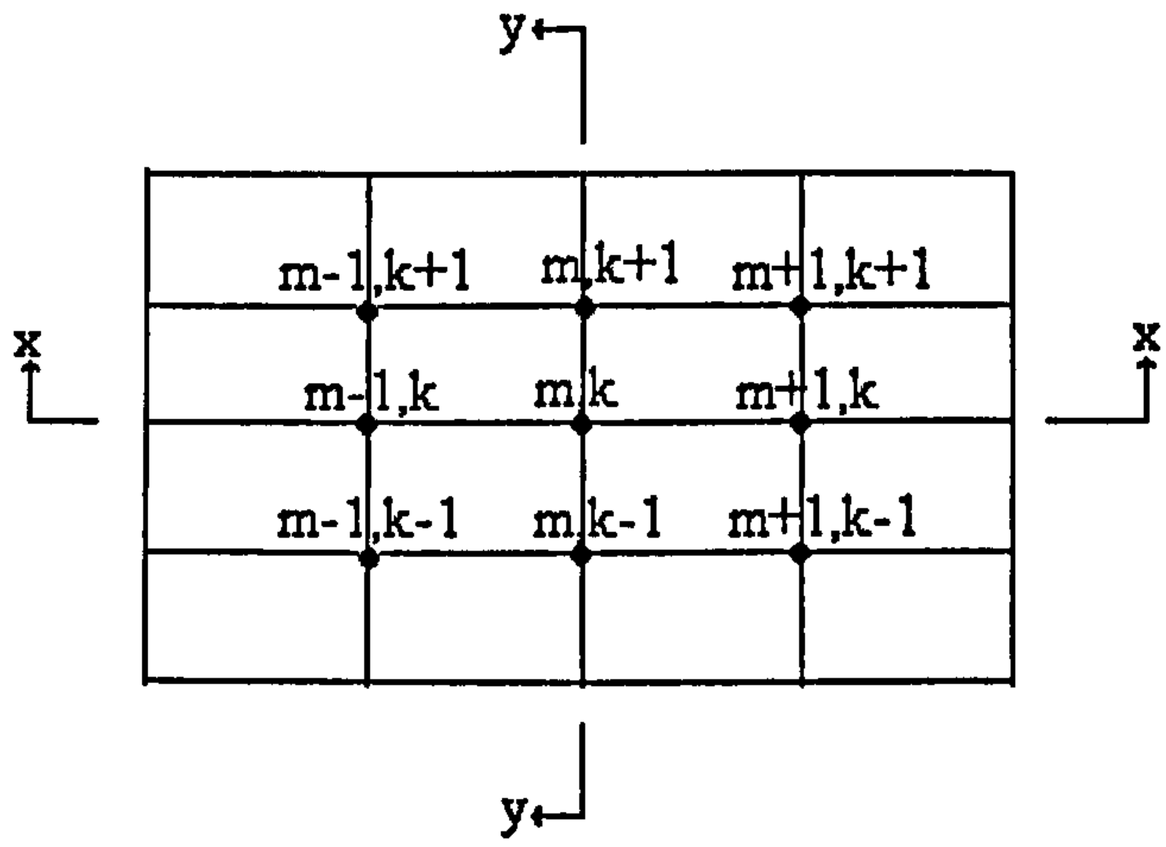

Fig. 3-10 Floor Plan

As stated above the solution is obtained by the finite difference method, the curvature then can be calculated in the two planes by using finite difference operators as in formula (3-40) for x-direction and formula (3-41) for y-direction:

$$\frac{d^2(w_o)_{m,k}}{dx^2} = \frac{(w_o)_{m,k+1} + (w_o)_{m-1,k} - 2(w_o)_{m,k}}{\Delta x^2} \qquad (3\text{-}42)$$

$$\frac{d^2(w_o)_{m,k}}{dy^2} = \frac{(w_o)_{m,k+1} + (w_o)_{m,k-1} - 2(w_o)_{m,k}}{\Delta y^2} \qquad (3\text{-}43)$$

The cross-section at Fig. 3-12 and Fig. 3-13 analyzed on the basis of the geometry, mechanical properties of the components (steel and concrete), and the temperature distribution obtained from the thermal analysis. The cross-sectional properties (moment capacity, rigidity, and deformation) are presented as a function of time and using stress-strain relations. To simplify the calculation, the same mesh is used as for the calculation of the temperatures of the floor's cross-section.

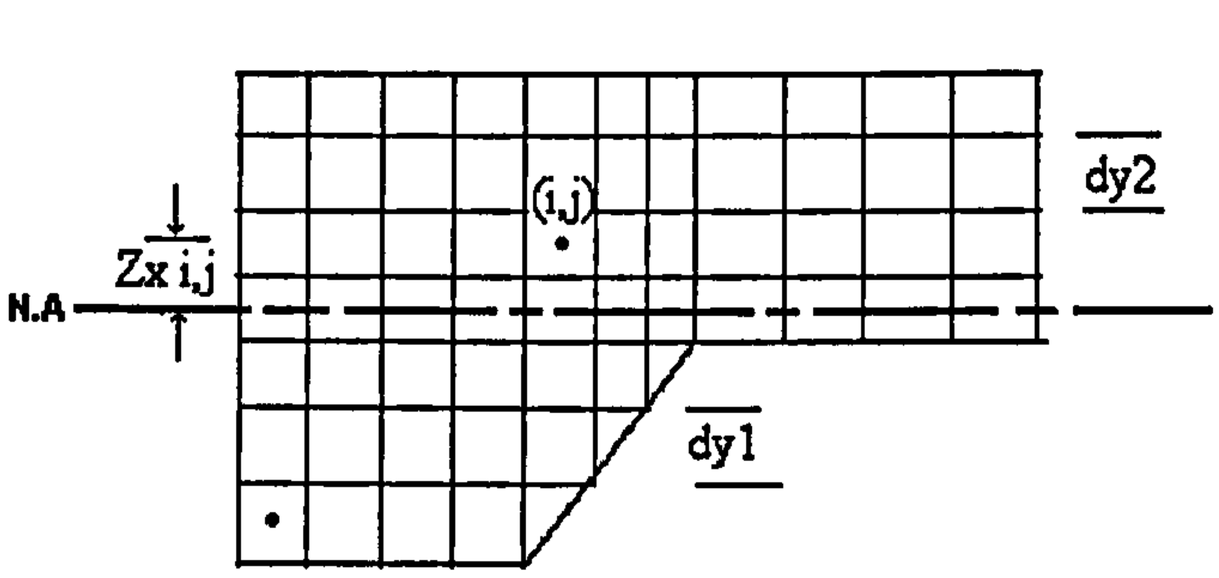

x — x

Fig. 3-11 Cross-section in X-Direction

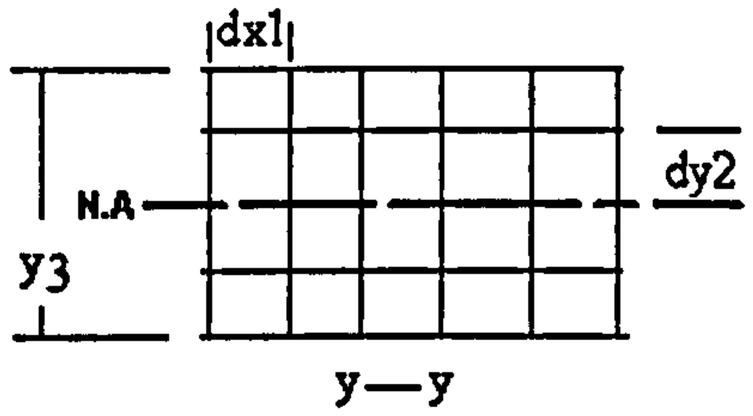

Fig. 3-12 Cross-section in Y-Direction

3.4.3 Strains Calculation

The thermal strains are superimposed on the mechanical strains associated with curvature to find the net strains. To calculate the strains, the following procedure is adopted:

a- Calculation of thermal strain

In each element of the cross section, temperature increase causes a thermal expansion and a decrease in strength and elastic properties. Consequently, the moment capacity

and flexural stiffness of the cross section decrease. The thermal expansion coefficients of concrete and steel increases with temperature as illustrated in Fig. 3-14. It shows that the expansion of concrete stops at high temperatures, (beyond 700 ^{o}C), [EUROCODE 4, 1994] because of shrinkage.

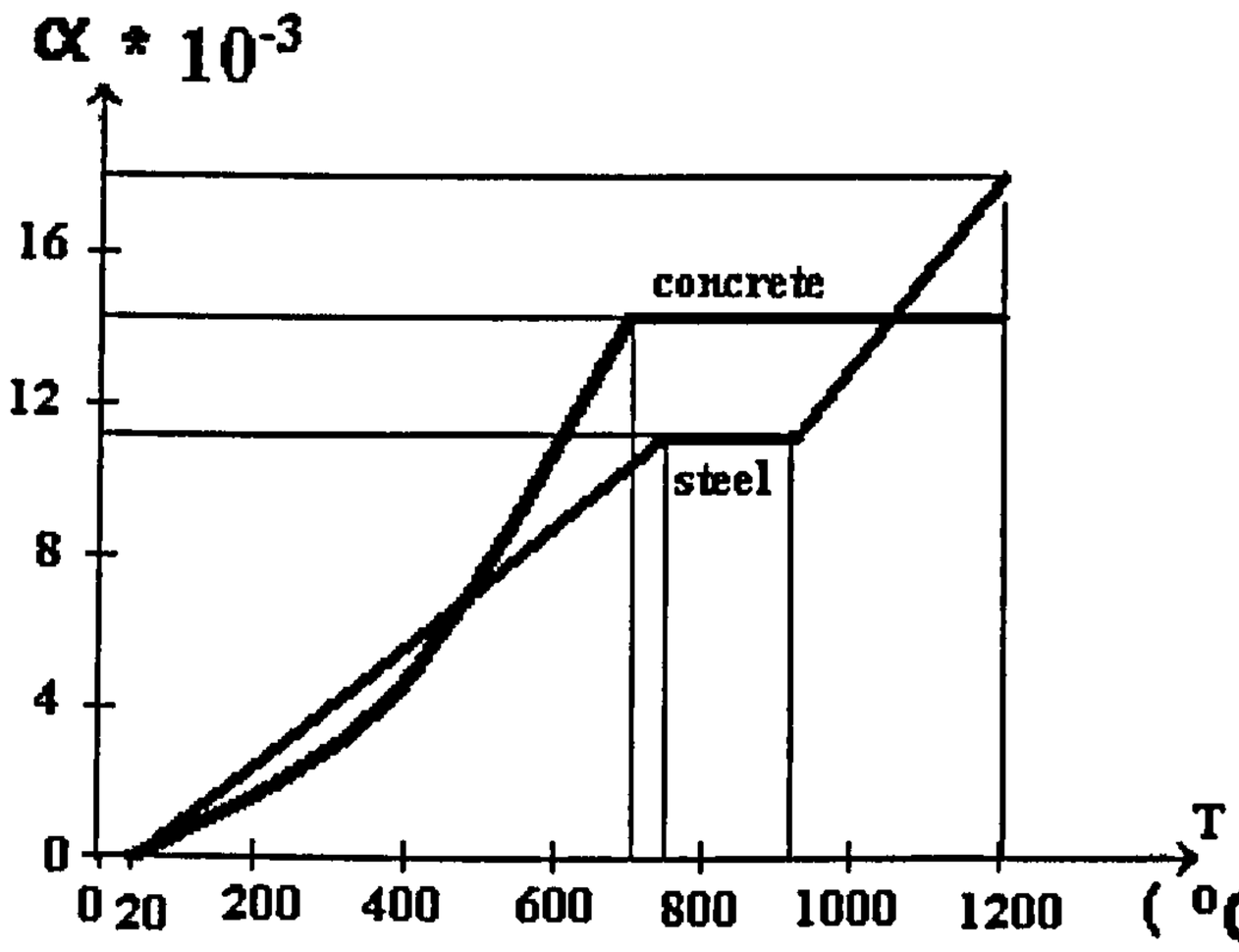

Fig. 3-13 Thermal expansion of concrete and steel as a function of the temperature

The rate of change of thermal expansion with temperature *(ΔL/L)*, denoted as the coefficient of thermal expansion (α), is not constant, especially for concrete.

The thermal strains that occur at free expansion are determined at every element of the cross-section by: $\varepsilon_{thermal} = \alpha \,.\, T$

According to the [Eurocode 4– 1994, Part 1-2], the following equations are used to determine the thermal strains in the elements of concrete cross section:

$$\varepsilon_{thermal} = -1.8\times10^{-4} + 9\times10^{-6}\times T + 2.3\times10^{-11}T^{3} \qquad \text{For } 20\,^{\circ}\text{C} \le T \le 700\,^{\circ}\text{C} \quad (3\text{-}44)$$

$$\varepsilon_{thermal} = 14\times10^{-3} \qquad \text{For } 700\,^{\circ}\text{C} < T \le 1200\,^{\circ}\text{C} \quad (3\text{-}45)$$

The following equations are used to determine steel thermal strain:

$$\varepsilon_{thermal} = -2.4\times10^{-4} + 1.2\times10^{-5}T + 0.4\times10^{-8}T^{-2} \qquad \text{For } 20\,^{\circ}\text{C} \le T \le 750\,^{\circ}\text{C} \quad (3\text{-}46)$$

$$\varepsilon_{thermal} = -11\times10^{-3} \qquad \text{For } 750\,^{\circ}\text{C} < T \le 860\,^{\circ}\text{C} \quad (3\text{-}47)$$

$$\varepsilon_{thermal} = -6.2\times10^{-3} + 2\times10^{-5}T \qquad \text{For } 860\,^{\circ}\text{C} < T \le 1200\,^{\circ}\text{C} \quad (3\text{-}48)$$

b- Calculation of Bending Strain

The bending strain can be obtained by multiplying the curvature with the vertical distances of each element in the cross-section from the neutral axis in the two planes:

$$\varepsilon_{bending} = Z.\, d^2y/dx^2 \qquad (3\text{-}49)$$

When:

Z: the vertical distances of each element in the cross-section from the neutral axis in the two planes

x and y: plane coordinates

$$\varepsilon_{X\,bending} = Z_{x\,i,j} \times \text{Ø}x_{m,k} \qquad (3\text{-}50)$$

$$\varepsilon_{Y\,bending} = Z_{y\,i,j} \times \text{Ø}y_{m,k} \qquad (3\text{-}51)$$

When:

$\varepsilon_{X\,bending}$ = bending strain in x-direction

$\varepsilon_{Y\,bending}$ = bending strain in y-direction

$Z_{x\,i,j}$ = the distance from element centre to the neutral axis in X-Direction

$Øx_{m,k}$ = curvature at point (m,k) in x-direction

$Z_{y\,i,j}$ = the distance from element centre to the neutral axis in Y-Direction

$Øy_{m,k}$ = curvature at point (m,k) in y-direction

In the present analysis, curvatures are approximated by the finite difference formulae.

c- Calculation of Strain due to Stress

The difference between the actual bending strains and the free thermal strains in a cross-section are defined as stress-related strain (ε_{stress}). See Fig. 3-14.

$$\varepsilon_{stress} = \varepsilon_{bending} - \varepsilon_{thermal} \quad (3\text{-}52)$$

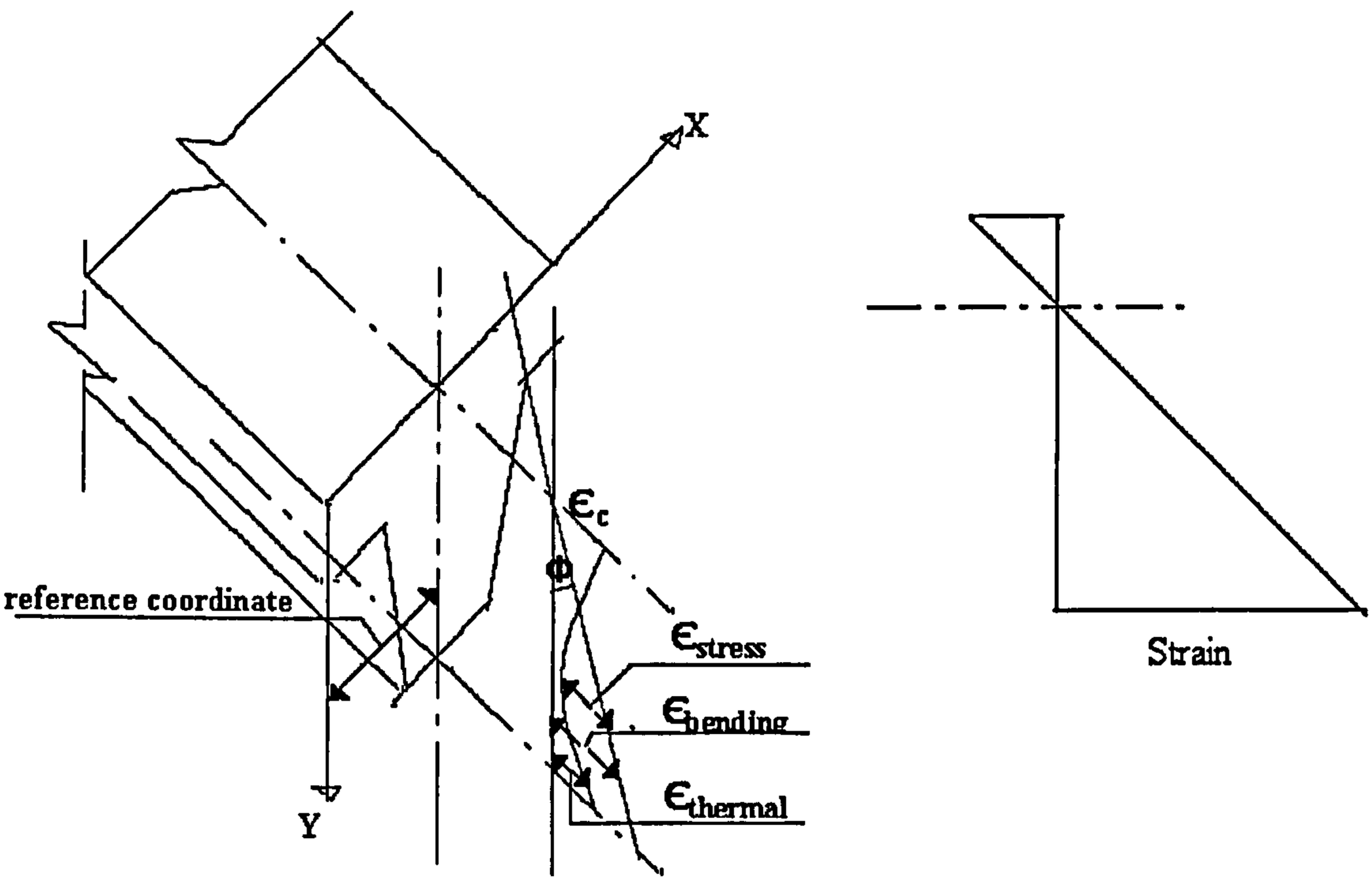

(a) (b)

Fig. 3-14 Strains on Reference co-ordinate of the cross-section

This would be the strain in the absence of any thermal effects.

3.4.4 Stresses in Concrete and Steel

The net strains form generated stresses in the elements of the cross-section.

Internal forces in the cross-section can be calculated from the following integrals:

$$p = \int \sigma dA \qquad (3\text{-}53)$$

$$M_x = \int \sigma_x dA Z_x \qquad (3\text{-}54)$$

$$M_y = \int \sigma_y dA Z_y \qquad (3\text{-}55)$$

In the context of plates, these forces are calculated for a unit width of the plate.

In view of the numerical procedure adopted, the integrations are replaced by summations over the rectangles and triangles of the cross-sectional grid.

Iteration needs to be performed for ensuring that the value of (p) matches the applied in-plane force. For unrestrained edges, (p) has to be zero.

The position of the neutral axis can be determined by trial and error; i.e., assuming a neutral axis, calculating the strain and stress at various points of the section and equating the compressive and tensile forces. Once the neutral axis is determined, the moment can be calculated easily by summing the moments of all the forces on the section.

3.4.5 Calculation of Rigidities

The moments are calculated as a function of the curvature which changes as a function of time. At a given point of time, the plate rigidities are calculated as follows:

$$D_x = \frac{M}{d^2w/dx^2} \qquad (3\text{-}56)$$

$$D_y = \frac{M}{d^2w/dy^2} \qquad (3\text{-}57)$$

As discussed in section 3.4, equation (3.35), an approximation is made to use

$D_{xy} = D_y$

3.5 Solution of the differential equation

The differential equation (3-36) of orthotropic plate can be used to determine the composite floor deflection. In the finite difference method, numerical solution of the differential equation for deflection is obtained for chosen points of the floor, referred to as nodes. To apply the finite difference method at a node, the differential equation is replaced by the finite difference expression, relating the given node. This method makes possible the analysis of rectangular plates for any of the usual types of edge conditions.

Solution by finite differences provides a means of determining a set of deflections for discrete points of a plate subjected to fire and edge conditions. The deflections are determined at all mesh points satisfying finite difference relations which correspond to the differential expressions of the usual plate theory.

The equilibrium shape is obtained using the Newton-Raphson iteration procedure. The plate rigidities are substituted in the governing differential equations alongside the finite difference formulae for each point of the mesh as presented in Fig.3-10.

The finite difference expression at nodes near the boundary has to be modified before solving for the unknown. The following sections demonstrate how this is done for a plate.

3.5.1 Finite difference equations at an interior node of plate

Fig. 3-15 represents a portion of the interior of a plate subdivided by grid lines into rectangular grid elements. The grid lines are spaced Δy units apart in the y-direction and Δx units apart in the x-direction. The intersections of the grid lines will be referred to as grid points. Certain of these, lettered for identification and the central point of the group will be called the pivotal point. The double letters refer in every case to the deflection at the individual point so lettered.

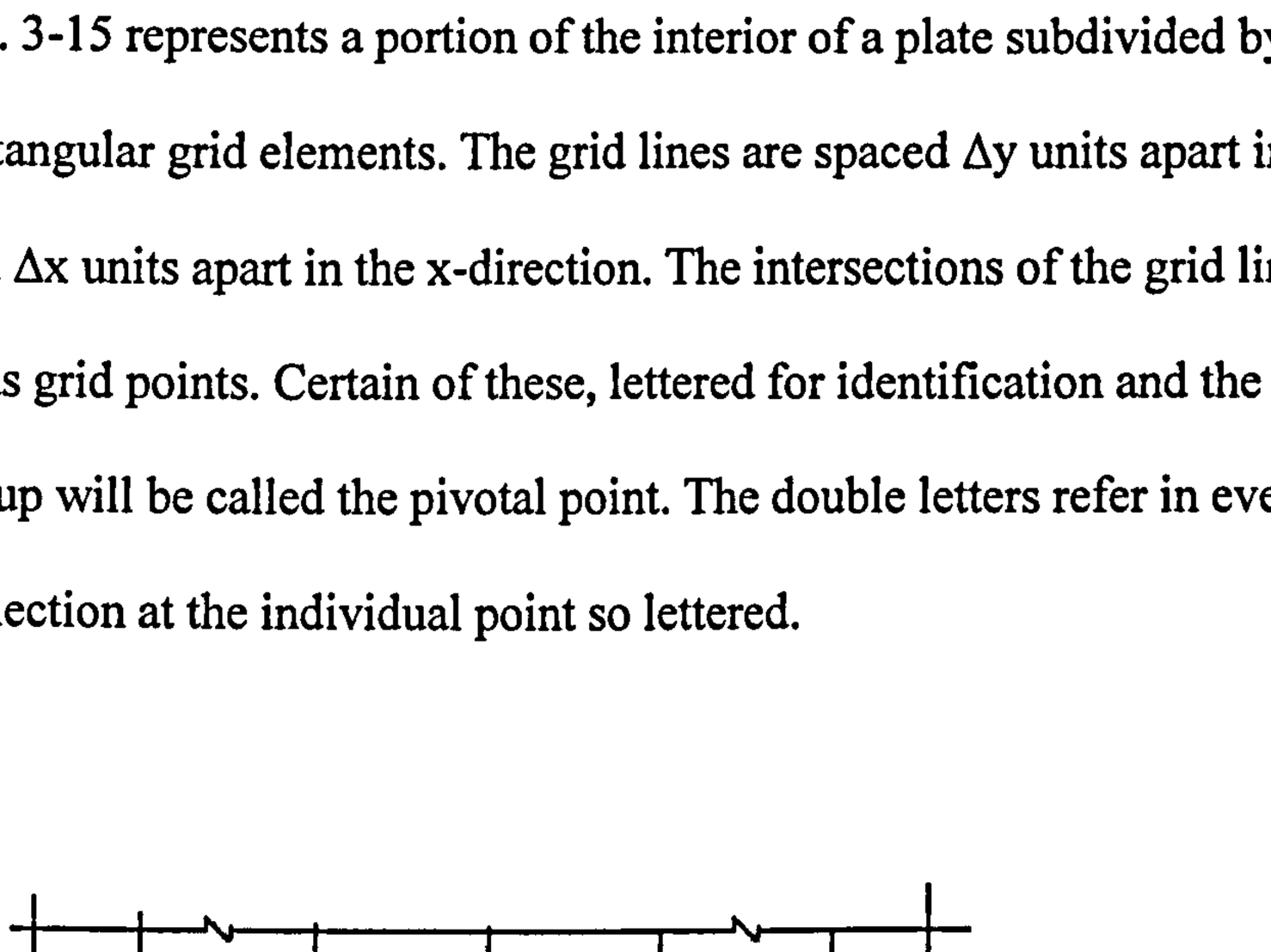

Fig. 3-15, a portion of the interior of a plate division

In order to solve equation (3-36) by a finite difference method, the identifying letters, which were used in Fig. 3-11, for each point will be used to represent the value of the deflection, w, of the floor at that point.

The finite difference expression for equation (3-36) can be written as:

$$\frac{d^4w}{dx^4} = \frac{w_{m-2,k} - 4w_{m-1,k} + 6w_{m,k} - 4w_{m+1,k} + w_{m+2,k}}{\Delta x^4} \qquad \text{(a)}$$

$$\frac{d^4w}{dx^2dy^2} = \frac{4w_{m,k} - 2(w_{m+1,k} + w_{m-1,k} + w_{m,k+1} + w_{m,k-1}) + w_{m+1,k+1} + w_{m+1,k-1} + w_{m-1,k-1} + w_{m-1,k+1}}{\Delta x^2 \Delta y^2} \qquad \text{(b)}$$

$$\frac{d^4w}{dy^4} = \frac{w_{m,k+2} - 4w_{m,k+1} + 6w_{m,k} - 4w_{m,k-1} + w_{m,k-2}}{\Delta y^4} \qquad \text{(c)}$$

When the above operators (a), (b), and (c) are substituted in equation (3-36), the following finite difference scheme is obtained:

$$D_x \frac{w_{m-2,k} - 4w_{m-1,k} + 6w_{m,k} - 4w_{m+1,k} + w_{m+2,k}}{\Delta x^4} +$$
$$2D_{xy} \frac{4w_{m,k} - 2(w_{m+1,k} + w_{m-1,k} + w_{m,k+1} + w_{m,k-1}) + w_{m+1,k+1} + w_{m+1,k-1} + w_{m-1,k-1} + w_{m-1,k+1}}{\Delta x^2 \Delta y^2} +$$
$$D_y \frac{w_{m,k+2} - 4w_{m,k+1} + 6w_{m,k} - 4w_{m,k-1} + w_{m,k-2}}{\Delta y^4} = q \qquad \text{(3-58)}$$

This equation can be represented by a stencil as given in Fig. 3-16. The stencil is moved from point to point in the mesh to obtain the required algebraic equations for the internal points.

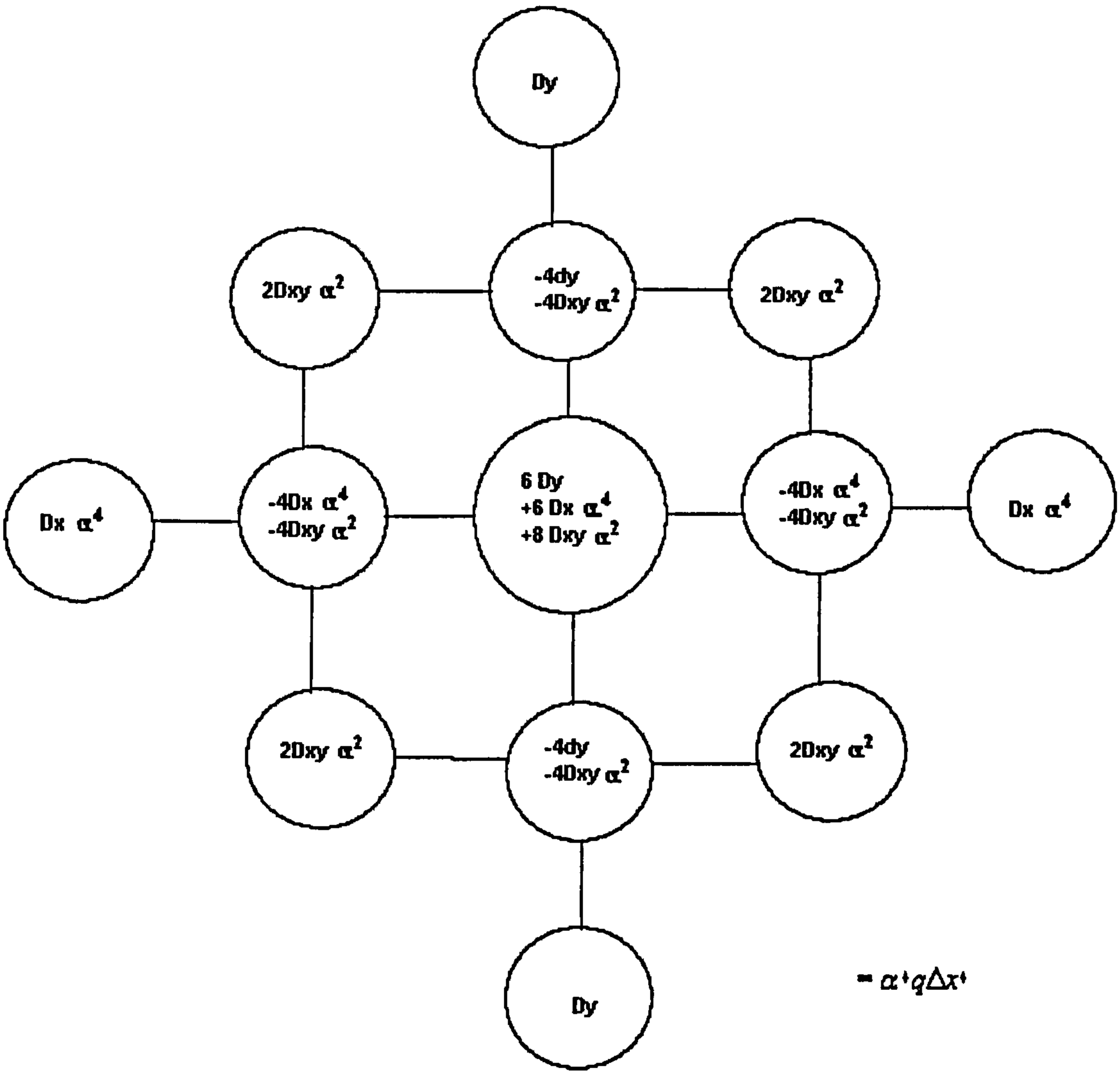

Fig. 3-16 Stencil for mesh-points. $\alpha^2 = \Delta y / \Delta x$

This may be considered as an operator to form an array. Each element of the array represents the coefficient of the deflection of one of the grid points in a group similar to that shown in Fig. 3-16 above.

Since the solution deals with discrete points the following form for a general interior node m,k is:

$[coefficients]\{w_{m,k}\}=q/D$

When $w_{m,k}$ represents the deflection at a general interior node, q represents the force at at a general interior node and D is the rigidity of the plate. Similar equations are written for all the nodes in a plate.

The solution of the equation (3-36) by the finite difference method also requires proper finite difference formulae for the boundary conditions. The coefficients of nodes at or near the boundary are modified with appropriate boundary conditions.

3.5.2 Finite Difference Equations at Boundaries of plate

Some boundary conditions usually encountered in engineering are presented in the following:

- Simply supported edge (movable in the plane of the plate)

- Hinged edge (or simply supported edge immovable in the plane of the plate)

-Rigidly clamped edge

-Free edge

-Elastically supported (stress-free) edge against rotation

A summary of some typical boundary conditions is given in Fig. 3-17.

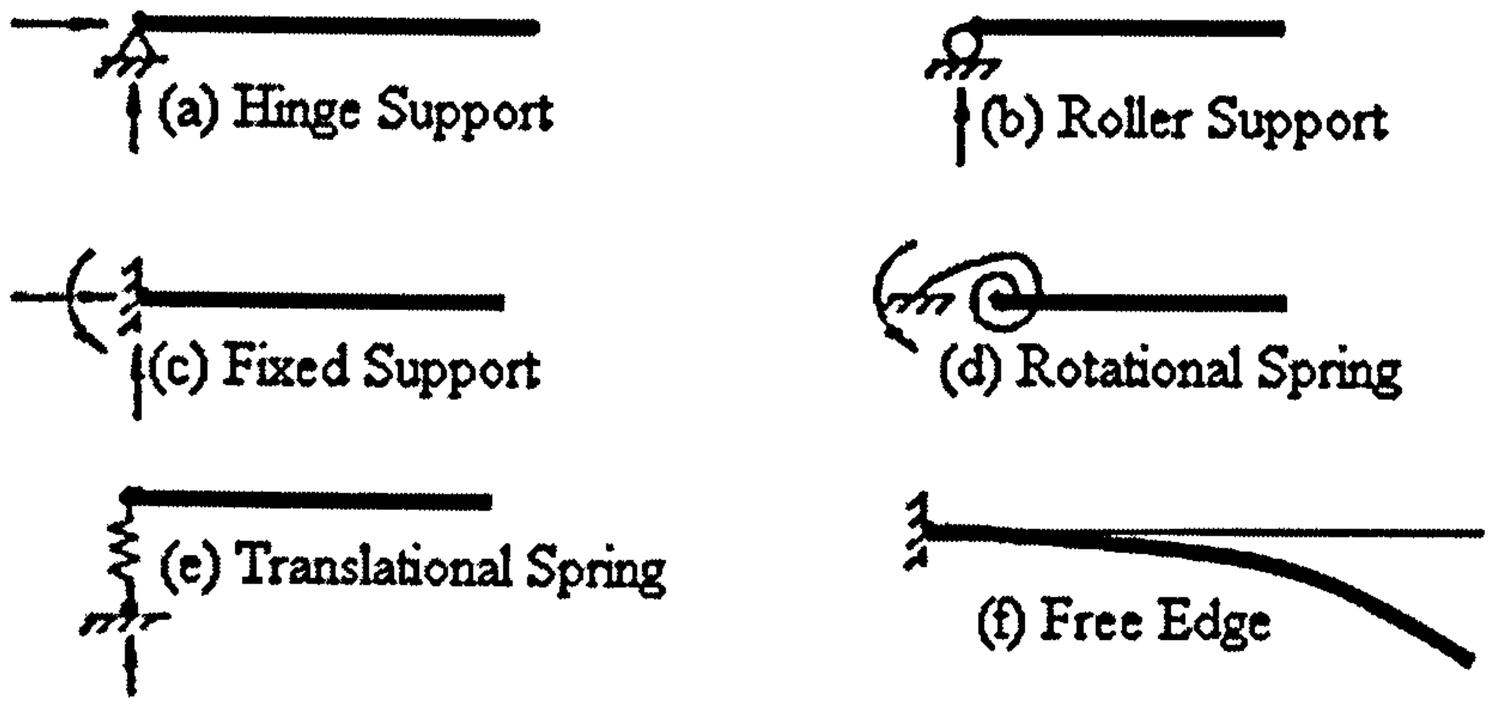

Fig 3-17 Various boundary conditions

(a) Hinge support:

A hinge support represent is a pin connection to a structural assembly and it does not allow translational movements as in Fig. 3-17a. It assumed to be frictionless and to allow rotation with respect to the others.

(b) Roller support:

A roller support is a kind of support that permits the attached structural part to rotate freely with respect to the foundational to translate freely in the direction parallel to the foundation surface as in Fig. 3-17b, no translation movement in any other direction is allowed.

(c)Fixed edge:

A fixed edge, Fig. 3-17c, does not allow rotation or translation in any direction.

(d) Rotational spring:

A rotational spring represents a support that provides some rotational restraint but does not provide any translational restraint, Fig. 3-17d.

(e) Translational spring:

A translational spring can provide partial restraints along the direction of deformation, Fig. 3-17e.

(f) Free edge:

Fig.3-17f shows the boundary condition for free edge. It is entirely free; there are no bending and twisting moments and also no vertical shearing forces.

(i) Simply supported edge

The deflections and moments along the edge of simply supported vanish at all boundary points. The analytical expression for the boundary condition in this case is:

$$w = 0, \qquad \frac{\partial^2 w}{\partial x^2} + \nu \frac{\partial^2 w}{\partial y^2} = 0 \qquad (3\text{-}59)$$

For the finite deference expression the fire condition translates to $w_{m,k} = 0$ for the grid points on the boundary of simply supported edge. At a straight edge parallel to y-axis.

$$\frac{\partial^2 w}{\partial y^2} = 0, \text{ which gives } \frac{\partial^2 w}{\partial x^2} = 0 \qquad (3\text{-}59a)$$

In order to formulate the boundary conditions with vanishing deflections, the equations for the adjacent node had to be established, so there is a need to identify some fictitious points obtained by continuation of the network beyond the boundary of the plate. By means of equation (3-59a), the simple support conditions in Fig. 3-18 shows that (LL) the value of w to be associated with w_{ll} is equal to - w_p.

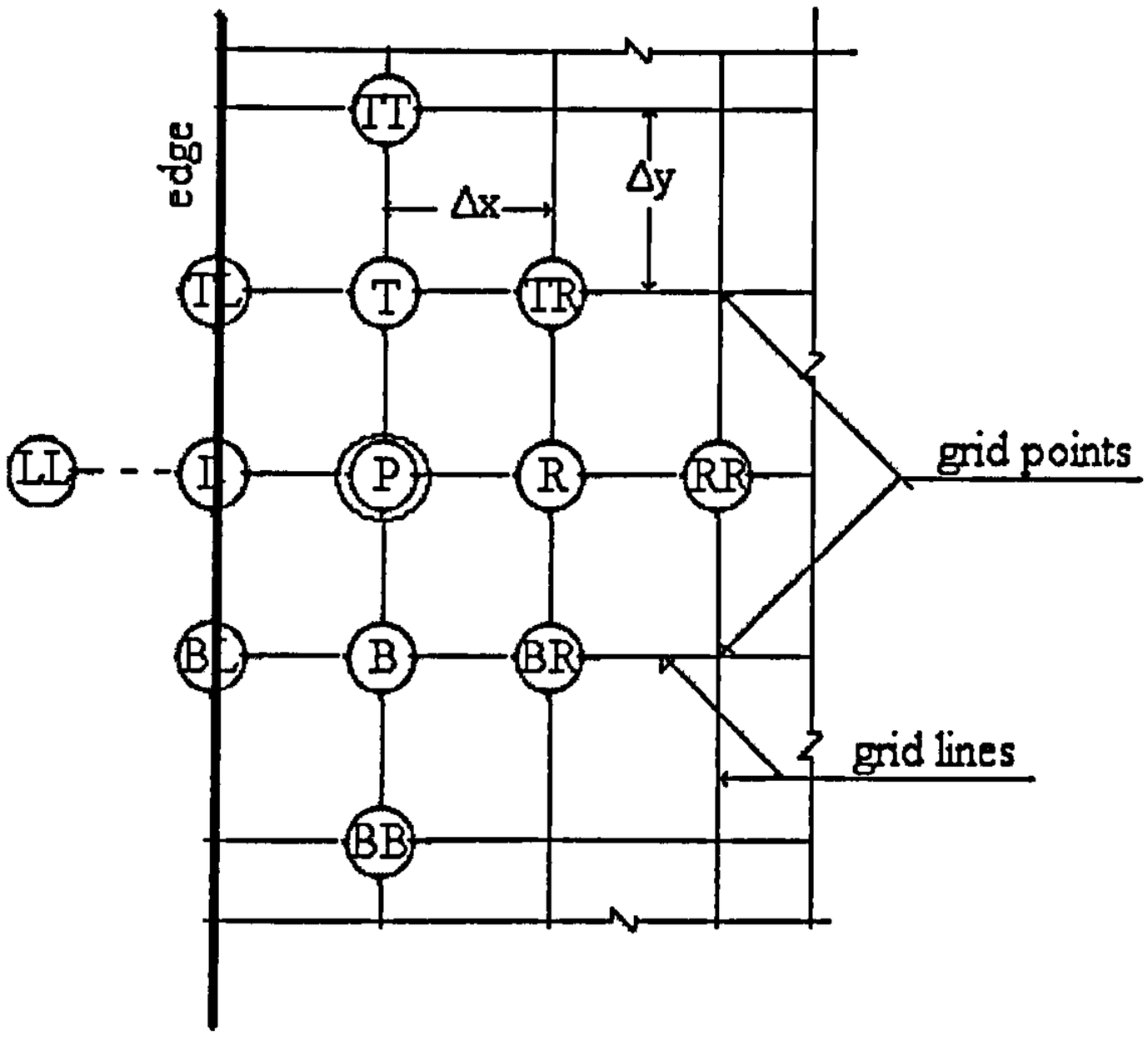

Fig. 3-18 Simply supported adjacent node

Hence, the values of the deflection points outside the grid should be introduced to express the grid points adjacent to the boundary and in the corner. Here w_p represents a deflection whose magnitude at any grid point is a function of the four adjoining grid elements. Then the deflection at the fictitious points, such as w_{ll} is equal in magnitude and opposite in direction at all adjacent points to the simply supported edge.

The finite difference form for deflections at fictitious points explained in Fig. 3-19 is stated as:

$$w_{ll} = -w_p$$

Fig. 3-19 Boundary condition for simple support

When w_i represent zero deflection

Fig. 3-20 and Fig. 3-21 show the method used in this case. The plate is divided into grid elements and the grid points numbered systematically for identification. Coefficients can be modified from equation (3-58) when a pivotal point is adjacent to the corner or to an edge.

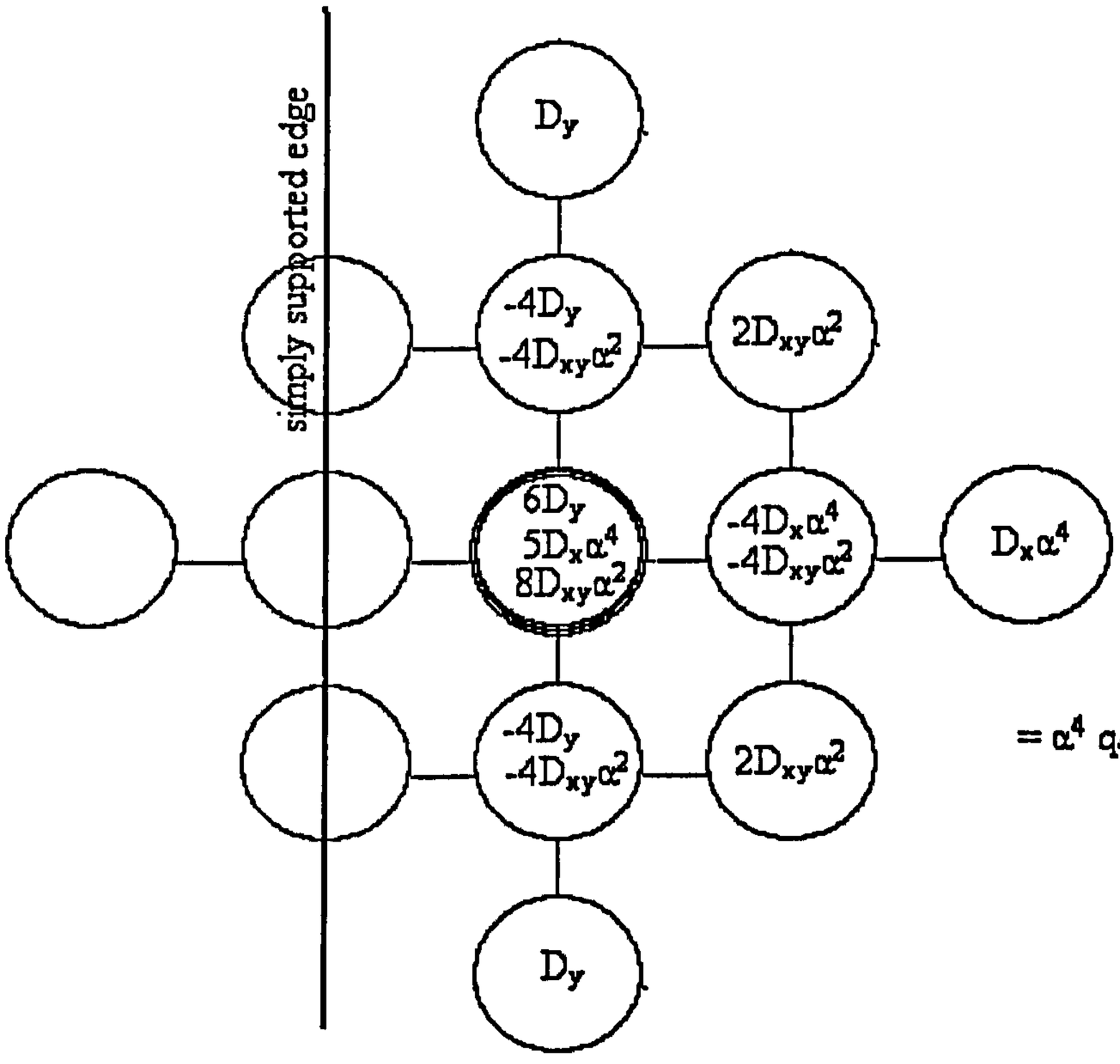

Fig 3-20 Pivotal point adjacent to a simply supported edge

Each coefficient multiplied by $w_{m,k}$ denotes the deflection at the respective point m,k to form a number of finite difference equations in matrix form. Thus, there remain only the deflections of the interior nodes so the total number of unknown deflections will not exceed the number of equations. In the case of rectangular mesh, Δx and Δy are mesh width in x and y direction respectively and based on $\alpha = \Delta y/\Delta x$.

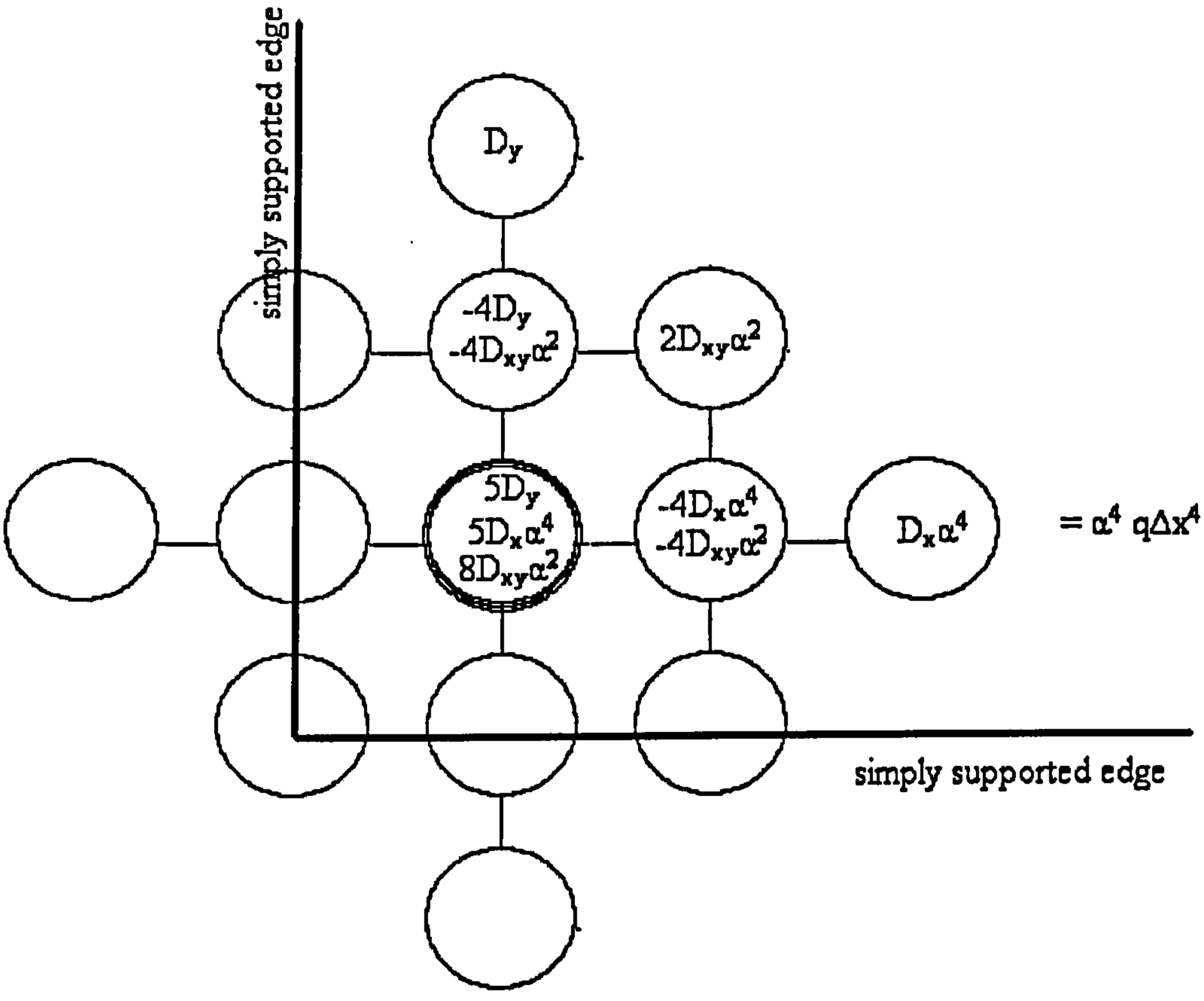

Fig 3-21 Pivotal point adjacent to a simply supported corner

(ii) Built-in edge (Fixed edge)

The boundary condition representing a fixed edge, Fig.3-22 and Fig. 3-24, can be treated in a same manner. The deflection at all points on a built-in edge and slope of the deflected surface normal to the edge are zero.

In order to formulate the boundary conditions for built-in edge, it should be first establish the equation for interior points next to the edge, Fig. 3-22 and Fig. 3-24, by applying the operator (3-58).

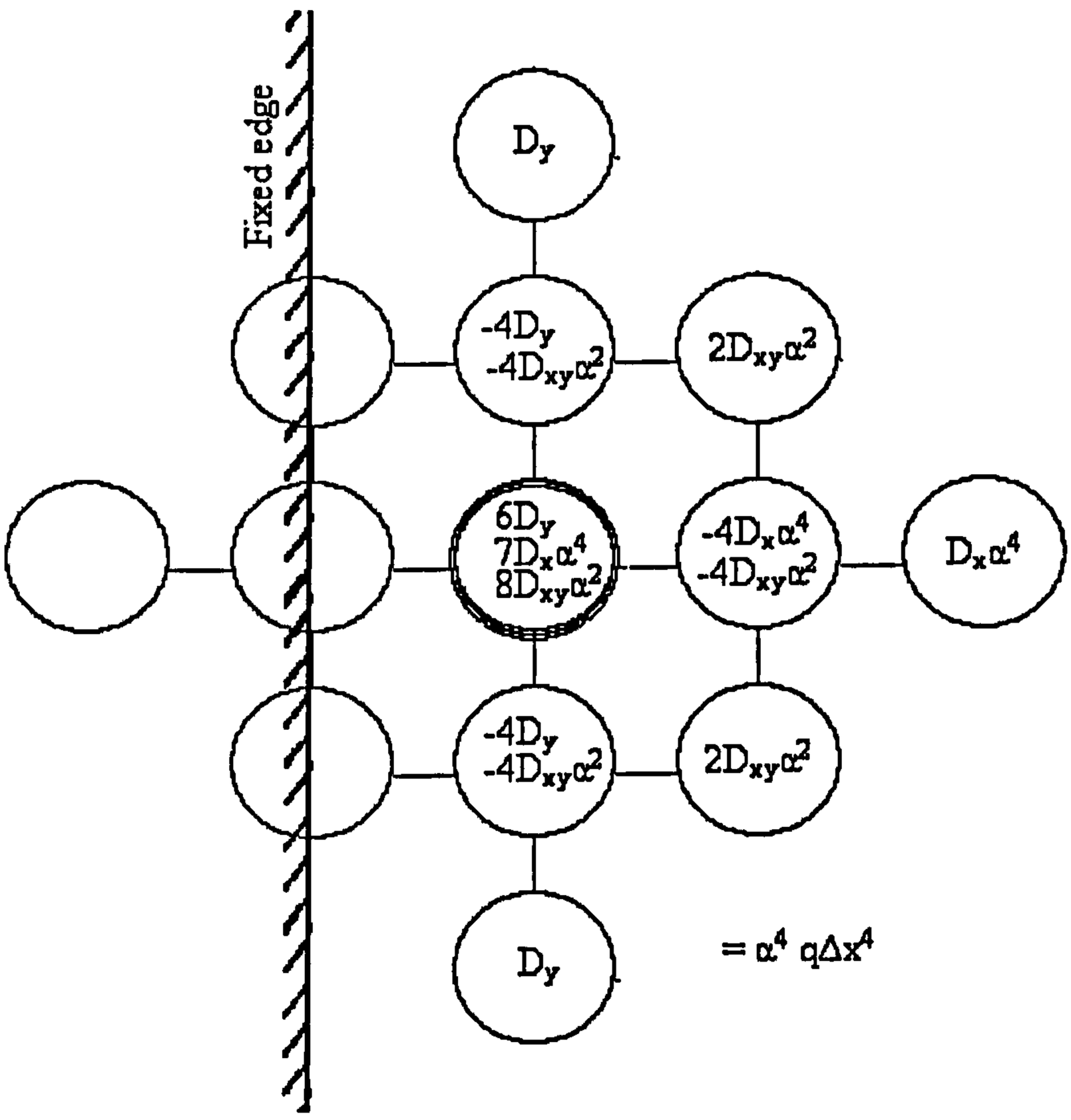

Fig 3-22 Pivotal point adjacent to a fixed edge

Next we have to eliminate the deflection at fictitious points outside the boundary of the plate. This is done by means of relation $w_{ll} = w_p$ for the points LL and P in Fig. 3-18. At a fixed edge, the slop and the deflection both have zero values. This results in the following expression, Fig 3-23, for the deflection of the fictitious point.

$$w_{ll} = w_p \qquad (3\text{-}60)$$

Which represent zero deflection and slop at point w_l.

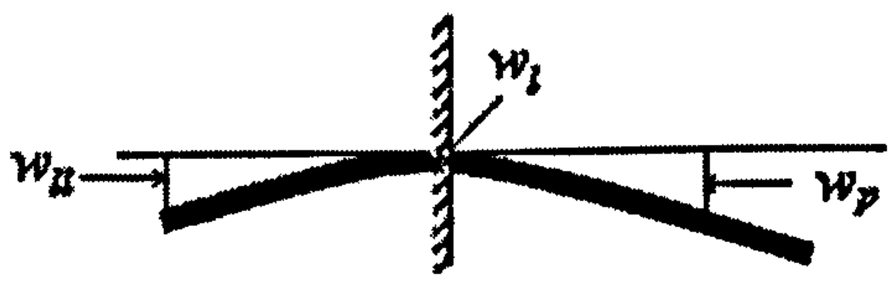

Fig. 3-23 Boundary condition for fixed edge

Thus, after modifying equation (3-58) to take care of the boundary conditions, remain only the deflections of the interior points in this equation and the total number of such unknown deflections will not exceed the number of equations of the type (3-58).

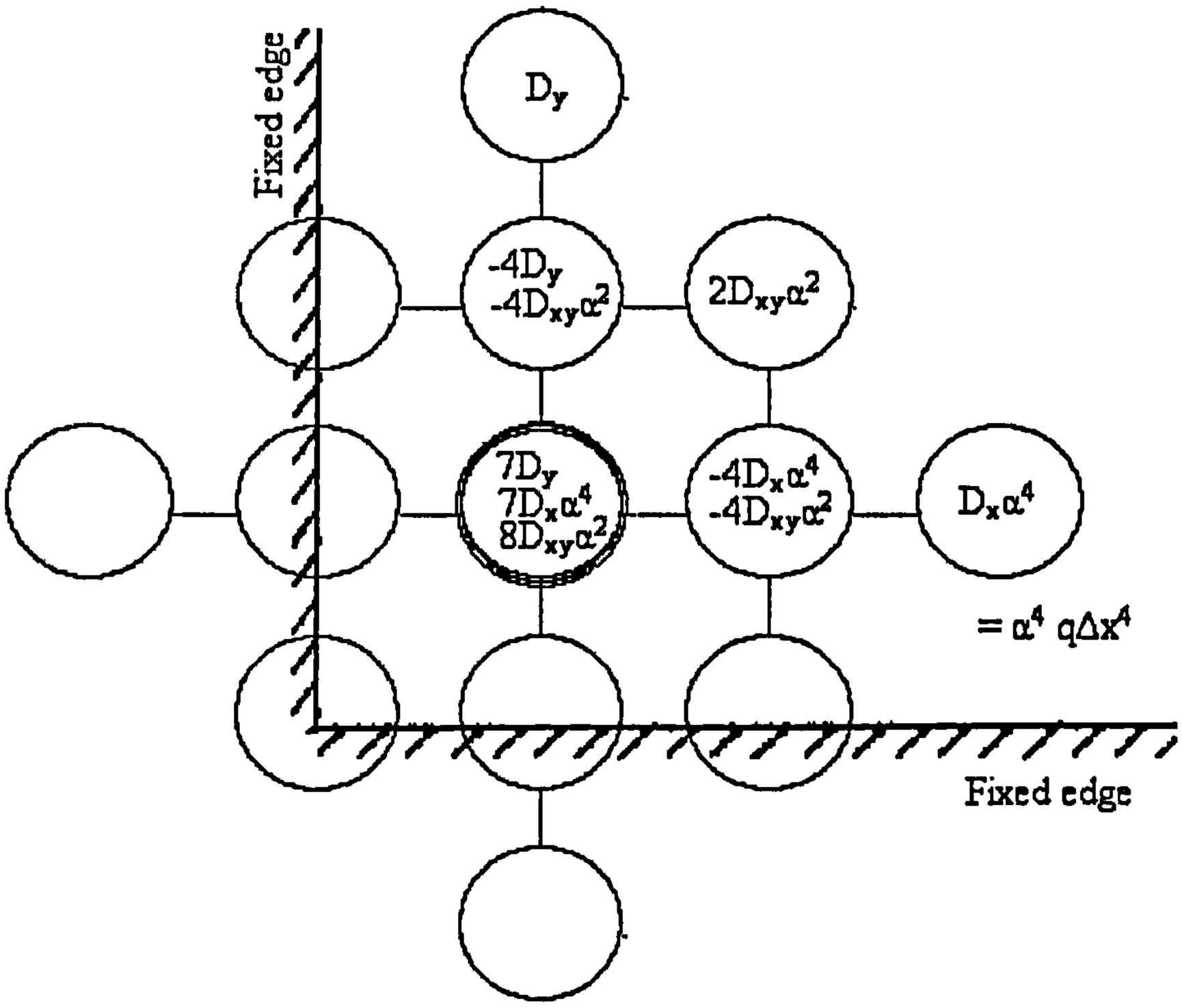

Fig 3-24 Pivotal point adjacent to a Fixed edge corner

(c) Free edge

In the case of a free edge the number of such difference equations will be increased by the numbers of such points beyond the boundary condition of the plate. At a free edge, the bending moment is zero and there should not be any transverse forces [Szilard, 1974].

For an edge parallel to the x-axis, following are the boundary conditions.

$$\frac{\partial^2 w}{\partial x^2}+\nu\frac{\partial^2 w}{\partial y^2}=0, \qquad [\frac{\partial^3 w}{\partial x^3}+(2-\nu)\frac{\partial^3 w}{\partial x\partial y^2}]=0 \qquad (3\text{-}61)$$

And for an edge parallel to the y-axis following are the conditions:

$$\frac{\partial^2 w}{\partial y^2}+\nu\frac{\partial^2 w}{\partial x^2}=0, \qquad [\frac{\partial^3 w}{\partial y^3}+(2-\nu)\frac{\partial^3 w}{\partial x^2\partial y}]=0 \qquad (3\text{-}62)$$

Poisson ratio is taken to be $\nu = 0.3$

If the point m,k is at the boundary as in Fig. 3-25, it requires four fictitious points placed outside the plate in order to give a better approximation to the boundary conditions.

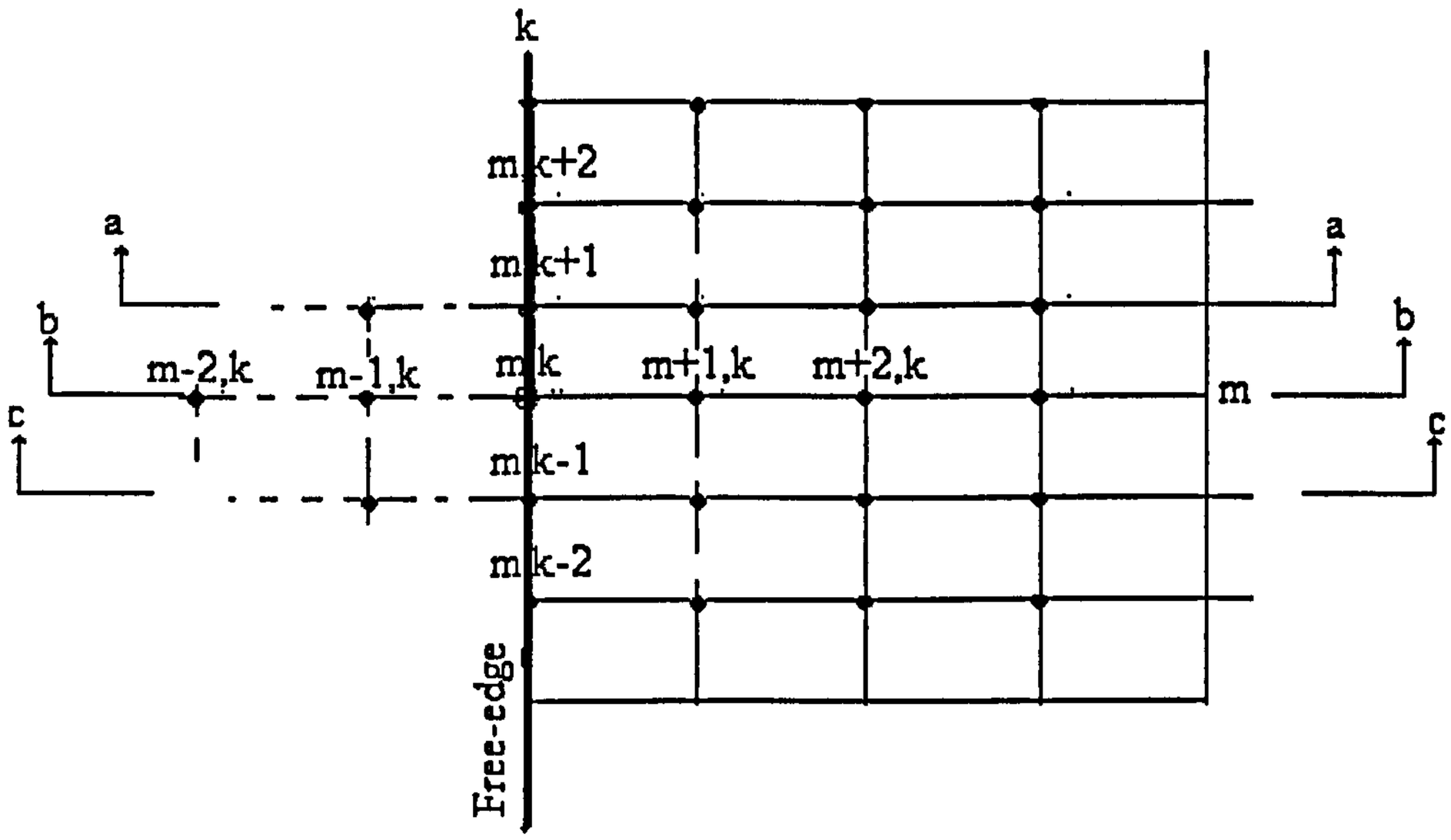

Fig 3-25 Boundary condition for free edge

Deflections at these fictitious points can be expressed in term of deflections of the mesh points located on the plate. An approximate solution of the equations (3-61) and (3-62) satisfying boundary conditions for free edge is formulated by finite difference method associated with the procedure as in Sec. 3.5.1. Using the notation of Fig 3-25, the finite difference form becomes:

$$
\begin{aligned}
(m_x)_{m,k} &= -(2+2\nu)w_{m,k} + w_{m+1,k} + w_{m-1,k} + \nu(w_{m,k+1} + w_{m,k-1}) = 0 \\
w_{m-1,k} &= (2+2\nu)w_{m,k} - w_{m+1,k} - \nu(w_{m,k+1} + w_{m,k-1})
\end{aligned}
\qquad (3\text{-}63)
$$

$$(\vartheta_x)_{m,k} = (6-2\nu)(w_{m+1,k} - w_{m-1,k}) + 2(1-\nu)(w_{m-1,k-1} + w_{m-1,k+1} - w_{m+1,k+1} - w_{m+1,k+1}) - w_{m+2,k} + w_{m-2,k} = 0 \tag{3-64}$$

$$w_{m-2,k} = -(6-2\nu)(w_{m+1,k} - w_{m-1,k}) - 2(1-\nu)(w_{m-1,k-1} + w_{m-1,k+1} - w_{m+1,k+1} - w_{m+1,k+1}) + w_{m+2,k} \tag{3-65}$$

$$(m_x)_{m,k+1} = -(2+2\nu)w_{m,k+1} + w_{m+1,k+1} + w_{m-1,k+1} + \nu(w_{m,k+2} + w_{m,k}) = 0$$

$$w_{m-1,k+1} = (2+2\nu)w_{m,k+1} - w_{m+1,k+1} - \nu(w_{m,k+2} + w_{m,k}) \tag{3-66}$$

$$(m_x)_{m,k-1} = -(2+2\nu)w_{m,k-1} + w_{m+1,k-1} + w_{m-1,k-1} + \nu(w_{m,k-2} + w_{m,k}) = 0$$

$$w_{m-1,k-1} = (2+2\nu)w_{m,k-1} - w_{m+1,k-1} - \nu(w_{m,k-2} + w_{m,k}) \tag{3-67}$$

The above four equations are substituted in equation (3-56) to eliminate the fictitious points. Then the following finite difference representation of the free edge condition is obtained.

$$\begin{aligned} &\{-(6-2\nu)(w_{m+1,k} - \{(2+2\nu)w_{m,k} - w_{m+1,k} - \nu(w_{m,k+1} + w_{m,k-1})\}) - 2(1-\nu) \\ &(\{(2+2\nu)w_{m,k-1} - w_{m+1,k-1} - \nu(w_{m,k-2} + w_{m,k})\} + \{(2+2\nu)w_{m,k+1} - w_{m+1,k+1} - \nu(w_{m,k+2} + w_{m,k})\} \\ &D_x \frac{- w_{m+1,k+1} - w_{m+1,k-1}) + w_{m+2,k}\} - 4\{(2+2\nu)w_{m,k} - w_{m+1,k} - \nu(w_{m,k+1} + w_{m,k-1})\} + 6w_{m,k} - 4w_{m+1,k} + w_{m+2,k}}{\Delta x^4} + \\ &4w_{m,k} - 2(w_{m+1,k} + \{(2+2\nu)w_{m,k} - w_{m+1,k} - \nu(w_{m,k+1} + w_{m,k-1})\} \\ &+ w_{m,k+1} + w_{m,k-1}) + w_{m+1,k+1} + w_{m+1,k-1} + \{(2+2\nu)w_{m,k-1} - w_{m+1,k-1} - \nu(w_{m,k-2} + w_{m,k})\} \\ &2D_{xy} \frac{+ \{(2+2\nu)w_{m,k+1} - w_{m+1,k+1} - \nu(w_{m,k+2} + w_{m,k})\}}{\Delta x^2 \Delta y^2} + \\ &D_y \frac{w_{m,k+2} - 4w_{m,k+1} + 6w_{m,k} - 4w_{m,k-1} + w_{m,k-2}}{\Delta y^4} = q \end{aligned}$$

Poisson ratio is substituted to get this expression:

$$D_x\frac{10.48w_{m,k}10.8w_{m+1,k}2w_{m+2,k}-4.06w_{m,k+1}+0.42w_{m,k+2}-4.06w_{m,k-1}+0.42w_{m,k-2}+2.8w_{m+1,k-1}+2.8w_{m+1,k+1}}{\Delta x^4}+$$

$$2D_{xy}\frac{-1.8w_{m,k}1.2w_{m,k+1}1.2_{m,k-1}-0.3w_{m,k-2}-0.3w_{m,k+2}}{\Delta x^2\Delta y^2}+$$

$$D_y\frac{w_{m,k+2}-4w_{m,k+1}+6w_{m,k}-4w_{m,k-1}+w_{m,k-2}}{\Delta y^4}=q$$

The equation is divided by Δx^4, and $\alpha = \Delta y/\Delta x$ is substituted

$$\alpha^4 D_x(10.48w_{m,k}10.8w_{m+1,k}2w_{m+2,k}-4.06w_{m,k+1}+0.42w_{m,k+2}-4.06w_{m,k-1}+0.42w_{m,k-2}2.8w_{m+1,k-1}2.8w_{m+1,k+1})+$$

$$\alpha^2 2D_{xy}(-1.8w_{m,k}1.2w_{m,k+1}1.2_{m,k-1}-0.3w_{m,k-2}-0.3w_{m,k+2})+$$

$$D_y(w_{m,k+2}-4w_{m,k+1}+6w_{m,k}-4w_{m,k-1}+w_{m,k-2})=q\Delta x^4\alpha^4$$

(3-68)

A similar procedure can be followed to define various boundary conditions with finite difference expression.

3.6 In-Plane Forces

In an orthogonal plate, the moment at a point depends on the local curvatures, and represented by the moment equations in the x and y directions as illustrated above in the previous section. If there are forces acting at the boundaries of the middle plane of the plate, n_x, n_y, and n_{xy}, these should be considered in deriving the differential equation of the deflection surface. As shown in Fig. 3-26 the plate deflects, carrying the original plane middle surface into curved shape.

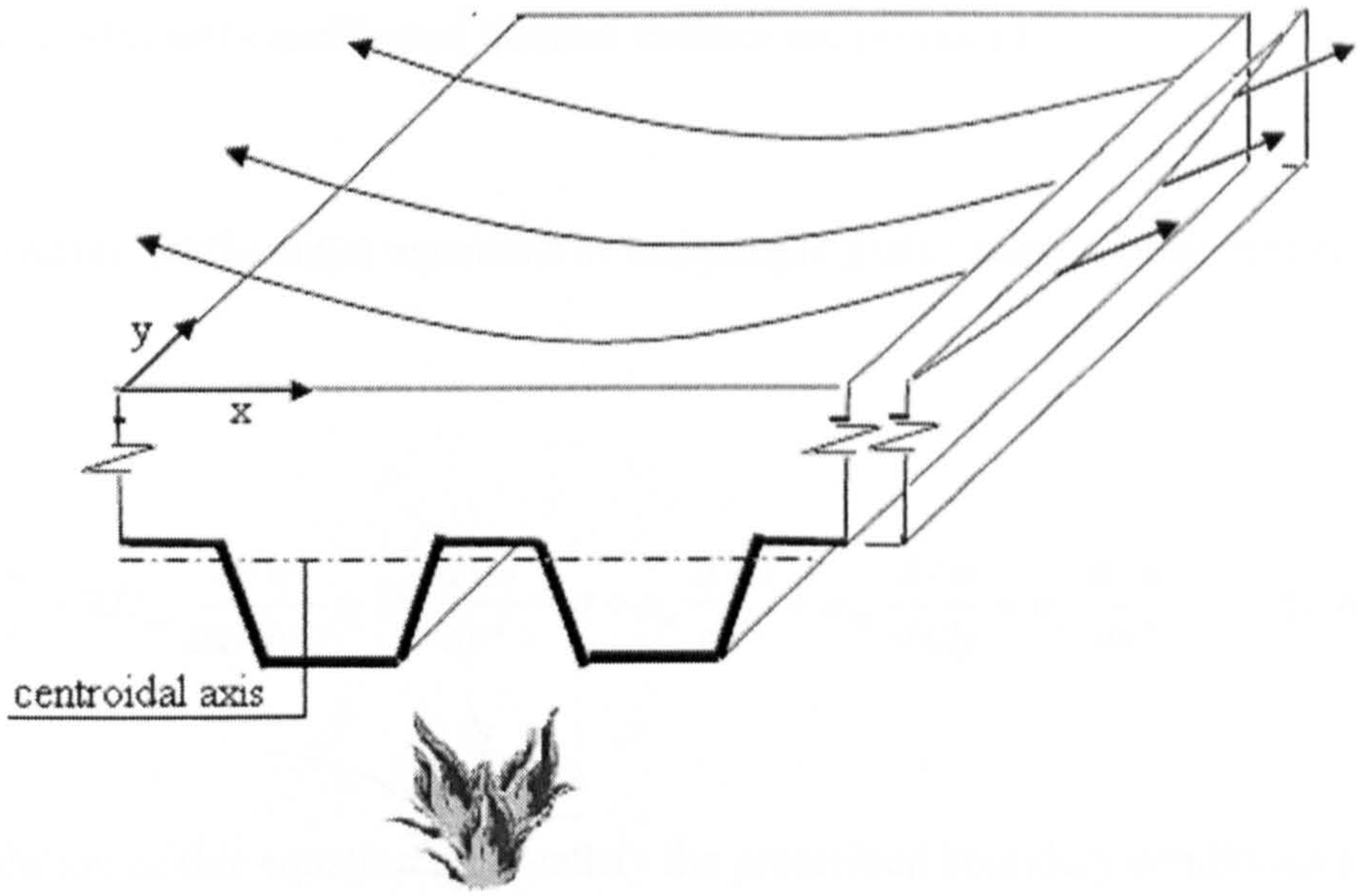

Fig. 3-26 Simply supported slab subjected to fire and in-plane force

3.6.1 In-Plane Forces Response of Boundaries

The response of a plate to in-plane actions is influenced by its boundary conditions. In-plane forces can occur when the displacements of the plate parallel to its middle surface are hindered by the support [Szilard, 1974]. Furthermore, they are applied directly at the boundaries.

If the temperature of the plate is raised, such expansion, for most structural materials, is directly proportional to the change in temperature. However, in the case of non-uniform heating across the plate thickness, the plate cannot expand freely because of the restriction of continuity which prevents their free elongation. Although the plate may be physically free to move at the boundaries, it is imposed by certain boundary conditions which account for in-plane stresses and moderate deflections. Another

cause of providing deflections, in-plane forces, arises due to temperature variations. Consequently, self-equilibrated thermal stresses are produced.

The governing differential equations of orthotropic plate under in-plane forces shown below:

$$D_x \frac{d^4w}{dx^4} + 2D_{xy} \frac{d^4w}{dx^2dy^2} + D_y \frac{d^4w}{dy^4} = q + n_x \frac{d^2w}{dx^2} + n_{xy} \frac{d^2w}{dxdy} + n_y \frac{d^2w}{dy^2} \qquad (3\text{-}69)$$

The solution of this equation must satisfy the prescribed boundary conditions for a given manner of loading and support.

3.6.2 Solution of In-plane Forces by Finite Difference Method:

Two types of edge conditions, for rectangular plate, simply supported and fixed edge, are described.

(i) Simply supported with in-plane forces

As for the simply supported case which was discussed in Section (3.5.2), the differential operators are replaced by the finite difference formula. This reduces the governing differential equation into a linear algebraic equation.

$$D_x \frac{w_{i-2,j} - 4w_{i-1,j} + 6w_{i,j} - 4w_{i+1,j} + w_{i+2,j}}{\Delta x^4} +$$

$$2D_{xy} \frac{4w_{i,j} - 2(w_{i+1,j} + w_{i-1,j} + w_{i,j+1} + w_{i,j-1}) + w_{i+1,j+1} + w_{i+1,j-1} + w_{i-1,j-1} + w_{i-1,j+1}}{\Delta x^2 \Delta y^2} +$$

$$D_y \frac{w_{i,j+2} - 4w_{i,j+1} + 6w_{i,j} - 4w_{i,j-1} + w_{i,j-2}}{\Delta y^4} -$$

$$nx \frac{w_{i+1,j} - 2w_{i,j} + w_{i-1,j}}{\Delta x^2} - ny \frac{w_{i,j+1} - 2w_{i,j} + w_{i,j-1}}{\Delta y^2} = q$$

$$D_x \frac{(w_{i-2,j} - 4w_{i-1,j} + 6w_{i,j} - 4w_{i+1,j} + w_{i+2,j})\Delta y^4}{\Delta x^4 \Delta y^4} +$$

$$2D_{xy} \frac{(4w_{i,j} - 2(w_{i+1,j} + w_{i-1,j} + w_{i,j+1} + w_{i,j-1}) + w_{i+1,j+1} + w_{i+1,j-1} + w_{i-1,j-1} + w_{i-1,j+1})\Delta x^2 \Delta y^2}{\Delta x^4 \Delta y^4}$$

$$D_y \frac{(w_{i,j+2} - 4w_{i,j+1} + 6w_{i,j} - 4w_{i,j-1} + w_{i,j-2})\Delta x^4}{\Delta x^4 \Delta y^4} -$$

$$nx \frac{(w_{i+1,j} - 2w_{i,j} + w_{i-1,j})\Delta x^2 \Delta y^4}{\Delta x^4 \Delta y^4} - ny \frac{(w_{i,j+1} - 2w_{i,j} + w_{i,j-1})\Delta x^4 \Delta y^2}{\Delta x^4 \Delta y^4} = q$$

Letting

$$\alpha = \frac{\Delta y}{\Delta x}$$

$$D_x(w_{i-2,j} - 4w_{i-1,j} + 6w_{i,j} - 4w_{i+1,j} + w_{i+2,j})\alpha^4 +$$
$$2D_{xy}(4w_{i,j} - 2(w_{i+1,j} + w_{i-1,j} + w_{i,j+1} + w_{i,j-1}) + w_{i+1,j+1} + w_{i+1,j-1} + w_{i-1,j-1} + w_{i-1,j+1})\alpha^2 +$$
$$D_y(w_{i,j+2} - 4w_{i,j+1} + 6w_{i,j} - 4w_{i,j-1} + w_{i,j-2}) -$$
$$n_x(w_{i+1,j} - 2w_{i,j} + w_{i-1,j})\Delta x^2 \alpha^4 - n_y(w_{i,j+1} - 2w_{i,j} + w_{i,j-1})\Delta x^2 \alpha^2 = q\Delta x^4 \alpha^4$$

(3-70)

Applying the above equation to all the mesh points, we obtain a matrix of finite difference equation. This equation can be formulated in stencil form as given in Fig. 3-27.

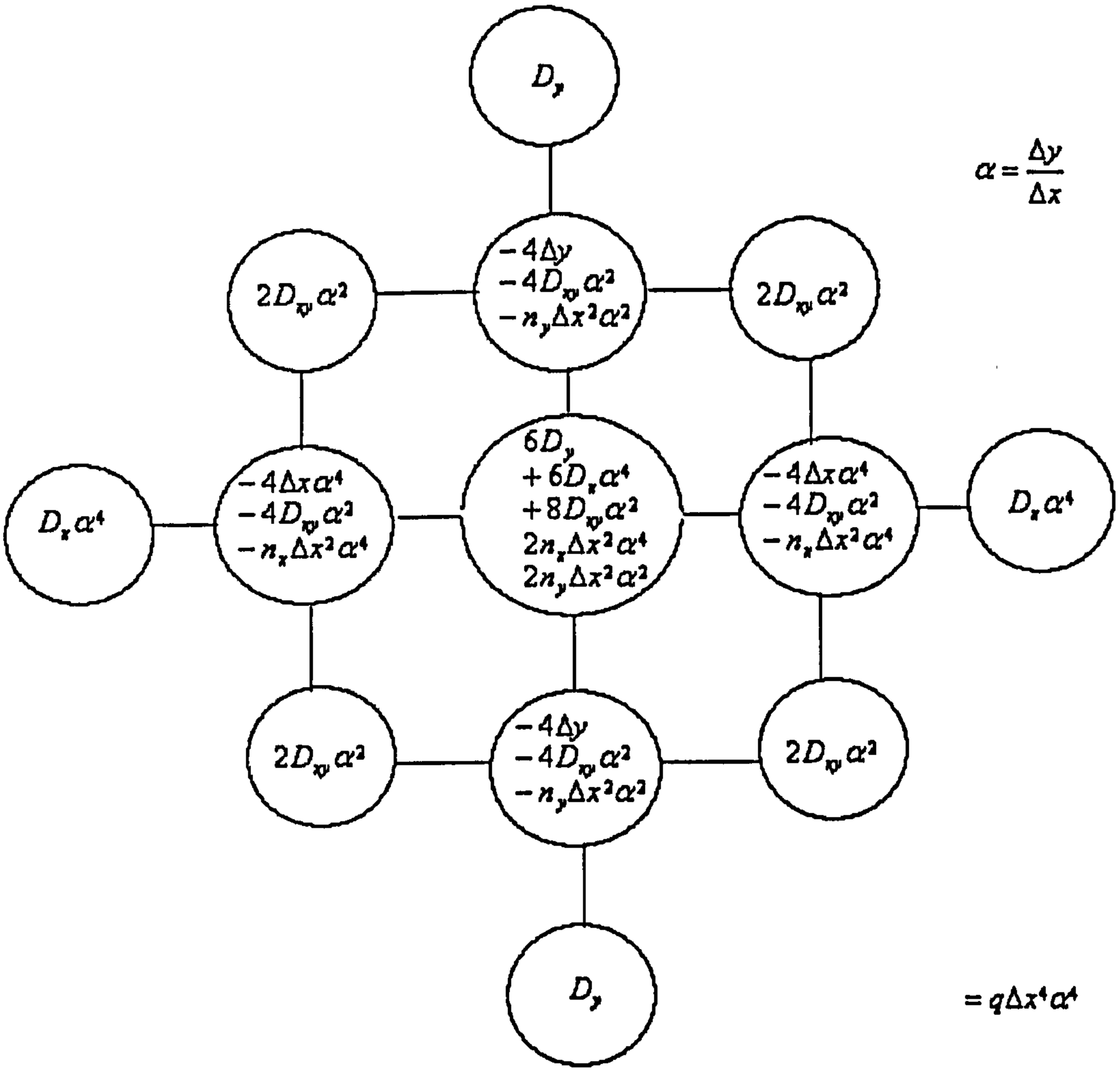

Fig. 3-27 Stencil for mesh point with in-plane force

Coefficients can be modified from equation (3-70) when Pivotal point is adjacent to a corner.

Therefore, the equation of the corner points is given in a diagrammatic form as in Fig. 3-28.

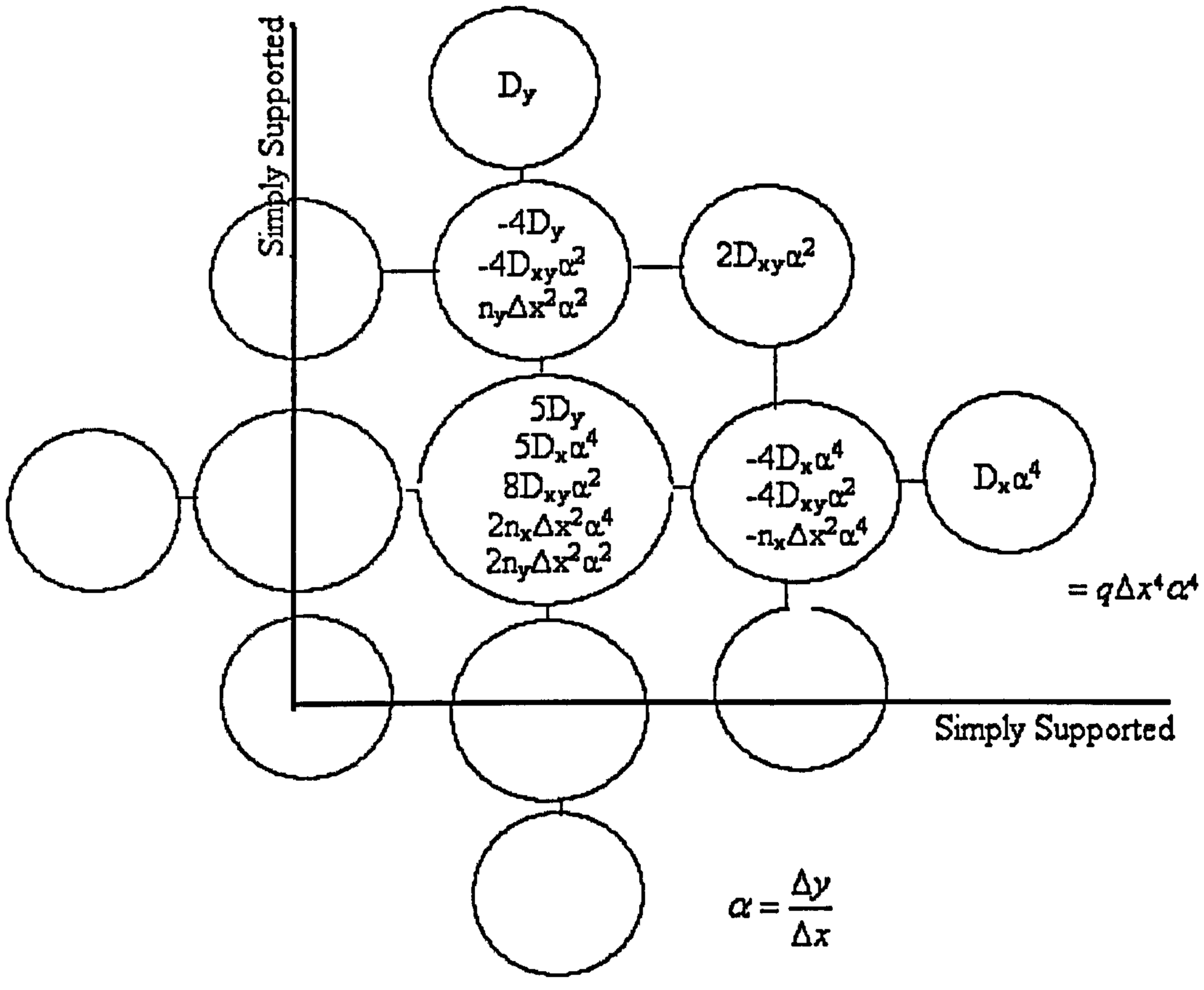

Fig. 3-28 Stencil for corner points for simply supported subjected to in-plane force

A similar procedure can be followed when the pivotal point is adjacent to the edge.

This is schematically shown in Fig. 3-29.

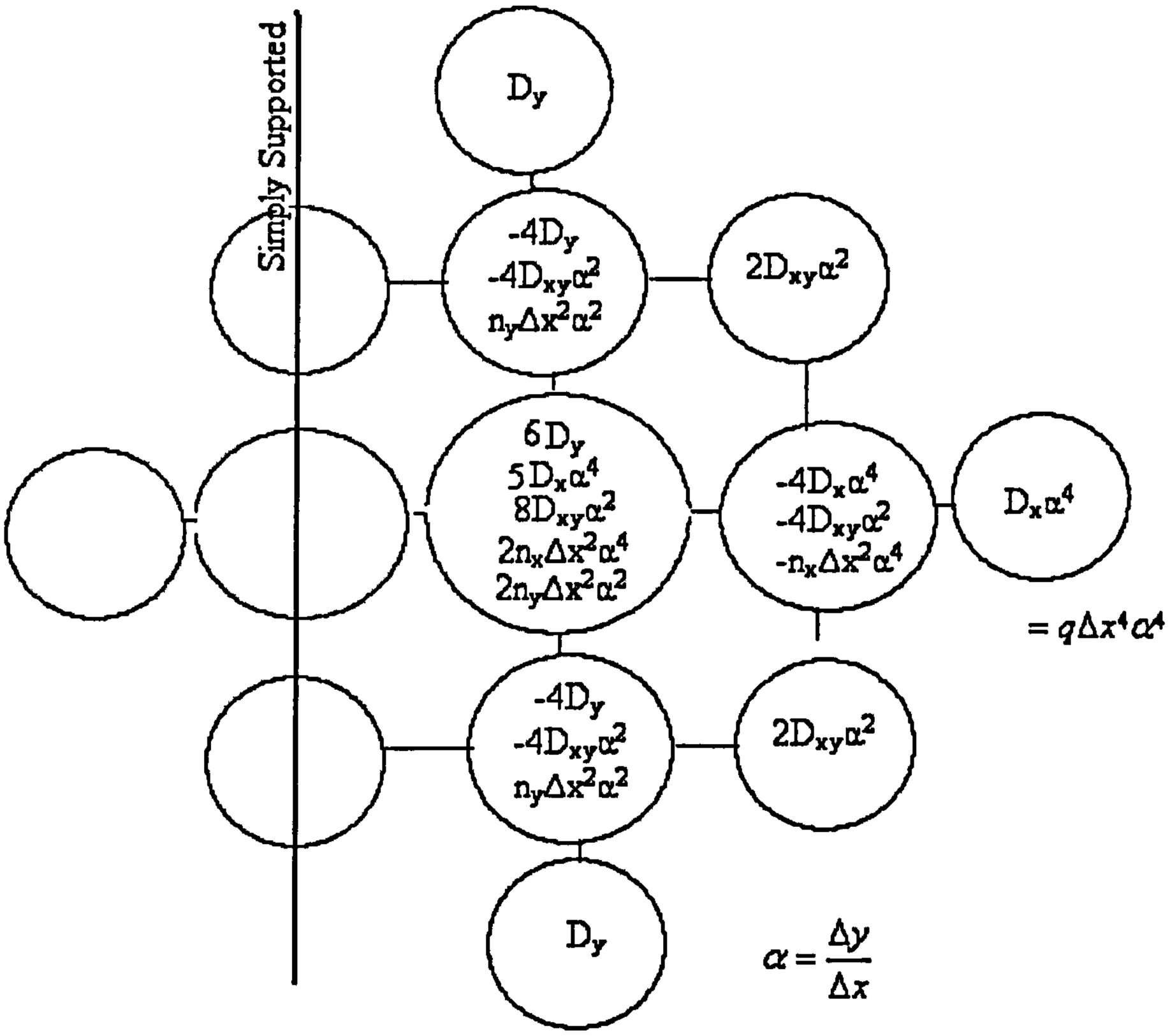

Fig. 3-29 Stencil for adjacent points for simply supported subjected to in-plane force

(ii) Built-in edge (Fixed edge) with in-plane forces

The boundary condition representing a fixed edge can be treated in a similar manner for both, corner and adjacent points.

Now all terms of the differential equation of the plate (3-69) which have finite difference form of (3-70), and using (3-60) to eliminate all derivatives of w can be expressed for fixed edges. The results of these mathematical treatments are given in a diagrammatic form in Fig. 3-30 for points adjacent to the corners and Fig. 3-31 for points adjacent to the edges.

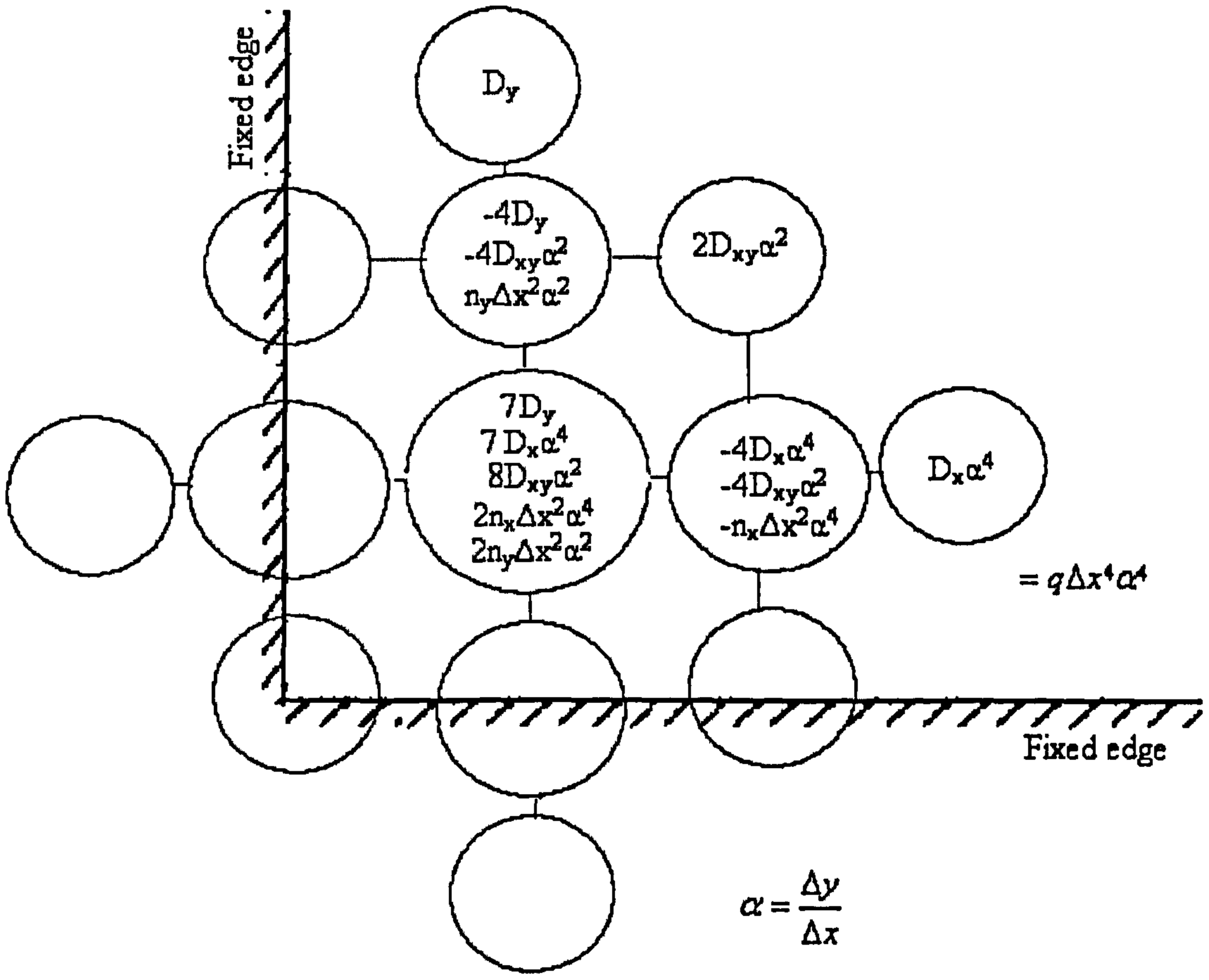

Fig. 3-30 Stencil for corner points for fixed edge subjected to in-plane force

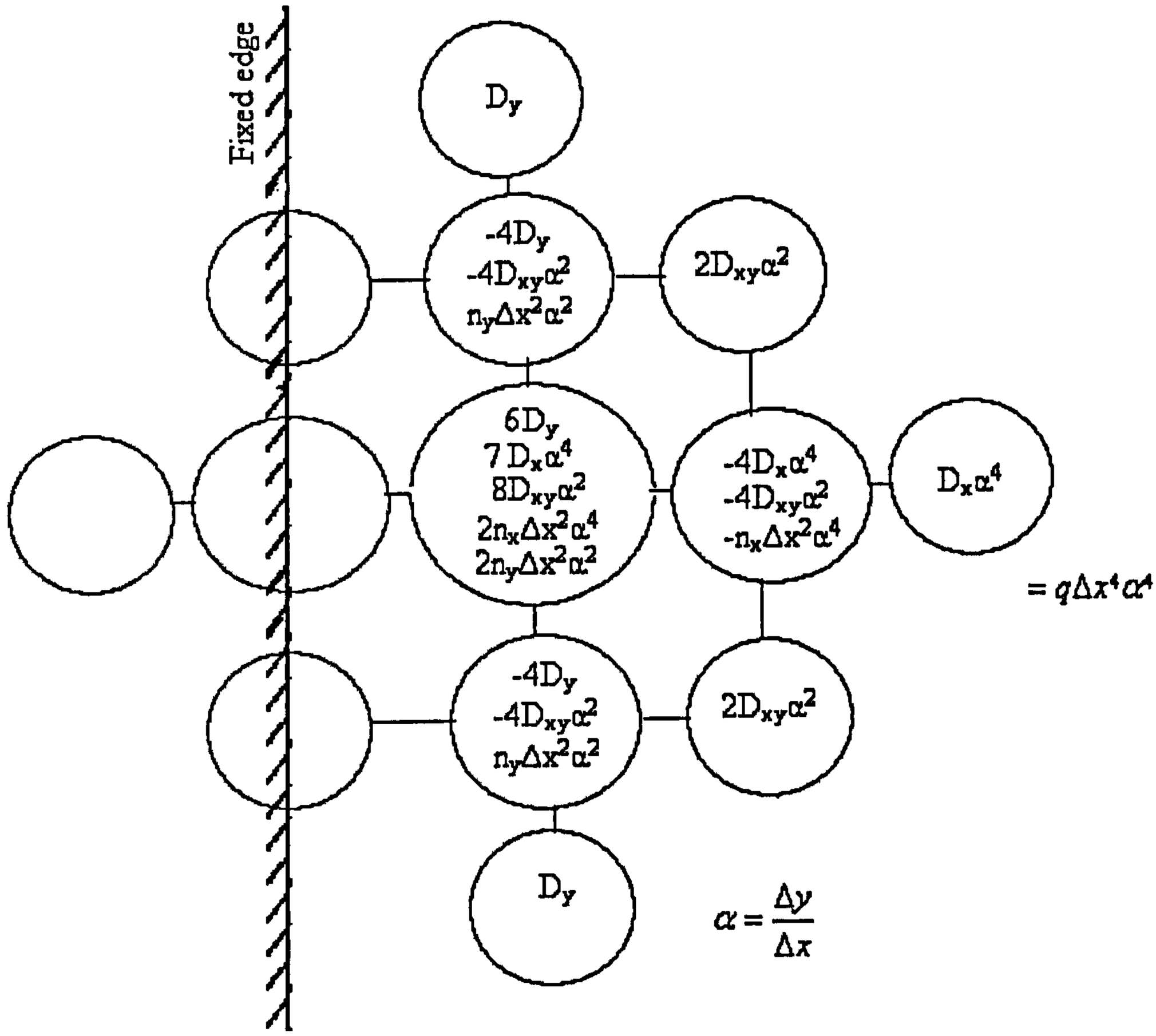

Fig. 3-31 Stencil for adjacent points for fixed edge subjected to in-plane force

Various edge conditions can be modified numerically as explained in the previous Sections by using similar formulation.

3.7 The effect of in-plane forces on shortening

At elevated temperature and increasing deflection the edges attempt to move inwards, forming deformation along edges.

The procedure to calculate the shortening Δx_i in Fig.3-32 is done by:

- Calculate the deflections for all mesh points of the floor plan
- Calculate Lx(i) for each line in x-direction, when i = 1,2,3,-----
- Finally, calculate Δx(i) for each line by:

$$\Delta x_i = \text{Span} - \sum Lx_i \qquad (3.71)$$

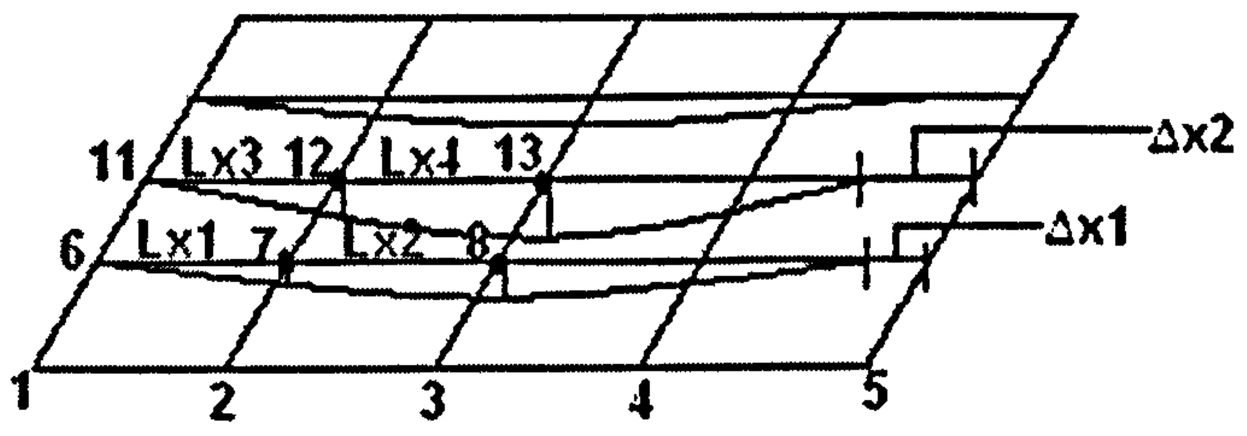

Fig. 3-32 Effect of in-plane force on shortening

3.8 Computer Program (CU-ACCEF)

In the present research a computer program has been developed to predict the performance of thermal and structural behaviour of composite floors at elevated temperatures. The program is labelled (CU-ACCEF) "City University- Analysis of steel Concrete Composite floor Exposed to Fire". It is written in Visual Basic and is based on finite difference method as explained in the previous sections.

The behaviour of the composite floor is simulated as a function of time using the temperature distribution in the cross-section of the floor which evaluated from the thermal analysis.

3.8.1 Thermal Analysis by (CU-ACCEF) Program

The thermal analysis is performed ahead of the mechanical analysis.

To perform the thermal analysis, the dimensions of the cross-section, number of division in each plane, and the duration of a fire are first defined. This is done with input data entered into the **Text Box** in the user interface Fig 3-33. To view the cross-section on the screen, one needs to run the program and then press **Draw** from the menu bar and choose **Section** and **Element**.

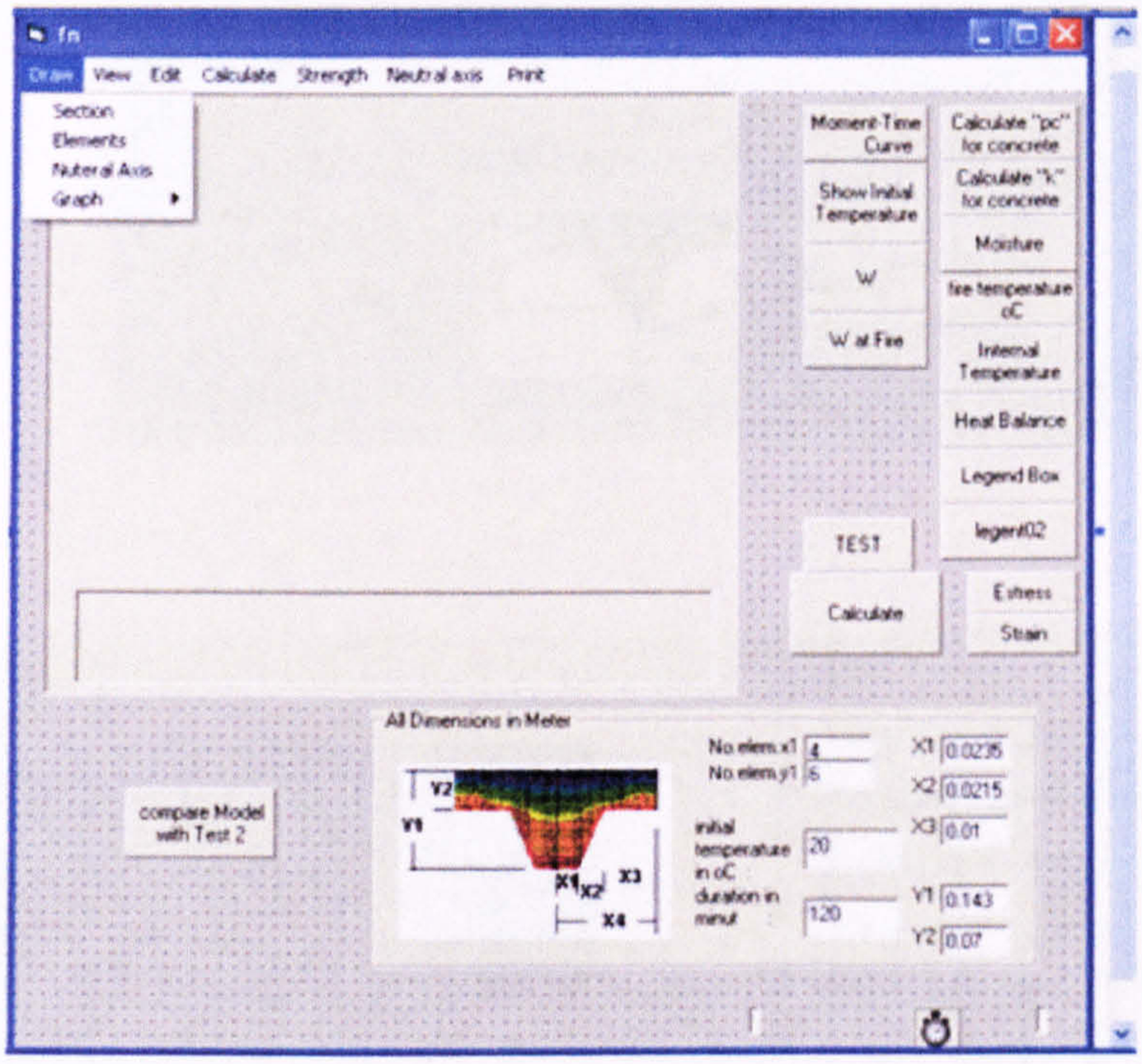

Fig 3-33 Input screen of the thermal analysis

The output screen shows the cross-section with descretized elements as in Fig.3-34.

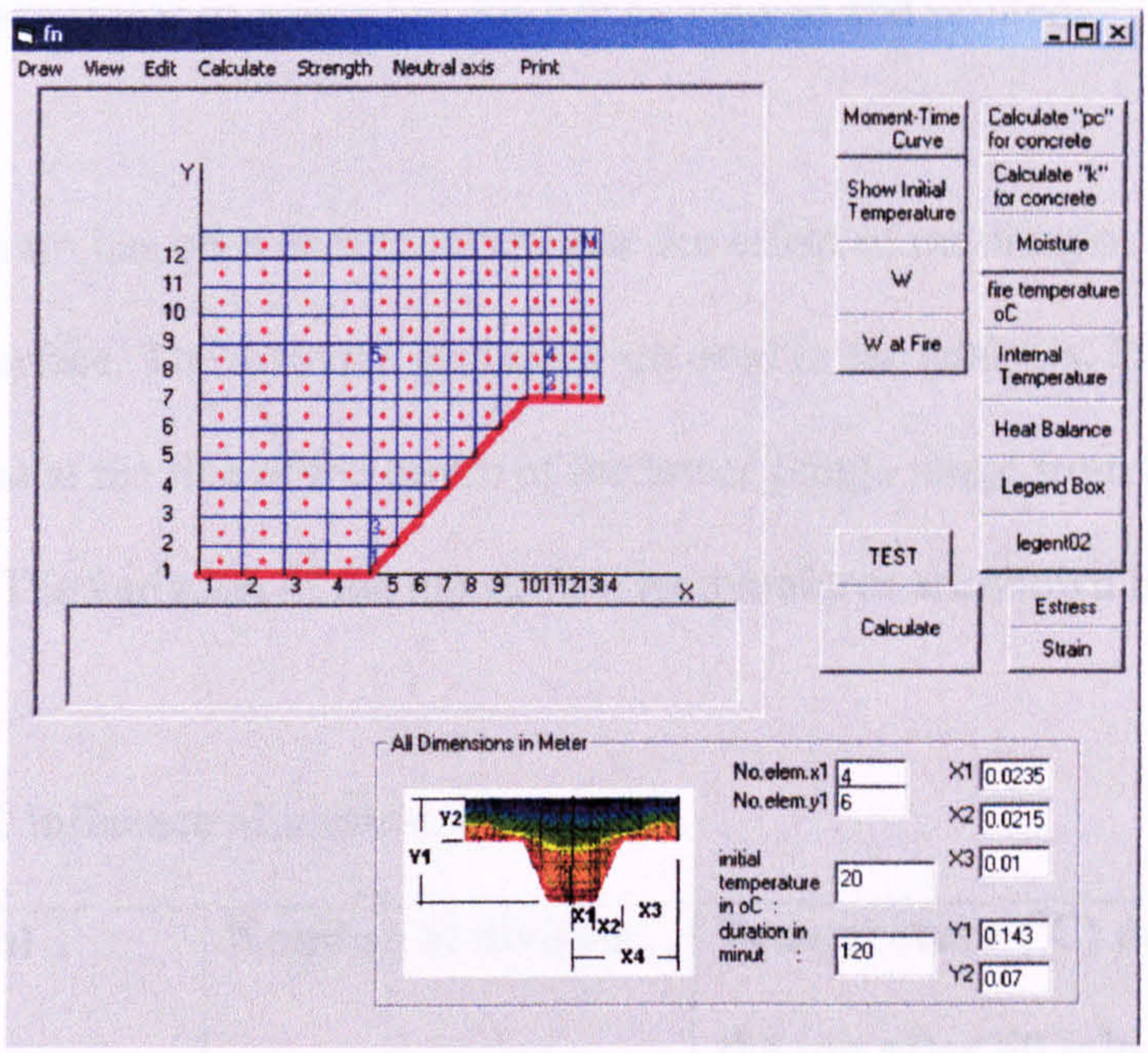

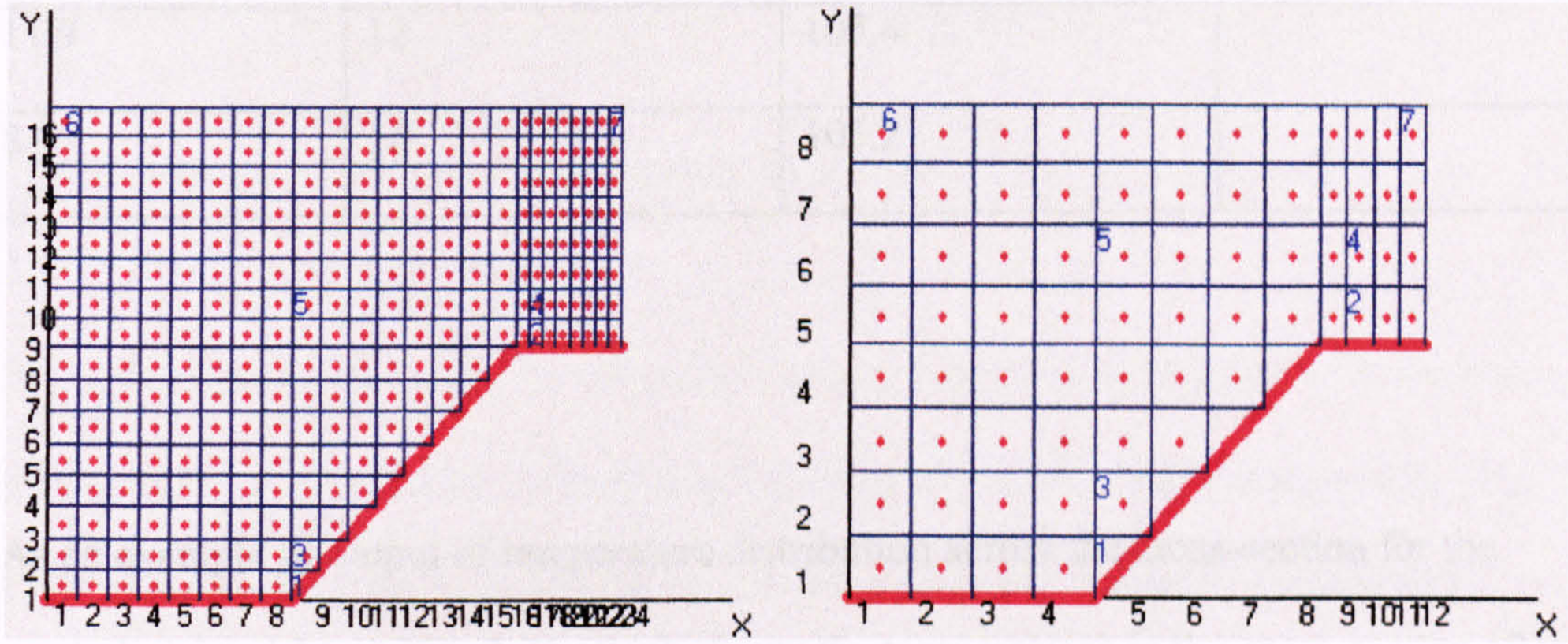

Fig. 3-34 Discretization of the cross-section of the Composite Floor and position of temperature nodes

Having descretized, the cross-section is then subjected to a time-temperature profile to determine the thermal distribution across the cross-section. The time-temperature profile applied to the thermal program can be based on either the standard fire curve

built into the program or for a user-defined fire curve. The results of the thermal analysis are stored in a data file and can be viewed and printed.

The program has been uses to investigate the effect of meshing on the temperature on the top surface. The different grid sizes are used in the analysis, Fig. 3-34. The number of element at the line of the centre of the lower flange range from 8 to 16 for the depth 143mm. The variation of the top surface temperatures are shown in the flowing table:

Table 3-1 Influence of mesh size

Size (mm) **Δy**	**Number of division**	**Temperature (^{o}C) at the top after 60 min**	
17.9	8	106.0	
11.9	12	105.4	
8.9	16	105.2	

As an example of output of temperature distribution across the cross-section for the mesh division 12, see Fig. 3-35 which shows the temperatures in the cross-section after 5, 30, 60, and 120 minutes fire exposure.

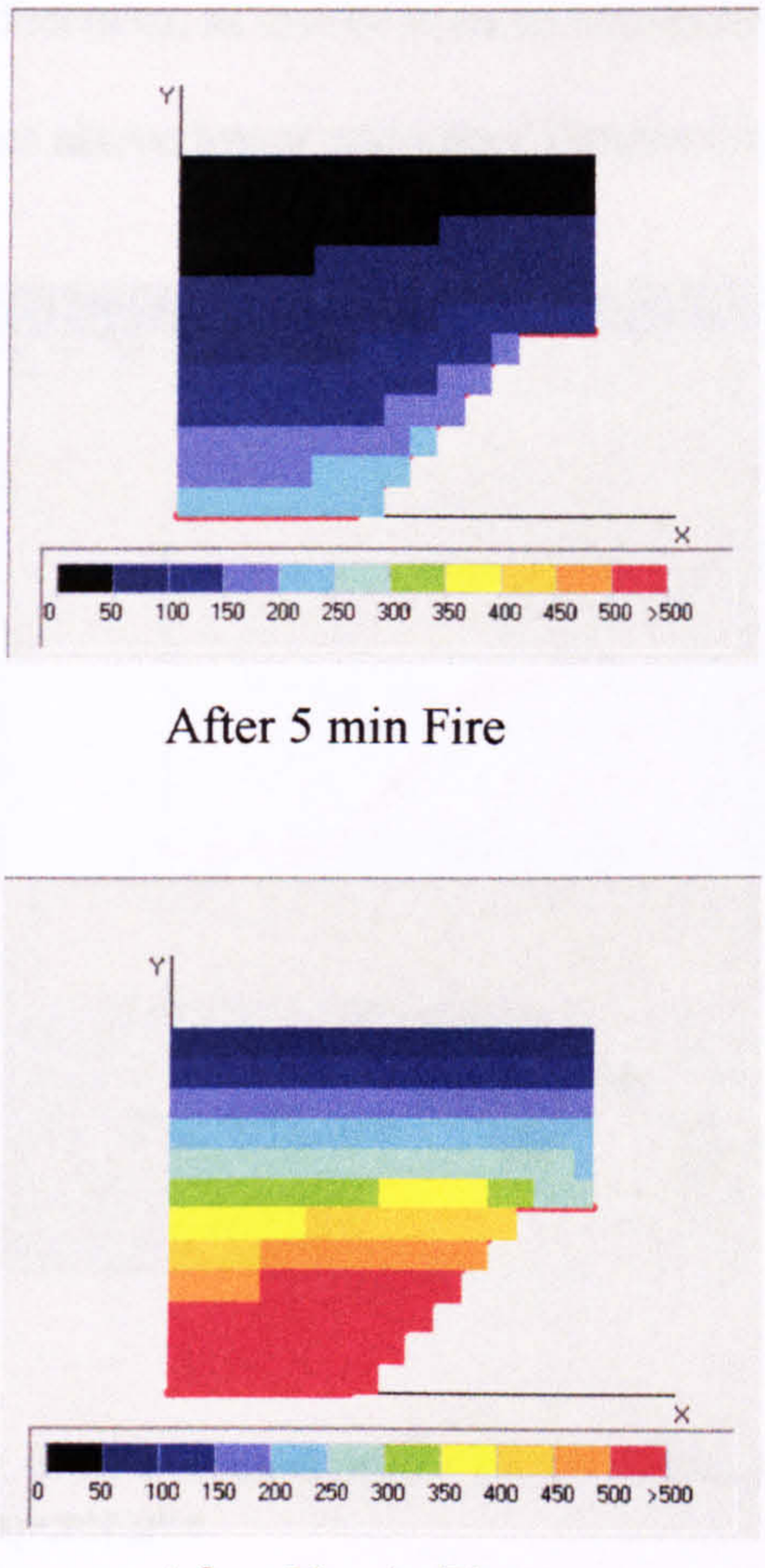

After 5 min Fire

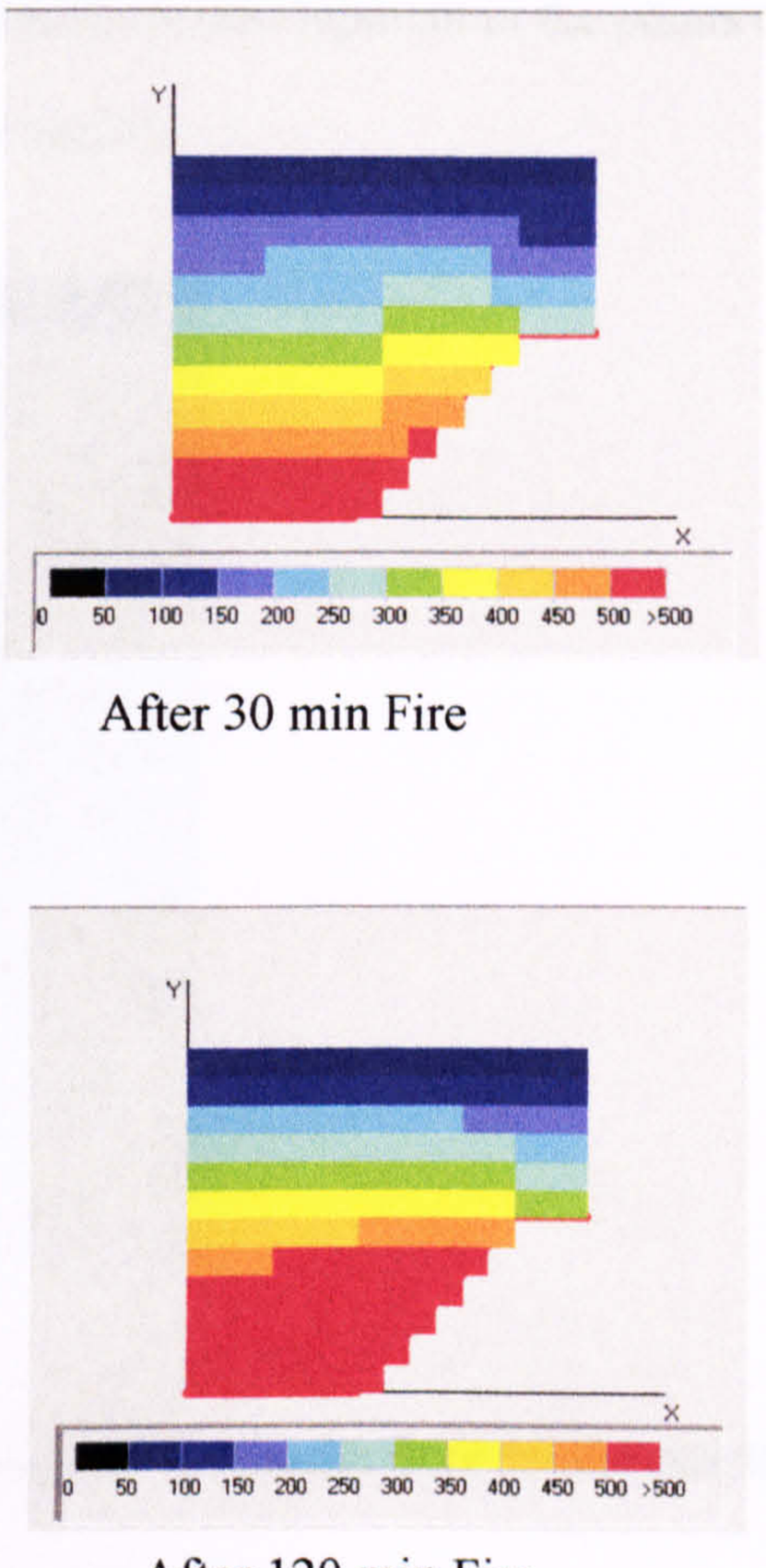

After 30 min Fire

After 60 min Fire

After 120 min Fire

Fig. 3-35 Temperature distributions when the composite floor exposed to fire

In practice, the behaviour of fire-exposed floors is generally determined with respect to fire exposure from below. Exposure at the upper side of the slab is less critical. Due to the profiled shape of the cross-section, the heat transfer in the floor is essentially two-dimensional with relative differences occur between temperatures of lower and upper face of the steel sheet. This is illustrated in the following graphs Fig. 3-36 and Fig. 3-37. The temperature at point 1 rapidly increases, the temperature located at point 2 increases less rapidly, at the temperatures by point 3 is higher than point 4 as a result of heat transfer from both the lower flange and the webs. The temperature increases located at point 5 and unexposed side (top surface) is relatively slow. Another effect is a variation of thickness in the cross section, causing temperature

differences, as can be seen by comparing temperature development in the points on lines above lower and upper flanges (points 4 and 5).

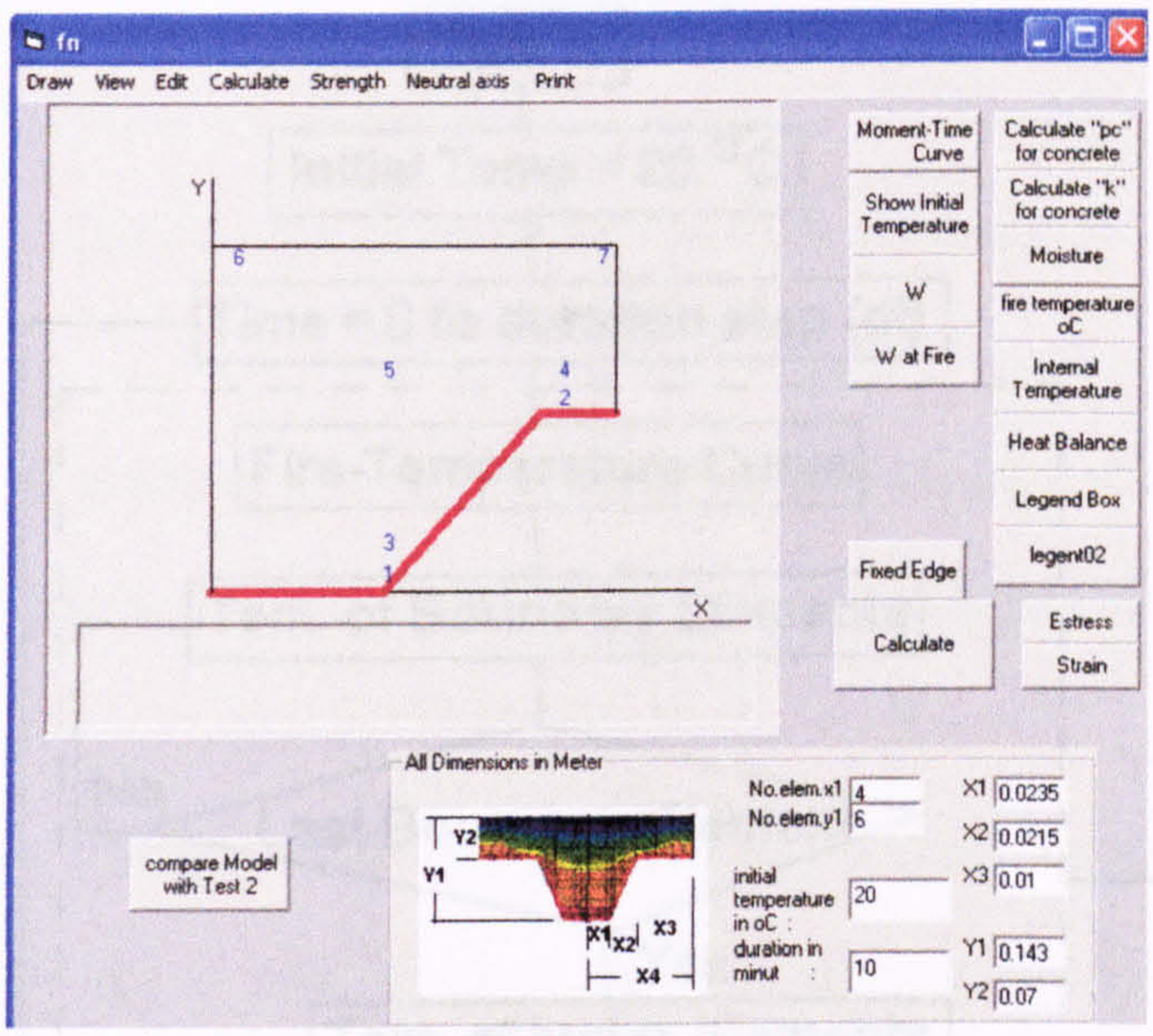

Fig. 3-36 Selected points on the cross-section of the composite floor to measure their temperatures

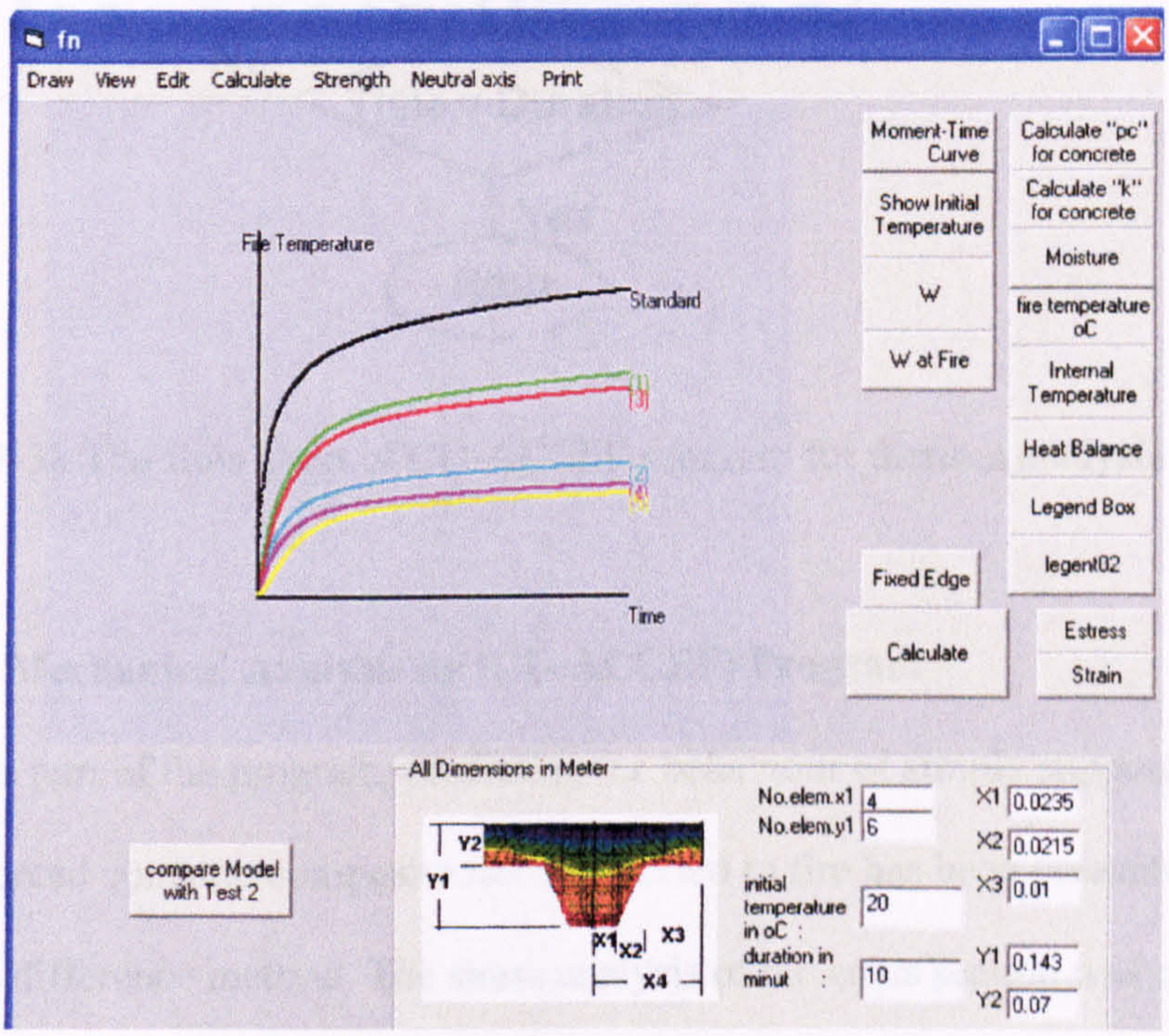

Fig. 3-37 Temperatures at selected points

The flow chart of the thermal analysis program is illustrated in the following Fig. 3-38.

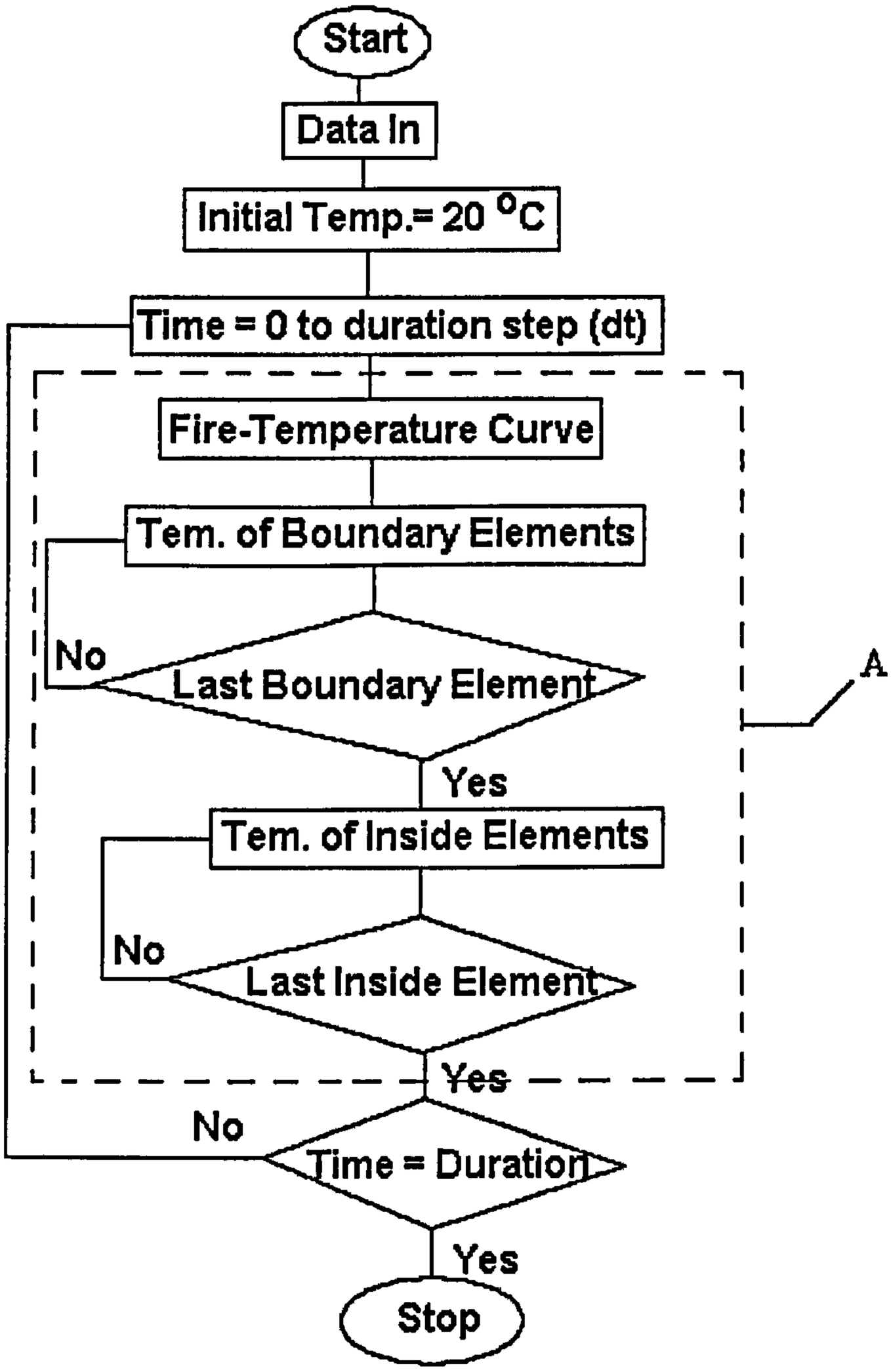

Fig. 3-38 The flow chart of CU-ACCEF program for thermal analysis

3.8.2 Mechanical Analysis by (CU-ACCEF) Program

In this part of the program, predicting the behaviour of simply supported and fixed reinforced concrete composite floor subjected to fire has been presented using the finite difference method. The stress analysis of the cross section was considered, incorporating the temperature-dependent strength degradation of the concrete, as well as the thermal strains.

The following required sequence of input is used for strength analysis for concrete and steel:

a) Compressive strength of concrete

b) Yield strength of steel

c) Coefficient of thermal expansion for steel and concrete

It is assumed that the lateral load remains the same during fire exposure. However, deformations increase and rigidity decreases due to increasing of thermal curvature.

3.8.3 Discretization of the floor and the cross-section

The floor is divided into a number of segments throughout its dimensions to take into account temperature distributions through the thickness of the floor. This is shown in Fig. 3-39.

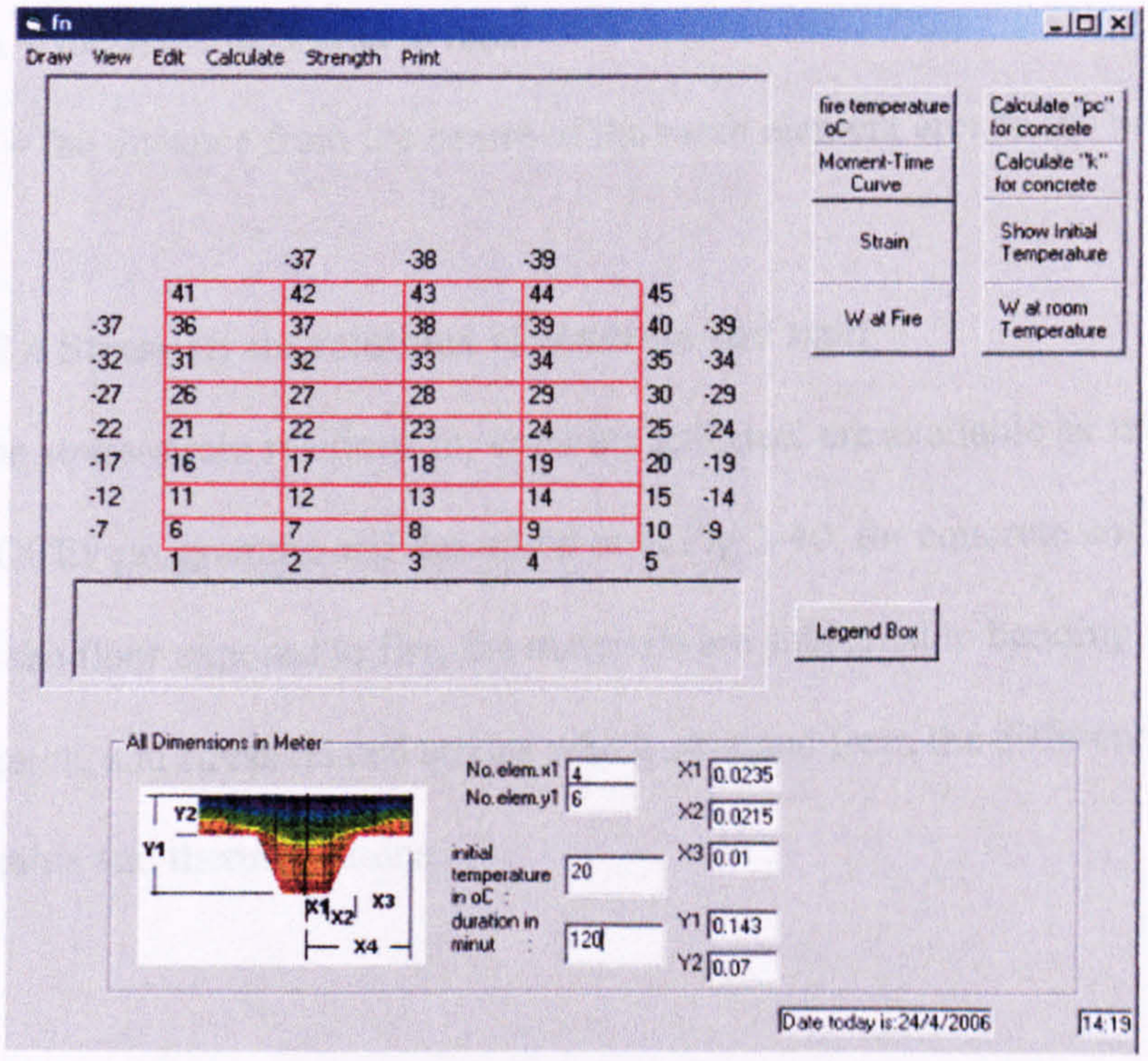

Fig. 3-39 Network of the floor elements

The cross-section is divided as in thermal analysis, consisting of rectangular and triangular shaped elements. The deformations and stresses in the cross section temperatures, deformations, and stresses of each element are represented by those of the centre for the element.

For two-dimensional (plane) problems, the axes are labelled x and y. The displacements are positive in the direction of x and y. The moments and rotations are positive in the counter-clockwise direction. The stresses are positive in compression and negative in tension. The bending moments in the floor are obtained as the summation of (σ.dA.Z) for each element in the cross-section.

When :

σ = stress

dA = mesh element area in mm^2

Z = the distance from the centre of the mesh element area to the neutral axis.

3.8.4 Stress-strain relations of concrete and steel

The stress-strain relations for concrete and steel are available as subroutine in the CU-ACCEF programme and described as in Fig 3-40 for concrete and Fig. 3-41 for steel.

In the floor exposed to fire, the materials are subjected to bending strains, thermal strains, and stress related strains which obtained from the difference between bending strains and thermal strains.

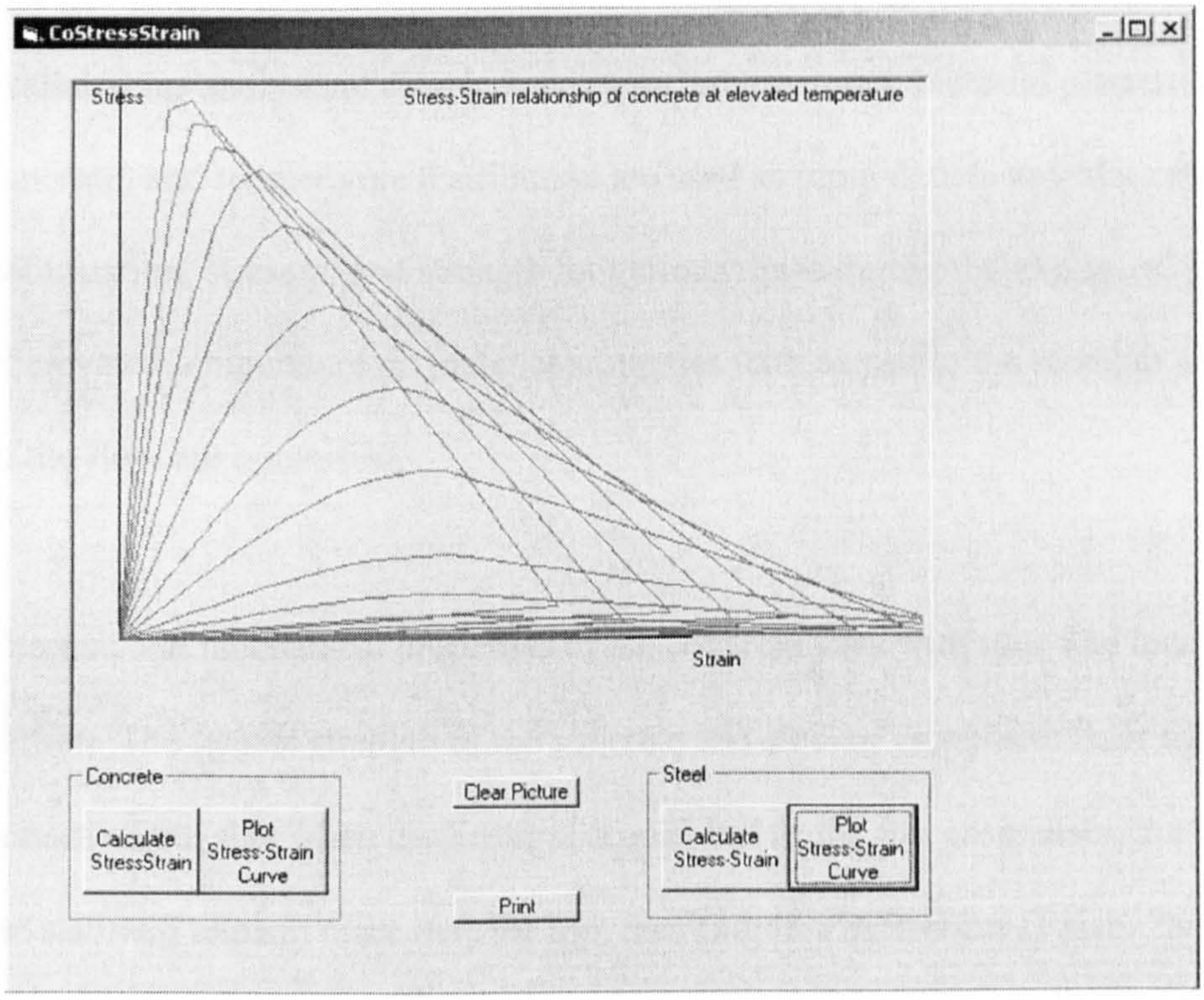

Fig. 3-40 Stress-Strain relationship of concrete at elevated temperature

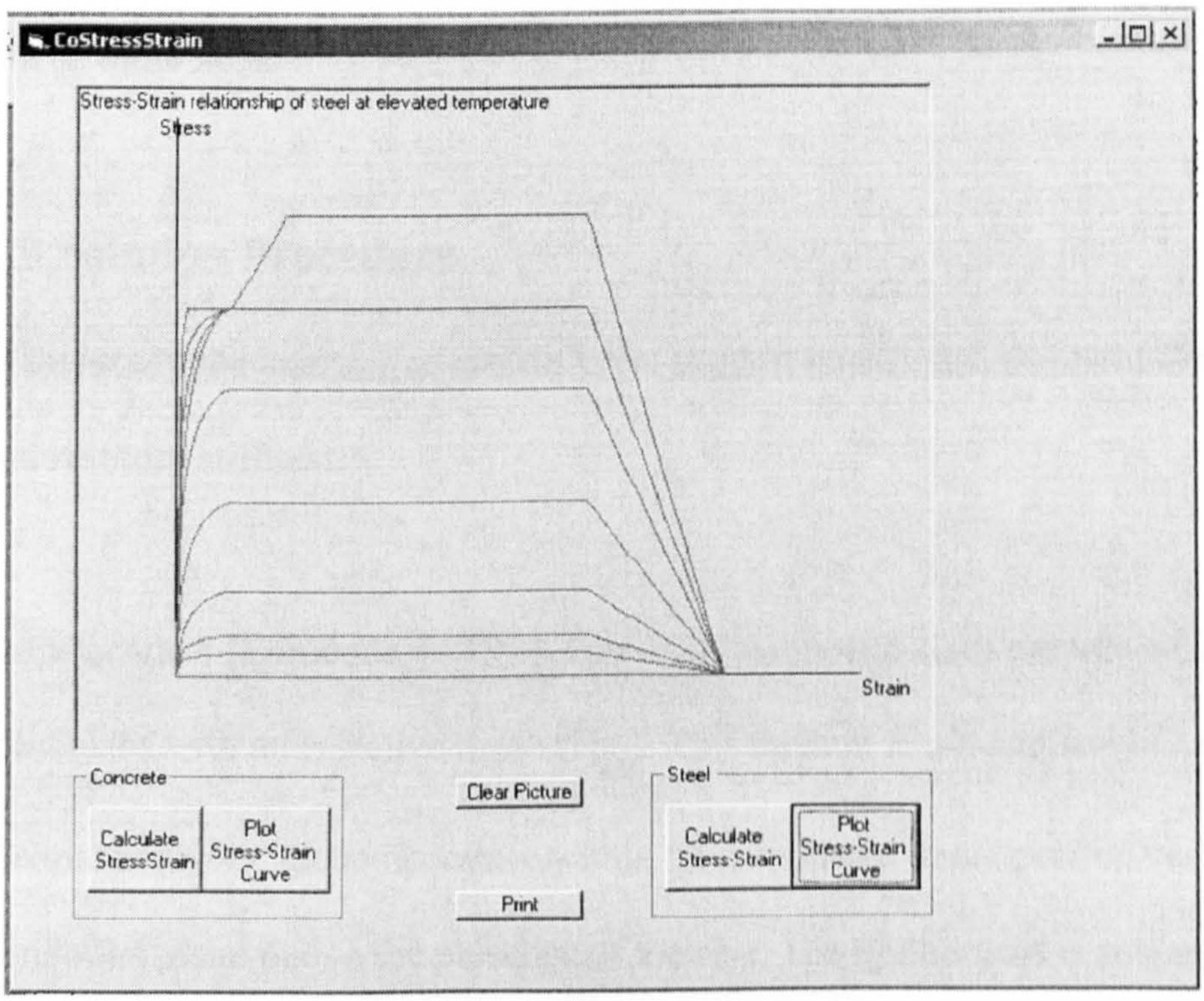

Fig. 3-41 Stress-Strain relationship of steel at elevated temperature

The material properties available in the CU-ACCEF programme, as subroutines, are available for analysis at elevated and room temperatures. Material properties (steel and concrete) and temperature distribution are used as input data to calculate the deformation, stresses, and strength for various times during the exposure. The effects of elevated temperature on material properties with regard to the strength and rigidity of the floor are quantified.

Thermal and mechanical properties of the concrete vary with time and location in the section. The tensile strength of the concrete and steel of composite floor acts near the bottom of the slab when the fire first occurs, but as the fire progresses, the bottom of the slab will expand more than the top, resulting in a deflection of slab. The tensile strength will decrease as the temperature increases and the difference in rigidity will generate. If the slab is thick and heavily reinforced, the compressive forces that occur can be quite large.

3.9 Solution Procedure

In this study the analysis covers different support conditions, different fire exposure and restraint stiffness.

In Eurocode 4 [Eurocode 4– 1994, Part 1-2], composite slabs are treated as equivalent solid slabs with an effective depth (H_{eff}). This method is not applicable here. In the thermal analyses, the temperature within its continuous upper portion varies in the horizontal plane due to the presence of the ribs. The thinner part is subject to higher

temperatures than the thicker part. The different temperatures in the thick and thin part of the floor have been considered in order to perform the structural analysis.

For these, fire resistance is usually expressed in standard classes, ranging from 30 to 120 minutes in 30-minute intervals. Only exposure from below is considered. In order to obtain reasonable agreement between the numerical and the experimental results which are discussed in Chapter 4, the contribution of the steel sheet decking was ignored for the fire limit state

Due to the shape of the profile in Fig. 3-3, the temperature distribution within the depth of the floor is non-uniform in both planes. In order to take into account this factor within the developed computer program CU-ACSEF, a simplifying assumption was made in this study; the temperatures distribution within the depth of the floor cross-section are divided into five zones as discussed in Fig.3-4.

3.9.1 The description of thermal response

The first step is determining the temperature distribution over the cross-section at discrete time is Δt during the fire. The two dimensional transient heat conduction problem was solved by the developed computer program. Thermal parameters, such as the conductivity k_c, Fig. 3-42, the convection heat transfer coefficient H_c and the thermal capacity $\rho_c C_c$, were selected in such a manner that the calculated temperatures in concrete agreed as much as possible. Coefficient of thermal expansion is not constant and followed the formulas in Sec 3.3.1. The remaining parameters, needed in the analysis of the temperature response, were estimated on the basis of Eurocode 4 [Eurocode 4– 1994, Part 1-2].

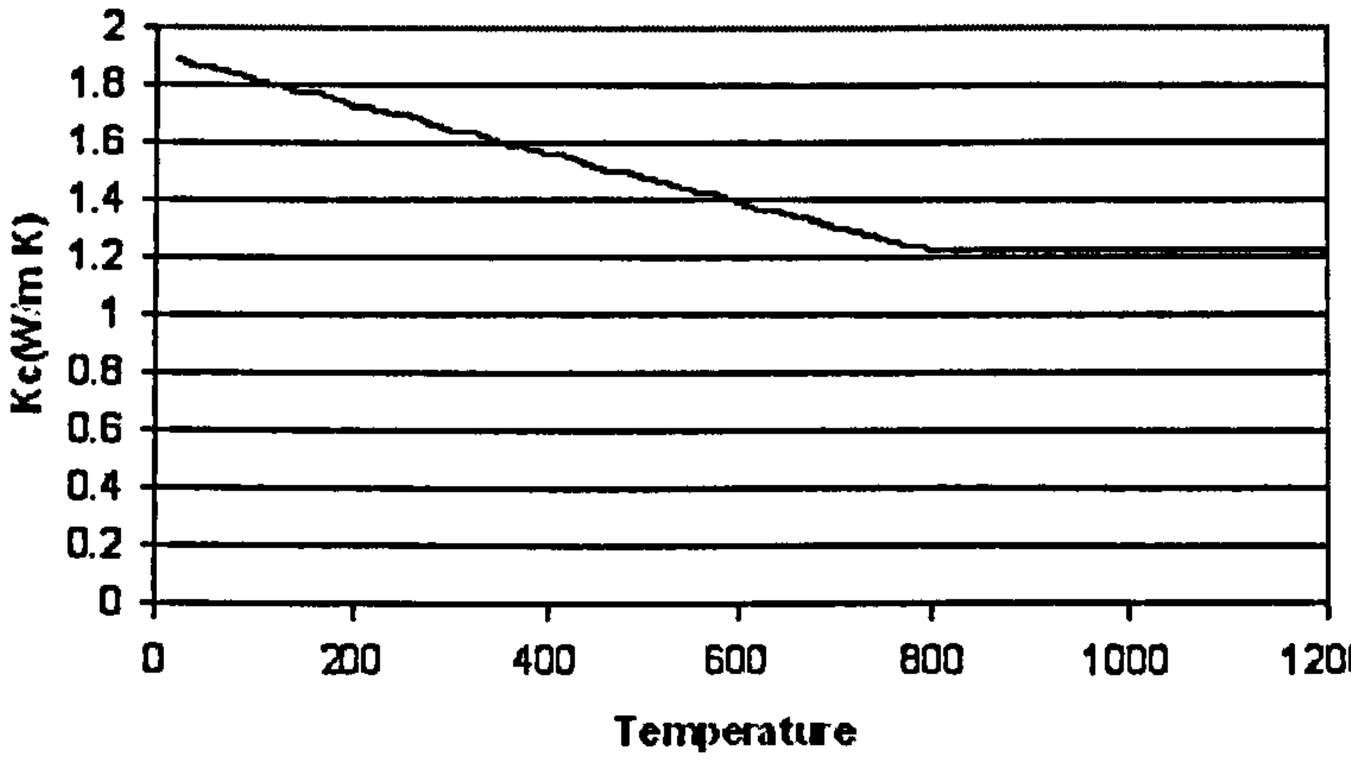

Fig. 3-42 The variation of concrete conductivity k_c with temperature

The temperature distribution over the cross-section of the floor, when exposed to the ISO standard fire, is illustrated in Fig. 3-35 for fire period 5, 30, 60, and 120 min, which is assumed to remain constant over the slab plan. That is, the fire underneath the floor is assumed to be uniform.

3.9.2 The description of mechanical response

Within an element, the curvature is considered to be changing with the temperatures and a resultant strain (and therefore stress) state at a boundary can be determined by satisfying the equilibrium conditions as illustrated in section (3.4.2), solution of orthotropic plate. Since the material properties vary with temperature and time, an incremental analysis procedure is adopted to evaluate the structural behaviour. The time steps taken by the condition was explained in Section (3.2).

For each time step, each node in the floor is analysed. The stress-related strains for the concrete and the steel for all elements of the cross-section are then obtained using the stress-strain formulas modified for the element temperatures. Equilibrium at the cross-

section is checked to determine whether the summation of internal forces match the applied external forces.

The strength is a function of the deflection in the floor. As the required strength now is known, this is used to determine the floor deflection at elevated temperature.

The plate can be divided into arbitrary number of elements in the x and y-directions. To obtain the deflection shape, initially, it is assumed that the maximum deflection is at the line of the centre of the lower flange and equal to 0.5mm. Applying equation (3-41) in a similar manner to determine the initial deflection at all points:

$$w_{o(1to45)} = A.Sin\frac{\pi(m-1).\Delta_x}{L_x}Sin\frac{\pi(n-1).\Delta_y}{L_y} \qquad (3\text{-}70)$$

When: m = 1, 2, 3,…,5 (in x-direction)

n = 1, 2, 3,…,9 (in y-direction)

.

This is illustrated as following in Fig. 3-43 :

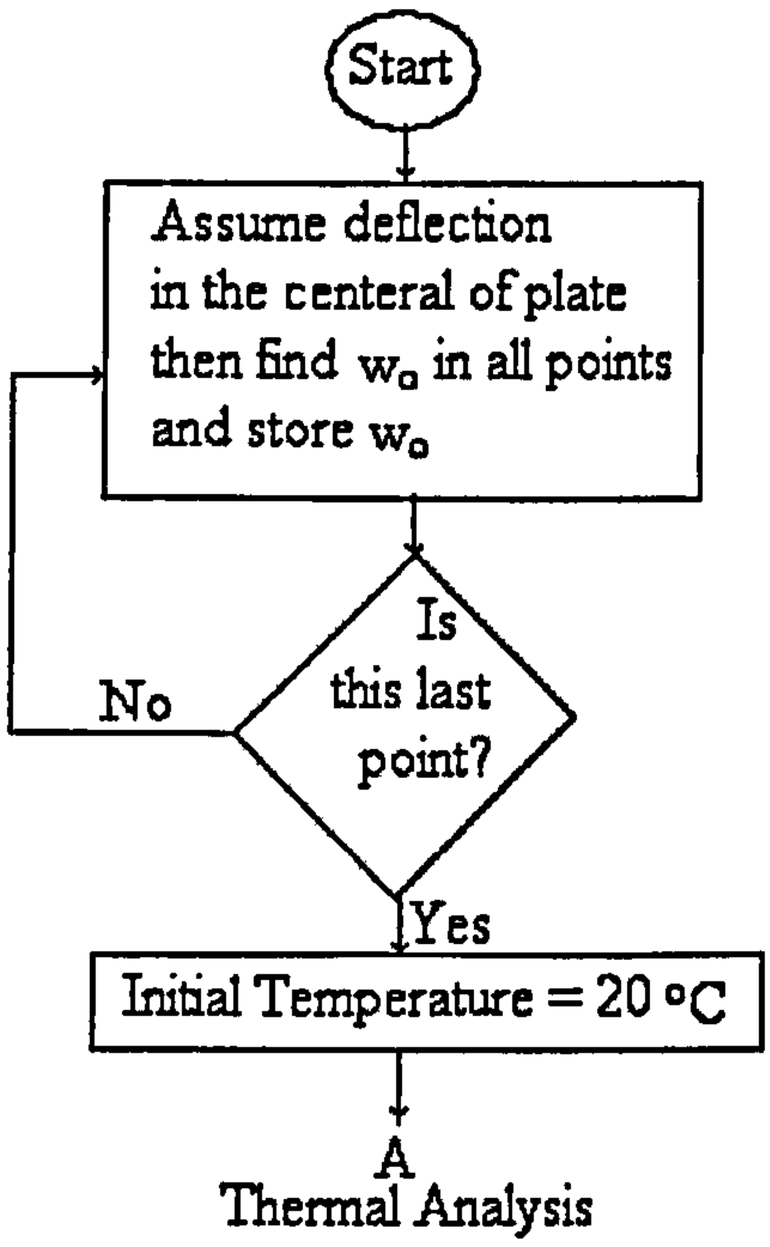

Fig. 3-43 Obtained initial deflection shape by CU-ACCEF program

The curvature in the two planes are derived as in equation (3-39) and (3-40).

When: i = 1, 2, 3,..., 45 (number of grid)

The edge deflections and curvatures are zero.

The following procedure was followed to find the predicted behaviour:

(1) The position of the neutral axis (NA1) is initially assumed at zero distance from the lower flange of the cross-section, to calculate the stresses at all points. Parameters of the stress-strain relation of concrete and steel are taken from Tables 3.3 and 3.4 in Eurocode 4 [Eurocode 4– 1994, Part 1-2] as well as concrete strain at the peak compressive stress, reduction factor for concrete and steel.

To find the net strains, the thermal and mechanical strains are determined as follow:

$$\varepsilon_{bending} = z_i \times \phi_x$$

(z_i) is present the distance from element centre to the (NA1)

At room temperature, 20 °C, thermal strain calculated from equation (3-42) which is as the following:

$$\varepsilon_{thermal} = -1.8\times10^{-4} + 9\times10^{-6}(T) + 2.3\times10^{-11}(T)^3$$

Then the net strains ε_{stress} are determined in all points.

As noted above, the temperature differentials develop between the upper and lower surfaces. These differentials lead to thermally induced bending which can increase deflections. A high temperature gradient through the depth of the floor will induce bending moments and additional deflections in the floor (see Equation 3-52 again).

Stress is calculated as a function of temperature and strains, for given room temperature properties according to the description in Sec 3.4.2. The internal forces are obtained as a summation of all the stresses.

Applying equations 2-3 to 2-13 to calculate the stress, the total internal force is found by:

$$p_1 = \sum \sigma \times \Delta A \qquad (3.73)$$

(2) Assume the position of the neutral axis (NA2) at the top surface. Then repeat the procedure (1) to calculate the internal forces p_2 with new position of the neutral axis.

Therefore the neutral axis (Z) determined by trial and error as follows:

$$Z = \frac{p_1 \times NA1 - p_2 \times NA2}{p_1 - p_2} \qquad (3.74)$$

(3) The procedure of the step (2) repeated with the new Z value until the convergence in the position of neutral axis.

(4) Once the neutral axis is determined, recalculate the strain and stress at all grid points of the section until compressive and tensile forces add up to zero.

$$\sum p = 0$$

After convergence, the moments for all mesh elements are obtained as follows:

$$M_x = \sum_{i=1}^{i=45} p \times z_i$$

The plate rigidities are calculated by:

$$D_x = \frac{M_x}{d^2 w / dx^2}$$

D_y is calculated in a similar manner for y-axis.

The procedure of steps 1, 2 and 3 is described in the following flow chart Fig.3-43a.

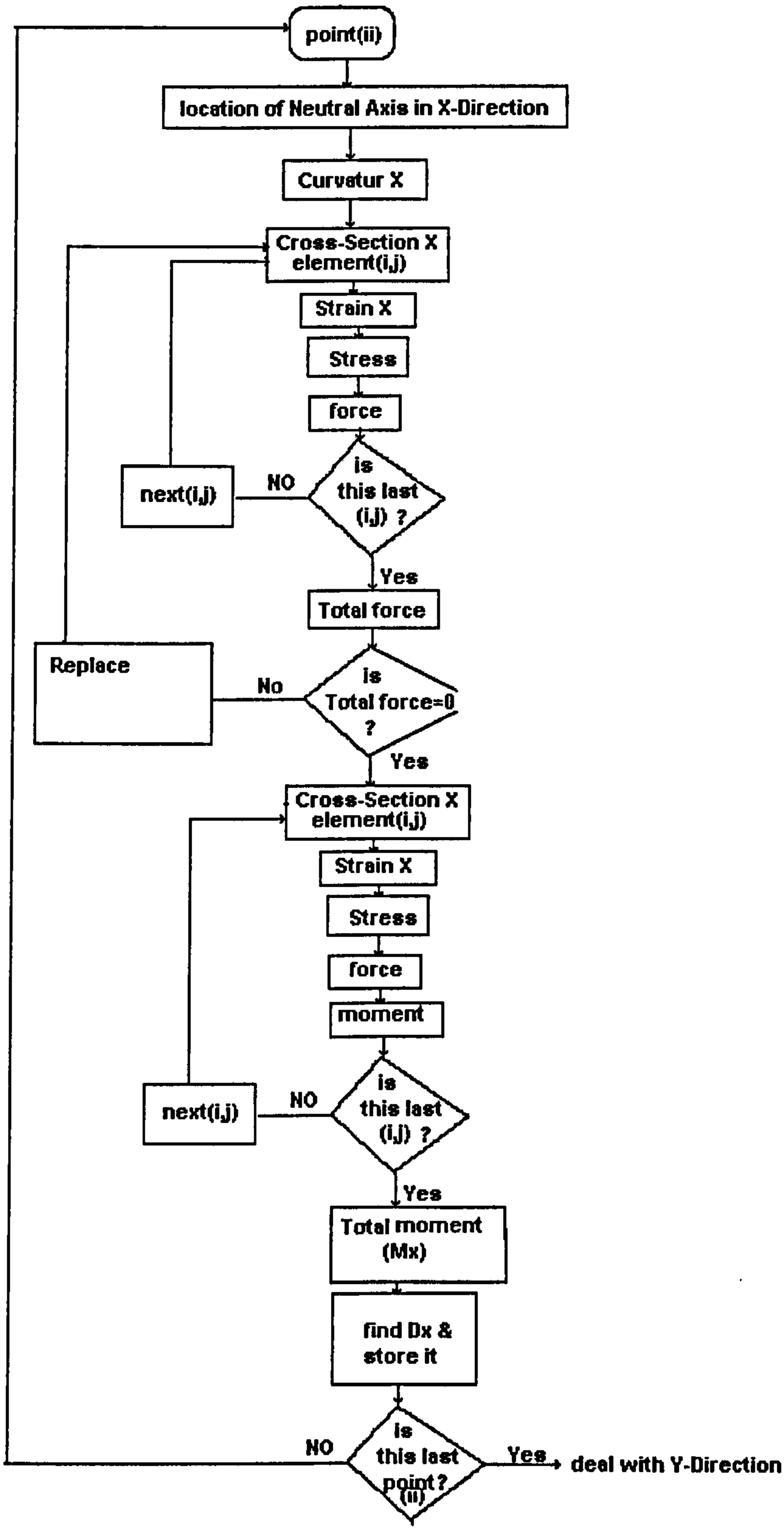

Fig. 3-43a The flow chart of the procedure of steps 1, 2 and 3

To calculate the deflections, the finite difference operator (3-58) is applied to all internal mesh points to form a matrix as shown in Fig. 3-43b.

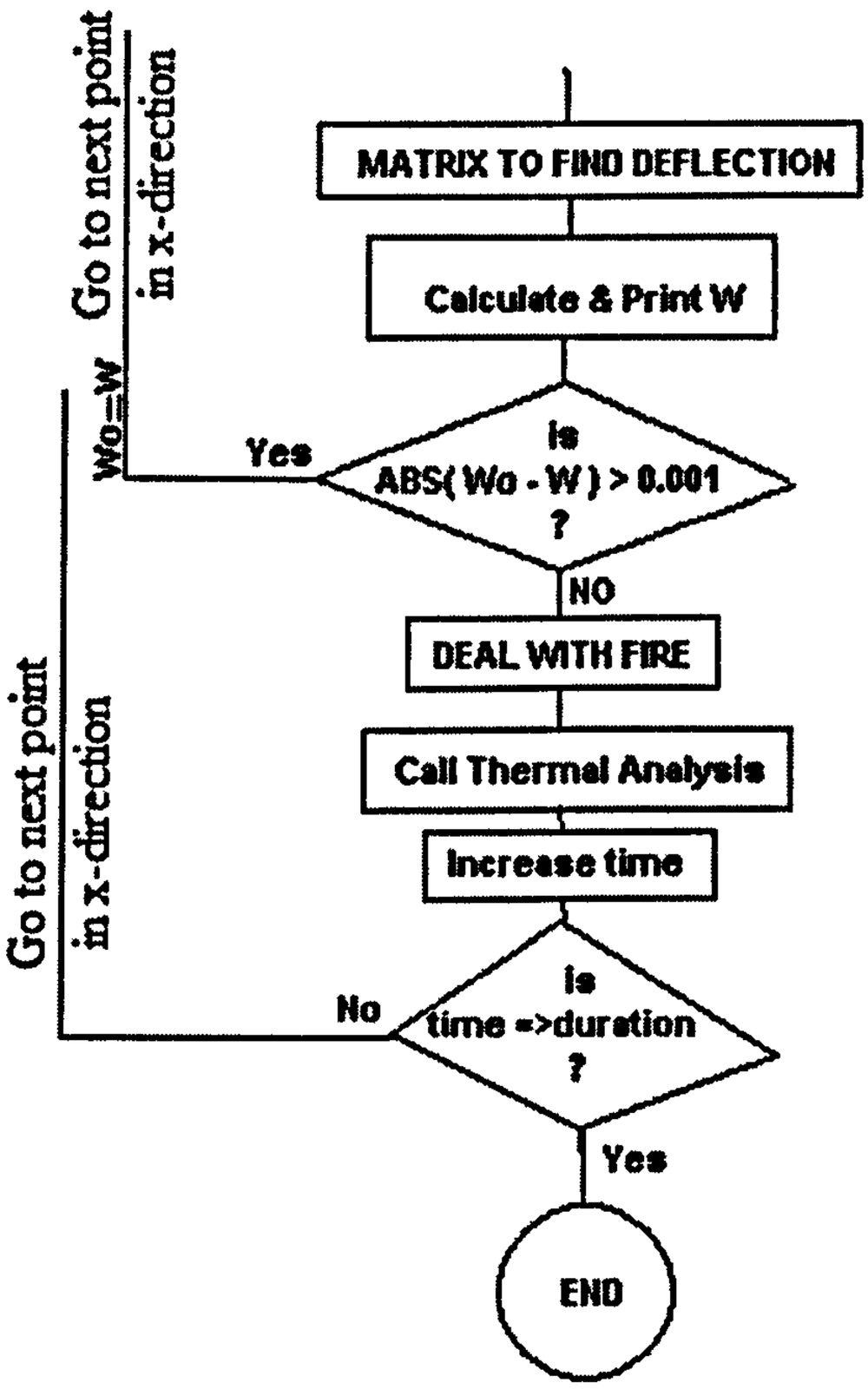

Fig. 3- 43b Matrix to find deflections during the time of fire

The time dependent deflection evolution of the different boundaries was established and a set of typical results is presented by the following Chapters.

The flow chart below describes the overall analysis procedure of the CU-ACCEF program, Fig. 3-44.

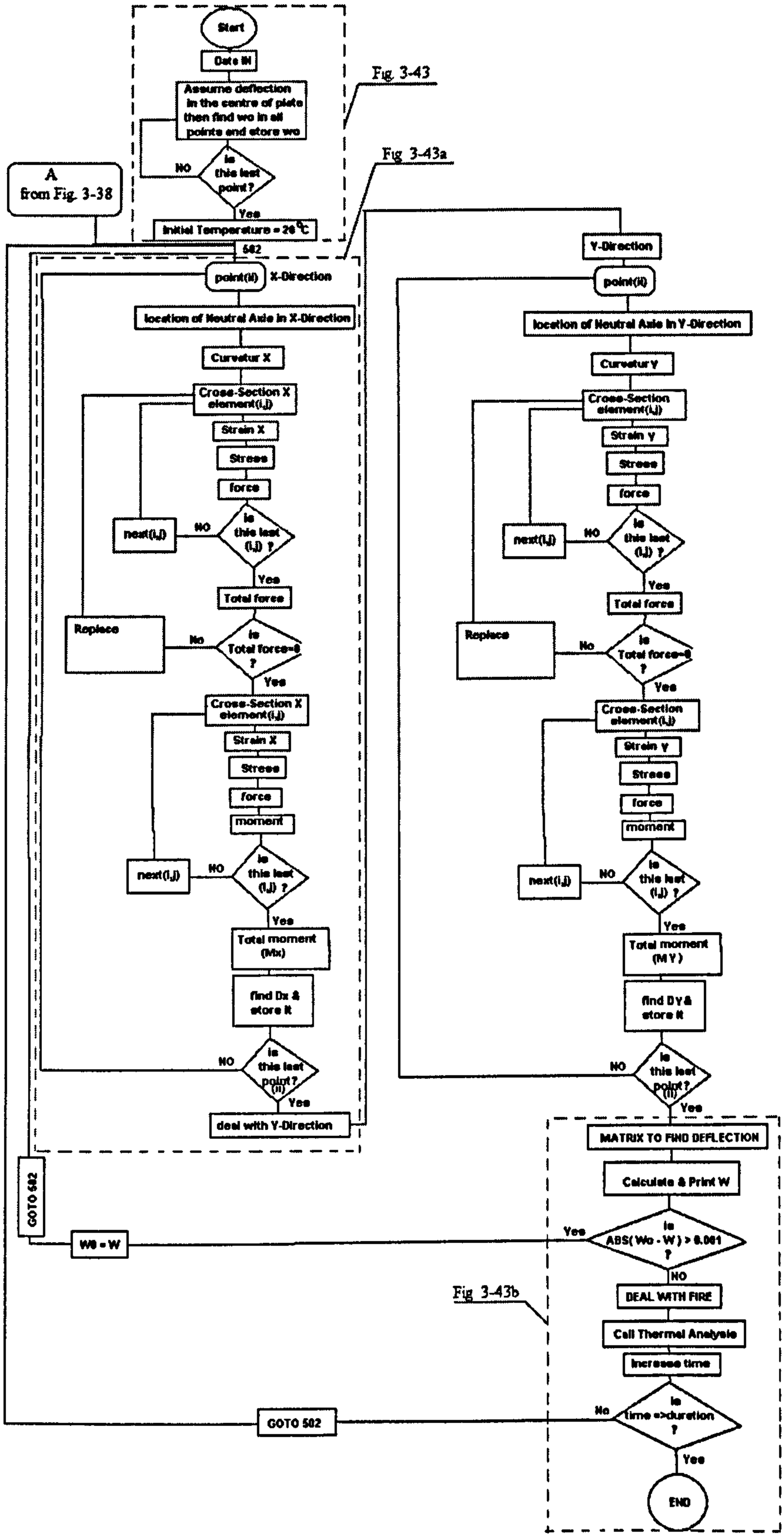

Fig. 3-44 The flow chart of the CU-ACCEF program

CHAPTER 4

Experimental Verification

4.1 Introduction

In this chapter, the results are presented on thermal and mechanical response of composite floors exposed to fire, and compared against published experimentally measured values.

The comparisons with fire tests have many objectives:

1- To investigate whether the new method is able to represent accurately the response of composite floors to fire.

2- To investigate prediction of the floor element temperatures.

3- To give a good estimation of the floor behaviour in fire.

4.2 Comparison of Thermal Analysis Results with Test Results

4.2.1 Hamerlinck and Twilt

Hamerlinck and Twilt [Hamerlinck et al., 1990] carried out tests on twelve specimens to investigate the thermal behaviour of composite floors during exposure to a standard fire. The variables were type of the steel sheet and concrete depth. Two different steel sheets were chosen. The specimen's dimensions were 1600×700 mm and the total depth was 143mm (for trapezoidal shape). Temperatures were measured on lines at the centre of the lower flange and upper flange of the steel sheet. The sheets were not

protected, additional reinforcement was applied, shrinkage-mesh reinforcement was used in the upper part of the specimens, and normal-weight concrete B25 was used.

A distinction has made between lines at the centres of the lower and upper flanges of the steel sheet. The test showed great difference in temperature between upper and lower flange. These differences increase with increasing distance to the top of the floor. The location of given points in the test is illustrated in Fig. 4-1. It presents 6 locations on a line at the lower flange and 2 locations on a line at the upper flange.

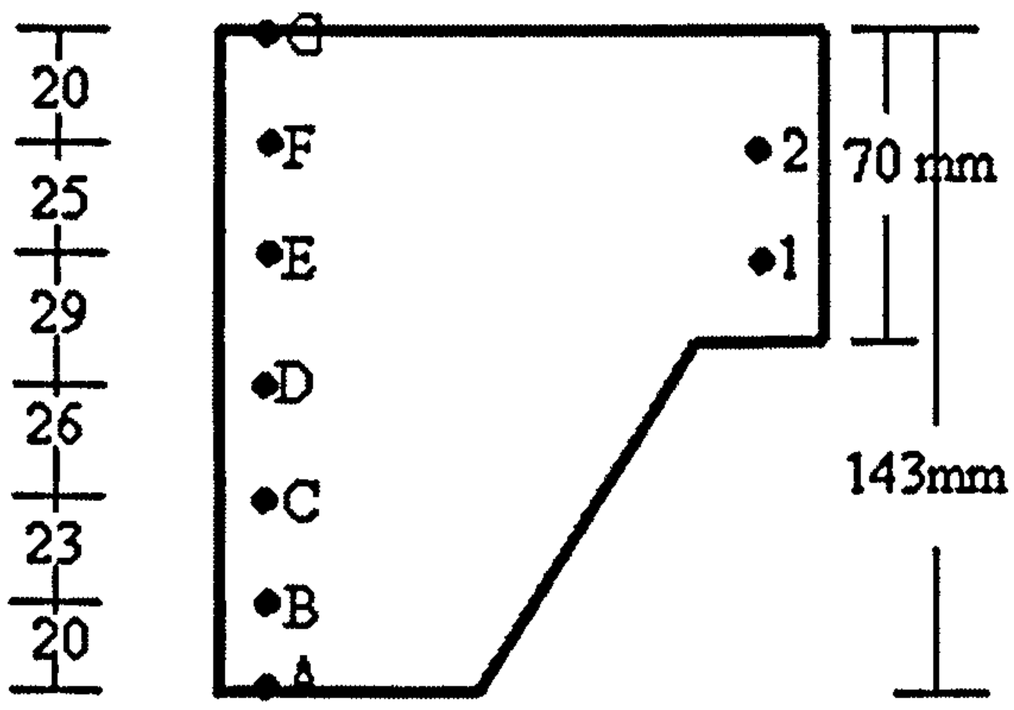

Fig 4-1 Position of given points and dimension of cross-section as in Hamerlinck and Twilt Test

After 120 minutes standard fire exposure, a comparison is made between the calculated temperature results for CU-ACCEF program and the test results is presented graphically in Fig.4-2 for a line at the lower flange, especially for temperature above 100 °C. The poor agreement below 100 °C might be because moisture is transported to cool area at the upper side of the floor, where evaporation takes place. In this area, for temperatures below 100 °C, analysis temperatures are higher than test temperature. The result may be improved by adapting moisture analysis, in which moisture transport is

taken into account. In the present analysis moisture simply evaporates from any element.

The temperature distribution at location D is significantly non-uniform. This may be influenced by a longitudinal reinforcing bar.

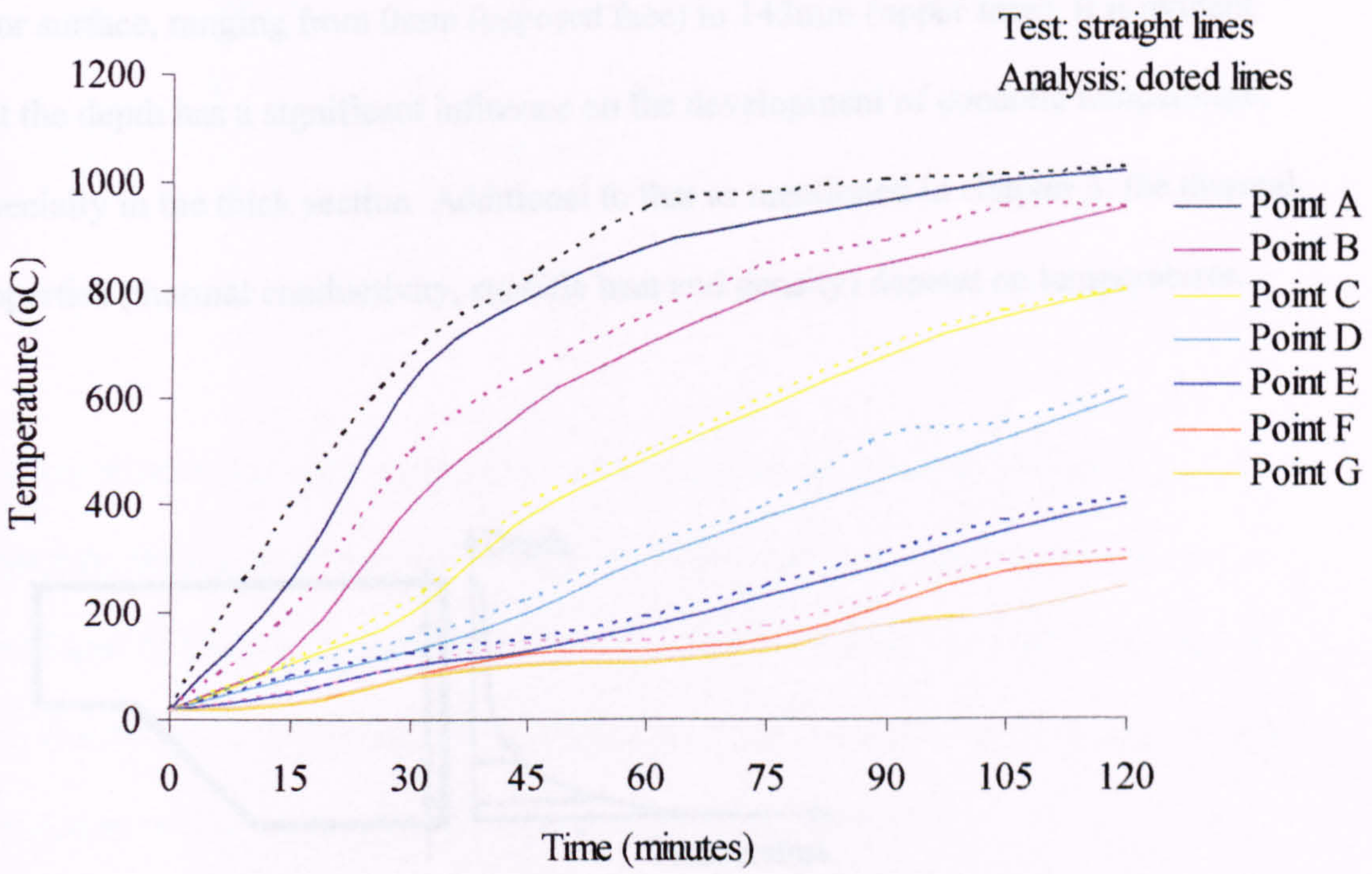

Fig 4-2 Comparison of analysis result with Hamerlinck and Twilt test result of developed temperature in different locations of the composite floor cross-section

The initial temperature on the unexposed side was 20°C. The average temperature of point F and G started to increase after 13 minutes. Between 39 and 81 minutes, the rate of temperature rise is lower compared to the other periods. This is possibly due to the increase of moisture on the top surface, therefore reducing the rate of temperature rise.

Furthermore, the temperatures at comparable points C, E, F and G are generally close to each other.

Overall the comparison between the measured and calculated temperatures is very good.

A temperature distribution through the depth of floor is illustrated in Fig. 4-3. It shows decreasing temperatures at increasing depth at various positions away from the heated floor surface, ranging from 0mm (exposed face) to 143mm (upper face). It is evident that the depth has a significant influence on the development of concrete temperature, especially in the thick section. Additional to that as mentioned in chapter 3, the thermal properties (thermal conductivity, specific heat and density) depend on temperatures.

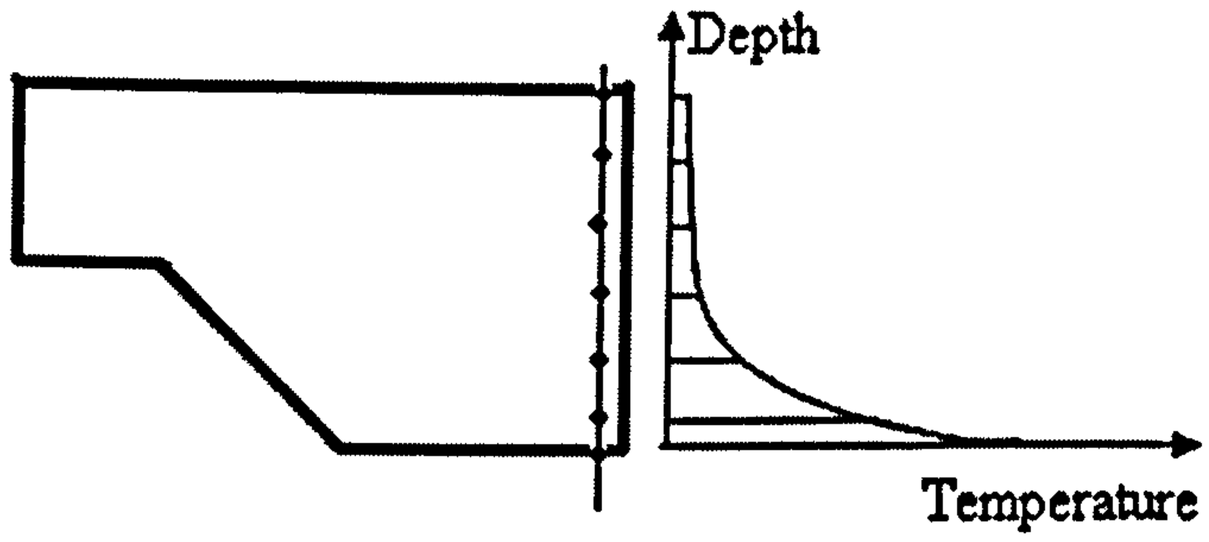

Fig. 4-3 Temperatures through the depth of composite floor

Different temperature developments in the locations and at the same level at upper and lower flange was graphically described as shown in Fig. 4-4. The graph shows significant variation, for both test and analysis method, between the temperature rise in point 1 and in point E. This is only to be expected because the first point is mounted on the thin section of the floor while the other point is mounted on the thicker part of the floor.

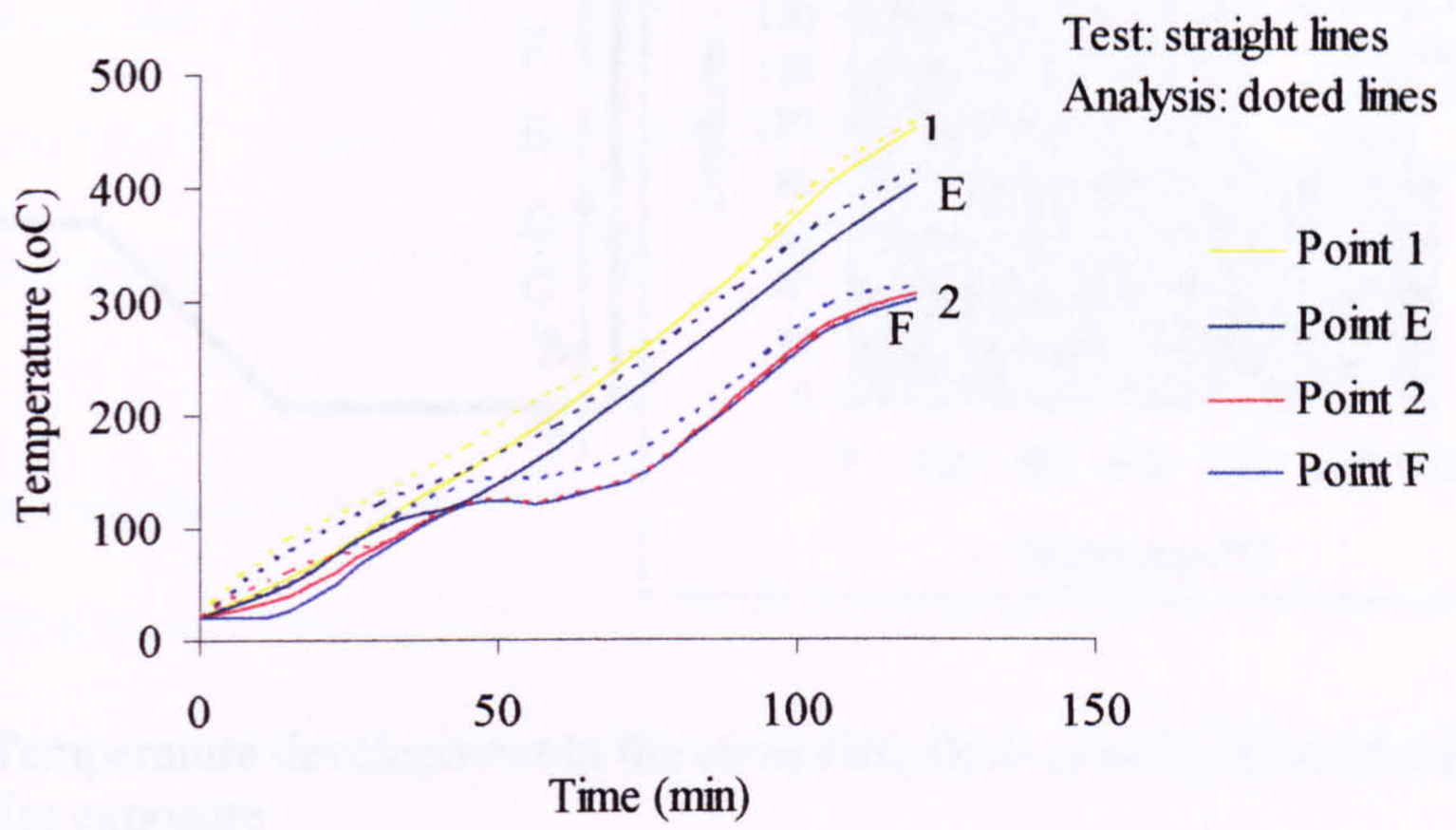

Fig 4-4 comparison of differences between location points at lower and upper.

In order to investigate the temperature distribution along the cross-section, Fig. 4-5 illustrates the output of the new method of analysis using concrete properties, as mentioned in Chapter 2, then compared with output of Hamerlinck and Twilt test. It also clearly shows temperature development between lower and upper surface after 60 minutes as in (Fig. 4-5a) and 120 minutes as in (Fig. 4-5b).

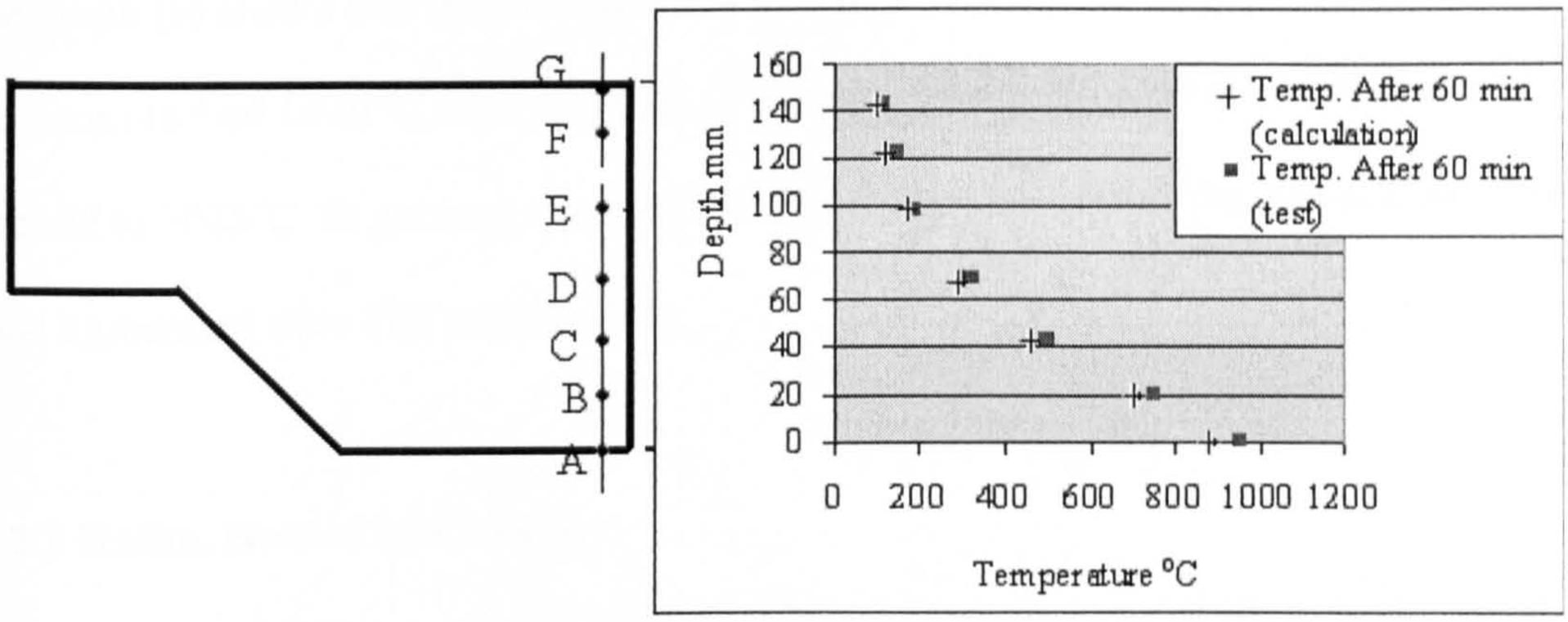

(a) Temperature development in the composite floor cross-section after 60 minutes fire exposure

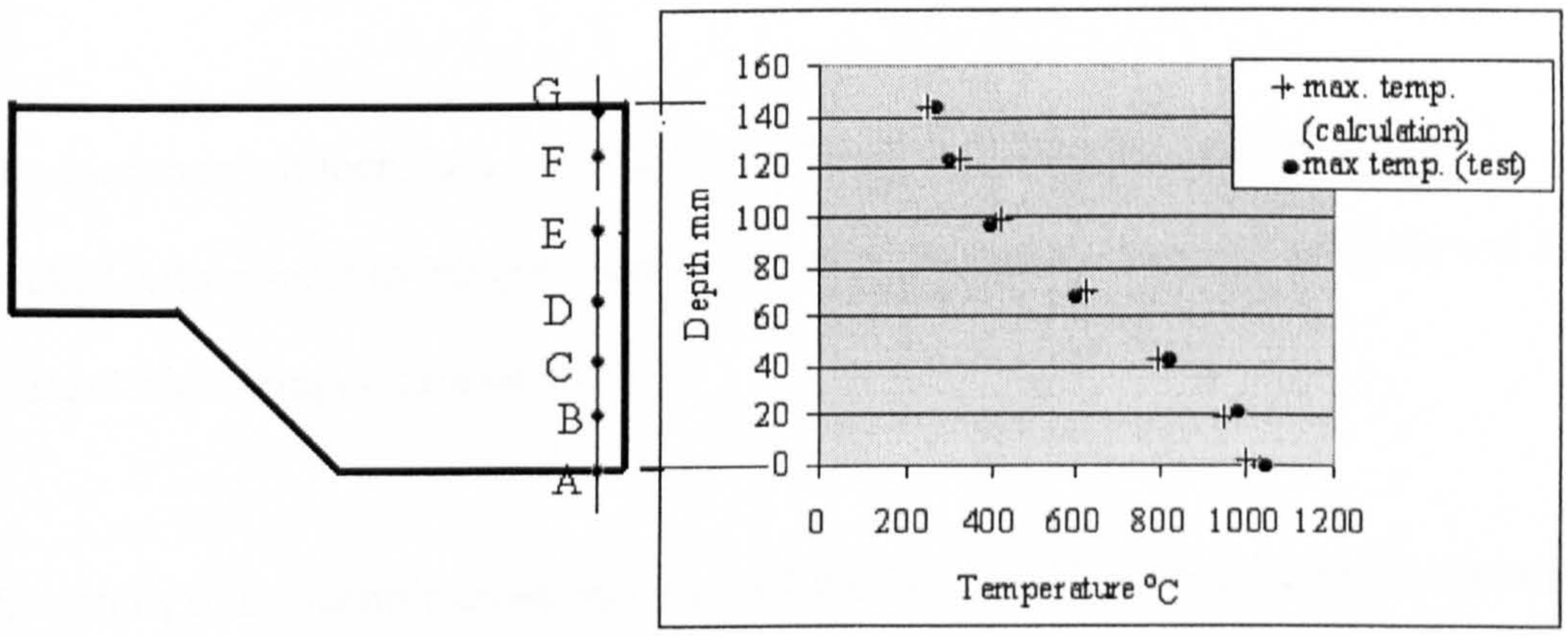

(b) Temperature development in the composite floor cross-section after 120 minutes fire exposure

Fig 4-5 temperature gradient through compared with Hamerlinck and Twilt test

Fig. 4-5 graph (a) presents the temperatures measured after 60 minutes fire exposure in different places as given in the test from point A-G. It can be observed that there are differences of about 70 °C at the lower surface in point A to 5 °C at the upper surface in point G. This has been discussed above and the differences are related to moisture content.

The graph (b) shows that the maximum temperature measured at the exposed face of the floor reached 1020 °C after 120 min of the test while in the new analysis method reached to 1025°C. In general, the temperatures at all comparative locations show very good agreement after 120 minutes fire.

4.2.2 Halim, Hakmi and Leary

Halim, Hakim and Leary [Halim et al., 1997] carried out tests to develop fundamental information on the behaviour of composite floors using a model fire test facility, on two specimens of composite floor subjected to fire in the laboratory of the Civil Engineering Department, University of Salford, UK.

The specimen's dimensions were 1200 ×900×110 mm. The fire resistance has checked with respect to integrity and insulation. The furnace temperature followed the standard time–temperature curve.

The details of the sample cross-sections and the location of selected points to measure concrete temperatures are shown in Fig. 4-6 for Sample 1 and Fig. 4-7 for Sample 2. In Sample 1, a light steel mesh was provided for fire resistance and to control cracking. Longitudinal bars were added in Sample 2 to study their effect on the fire resistance of composite floors. Also other positions were selected in the test to measure steel temperatures on the steel sheet, shrinkage steel mesh and longitudinal steel bars.

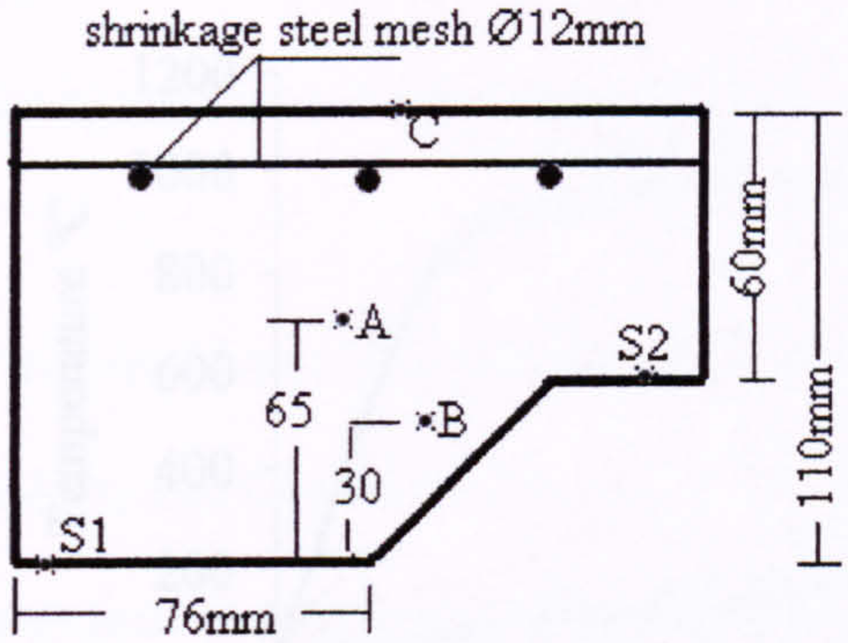

Fig. 4-6 Position of given points and dimension of cross-section as in Halim, Hakim and Leary test Sample 1

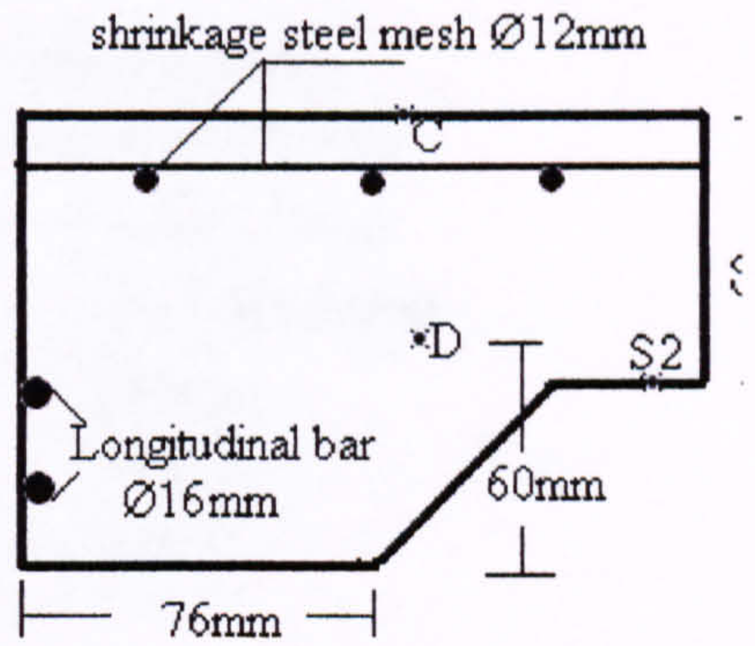

Fig. 4-7 Position of given points and dimension of cross-section as in Halim, Hakim and Leary test Sample 2

The temperature gradients through the depth of the floor have been calculated, with the same assumptions as for the above test, by the new analysis method. In Fig. 4-8 and 4-9, a comparison is made between the test results and calculation results.

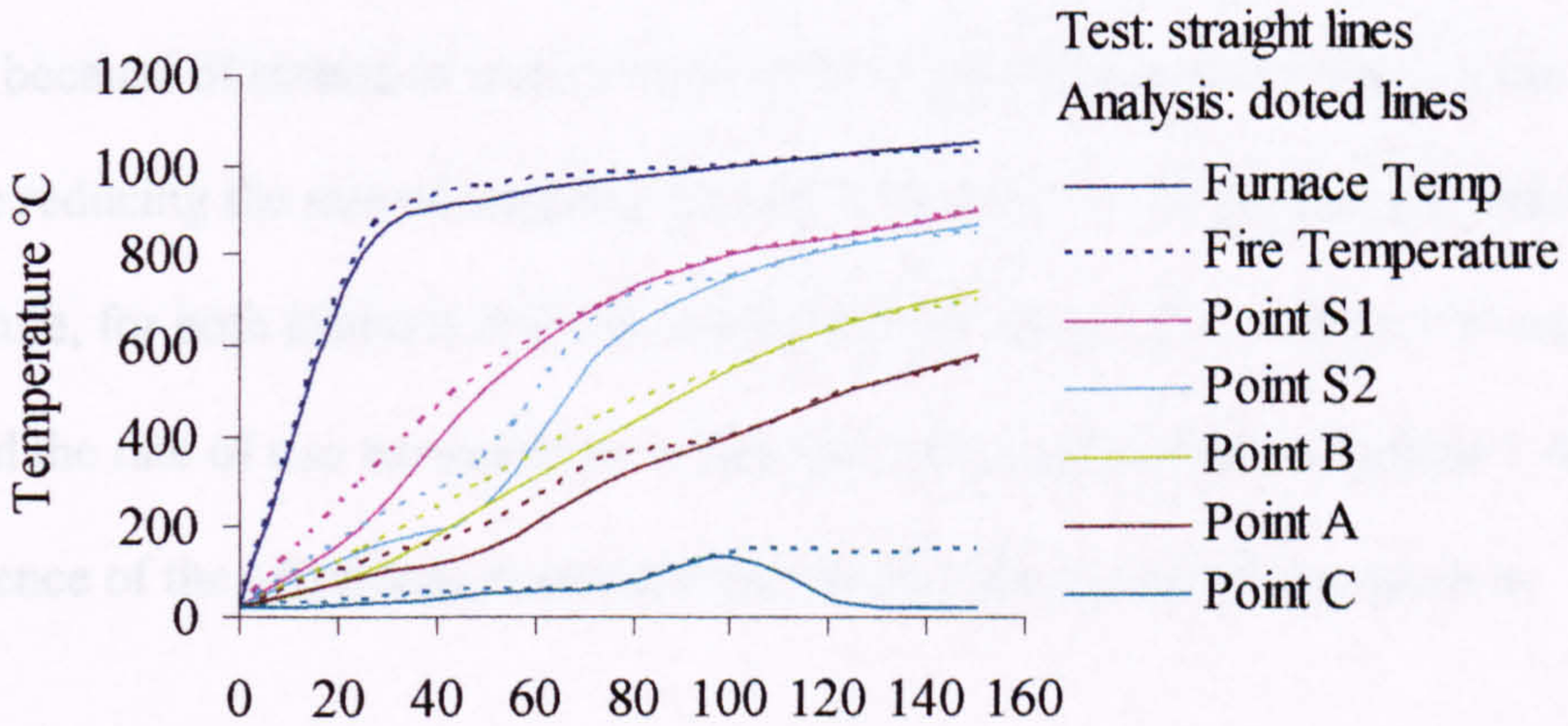

Fig 4-8 Comparison of analysis result with Halim and Hakim Test result (Sample 1) of developed temperature in different location of the composite floor cross-section

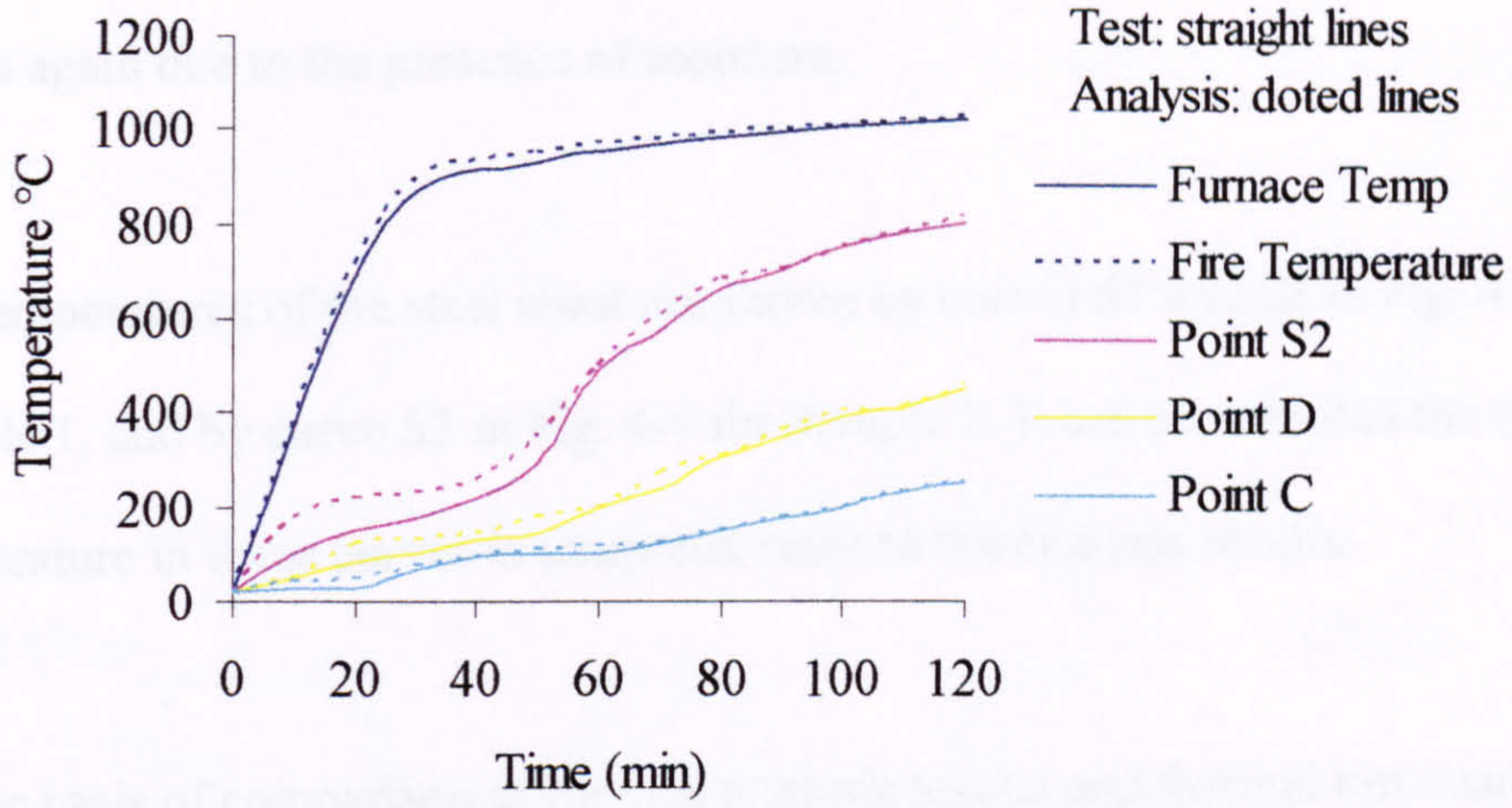

Fig 4-9 Comparison of analysis result with Halim and Hakim Test result (Sample 2) of developed temperature in different location of the composite floor cross-section

The curves for point C in Figs. 4-8 and 4-9 show the temperature distribution on the unexposed surface of each test sample throughout the fire test. The graph shows the maximum temperature value of 137 °C at 100 min fire time in case of Sample 1, while in the analysis method the unexposed surface temperature continued to rise. This is possibly because of spread of water evaporation on the unexposed surface in the tests, therefore reducing the rate of temperature rise. In Sample 2, the unexposed surface temperature, for both analysis and test results reached about 200 °C after 100 min fire times and the rate of rise temperature in Sample 2 was higher than in Sample 1 due to the existence of the additional reinforcement bars beside the shrinkage mesh in Sample2.

Temperatures within the concrete depth are shown by curves A and B in Fig. 4-8 for Sample 1, and by curve D in Fig. 4-9 for Sample 2. Points A and B are at distances 30 mm and 65 mm from the bottom of the floor, respectively; and D at 60 mm from the

bottom of the floor. The rise in the test temperatures is slower than for the analysis results again due to the presence of moisture.

The temperatures of the steel sheet are shown by curves S1 and S2 in Fig. 4-8 for Sample 1, and by curve S2 in Fig. 4-9 for Sample 2. It can be seen that the rise in temperature in these curves is sharp and close to the analysis results.

On the basis of comparison of thermal analysis results and thermal test results, it can be concluded that the present thermal analysis gives satisfactory prediction of the thermal behaviour of the composite floor exposed to fire.

4-3 Comparison of Numerical Results with Mechanical Test Results

4.3.1 Hamerlinck and Twilt

The cross-section of simply supported and continuous slab illustrated in Fig. 4-10. The span was 3200mm, width of 650mm, total depth 143mm, and steel sheet thickness 0.75mm, unprotected. The imposed load is equivalent to 3kN/m^2, which is an in-service load usually applied in design office buildings.

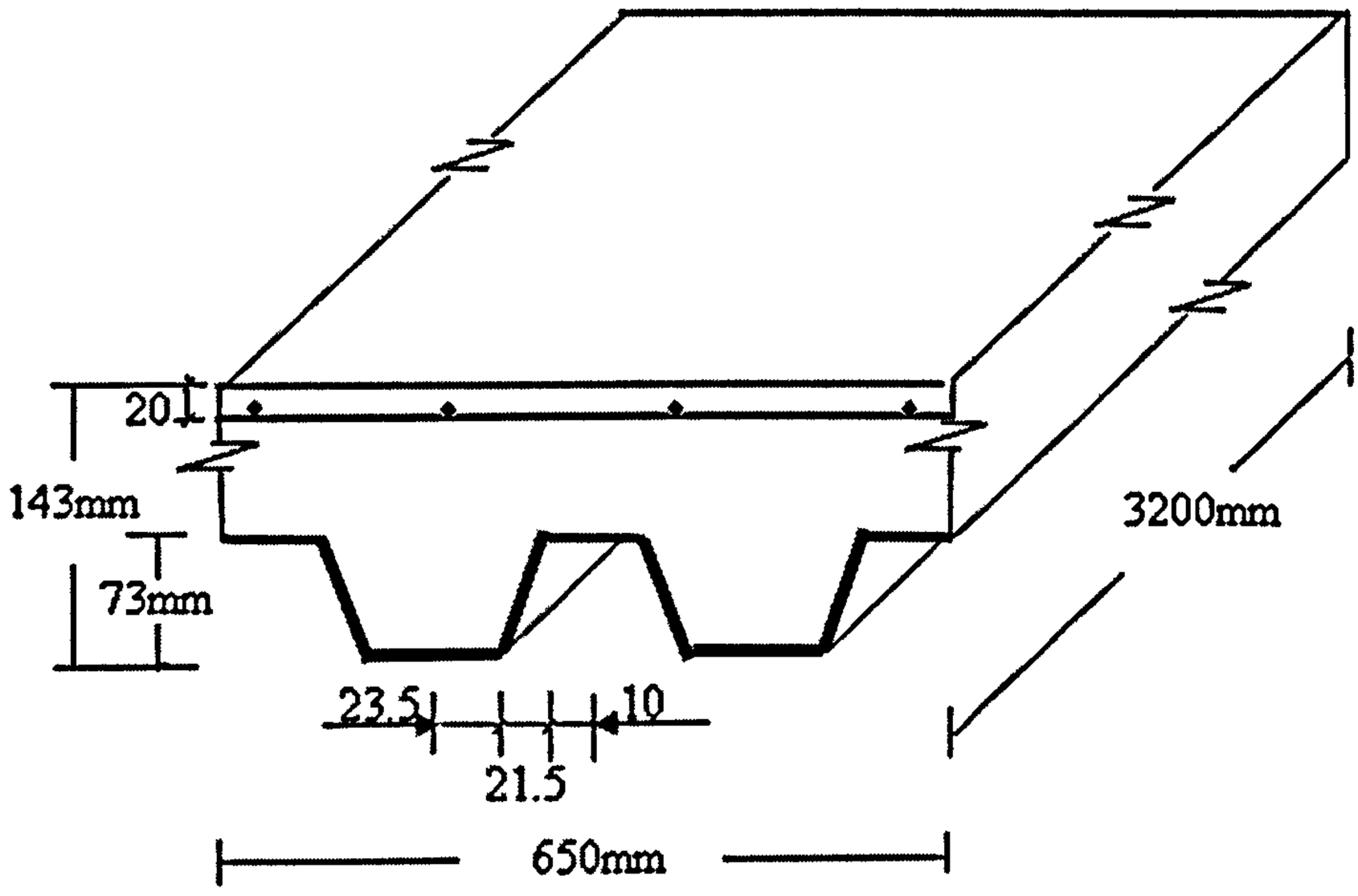

Fig. 4-10 The composite floor as in Hamerlinck and Twilt tests

All tests were performed on floors with 73mm steel sheet and 70mm concrete depth. This concrete depth corresponds to a fire resistance of 120 minutes as regards the thermal-insulation criterion, which was calculated according to the European Technical Note [ECCS, 1983]. Yield stress of the steel sheet was 280 N/mm^2 and not protected by insulation or suspended ceiling. The moisture content of each specimen was measured at several points of the cross-section. The average measured moisture content at the beginning of the tests amounted to 3.5% by dry weight.

Temperature distribution was determined in different positions. They were performed on the steel sheet and in a number of points in the concrete as stated in the thermal test in 4-2-1. Hence calculated temperatures were available for the points to influence on the mechanical behaviour.

Input parameters were taken, such as geometry, mechanical properties at room temperature and at elevated temperature. The most important parameter varied in the test with considering the amount of additional reinforcement, both positive and negative. The centre of the longitudinal bars of the shrinkage mesh was situated 20mm from the top of the slab.

Two tests on simply supported slabs were carried out to study the behaviour. In test specimen 1, no additional reinforcement was applied, in test specimen 2, 1 Ø10 bar in every 2 troughs as in Fig. 4-11

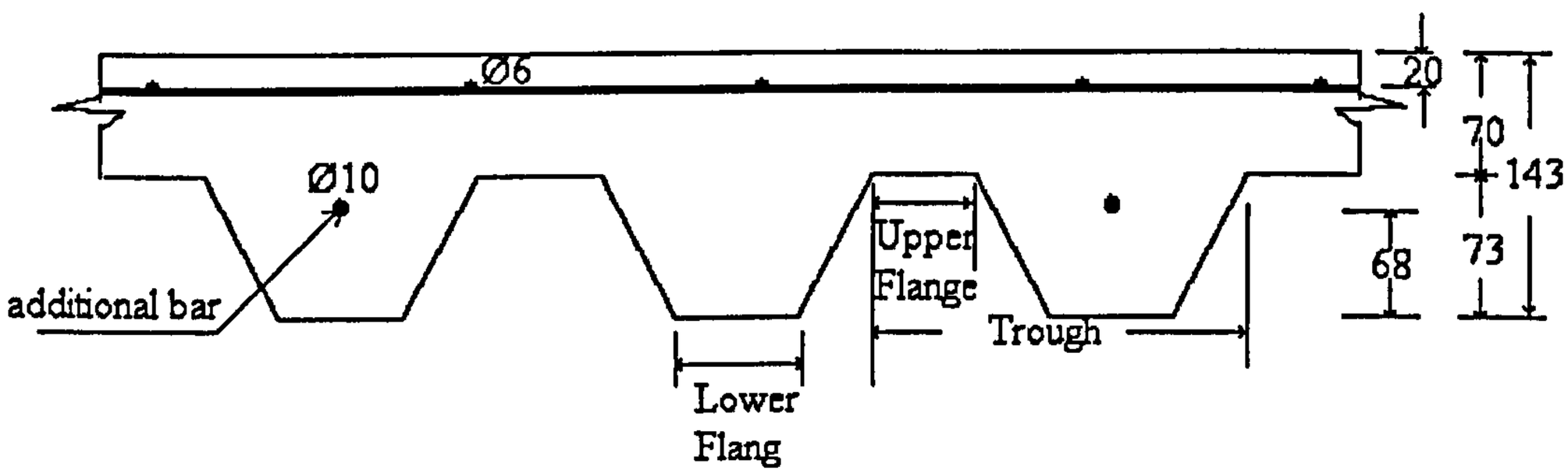

Fig. 4-11 Positions of the mesh reinforcement and additional bars as in Hamerlinck and Twilt test. All dimensions in mm

Since it was shown in Section 4.2.1 that the discrepancies for temperature are slight, it may be expected that the mechanical analysis with the calculated temperature will provide results comparable to those of test results with measured temperatures. This will be illustrated by means of Hamerlinck and Twilt Test 1 and Test 2.

Hamerlinck and Twilt Test 1

Test 1 was carried out on a simply supported slab with no additional reinforcement. It was used to verify a fire resistance of 30 minutes. The loading was 5.7kN/m^2 inclusive the dead weight. A fire resistance of 39 minutes was obtained taking the span/20 deflection criterion (3200/20=160mm).

As temperatures were not measured at all elements of the cross section in the test, so in the analysis, temperatures were determined by interpolation between known temperatures.

Other properties were adopted from [Eurocode-4], such as thermal expansion and mechanical properties at elevated temperatures. A fire resistance of 42.5 minutes was obtained taking the same criterion of span/20 deflection. This result is in line with ECCS Technical Note [ECCS, 1983], in which it is stated that a fire resistance of 30 minutes can be assumed for slabs without additional reinforcement.

Comparison of mid-span deflections between the analysis method and Hamerlinck test 1 is illustrated in Fig. 4-12. Good correlation with deflection is shown for the full range of the analyses.

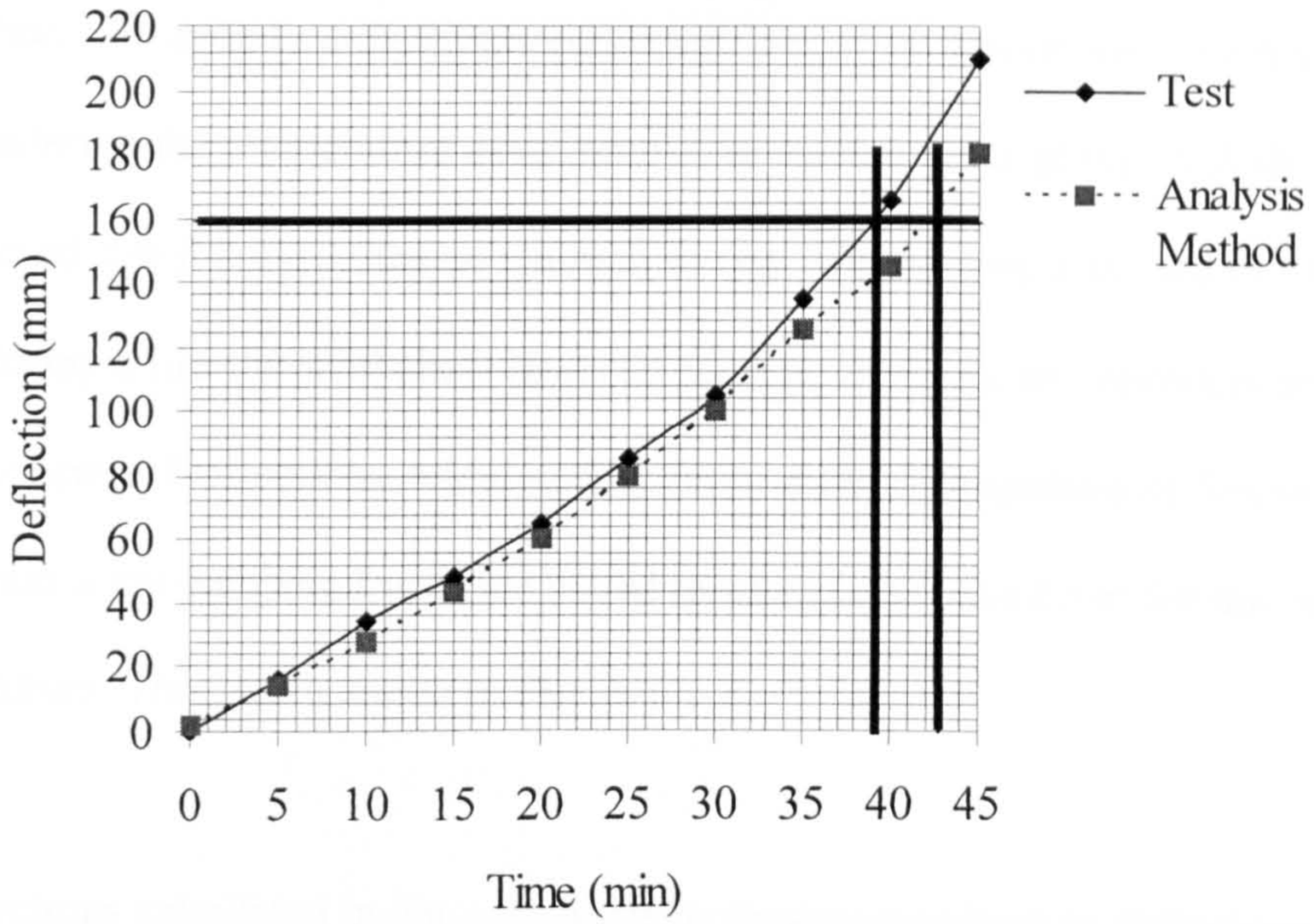

Fig.4-12 Comparison of mid-span deflections for the analysis method with Hamerlinck and Twilt test1.

Hamerlinck and Twilt Test 2

Test 2 was designed to obtain fire resistance of 90 minutes applying the Span/20 deflection criterion. A span of 3200mm was adopted. One of the supports was a hinge. The floor was supported from a frame by means of a flexible swing. The steel sheets were not protected by insulation. The additional bar reinforcement was positioned in the concrete trough with the height of 68mm above the lower flange of the steel sheet as in Fig. 4-11.

Yield stress of the reinforcement was 500 N/mm^2 and the concrete compressive strength was 33.6 N/mm^2. The test was terminated when the mid span deflection reached 266mm (Span/12). This occurred after 115 minutes.

The behaviour of the specimen in Test 2 was simulated using the developed numerical method. Temperature distribution through the cross-section was determined by considering the temperature development in various parts of the steel sheet. It has assumed that it contributes no strength in fire. This approach is used in EN 1994.1.2. As during a fire the steel sheet heats up rapidly, expands, and normally separates from the concrete. Deflections calculated by finite difference method as described in Chapter 3 are compared with the tested results at different times for mid span deflection. This is illustrated in Fig. 4-13.

Deflections calculated by the new analysis method are close to deflections measured by the tests. Thus, the agreement is good as shown in the graph.

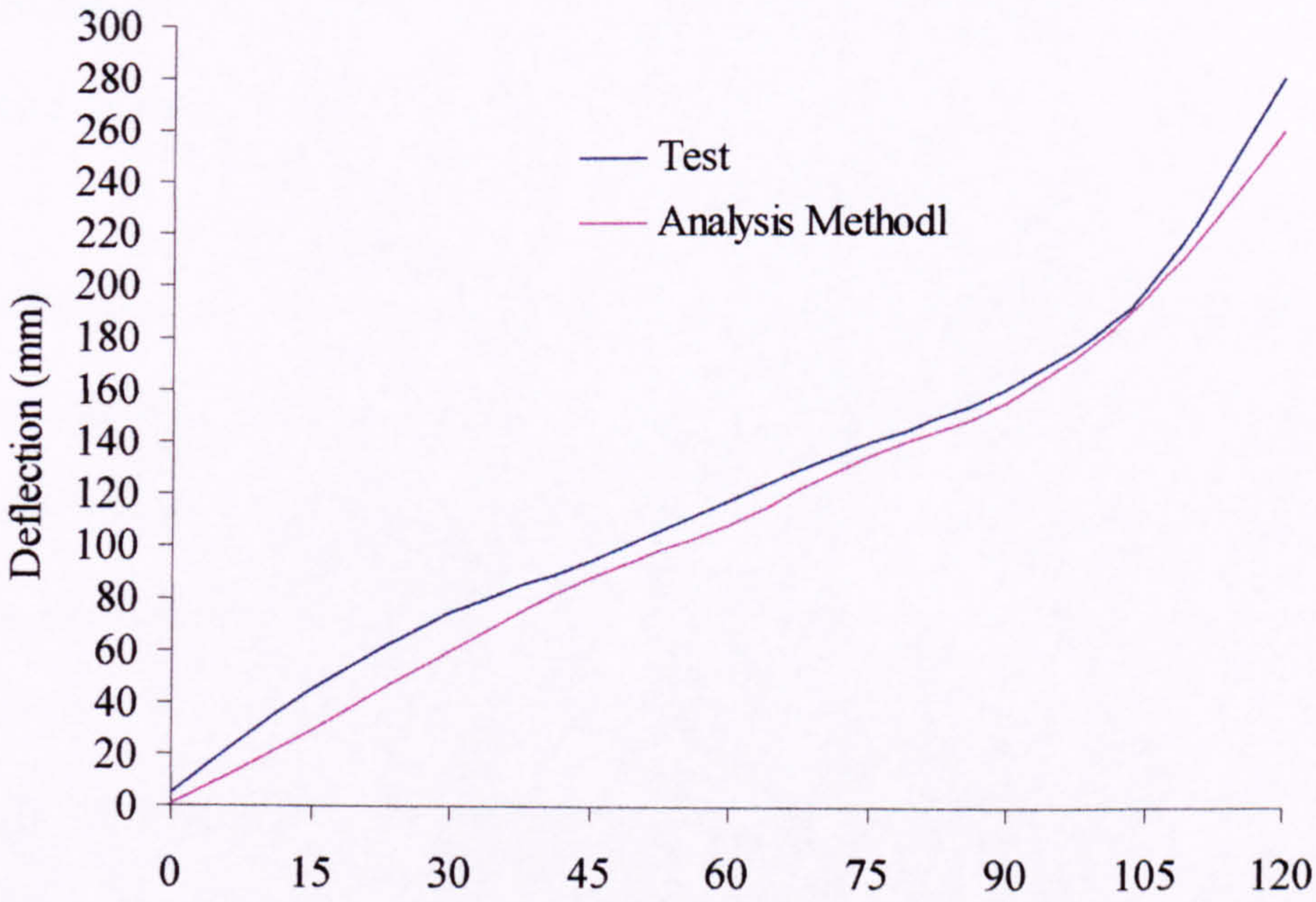

Fig. 4- 13 Comparison between numerical analysis method and Test 2 for mid-span deflections with additional reinforcement

The conclusion is drawn that the strength analysis method gives validated results for composite floor with and without additional reinforcement as in the tests.

The main conclusion that can be drawn from the above comparisons is that the developed numerical analysis method which includes both thermal and structural analysis is appropriate to describe the overall deformation behaviour for composite floor exposed to fire.

CHAPTER 5

Effect of In-Plane Forces and Edge Supports for Composite Floor Exposed to Fire

5-1 Introduction

In Chapter 3, the two dimensional orthotropic plate analysis was developed on the basis that the composite floor has various edges supported and is subjected to in-plane forces. For understanding the true behaviour of a composite floor when subjected to a fire, the influence of boundary conditions on the structural behaviour will now be examined. Several different boundary conditions have been used in the parametric studies described in this Chapter.

The influence of the support conditions at room temperature and in fire response of the composite floor are examined by varying the in-plane force and supports along perimeter edges of the vertically-supported slab, where four different cases are considered as follows:

(i) Simply supported without in-plane force

(ii) Simply supported with in-plane force

(iii) Fixed without in-plane force

(iv) Fixed with in-plane force

The floor in cases (i) and (iii) is subjected to zero in-plane forces in x and y direction, whereas in cases (ii) and (iv) is prevented from pull-in along the edges thus in during in-plane forces.

5.2 Properties of the Floor

The composite floor, shown in Fig. 5-1, is considered here in a parametric study aimed at establishing the importance of various types of edge under fire conditions and in-plane forces. Two boundary conditions are considered, a rectangular plate with simply supported edges and a rectangular plate with fixed edges.

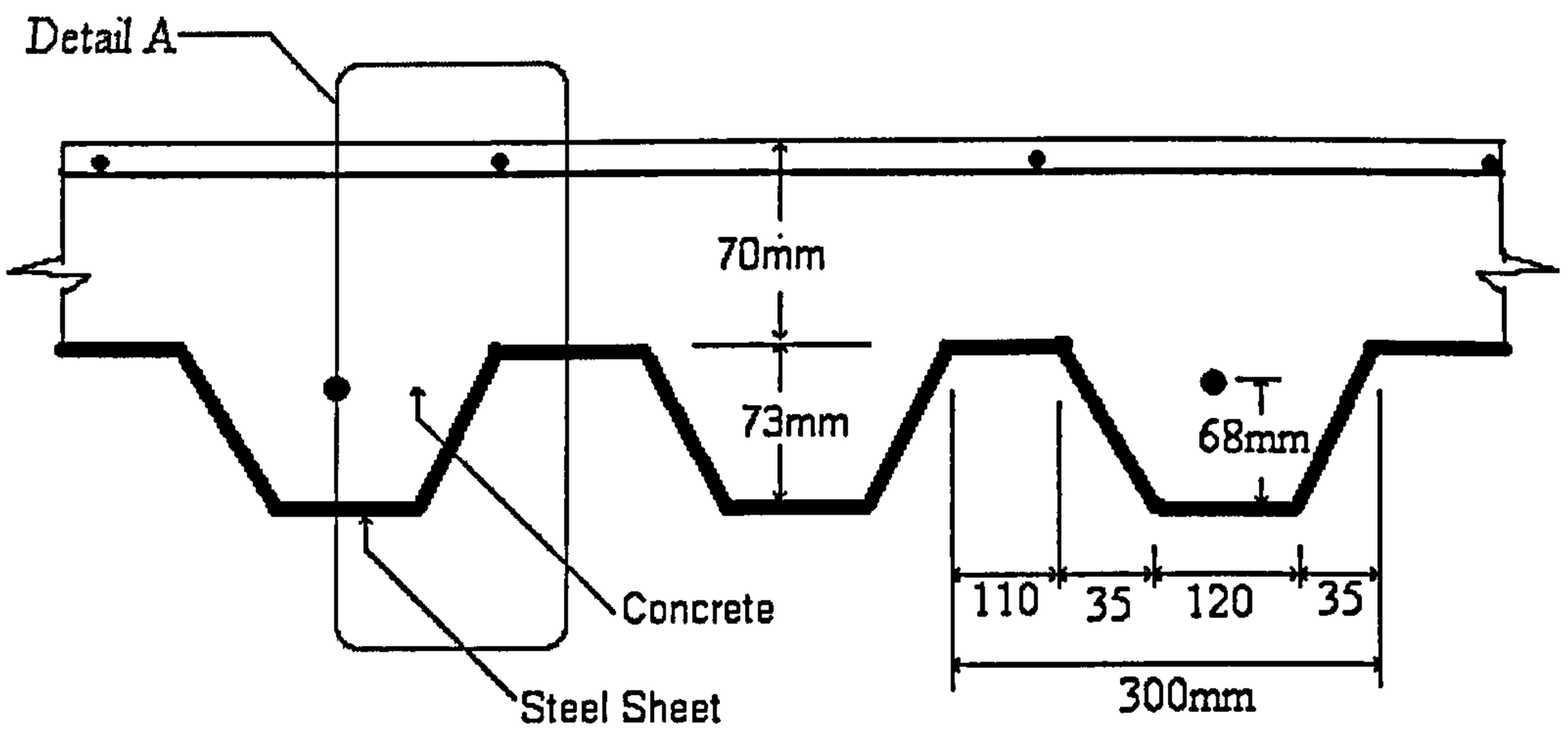

Fig. 5-1 Cross-Section of the Composite Floor

The span L_x is of 4600mm in the x-direction and L_y is of 3200mm in y-direction. The total thickness of the floor is 143mm. The load including self-weight was typical office building load intensity.

The characteristic values are as follows in Table 5-1:

Table 5-1:

Span (y-direction)	= 3200 mm
Span (x-direction)	= 4600 mm
Total Floor Depth	= 143 mm
Concrete Strength at 20 °C	= 35 N/mm^2
Concrete tensile strengths	= 0
Shrinkage reinforcement mesh	= Ø6mm @ 150mm
Additional reinforcement mesh	= Ø10mm @ 300mm
Deck type	= Trapezoidal
Deck Depth	= 73 mm
Steel Sheet Thickness	= 1.5 mm
Yield stress of steel at 20 °C	= 460 N/mm^2
Youngs Modulus of steel at 20 °C	= 210000 N/mm^2

The fire temperature is assumed to follow the ISO standard curve. The temperature distribution and variation with time were calculated using the developed computer program CU-ACCEF. The program runs for 120 minutes fire exposure.

5.3 Fixed and Simply supported edges without in-plane restraint

The geometry and dimensions of the cross section data are given in Fig, 5-2 which also shows the mesh used. At each mesh element, the material properties and thermal expansion are calculated according to the corresponding temperature.

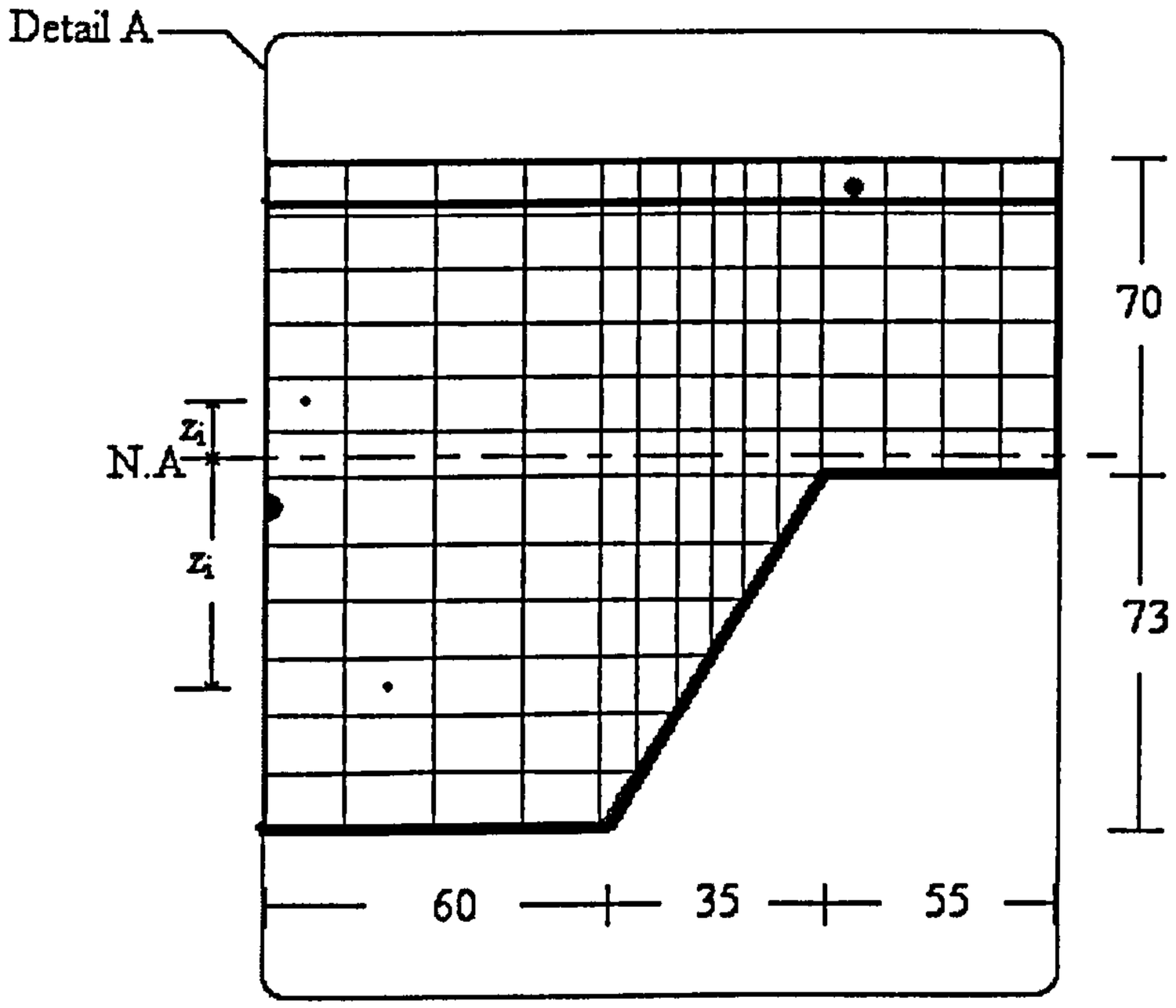

Fig 5-2 Geometry and dimensions of the cross section

Fig. 5-3 compares the mid-span deflections from the previous analysis results for simply supported and fixed edge composite floor. The graph shows a fire resistance of 101.5 minutes was obtained taking the L_x / 20 [BSI 1990] deflection criterion 230 mm for simply supported composite floor. The fire resistance of 116.5 minutes which is the time taken to reach the same value of L_x / 20 can be assumed for fixed supported for the same composite floor. The analyses stop when the time reaches to 120 minutes.

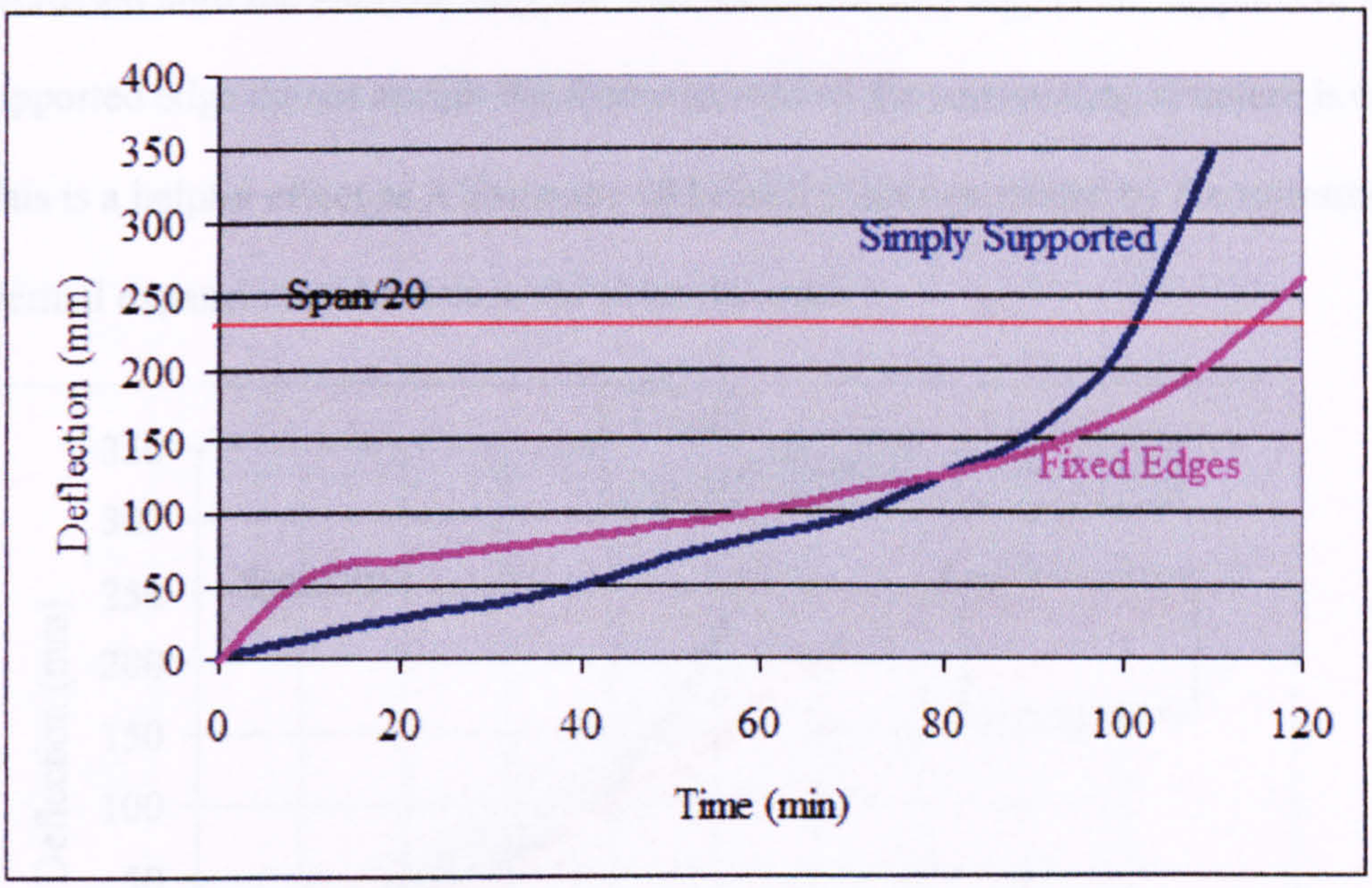

Fig. 5-3 Comparison of Central Deflection for Simply Supported and Fixed Edges Composite Floor subjected to fire

5.4 Effect of edge restraint

The role of in-plane forces in describing the behaviour of composite floor will be examined in this Section.

Figs. 5-4 and 5-5 show the influence of in-plane forces and the effect of supports in the fire resistance. Fig. 5-4 compares the mid-span deflections for the simply supported composite floor during the fire affected by in-plane forces. The graph shows that in-plane forces had no effect on deflection rates during the initial stage of the fire up to about 40 min. The effect of in-plane forces only appeared at the later stage. The large decrease in deflection can be noticed when the floor is subjected to in-plane force in x-direction only. That may result from restrained thermal expansion during the fire. After 80 minutes the floor deflected rapidly to about 105mm. its deflection rates gradually

decreased until the analysis stopped. The reason for this drop is the supports of simply supported edge do not anchor the forces as well as the surrounding structure is cooler. This is a helpful effect as it limits the additional forces generated by the restrained thermal expansion and increase the fire resistance.

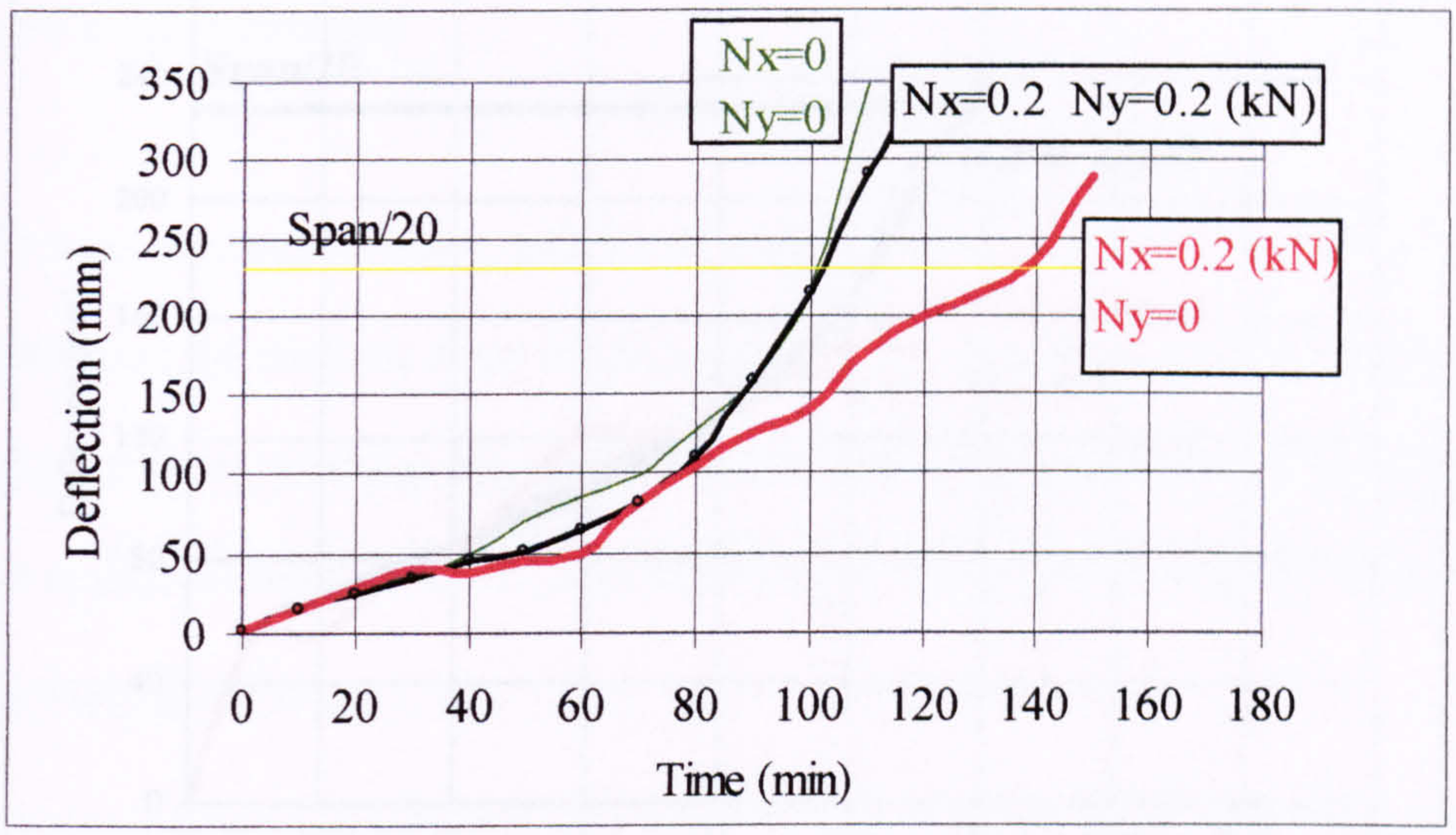

Fig.5-4 Comparison of Central Deflection for Simply Supported Composite Floor subjected to fire with and without in-plane force

With in-plane force in both directions, the difference in central deflections compared with the deflections without in-plane forces are still relatively small. The deflection curve shows a dip after 40 minutes and gradually increased until reach the same rate of the deflection without in-plane forces at 88 minutes and again decreases after 100 minutes until the analysis stopped. Therefore there is no anchorage effect as the floor is free to pull. This is clearly a desirable behaviour here, as it reduces the force imposed on the floor by the expansion forces.

The same floor, but assumed spanning between rigid end restraints, fixed edges. The changed behaviour is shown in Fig. 5-5. The key difference is that availability of in-plane forces. The graph shows the growth of deflections during the fire in three cases

with applying in-plane forces. In both x and y direction it is notable different in comparison with the actual levels of deflection in the absence of in-plane forces.

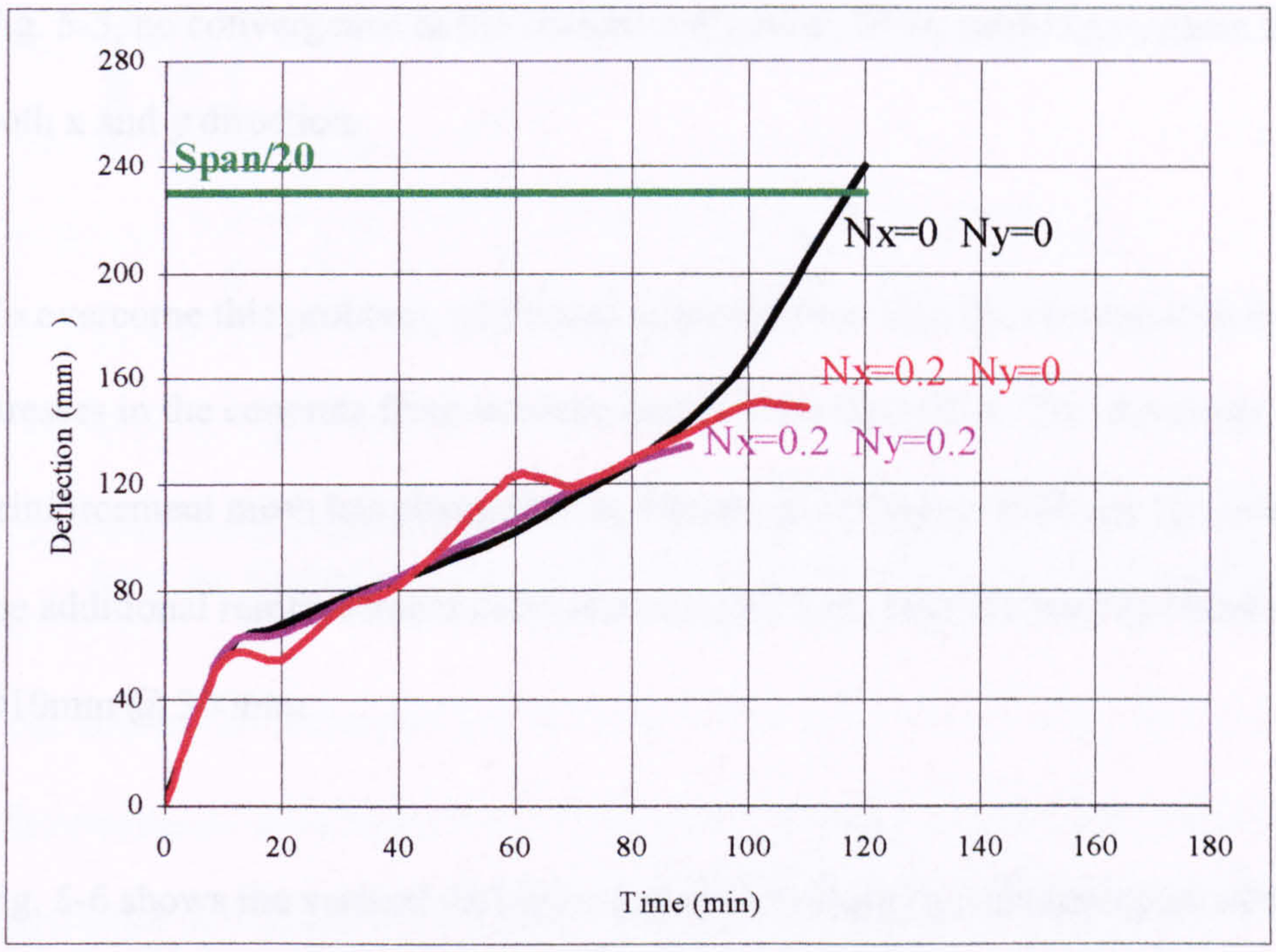

Fig.5-5 Comparison of Central Deflection of Fixed edges with and without in-plane force for Composite Floor subjected to fire

When applying in-plane forces in x-direction only, the deflection rates showed a fluctuated rate reduction for all the duration of the fire. The reason for this, the forces from fixed supports may increase the rigidity of the floor and prevent large downward deflections.

But it can be seen that the deflection rate had significant change when applying in-plane forces in two directions in steady state until 92 minutes. After that there was no convergence on the result of the computer program. This change had a significant effect on the fire resistance. It clearly indicates tensions in the mid-span region of the floor and loses its strength. Since the slab expansion occurs in its own plane, and this is the plane in which the surrounding slab provides restraint, large thrusts can develop in

two directions. The fixed supports will form large compressive forces in the slab, even for small deflection. Therefore, the flexural resistance at mid-span can also be exceeded for a rigidly restrained. This will result in a reducing the strength as shown in Fig. 5-5, no convergence in the computer program, when applying in-plane forces in both x and y direction.

To overcome this problem, additional reinforcement may then be required to resist stresses in the concrete from in-plane force in two directions. The shrinkage reinforcement mesh has changed from Ø6mm @ 150mm to Ø10mm @ 150mm and the additional reinforcement mesh has changed from 1bar Ø10mm @ 300mm to 2 bars Ø10mm @ 300mm.

Fig. 5-6 shows the vertical deflections after increasing the reinforcement of the same point shown in Figure 5-5. It can be seen that the fire resistance in the case of increase reinforcement is higher than the previous one for three cases, using the L/20 criterion. The rate of deflection for the floors with additional reinforced can be seen to be less deflection than those for the equivalent floors. All the cases showed similar rates of deflection between 0 and 100 minutes. The floor with in-plane forces in x-direction had deflections lower than those without in-plane forces or forces in both directions as shown in Fig. 5-6.

In addition the restraint to the floor comes from the surrounding cold structure, which is assumed to be 20 °C in this analysis. The Cardington tests suggest that even edge panels can benefit enormously from transfer of loads from the weakening systems of bending and shear towards other mechanisms [Newman, 1999].

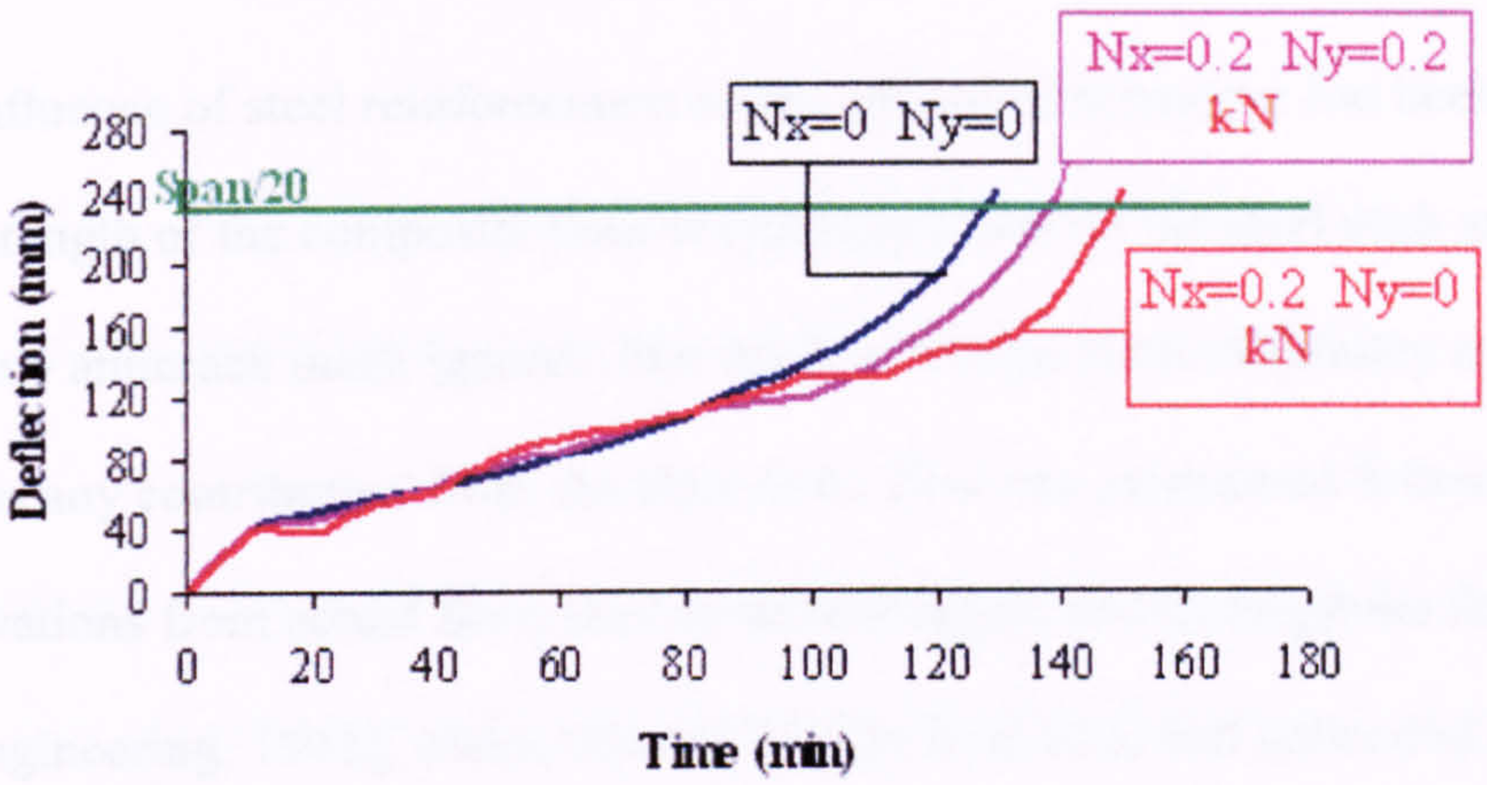

Fig. 5-6 Comparison of Central Deflection of Fixed edges with and without in-plane force for Composite Floor subjected to fire after increasing the reinforcement

The conclusion is reached that the effect of in-plane to fixed edges does not increase fire resistance up to about 90 minutes, but that beyond this it can increases the fire resistance in the floor if it is applied in x direction only or increased with reinforcement.

Most importantly, the presence or absence of in-plane forces and different edges, played a significant role in the behaviour, as observed in the analysis presented by the above graphs. This is particularly evident in the response of the composite floor in which the edge restraints restrict the deflection during the fire. The deflection for restrained slab is lower compared to an equivalent unrestrained slab. The difference in applying the Nx and Ny can be seen.

Since the reinforcement makes a significant contribution and it is an important performance factor to achieve a fire resistance period, it is important to investigate this phenomenon in the next Section.

5.5 Effect of reinforcement

The influence of steel reinforcement on the structural behaviour has been investigated. The strength of the composite floor is typically based on the steel deck and concrete, with any anticrack mesh ignored. But the Fire Design method, [Bailey et al, 2000], ignores any contribution from the steel deck. This was considered following observations from actual fires, such as the Broadgate and Basingstoke fires [Structural fire engineering, 1991], which showed that the steel deck had debonded and the composite floor suffered very large mid-span deflections but did not collapse. Full scale fire tests at the Cardington Large Building Test facility have also confirmed this behaviour.

Since the deck is ignored, the strength of slab in a fire is based on the mesh reinforcement and concrete. Therefore, this parametric study has been carried out to demonstrate the effect of the floor reinforcement on the structural behaviour of the composite floor by using the current analysis method and then showing some detail comparison with Bailey's Design Method [Bailey et al, 2000]. The choice of the type of reinforcement floor depends on several factors such as economy of construction, span and strength of serviceability requirements.

In order to make more precise comparison with the Bailey Design Method two analyses for 9×9m square composite floors at elevated temperatures have been performed, Slab (1) was simply supported along two edges and clamped along the others. Slab (2) was clamped along all the four edges. The investigation was carried out by dividing the floor into equal sections in each the x and the y directions.

Two different anticrack meshes have been used for both slabs:

A142: which means that area of steel equal 142mm^2/m, 6Ø@ 200mm.

A393: which means that area of steel equal 393mm^2/m, 10Ø@ 200mm.

The position of the mesh is based on an average axis distance of 45mm below the top of the slab as recommended by the design tables [Bailey, et al., (2006),] with yield strength of 500N/m^2.

The composite floor is assumed to be lightweight concrete constructed using a trapezoidal profiled steel decking. The concrete strength is 35 N/m^2. The total depth of the floor is 130mm including 65mm deep ribs. The design tables [Bailey, C.G., (2006), et al.] are applicable to profiled steel decking up to 70 mm deep and for depth of concrete above the steel decking from 60 to 80 mm.

The characteristic dead and imposed loads were assumed to be 4.1kN/ m^2 and 2.5kN/ m^2 respectively. From BS 5950: Part 8 [BSI 1990], the partial safety factors in fire are 1.0 for dead loads and 0.8 for imposed loads, giving a total design load of 6.1kN/ m^2 at the fire limit state.

Bailey's design method assumes that the slab temperature varies linearly through its thickness. This assumption has not been used in this analysis. A non linear temperature distribution has been used across the thickness of composite floor. It is based on the ISO standard fire and the finite difference thermal analysis which has been explained in the previous Sections. The temperature of the lower flange of the composite floor is

used against the result of the deflections in the centre of the floor to analyze the various boundary conditions. This is described in Fig. 5-7 in the following section.

5.5.1 Results of the analysis

Fig. 5-7 compares the maximum vertical deflection predicted by this analysis method for the two reinforcement mesh for both slabs simply supported edge condition and clamped edge condition. Fire resistance with A393 reinforcement for both floors is higher compared to equivalent floor when using A142 reinforcement using the L/20 criterion. It can be noticed that the influence of reinforcement for simply supported case can be negligible up to about 420 °C, but beyond this point it becomes increasing significant.

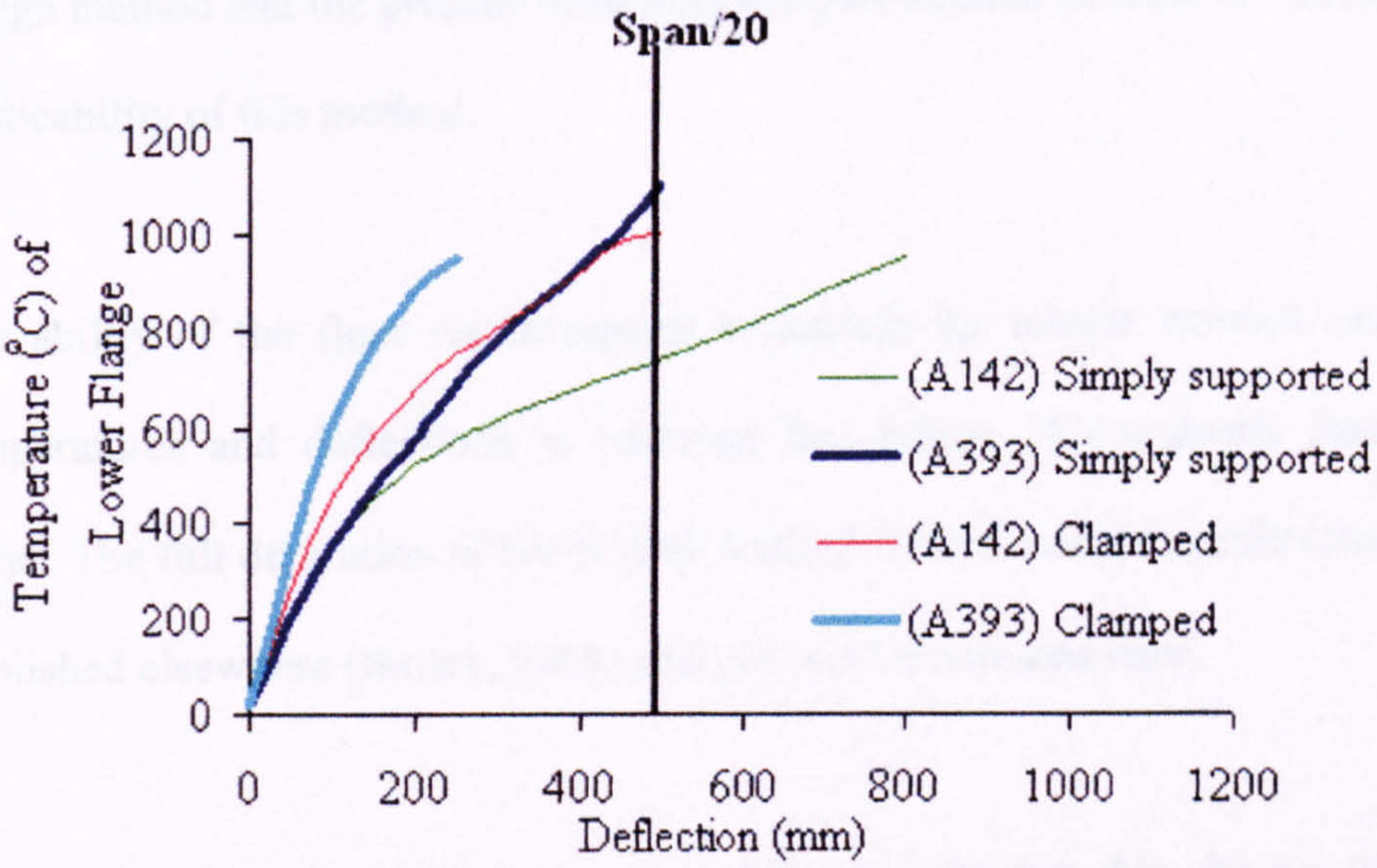

Fig. 5-7 Central deflection with different reinforcement

The maximum deflection of the composite floor also shows considerable difference between clamped and simply supported condition. Central deflections of the simply

supported slab are greater than the deflections for the clamped edge condition at elevated temperature. The clamped floor is restrained by the surrounding structure while being exposed to the fire. In this case, the boundary conditions have a more dominant effect on the deflection as the temperature is increased. It is evident that it becomes important to take into account the boundary support condition at high temperature. Although the limit of span/20 for deflection had been needed, there was no collapse of the floor at this stage.

5.5.2 Comparison with Bailey Design method

A simple design method has been recently developed by [Bailey et al, 2000] for calculating the performance of composite flooring systems subject to fire. The objective of this section is to show some detailed comparisons between the simple design method and the present numerical analysis method in order to check the applicability of this method.

The ability of the floor reinforcement to sustain the tensile stresses caused at high temperatures and deflections is ensuring that failure of composite floors does not occur. The full derivation of the Bailey method for orthotropic reinforcement has been published elsewhere [Bailey, 2003] and will not be repeated here.

Fig.5-8 compares the maximum vertical deflections predicted by this analysis method and the Bailey Design Method for the two reinforcing meshes.

The maximum deflection allowed according to Bailey's method is 435 mm and the corresponding failure temperature is 740 °C with A142 mesh. Table 5-1 describe this

comparison. However, for A142 mesh in this analysis study shows the mid-span deflection 450mm, span/20, at a temperature of about 710 °C which corresponds closely to the temperature at Bailey's method. For A393 mesh the Bailey's method gives failure temperatures in excess of 1100 °C which is also close to that indicated by this analysis study which reached to 1052 °C at a deflection level span/20.

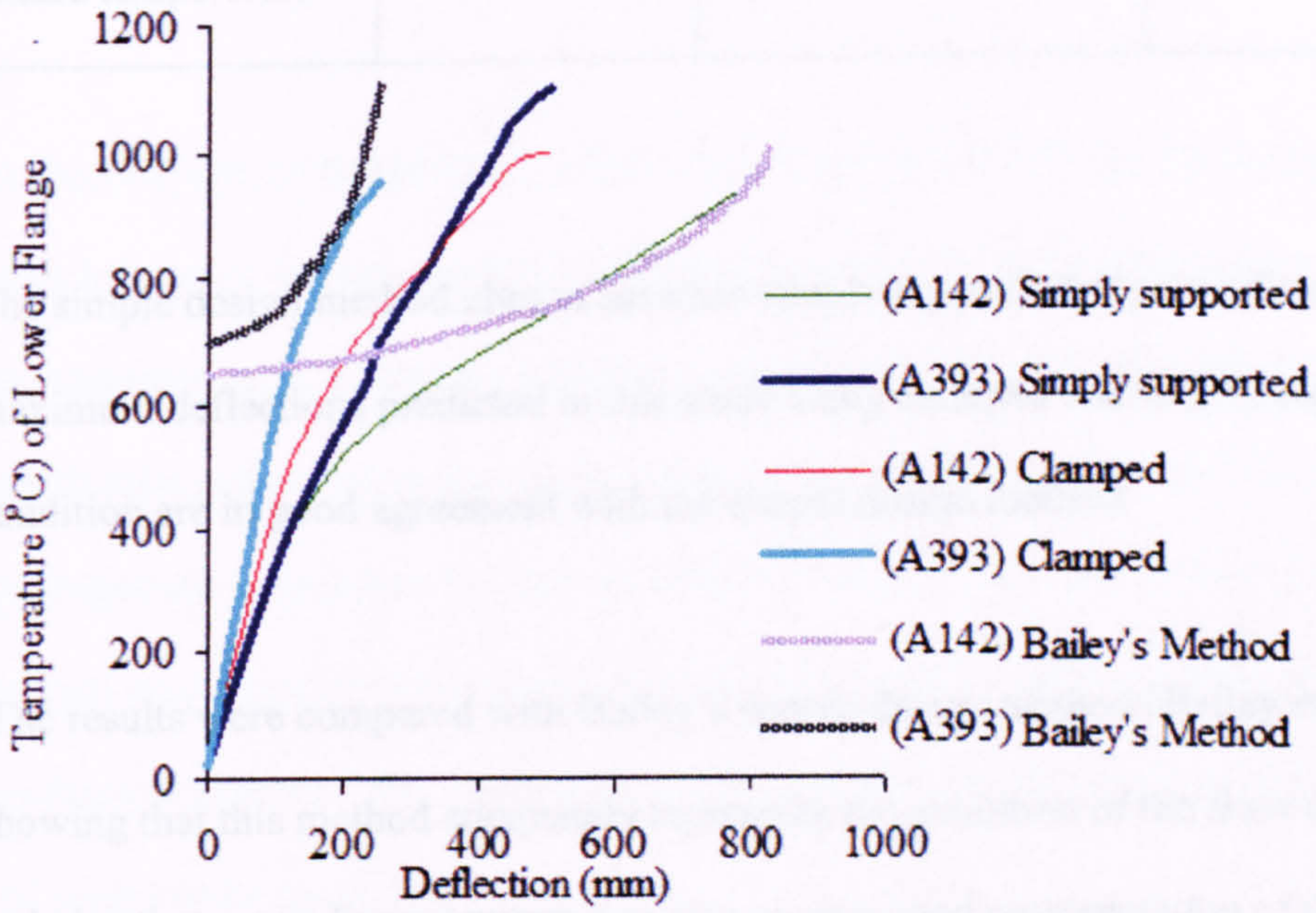

Fig. 5-8 Comparison deflections of different reinforced floor with Bailey Design Method

Table 5-2: Comparison between Bailey method and the developed analysis method

	Bailey Method	**Current Analysis Method**	**Mesh Reinforcement**
Maximum deflection	435 mm	450 mm	A124
Corresponding failure temperature	740 °C	710 °C	
Corresponding failure temperature	1100 °C	1052 °C	A393

The simple design method always assumes simply supported edge conditions. The maximum deflections predicted in this study using clamped and simply supported condition are in good agreement with the simple design method.

The results were compared with Bailey's simple design method [Bailey et al, 2000] showing that this method adequately represents the evolution of the floor deflection and also that a non-linear temperature rise gives a good representation of the temperature histories.

CHAPTER 6

CONCLUSION

6.1 New Method of Analysis

The research described in the preceding chapters investigated the behaviour of composite floors exposed to fire. In particular a new method for describing their structural response has been developed. This is a three-step process involving estimate of fire exposure, heat flow analysis, followed by a strength analysis.

As the first step in this method, a fire temperature calculation has been employed in order to predict the temperature development in the fire compartment as a function of fire exposure time. Secondly, a thermal response was used to calculate the temperature distribution and development in the cross section of the composite floor, considering the important parameters for thermal analysis, such as geometry of the steel sheet, thermal properties of components materials and concrete depth. Finally, by means of a mechanical response and given the thermal response, the structural performance of the full floor can be predicted.

Heat balance equations were formulated using the finite difference method. For calculation of temperatures at a given time, the cross-section is divided into elements. The heat transfer from the fire to the surface is considered for the volume of boundary elements. Also heat conduction to the neighbouring points is considered. At internal elements of the cross-section, heat conduction to all neighbouring elements is considered. Both the conductivity and specific heat of concrete are included.

By using the developed program, the temperature distribution within the composite floor in fire can be evaluated without the necessity of testing.

The mechanical analysis is based on orthotropic plate theory using the governing differential equation as described in Chapter 3. Finite difference method is used to solve the orthotropic plate differential equation to determine equilibrium deflections at a given stage of fire growth. The new method takes into account fully nonlinear stress-strain relationships for steel and concrete.

The procedure is to calculate curvatures in the two planes for each element in the cross-sectional grid using the finite difference operators. The thermal strain are superimposed on the mechanical strains associated with curvatures to find the net strain then stresses are calculated using the nonlinear temperature dependent stress-strain curves. Integrating the stresses, the internal stress resultants are calculated then the internal force and the moment in both directions calculated. In view of the numerical procedure adopted, the integrations are replaced by summations over the elements of the cross-sectional grid. Iteration needs to be performed for ensuring that the value of internal force matches the applied in-plane force. For unrestrained edges, the internal force is assumed to be zero. The proposed method used a novel approved for the calculation of plate rigidities in both directions, which are needed in the solution of the orthotropic plate equation, taking into account the effect of temperature on the internal stress, which in turn contribute to the internal moment.

The differential operators are replaced by the finite difference formulae to reduce the governing differential equation into a linear algebraic equation. The stiffness in the

weak direction comes from the smaller thickness in the composite floor, ignoring the trapezoidal part of the deck. In the strong direction the full profile of the deck is used.

Due to increasing temperature, the materials (concrete and steel) expand and their strength decreases. Moment capacity decreases and a thermal curvature is developed, resulting in an increase in deflections.

6.2 Validation

This method was successfully validated against experimental fire tests which have been carried out at the Centre for Fire Research-TNO Building and Construction Research [Hamerlinck and Twilt, 1989]. The tests comprised details for studying the thermal behaviour and the mechanical behaviour of composite floors during a fire as illustrated in Chapter 4). Also used were tests by [Halim, Hakmi and Leary, 1997] on two floors in the laboratory of the Civil Engineering Department, University of Salford, UK. The results show very good correlation between the tests results and this method results. This indicates that, the analysis method predicts behaviour very similar to that shown in the tests.

The information produced by the developed computer program gives a picture of the strength and deformation of the floor at any given stage of the heat exposure.

6.3 Parametric Study

A parametric study using various boundary conditions was carried out. Particular consideration was given to the influence of various edges restraint conditions on the predicted responses. Examples undertaken with two conditions, simple support and

fixed edges, further conditions for different boundaries can be taken by following the described procedure in Chapter 3. However, some general conclusions can be drawn, as follows:

- It is shown that fixed edges have better fire resistance than simple support which are not subjected to in-plane forces.
- Simply supported composite floor has better fire resistance when subjected to in-plane force in one direction.
- The effect of in-plane forces on floors with fixed edges has little influence on the deflection up to about 90 minutes.
- In-plane forces can increase the fire resistance of floors with fixed edges the forces are applied in one direction only.

The enhancement of performance by addition reinforcement area was also studied. The analysis has demonstrated the enhancement of fire resistance which can be achieved by increasing the area of reinforcement mesh. The influence of reinforcement for simply supported floors can be negligible up to about 420 °C, but beyond this point it becomes increasing significant.

Effects of boundary conditions and in-plane forces have been studied. It is clear from this study that surrounding structure provides restraint increasing the fire resistance of the structure within the fire compartment. The analyzed results indicate that in-plane forces provided by the surrounding parts cause an influence on the deformational and mechanical responses of the composite floor in fire. The restraints essentially cause the change in the strength in fire, which can be quantified using the calculated deflection by the developed method.

The composite floor behaviour could be well represented through this method of analysis which can provide information for design of composite floor in fire.

6.4 Suggestions for future work

Future work in developing this work could include the following:

- Additional boundaries conditions can be added to the present program. In particular, boundaries with edge-beams would enable a more accurate simulation of modern composite floors.
- This method of analysis assumes uniform moisture content throughout the concrete floor. The analysis can be improved by properly considering transport of moisture from the fire zone to the cooler non-fire zones.

REFERENCES

- Abrams, M. S., 1979

"Behaviour of inorganic materials in fire", ASTM Special Technical Publication, 685, American Society for Testing and Materials, Philadelphia

- Abrams, M. S., & Gustaferro, A. H. (1968)

"Fire endurance of concrete slabs as influenced by thickness, aggregate type, and moisture" Journal of the PCA Research and Development Laboratories, 10(2), 9-24

- Anderberg Y., 1988

"Modelling Steel Behaviour", Fire Safety Journal, 13(1), p 17-26

- Anderberg, Y. and Forsen, N.E., 1982

"Fire resistance of concrete structures", Division of Structural Mechanics and Concrete Construction, Lund Institute of Technology, Lund Sweden

- Anthony, F. Mills, 1995.

"Basic Heat and Mass Transfer ", University of California at Los Angeles, Richard D. Irwin, INC

- ASTM, 1988

"Standard test methods for fire tests of building construction and materials", E119-88, American Society for Testing and Materials

- Australian Building Codes Board, 1996

"Building Code of Australia".

- **Bailey, C.G., 2003**

"Efficient arrangement of reinforcement for membrane behaviour of composite floor slabs in fire conditions". J. Construct. Steel Research, 59, pp931-949

- **Bailey, C.G., Lennon, T. and Moore D.B. 1999**

"The behaviour of full-scale steel-framed buildings subjected to compartment fires", The Structural Engineer. Vol. 77 No. 8., pp. 15-21.

- **Bailey, C.G., and Moore, D.B., 2000**

The structural behaviour of steel frames with composite floor slabs subject to fire, The Structural Engineer, Vol. 78, No. 11. pp 19-33

- **Bailey, C.G., White, D.S. and Moore, D.B., 2000**

The tensile membrane action of unrestrained composite slabs simulated under fire conditions, Engineering Structures, Vol. 22, No. 11, pp 1583-1595

- **Bailey, C.G., Newman G M, Robinson J T, 2006**

"Fire Safety Design: A new Approach to Muti-Storey Steel-Framed Buildings", 2nd edition, The Steel Construction Institution, UK

- **Barnett, C. R., 2002**

"A new empirical model for fire compartment temperatures", Fire Safety Journal, Volume 37, Issue 5, pages 437-463.

- **Bashur, F.K, and Darwin, D., 1978**

"Nonlinear Model for Reinforced Concrete Slabs", Journal of Structural Division, ASCE, Vol. 104, No ST1, pp. 157-170

- Bergmann, R. and Pantazopoulou, V. A., 1988

"Finite Element for R/C Shear Walls Under Cyclic Loads" Department of Civil Engineering, Report UCB/SEMM-88/09, University of California, Berkeley, 1988.

- Bocca, Pietro Giovanni and Crotti, Marco, 2000

"Testing Procedure Based on Thermal and Mechanical Analysis for the Evaluation of Concrete Damage", Roma,

- Both, C., 1998

"The Fire Resistance of Composite Steel-Concrete Slabs", ISBN 90-407-1803-2-Y / CIP, Delft University

- BR2000

UK Building Regulations 2000 Fire Safety, Amendments 2002 to Approved Document B, (Fire safety) published by TSO (The Stationary Office) and available online www.tso.co.uk/bookshop.

- BR2006

UK Building Regulation part B 'Fire', 2006

-Bravery, P.N.R., 1993

Cardington Large Building Test Facility, Construction details for the first building, Building Research Establishment, Internal paper, Watford.

- Bresler, B., and Iding, R. H., 1982

"Effect of Fire Exposure on Steel Frame Buildings", Report WJE No. 78124, prepared for American Iron and Steel Institute, Wiss, Janney, Elstner and Associates, Northbrook, IL, March.

- **BS 476, 1987**

"Fire Tests on Building Materials and Structures,". BSI British Standards: Part 20: London.

- **BS7974**

Application of Fire Safety Engineering Principles to the "Design of Buildings- Code of Practice", available from The British Standards Institution

- **BSI5950, 1990**

"Code of Practice for Fire Resistance design", British Standards Part 8, London

- **BS EN 1991-1-2-2002 Eurocode 1**

Actions on Structures, General Actions, Actions on structures exposed to fire, BSI

- **Buchanan, Andrew H., 2001**

"Structural Design for Fire Safety", John Wiley & Sons Ltd

- **CEC, 1988**

Construction Products Directive, Commission of European Community, N°L40/12, Luxembourg, December.

- **CEC, 1990a**

"Design of concrete structures", Eurocode No.2, Part 10, Structural fire design

- **CEC, 1990b**

"Design of composite structures", Eurocode No.4, Part 10, Structural fire design

- **Cervenka, V., Eligehausen, R. and Pukl R., 1990**

"SBETA-Computer Program for Nonlinear Finite Element Analysis of Reinforced Concrete Structures", Report 90/1, Institute of Building Materials, University of Stuttgart

- **Chiapetta, R. L., Longinow, A., and Stepanek, O. J., 1972**

"The Effect of Fire Temperatures on Buildings with Steel Frames", IITRI Project J8096, Final Report, Illinois Institute of Technology Research Institute, Chicago, IL, April

- **CIRIA 1986**

"Fire resistance of composite slabs with steel decking", the Construction Industry Research and Information Association

- **Cioni, P., Croce, P., Salvatore, W., 2001**

"Assessing fire damage to r.c. elements", Fire Safety Journal 36, 181–199

- **Cote, A. E. and J.L. Linville (eds.) 1986**

"Fire Protection Handbook", 16th Edition, Fire Safety in Building Design and Construction, National Fire Protection Association, Quincy, MA, pp. 7-82 to 7-108.

- **Corus Construction Centre website: http://www.corusconstruction.com.**

- **Corus Construction & Industrial, 2006**

Fire resistance of steel-framed buildings

- **ECCS, 1983**

"Calculation of the fire resistance of composite concrete slabs with profiled steel sheet exposed to the standard fire", ECCS, Committee T3-Fire safety of steel structures, technical note

- ECCS, 1988

European Convention for Constructional Steelwork, "Calculation of the Fire Resistance of Centrally Loaded Composite Steel-Concrete Columns Exposed to the Standard Fire", Publication 55

- Elghazouli, A.Y. and Izzuddin, B.A., 2001

"Analytical Assessment of the Structural Performance of Composite Floors Subject to Compartment Fires", Fire Safety Journal, 36, pp769-793

- Ellingwood, B., and Lin, T.D., 1991

"Flexure and shear behaviour of concrete beams during fires", Journal of Structural

- Eurocode 1 –EN1991-1-2

Actions on Structures – Part 1-2: General Actions-Actions on structures exposed to fire. CEN, Brussels, November 2002

- Eurocode 1 –ENV1991-1-2-, 1993

Actions on Structures – Part 1-2: General Actions-Actions on structures exposed to fire, CEN, Brussels.

- Eurocode 1, 1995.

Basis of Design and Actions on Structures, Part 2-2: Actions on structures–Actions on structures exposed to fire, ENV 1991-2-2.

- Eurocode 4 – 1989

"Composite Steel and Concrete Structures" part 10

- Eurocode 4 – 1994, Part 1-1

"Design of Composite Steel and Concrete Structures": ENV1994-1-1: Part 1-1: General rules and rules for building.

- Eurocode 4– 1994, Part 1-2

Design of Composite Steel and Concrete – Part 1-2: General rules- Structural Fire Design,

- European Convention for Constructional Steelwork, 1986

"Calculation of the Fire Resistance of Composite Columns Exposed to the Standard Fire"

- European Convention for Constructional Steelwork, 1984

"Calculation of the Fire Resistance of Composite Concrete Slabs with Profiled Steel Sheet Exposed to the Standard Fire"

- European Joint Research Programme 1999

"The Behaviour of Multi-Storey *Steel-Framed Buildings in Fire*", *Swinden* Technology Centre, British Steel plc, Rotherham, UK,

- Eymard, R., Galloue t, T., and Herbin, R., 2000

''The fine volume methods'' Handbook of numerical analysis, P. G. Ciarbet and J. L. Lions, eds., North Holland, Amsterdam

- Eymard, R., Galloue"t, T., Hilhorst, D., and Slimane, Y. N., 1998

''Finite volumes and nonlinear diffusion equations'', RAIRO-Mathematical Modelling and Numerical Analysis, Engineering, ASCE, 117 (2), pp.440-458

-Frank Kreith, Mark S. Bohn, 1993

"Principle of Heat Transfer", 5th ed. West Publishing Company, USA

- Franssen, Jean 2003

"Compartment Fire Models for Structural Engineering", University of Liege, Belgium

-Franssen, J.M. and Dotreppe, J.C., 1992

"Fire Resistance of Columns in Steel Frames", Fire Safety Journal 1992; 19: 159-175

- Gewain, R. G. (1982a),

"Building Fire Tests Computer Solution for Structural Fire Protection", SFPE Bulletin, Society of Fire Protection Engineers, Boston, MA, April

- Gewain, R. G. (1982b),

"Predicting Fire Resistance for Steel Floor Systems", presented at the Canadian Structural Engineering Conference., 1982

- Gewain, G. Richard and Troup, W. J. Emile, 2001

"Restrained Fire Resistance Ratings in Structural Steel Buildings", Engineering Journal / Second Quarter

- Gillie, M., Usmani, A., Rotter, M. and O'Connor, M., 2001

"Modelling of Heated Composite Floor Slabs with Reference to the Cardington Experiments", Fire Safety Journal, 36, pp745-767

- Gosselin, G.C. and T.T. Lie, 1987

"Provision of fire resistance -evolution of design approaches", Proceedings of Canadian Society for Civil Engineering Centennial Conference, Montreal, Quebec, Vol. 1, pp. 3-19.

- Halim, A.H., Hakmi, M.R., D.C. O'Leary, 1997

"Fire resistance of Composite Floor Slab", published by: Engineering Structures – ELSEVIER, 21 (1999) 176–182

- **Hamerlink, A.F., 1990**

"Preliminary calculation of Fire Test on Composite Steel/Concrete Slab", Eindhoven University of Technology, Report TUE-BKO-KO, The Netherlands,.

- **Hamerlink, A.F., Twilt, L. 1989**

"ECSC sponsored research on The Behaviour of Fire-Exposed Composite Steel/Concrete Slab", TU Eindhoven,/ TNO Delft, Test report BI 89-016 The Netherlands.

- **Hamerlink, A.F., Twilt, L. 1990**

"The Thermal Behaviour of Fire-Exposed Composite Steel/Concrete Slab", Eindhoven University of Technology,/ TNO Delft Test report The Netherlands

- **Harmathy, T.Z., 1970,**

"Thermal properties of concrete at elevated temperatures". ASTM Journal of Marerials no. 1, pp. 47-74,

- **Harmathy, T. Z., 1983,**

" Properties of building materials at elevated temperatures ", Division of building Research, National Research council of Canada, Paper No. 1080, Ottawa, NRCC 20956.

- **Harmathy, T.Z. and W.W. Stanzak, 1970**

"Elevated temperature tensile and creep properties of some structural and prestressing steels", American Society for Testing and Materials, Special Technical Publication 464 on Fire Test Performance, Philadelphia, PA, pp. 186-208.

- **Hertz, Kristian 1999**

"Analyses of Concrete Structures Exposed to Fire", Department of Buildings and Energy Technical University of Denmark.

- **Holman J.P., 1986**

Heat transfer, McGraw Hill-Book Company, New York

- **Huang, Z., 1995**

"The Analysis of Thermal and Fire Performance of Cementitious Building Components", PhD thesis, University of Central Lancashire

- **Huang Z., Burgess I.W. and Plank R.J., 1999**

Non-linear analysis of reinforced concrete slabs subjected to fire, ACI Structural Journal, 96(1), pp127-135.

- **Huang, Z., Burgess, I.W. and Plank, R.J., 2003**

"Modelling Membrane Action of Concrete Slabs in Composite Buildings in Fire Part I: Theoretical development", Journal of Structural Engineering, ASCE, 129 (8), pp1093-1102

- **Huang, Z., Burgess, I.W. and Plank, R.J., 2004**

"3D Modelling of Beam-Columns with General Cross-Sections in Fire", Paper S6-5, Third International Workshop on Structures in Fire, Ottawa, Canada, pp323-334

- **Huang, Z., and Platten, A., 1997**

"Non-linear finite element analysis of planar reinforced concrete members subjected to fire", ACI Structural Journal, 94 (3), pp.272-282

- **Iaonnides, S. A. and Mehta, S. (1997)**

"Restrained Vs. Unrestrained Fire Ratings: A Practical Approach, Modern Steel Construction", American Institute of Steel Construction, Chicago, IL, May.

- **Iding, R.H., Bresler, B., and Nizamuddin, Z., July 1977**

"FIRES-RC II – Structural Analysis Program for the Fire Response of Reinforced Concrete Frames," UCB-FRG Report 77-8, Fire Research Group, Department of Civil Engineering, University of California, Berkeley,

- **Iding, R. Bresler B. and Nizamuddin Z., October 1977**

"FIRES-T3", a computer program for the fire response of structures-thermal, University of California, Berkeley, October 1977

- **Iding, R.H., and Bresler, B., April 30, 1987**

"FASBUS II User's Manual" prepared for the American Iron and Steel Institute, Wiss, Janney, Elstner Associates, Inc.

- **Ingberg, S.H.1928**

"Test of Severity of Building Fires", Quarterly, National Fire Association, vol.22

- **ISO 834, 1975**

"Fire resistance tests-Element of building construction", International Standard ISO834, International Organization for Standardization Geneva

- **Issen, L.A., Gustaferro, A.H. and Carlson, C.C., 1970**

"Fire tests of concrete members; an improved method for estimating thermal restraint forces", Fire Test Performance, ASTM, STP 464, American Society for Testing and Materials, pp. 153-185

- Jaluria, Y., Torrance, K. E., 1986

"Computational heat transfer", Hemisphere Publishing Corporation

- James A. Milke, October 1999

"Analytical Methods to Evaluate Fire Resistance of Structural Members", J. Struct Engrg., Volume 125, Issue 10, pp. 1179-1187

- Jeanes, D.C., 1985

"Application of the computer in modeling fire endurance of structural steel floor systems", Fire safety journal 9, pp. 119-135

- Johnson, R.P., 1985

"Composite Construction 1 and 2", Hart, F., Henn, W., Sontag H., "Multi-storey Buildings in Steel", Second Edition, Collins, London

- Jose Torero, 21 April 2004

"Fire and Structures Conference", University of Edinburgh, Report of a Conference held at The Royal Society of Edinburgh on

- Kawagoe, K., 1958

"Fire Behaviour in Rooms", Report No. 27, Building Research Institute, Tokyo, Japan

- Kawagoe, K., Sekine, T., 1963

"Estimating of temperature-time curves in room", Report No. 11, Building Research Institute, Tokyo, Japan

- Kirby B.R. and Preston R.R., 1988

"High Temperature Properties of Hot-Rolled, Structural Steel for use in fire engineering design studies", Fire Safety Jurnal 13, p 27-37

- Kirby B.R. 2000

"British Steel data on the Cardington fire tests", Technical report, British Steel

- Kodur, V.K.R. and Lie, T.T., 1996

"A Computer Program to Calculate the Fire Resistance of Rectangular Reinforced Concrete Columns", Third Canadian Conference on Computing in Civil and Building Engineering, Ottawa, Canada, 1996, pp. 11-20

- Kruppa j. and Zhao B., 1995

"Fire resistance of composite beams", Journal Construction Steel Research 33

- Kwak, H.G., 1990

"Material Nonlinear Finite Element Analysis and Optimal Design of Reinforced Concrete Structures", Ph.D. Dissertation, Department of Civil Engineering, KAIST, Korea

- Lamont S., 2002

"The behaviour of multi-storey composite steel framed structures in response to compartment fires" PhD thesis The University of Edinburgh

- Law M., 1971

"A relationship between fire grading and building design and contents", Technical Report

- Lawson, R.M., 1989

"Design of Composite Slabs and Beams with Steel Decking", SCI-Publication 055.

- Ley, J., Sansom, M and Kwan A., 2002

"Material flow analysis of the UK steel construction sector", IISI World Conference 2002, Luxembourg

- Lie T.T. 1974

"Characteristic Temperature Curves for Various Fire Severities", Fire Technology, 10, 4.

- Lie T.T. 1984

"A procedure to calculate fire resistance of structural members", Fire and Materials, Vol. 8, No. 1, NRCC 23574, pp. 40-48

- Lie T.T. 1992

"Structural Fire Protection", American Society of Civil Engineers

- Lie, T. 1994

"Fire resistance of circular steel columns filled with bar reinforced concrete", Structural Engineering.

- Lie, T.T. 1995

"Fire Temperature-Time Relations", SFPE Handbook of Fire Protection Engineering, Society of Fire Protection Engineering, USA.

- Lie, T.T., and Celikkod, B., 1991

"Method to calculate the fire resistance of circular reinforced concrete columns", ACI Material Journal, 88(1), pp.84-91

- Lie, T.T., T.D. Lin, D.E. Allen and M.S. Abrams, 1984.

" Fire resistance of reinforced concrete columns", Division of Building Research, National Research Council of Canada, Technical Paper No. 1167, Ottawa, NRCC 23065, 32 p

- Lie T.T. and R.J. Irwin, 1993

"Method to calculate the fire resistance of reinforced concrete columns with rectangular cross section", ACI Structural Journal 90 (1993) (1), pp. 52–60

- **Lim, Linus, 2002**

"Experimental Fire Tests of Two-Way Concrete Slabs", University of Canterbury, & Colleen Wade, BRANZ Limited, New Zealand, Fire Engineering Research Report 02/12

- **Lin, C.S. and Scordelis, A.C., 1975**

"Nonlinear Analysis of RC Shells of General Form", Journal of Structural Division, ASCE, Vol. 101, No ST3, pp. 523-538

- **Lin, T.D. and Abrams, M.S.1983**

"Simulation of realistic thermal resistant during fire tests of floors and roofs", in: Fire Safety of Concrete Structures, Ed: M.S. Abrams, Publication SP-80. American Concrete Institution, Detroit.

- **Ma Z. and Makelainen P., 1999**

"Temperature Analysis of Steel-Concrete Composite Slim Floor Structures Exposed to Fires". Laboratory of Steel Structures Publications 10, Helsinki University of Technology, Espoo

- **Ma, Z. and Makelainen P., 2000**

"Parametric temperature-time curves of medium compartment fires for structural design", Fire Safety Journal, Volume 34, Issue 4, June, Pages 361-375.

- **Malhotra, H.L., 1956**

"The effect of temperature on the compressive strength of concrete", Magazine of Concrete Research, Vol. 8, No. 23, pp. 85-94

- **Malhotra, H.L. 1982**

"Design of fire resisting structures", Surrey University Press, London

- **Newman G M, 1989**

"The Fire Resistance of Composite Floors with Steel Decking", the Steel Construction Institute (SCI P-056)

- **Newman G M, 1991**

"The Fire Resistance of Composite Floors with Steel Decking", The steel construction institute 2nd ED (SCI P-056)

- **Newman, G., 1999**

"The Cardington Fire Tests", Proceedings, North American Steel Construction Conference, New Orleans, LA, American Institute of Steel Construction, Chicago

- **NIST, (National Institute of Standards And Technology), July 14, 2005**

"Fire Resistive Materials: Thermal Performance testing", www.scincedaily.com

- **Patankar S.V., 1980**

"Numerical Heat Transfer and Fluid Flow", Hemisphere Publishing Corp, Washington, D.C

- **Petterson, O., Magnuson, S.E. and Thor, J., 1976**

"Fire Engineering Design of Structures", Swedish Institute of Steel Construction, Publication 50,

- **Rajagopal, K.R., 1976**

"Nonlinear Analysis of Reinforced Concrete Beams, Beam-Columns and Slabs by Finite Elements", Ph.D. Dissertation, Iowa State University

- **SAA, 1990**

"Fire resistance tests of structure" AS1530.4-1990, Standards Association of Australia

- **Sala A. 1986**

Radiant properties of materials, Elsevier

- **Schneider U., 1983**

"Behaviour of concrete at high temperature", RILEM Committee

- **SCI, 2006**

"Composite Construction at the SCI", the Steel Construction Institute, Issue: 016.

- **Sebastjan Bratina, Bojan Cas, Miran Saje' and Igor Planinc, 2004**

"Numerical modelling of behaviour of reinforced concrete columns in fire and comparison with Eurocode 2", ScienceDirect, University of Ljubljana, Slovenia

- **S. Lamont A. S. Usmani and D. D. Drysdale,**

"Heat transfer analysis of the composite slab in the Cardington frame fire tests", Edinburgh University, UK, Available online 9 October 2001

- **(SNBCC) Supplement to the National Building Code of Canada 1985**

"Associate Committee on the National Building Code", National Research Council of Canada, Ottawa, NRCC

- **Stadling, R.E. and Brady, F.L. 1927**

"Fire Resistance Construction", Building Research Special Report No. 8, HMSO, London

- **Sterner, E., and Wickstr U., 1990**

"TASEF --Temperature Analysis of Structures Exposed to Fire," SP Report 1990:05, Swedish National Testing and Research Institute, Borays

-Stradling R. and Lea F., 1922

"The resistance to fire of concrete and reinforced concrete", Engineering

-Structural fire engineering (1991)

Steel Construction Industry Forum, "Investigation of Broadgate Phase 8 fire", Steel Construction Institute (SCI).

- Sullivan, P.J.E., Terro, M.J. and Morris, W.A., 1997

"Critical Review of Fire-Dedicated Thermal and Structural Computer Programs", Journal of Applied Fire Science, Vol. 3, No. 2, 1993, pp. 113-135

- Szilard, Rudolph, 1974

"Theory and Analysis of Plates classic and numerical methods", Prentice-Hall, INC, New Jersey

- Timoshenko P. Stephen, 1959

"Theory of Plates and Shells", 2nd Edition, McGraw-Hill international editions,

- Torero, J.L. and Steinhaus, T., June, 2004

"Applications of Computer Modelling to Fire Safety Design," Essen, Germany,

- Trinks,W., and Mawhinneg, M. W. 1961

"Industrial Furnaces ", Carnegie Inst. Technology, Wiley, New York

- ULC, 1989

"Standard methods of fire endurance tests of building construction and materials", CAN/ULC-S101-M89, Underwriters Laboratories of Canada, Ontario, Canada

- Usmani A.S., Rotter J.M., Lamont S., Sanad A.M. and M.Gillie

"Fundamental principles of structural behaviour under thermal effects", Fire Safety Journal Vol. 36 No. 8, 2001

- Virdi K.S. and Dowling P.J., 1976

"A Unified Design Method for Composite Columns", International Association for Structural Engineering, Zurich

- Wade, C., 1992

"Fire resistance of New Zealand concretes" (Study Report No. 40). Judgeford: BRANZ, The Resource Centre for Building Excellence.

- Zhao J.-C., 2000

"Application of the direct iteration method for non-linear analysis of steel frames in fire", Fire Safety Journal 35 (2000), pp. 241–255

- Zhongcheng Ma and Pentti Makelainen, 2000

"Parametric temperature–time curves of medium compartment fires for structural design", Fire Safety Journal Volume 34, Issue 4, June 2000, Page 361-375

- Zhuman Fu and George Hadjisophocleous

A two-zone fire growth and smoke movement model for multi-compartment buildings, Fire Safety Journal, 34, 2000, pp. 257-285